

Lincoln University Digital Thesis

Copyright Statement

The digital copy of this thesis is protected by the Copyright Act 1994 (New Zealand).

This thesis may be consulted by you, provided you comply with the provisions of the Act and the following conditions of use:

- you will use the copy only for the purposes of research or private study
- you will recognise the author's right to be identified as the author of the thesis and due acknowledgement will be made to the author where appropriate
- you will obtain the author's permission before publishing any material from the thesis.

**An Act of Fruitility: Investigating the Causes of Outer Arm
Formation in Grapevine (*Vitis vinifera* L.)**

A thesis
submitted in partial fulfilment
of the requirements for the Degree of
Doctor of Philosophy

at
Lincoln University
by
Rebecca Michiko Tashiro

Lincoln University
2014

Abstract of a thesis submitted in partial fulfilment of the
requirements for the Degree of Doctor of Philosophy.

An Act of Fruitfulness: Investigating the Causes of Outer Arm Formation in
Grapevine (*Vitis vinifera* L.)

by

Rebecca Michiko Tashiro

A major factor affecting quality in wine grapes is the varying levels of ripeness within a bunch. A significant cause of within bunch variation is the formation of an additional branch at the base of the main bunch, called the outer arm. As part of an industry-driven initiative, this work was tasked with identifying the molecular causes of fruitful outer arm development in grapevine. Two maize mutants shown to affect inflorescence architecture are the *ramosa3* and the *barren stalk1* genes. The *ramosa3* phenotype is due to a mutation in a TREHALOSE PHOSPHATE PHOSPHATASE (TPP) gene, a member of the trehalose biosynthesis pathway. The BARREN STALK1/LAX PANICLE (BA1/LAX1) bHLH transcription factor gene family regulates branching by limiting auxin into pluripotent cells. There were no published studies on these genes in grapevine when this research began. The focus of this work was to identify and characterize the TREHALOSE-6-PHOSPHATE SYNTHASE (TPS), TPP, and BA1/LAX1 gene families.

Seven TPS and seven TPP genes were identified in grapevine. Yeast complementation studies showed that only one TPS gene but all TPP genes examined are capable of trehalose biosynthesis. Transcription assays showed varying expression patterns of the VvTPS and VvTPP homologues across different grapevine tissues. Of particular interest was the high expression of some VvTPS and VvTPP genes during inflorescence initiation and differentiation. The VvBA1/LAX1 gene identified in grapevine also showed a range of transcription levels in the tissue types tested, with high expression in tissues undergoing rapid developmental changes. This is in agreement with other studies indicating a role for this transcription factor in auxin signalling.

To examine if carbohydrate supply affects fruitful outer arm development in grapevine, physiological and molecular experiments were carried out. Shoots of small or large diameter were harvested from a pruning trial, from which single node cuttings were planted and examined for fruitful outer arm development. Cuttings taken from large diameter shoots had a higher frequency of fruitful outer arms than small diameter shoots for both pruning treatments. Shoots from the severe pruning

treatment (pruned to 6 nodes) had a lower frequency of fruitful outer arms. The difference in fruitful outer arm development between the two pruning treatments could not be attributed to diameter size (and carbohydrate status) alone, as both treatments had similar diameter sizes. Transcript screening of several VvTPS and VvTPP genes in four bud developmental stages showed that these genes are expressed similar to several floral pathway genes. This leads us to hypothesize that the level of VvTPS and VvTPP expression, or the metabolites formed during trehalose biosynthesis, may be used as a signal by the plant to indicate carbohydrate status during primordia development to regulate inflorescence architecture. Comparison of buds from the same developmental stage, but collected from the two shoot diameter classes, indicated that diameter may have an effect on transcript levels for many of the VvTPS and VvTPP genes tested. When VvBA1/LAX1 was screened on the same bud tissues, there was a two-fold difference in expression during the budswell developmental stage, indicating that this transcription factor is most active just after dormancy during inflorescence differentiation. There was no significant shoot diameter difference in VvBA1/LAX1 expression, so this gene is not believed to have a role in carbohydrate signalling.

The results of this research show that the VvTPS and VvTPP gene families are present and active in grapevine, with a possible role in carbohydrate signalling during important developmental stages. We hypothesize that this signalling is partly responsible for fruitful outer arm development when there is a surplus of carbohydrates in the plant at the time of inflorescence primordia initiation. Furthermore, the expression of VvBA1/LAX1 before budburst indicates that this gene may also play a role in outer arm formation by regulating the differentiation of this organ during the second season of development. Although the results of this research cannot confirm these hypotheses, it has built a foundation to further investigate the role of these gene families in fruitful outer arm development.

Keywords: Grapevine, inflorescence, outer arm, signalling, trehalose, carbohydrate, bud, auxin, BA1/LAX1, plasmid, qRT-PCR.

Acknowledgements

I would like to acknowledge the superb support that I received from my supervisory committee during the course of this work. Dr. Winefield is a brilliant scientist with a strong commitment to improving the skills of his students. Dr. Jordan has many years of experience in molecular biology and a great intuition for good research topics. Dr. Trought is well known for his extensive knowledge of grapevine physiology and the enthusiasm he has for his work is contagious.

In addition to my supervisory committee, I would like to thank the members of the Winefield and Jordan research groups for their help and support throughout the course of this research. In particular, I would like to thank the technicians Jackie White and Joshua Philips for their assistance in the lab, especially for all the times that they focused more on my research than their own.

I would also like to thank the various research groups around the world that have assisted me during the course of this work. Thanks to the Lincoln University Center for Viticulture and Oenology for allowing me to collect samples from the vineyard, often with little advance notice, and to the Lincoln University greenhouse staff for the care of my single node cuttings. I am thankful to the Brancott Estate in Marlborough for the opportunity to collect samples from their commercial vineyard- again, often with little advance notice. I also gratefully acknowledge the Marlborough Wine Research Center for their support throughout the course of this research. I would like to thank the Hohmann Lab from the University of Gothenberg, Sweden, for providing the yeast mutant strains used in this research. I also thank the Malcomber research group from California State University, USA, for supplying the VvBA1/LAX1 sequence data.

Finally, I would like to acknowledge the funding I received during the course of this research. My research expenses were funded by the Foundation for Research Science and Technology (FRST) through the Designer Grapevines Research Program. My scholarship and fees were funded by the Lincoln University PhD Scholarship.

Table of Contents

Abstract	ii
Acknowledgements	iv
Table of Contents	v
List of Tables	viii
List of Figures	ix
 Chapter 1 Introduction	 1
1.1 Regulation of outer arm development	3
1.1.1 Overview of flowering in angiosperms	3
1.1.2 Flowering pathway initiation genes	4
1.1.3 Floral pathway integrator genes	5
1.1.4 Flowering meristem identity genes	6
1.1.5 Trehalose pathway genes	8
1.1.6 BARREN STALK1/LAX PANICLE1 (BA1/LAX1)	9
1.1.7 Carbohydrate status of the plant	10
1.2 Preview of research done during this thesis	11
1.2.1 Trehalose pathway genes in grapevine	11
1.2.2 The BA1/LAX1 gene in grapevine	11
1.2.3 Carbohydrate status effect on outer arm development	12
 Chapter 2 Development of yeast expression plasmids for grapevine TPS and TPP complementation study	 13
2.1 Introduction	13
2.2 Materials & methods	14
2.2.1 Yeast mutant strains pedigree	15
2.2.2 Plasmid construction	15
2.3 Results & discussion	19
2.4 Conclusions and future prospects	22
 Chapter 3 Development of reference genes to use for transcriptional analysis in grapevine	 23
3.1 Introduction	23
3.2 Materials & methods	24
3.2.1 Candidate reference gene identification	24
3.2.2 Primer design	25
3.2.3 Plant material collected for qRT-PCR assays to test potential grapevine reference genes for stability across the samples tested	25
3.2.4 RNA extraction and cDNA synthesis	27
3.2.5 qRT-PCR assays	27
3.2.6 Statistical analysis	28
3.3 Results & discussion	29
3.4 Conclusions and future prospects	36
 Chapter 4 <i>In silico</i> identification of grapevine genes encoding trehalose biosynthetic enzymes and homologues of the transcription factor BARREN STALK1/LAX PANICLE1 (BA1/LAX1)	 37
4.1 Introduction	37

4.2	Materials & methods	39
4.2.1	Gene identification and annotation.....	39
4.2.2	Phylogenetic tree development.....	39
4.2.3	Karyotype development.....	40
4.3	Results & discussion.....	40
4.3.1	Grapevine trehalose pathway genes	40
4.3.2	Grapevine BA1/LAX1	49
4.4	Conclusions and future prospects	51
Chapter 5 Characterization of the TPS/TPP gene family in grapevine.....		53
5.1	Introduction	53
5.1.1	Trehalose-6-phosphate (T6P) in carbohydrate synthesis	54
5.1.2	Trehalose-6-phosphate (T6P) as a signal molecule	54
5.1.3	Trehalose-6-phosphate (T6P) in inflorescence architecture.....	56
5.2	Materials & Methods	57
5.2.1	Cloning of VvTPS and VvTPP genes	57
5.2.2	Yeast complementation	58
5.2.3	Quantitative gene expression assays in grapevine tissue by qRT-PCR	61
5.3	Results & discussion.....	62
5.3.1	Complementation assays for grapevine TPS and TPP gene function in mutant strains of <i>Saccharomyces cerevisiae</i>	62
5.3.2	Quantitative assays for TPS and TPP gene expression in grapevine tissues by qRT-PCR	67
5.4	Conclusions and future prospects	83
5.4.1	Grapevine TPS and TPP genes can complement yeast mutant strains.....	84
5.4.2	Transcript variation of grapevine TPS and TPP genes among different tissues	85
5.4.3	Future work in grapevine TPS and TPP characterization	86
Chapter 6 Characterization of the BA1/LAX1 gene in grapevine.....		88
6.1	Introduction	88
6.2	Materials & Methods	91
6.2.1	Cloning of VvBA1/LAX1	91
6.2.2	Quantitative expression assay of VvBA1/LAX1 in grapevine tissue by qRT-PCR	91
6.3	Results & discussion.....	93
6.3.1	Transcript variation of grapevine VvBA1/LAX1 genes among different tissues.....	93
6.4	Conclusions and future prospects	96
Chapter 7 Investigating the impact of carbohydrate supply on the flowering process in grapevine		98
7.1	Introduction	98
7.1.1	Carbohydrate in flowering	98
7.1.2	Carbohydrate in grapevine	99
7.1.3	Molecular biology of flowering in grapevine	100
7.2	Materials & methods	101
7.2.1	Single node cuttings	101
7.2.2	Quantitative gene expression assays in grapevine bud developmental stages by qRT-PCR.....	102
7.3	Results & discussion.....	104
7.3.1	Determination of fruitful outer arm development with limited carbohydrate by single node cuttings	104

7.3.2	Transcript variation of grapevine trehalose pathway families, VvBA1/LAX1, and flowering pathway genes in grapevine developmental bud stages	108
7.4	Conclusions and future prospects	124
Chapter 8 Conclusions and future prospects		127
Appendix A General protocols.....		135
A.1	Polymerase chain reaction (PCR)	135
A.2	Qualitative reverse-transcriptase PCR (qRT-PCR) data analysis	139
Appendix B Primers used for this research.....		141
B.1	Plasmid backbone primers.....	141
B.2	Reference gene fragment cloning primers	141
B.3	Whole gene amplification primers	142
B.4	RT-PCR primers	143
B.5	qRT-PCR primers	144
Appendix C Media used for this research.....		145
C.1	Bacterial media	145
C.2	Yeast media.....	145
Appendix D Sequence data for this work		146
D.1	Sequence results after cloning yeast promoters into pYexBx	146
D.2	Class II TPS genes sequence alignment of the glycosyltransferase and phosphatase regions.....	152
Appendix E RT-PCR assay on grapevine tissues		157
E.1	Trehalose biosynthesis pathway gene families	157
E.2	VvBA1/LAX1	160
Appendix F Additional tables and charts for this work		163
F.1	ANOVA table of reference genes tested on the 'Pinot noir' confirmation population tissue types.....	163
F.2	Single node cuttings supplementary charts.....	169
References		174

List of Tables

Table 2.1	Primers used to amplify <i>S. cerevisiae</i> promoters for cloning into pYexBx to develop new plasmids for complementation experiments.....	16
Table 2.2	Primers used to amplify <i>S. cerevisiae</i> TPS genes for cloning into pYexTEF1MCS, pYexTPS1MCS, or pYexTPS2MCS to test promoter function in the new plasmids developed for complementation experiments.....	17
Table 3.1	Grapevine qRT-PCR reference gene primer sequences used to identify the most stably expressed genes in this study.	26
Table 3.2	Reference genes screened for stability in this study.....	31
Table 3.3	Ranking of reference genes screened for stability in ‘Sauvignon blanc’ tissue based on geNorm analysis (Vandesompele et al., 2002) and the tissue types used in each dataset.	33
Table 3.4	ANOVA testing of candidate reference genes to determine the stability value for each gene from three biological replicates of nine ‘Pinot noir’ tissue types (Khanlou and Van Bockstaele, 2012).	34
Table 3.5	Ranking of reference genes screened for stability in three biological replicates of ‘Pinot noir’ based on geNorm (Vandesompele et al., 2002) and ANOVA (Khanlou and Van Bockstaele, 2012) analysis.....	35
Table 4.1	Grapevine trehalose pathway genes	42
Table 4.2	Grapevine BARREN STALK1/LAX PANICLE1 (BA1/LAX1) gene	50
Table 5.1	Primers used to clone TPS and TPP genes into pYexTEF1/TPS1/TPS2 plasmids for yeast complementation.....	60

List of Figures

Figure 1.1	A ‘Pinot noir’ grape bunch bearing a fruitful outer arm whose berries are at an earlier stage of ripening when compared to the main bunch.	2
Figure 1.2	Genetic cues for floral development in grapevine.	5
Figure 2.1	Plasmids developed for yeast transformation.	20
Figure 2.2	<i>S. cerevisiae</i> <i>tps</i> mutant strains transformed with three different plasmids containing the endogenous yeast TPS1 or TPS2 gene to test for promoter function.....	21
Figure 3.1	Box and whisker plot showing the C_q range of the reference genes tested across 24 ‘Sauvignon blanc’ tissue types.....	30
Figure 3.2	Stability of the reference genes tested on 24 ‘Sauvignon blanc’ tissues as determined by geNorm (Vandesompele et al., 2002).	32
Figure 3.3	Stability of the reference genes tested on three biological replicates of ‘Pinot noir’ as determined by geNorm (Vandesompele et al., 2002).	35
Figure 4.1	Grapevine karyotype showing the locations of the VvTPS and VvTPP genes.	41
Figure 4.2	Sequence alignment of the glycosyltransferase region of Class I TPS genes.	43
Figure 4.3	Phylogenetic tree of TPS genes.	45
Figure 4.4	Sequence alignment of the phosphatase region of TPP genes.	47
Figure 4.5	Phylogenetic tree of TPP genes.	49
Figure 4.6	Sequence alignment of the BA1/LAX1 clade of bHLH genes.....	50
Figure 4.7	Phylogenetic tree of the BA1/LAX1 clade of bHLH genes.	51
Figure 5.1	The trehalose biosynthesis pathway in plants.	53
Figure 5.2	Simplified diagram of SnRK1 signalling in plant cells.....	55
Figure 5.3	Complementation of the yeast <i>tps1Δ</i> :TRP1 genotype with grapevine TPS gene family genes using the endogenous yeast TPS1 promoter.	63
Figure 5.4	Complementation of the yeast <i>tps1Δ</i> :TRP1 genotype with grapevine TPS gene family genes using the constitutive yeast TEF1 promoter.	65
Figure 5.5	Complementation of the yeast <i>tps2Δ</i> : <i>LEU2</i> genotype with grapevine TPP gene family genes using the endogenous yeast TPS2 promoter.	66
Figure 5.6	Grapevine ‘Pinot noir’ tissue types used to quantify VvTPS and VvTPP transcript activity by qRT-PCR.	67
Figure 5.7	Relative expression of VvTPS1 assayed across nine ‘Pinot noir’ tissue types.	68
Figure 5.8	Relative expression of VvTPS2 assayed across nine ‘Pinot noir’ tissue types.	71
Figure 5.9	Relative expression of VvTPS3 assayed across nine ‘Pinot noir’ tissue types.	72
Figure 5.10	Relative expression of VvTPS4 assayed in nine ‘Pinot noir’ tissue types.	73
Figure 5.11	Relative expression of VvTPS5 assayed in nine ‘Pinot noir’ tissue types.	74
Figure 5.12	Relative expression of VvTPS6 assayed in nine ‘Pinot noir’ tissue types.	75
Figure 5.13	Relative expression of VvTPPA assayed in nine ‘Pinot noir’ tissue types.....	77
Figure 5.14	Relative expression of VvTPPB assayed in nine ‘Pinot noir’ tissue types.	78
Figure 5.15	Relative expression of VvTPPC/G assayed in nine ‘Pinot noir’ tissue types.....	80
Figure 5.16	Relative expression of VvTPPD assayed in nine ‘Pinot noir’ tissue types.....	81
Figure 5.17	Relative expression of VvTPPE assayed in nine ‘Pinot noir’ tissue types.	82
Figure 6.1	Grapevine ‘Pinot noir’ tissue types used to quantify VvBA1/LAX1 transcript activity by qRT-PCR.	94
Figure 6.2	Quantitative relative expression of grapevine VvBA1/LAX1 gene activity in three biological replicates of nine ‘Pinot noir’ tissue types.....	95
Figure 7.1	Mean diameter (mm) of small or large diameter class single node cuttings per shoot position from 6-node (a) or 12-node (b) pruned shoots.	105
Figure 7.2	Mean volume (mm) of small or large diameter class single node cuttings per shoot position from 6-node (a) or 12-node (b) pruned shoots.	106
Figure 7.3	Mean frequency of fruitful outer arms from single node cuttings grown from small or large diameter class shoots from 6-node (a) or 12-node (b) pruned shoots.	107

Figure 7.4	Relative expression of VvCO1 in grapevine bud developmental stages. VvCO1 expression levels are shown as grouped developmental stages (a) or separated into small or large diameter class shoots (b).	110
Figure 7.5	Relative expression of VvFL in grapevine bud developmental stages. VvFL expression levels are shown as grouped developmental stages (a) or separated into small or large diameter class shoots (b).	110
Figure 7.6	Relative expression of VvTFL1A in grapevine bud developmental stages. VvTFL1A expression levels are shown as grouped developmental stages (a) or separated into small or large diameter class shoots (b).	111
Figure 7.7	Relative expression of VvBA1/LAX1 in grapevine bud developmental stages. VvBA1/LAX1 expression levels are shown as grouped developmental stages (a) or separated into small or large diameter class shoots (b).	112
Figure 7.8	Relative expression of VvTPS1 in grapevine bud developmental stages. VvTPS1 expression levels are shown as grouped developmental stages (a) or separated into small or large diameter class shoots (b).	114
Figure 7.9	Relative expression of VvTPS5 in grapevine bud developmental stages. VvTPS5 expression levels are shown as grouped developmental stages (a) or separated into small or large diameter class shoots (b).	115
Figure 7.10	Relative expression of VvTPPA in grapevine bud developmental stages. VvTPPA expression levels are shown as grouped developmental stages (a) or separated into small or large diameter class shoots (b).	116
Figure 7.11	Relative expression of VvTPPB in grapevine bud developmental stages. VvTPPB expression levels are shown as grouped developmental stages (a) or separated into small or large diameter class shoots (b).	117
Figure 7.12	Relative expression of VvTPPE in grapevine bud developmental stages. VvTPPE expression levels are shown as grouped developmental stages (a) or separated into small or large diameter class shoots (b).	118
Figure 7.13	Relative expression of VvSPS1 in grapevine bud developmental stages. VvSPS1 expression levels are shown as grouped developmental stages (a) or separated into small or large diameter class shoots (b).	121
Figure 7.14	Relative expression of VvSPP1A in grapevine bud developmental stages. VvSPP1A expression levels are shown as grouped developmental stages (a) or separated into small or large diameter class shoots (b).	122
Figure 7.15	Relative expression of VvSPP1B in grapevine bud developmental stages. VvSPP1B expression levels are shown as grouped developmental stages (a) or separated into small or large diameter class shoots (b).	123

Chapter 1

Introduction

The common grapevine (*Vitis vinifera*) is cultivated in temperate climates worldwide for fresh and dried fruit consumption, and its juice is consumed fresh or fermented into alcoholic beverages such as wine. In 2011, grapes were being grown on over 7.5 million hectares worldwide (OIV, 2012). Up to 80% of all grapes harvested are converted into wine (Mullins, 1992) with the majority of wine being produced in Europe (Jackson, 2000). According to New Zealand Winegrowers (2013), an industry association, wine was New Zealand's 8th largest export product in 2013, with an estimated 345,000 tons harvested at a value of around \$1.2 billion. Nearly all grapes harvested in New Zealand are used in wine production (OIV, 2010). In 2013, grapevine was grown on an estimated 35,500 hectares in New Zealand, an increase of 1% from the previous year and a nearly 100% increase from a decade ago (New Zealand Winegrowers, 2013). The increase in production area has resulted in increased vintages, with 2008 having the largest harvest to date, at an average of 9.7 tonnes per hectare harvested (Winegrowers, 2009). The record harvest in 2008 was followed with a predicted second year of record harvest in 2009 (Winegrowers, 2009). To avoid flooding the market, vineyard managers took the drastic step of reducing crop loads before harvest to end up with an average yield of 9.2 tonnes per hectare (Winegrowers, 2009). As a result of the 2008 and 2009 harvests, vineyard managers and growers are recognizing the importance of producing high-value product rather than large-quantity yields when growing grapes for winemaking.

When grapes are used for winemaking, one factor affecting crop quality is the varying levels of maturity for individual berries within a bunch at harvest. In viticulture, berry maturity is measured by the amount of soluble sugars available (defined as °Brix) (Krstic, 2003). If the berries within a bunch are at differing stages of maturity at harvest, some fruit will be below the correct °Brix range for the cultivar, which in red wines ultimately results in a reduced value for the harvest and a lower quality wine produced. 'Pinot Noir' grapes are typically harvested when the berries are between 22.5-24.3 °Brix (Krstic, 2003). The narrow harvest range (less than 2 °Brix) for this cultivar means that there is a higher chance that individual berries both within the bunch and throughout the vineyard will be outside the acceptable range at harvest time. When red grape berries that are harvested below the standard °Brix are used to make wine, the resulting vintage has sensory descriptions of "green" or "bell pepper" (Tesci et al., 2002), which is undesirable in red wines and results in lower taste scores and hence lower value wines.

One of the factors affecting berry maturity within a bunch is the shape of the cluster itself. Many grape inflorescences have an additional branch form at the base which develops into either a tendril, an inflorescence branch, a combination of both organs, or abscise and fall off (Morrison, 1991; Carmona et al., 2008; Vasconcelos et al., 2009). This additional branch is described by various authors as “shoulders,” “wings,” “outer arms” or “ramifications” (Galet, 2000; Krstic, 2003; Dunn and Martin, 2007; Carmona et al., 2008; Tarter and Poni, 2010). It is unknown what causes the branch (hereafter referred to as “outer arm”) to determine its fate, but anecdotal evidence points to environmental factors as a major source of the variation (Dunn and Martin, 2007). When the outer arm develops into an inflorescence branch, it is often found on bunches that are larger than average (Tarter and Poni, 2010) and the berries from the outer arm can increase yield by as much as 40% (J. Bennett, pers. comm.). While yield can be significantly affected by the presence of fruitful outer arms, berries within the structure can be delayed by up to two weeks in reaching maturity when compared to berries within the main bunch (Figure 1.1). This wide range of maturity can negatively impact crop values and wine quality if the entire bunch is harvested at the same time. To increase the quality of harvest, vineyard managers growing red grape varieties such as ‘Pinot Noir’ often have to spend additional time and money selectively pruning outer arm bunches during the growing season or immediately before harvest.



Figure 1.1 A ‘Pinot noir’ grape bunch bearing a fruitful outer arm whose berries are at an earlier stage of ripening when compared to the main bunch.

In New Zealand, 'Pinot noir' is the second most popular grapevine variety grown (New Zealand Winegrowers, 2013). As 'Pinot noir' is often used to make red wines, the development of fruitful outer arms and subsequent delay of berry ripening on this variety requires removal of the outer arms before the bunch is harvested. As part of an industry-driven project to improve grapevine varieties in New Zealand, the goal of this study was to identify the molecular causes of fruitful outer arm development in grapevine- specifically in 'Pinot noir' vines. Since fruitful outer arm development in grapevine is highly variable, this research project focused on the genes and signalling involved in inflorescence development.

In grapevine, the inflorescences for the following growing season are formed during the current growing season within the compound latent bud located on the base of each petiole along the shoot (Morrison, 1991). The inflorescence primordia develops from undifferentiated primordia (anlagen) that appears after 3 to 8 leaf primordia develop within the latent bud (Srinivasan and Mullins, 1981). The time of anlagen formation within the bud depends on the genotype, environment, and location of the bud on the shoot (Vasconcelos et al., 2009). Anlagen can develop into inflorescence primordia, tendril primordia, or a combination of the two tissue types (May, 2004). Again, genotype, environment, and bud location appear to strongly influence the final anlagen structure, with the first few anlagen formed becoming inflorescences and anlagen formed during periods of active shoot growth becoming tendrils (Boss et al., 2003). Differentiation of the anlagen into the final tissue type begins during anthesis of the current year's inflorescences (Morrison, 1991). For anlagen that become inflorescences, the tissue undergoes an initial division which will later become the main inflorescence and the outer arm (Srinivasan and Mullins, 1981). The main inflorescence primordia undergoes several rounds of branching to form secondary and tertiary branch primordia before entering dormancy (Srinivasan and Mullins, 1981; May, 2004; Vasconcelos et al., 2009). The outer arm primordia also undergoes some branching (Srinivasan and Mullins, 1981), but significantly less than the main branch primordia. As stated above, little is known about what causes the outer arm to form inflorescences rather than tendrils but three causes have been postulated: genes, environment, and carbohydrate status of the plant.

1.1 Regulation of outer arm development

1.1.1 Overview of flowering in angiosperms

As shown in Figure 1.2, multiple overlapping cues stimulate the flowering process in plants. A complete review of all of the genes involved in the flowering process in plants is beyond the scope of this research, but the major genes involved in floral initiation are described below. Upon recognition

of the flowering stimulus, usually FLOWERING LOCUS T (FT), the plants then transcribe genes involved in the development of inflorescence meristems, flower meristems, and floral organs. In *Arabidopsis*, a facultative long-day annual, environmental cues such as temperature and day length are triggers for flowering; in grapevine, a facultative long day perennial (Sreekantan et al., 2010), cues such as light intensity and plant age are also factors that affect the transition to flowering (Carmona et al., 2008). Genes that play major roles in promoting the transition to flower, such as LEAFY (LFY) and FT, are also known to affect the overall architecture of the inflorescence (Bomblies et al., 2003; Hiraoka et al., 2013).

1.1.2 Flowering pathway initiation genes

There are four pathways recognized as being involved in the initiation of flowering in plants. One of the major pathways involved in floral initiation in plants is the photoperiod pathway, which integrates day length signals from numerous sources into the floral promoting gene *CONSTANS1* (CO1; Ito et al., 2012). Once the proper day length is achieved, the level of CO1 expression is sufficient to activate FT transcription, which in turn leads to activation of the floral meristem identity genes *APETALA1* (AP1) and *LFY* (He, 2012). These genes then promote flowering by activating the genes responsible for flower primordia development and differentiation (Samach and Smith, 2013). Another pathway involved in the initiation of flowering in some plants is the vernalization pathway, which recognizes temporal cues to promote or repress flowering. The major integrator gene in this pathway is the transcription factor *FLOWERING LOCUS C* (FLC), which represses transcription of the floral integrator genes *FT*, *SOC*, and *LFY* (Boss et al., 2004) until the proper vernalization requirements have been met. Besides the environment-dependent pathways described above, flowering plants also rely on internal cues such as hormones and age. Several hormones, such as gibberellins or auxin, either promote or repress flowering (Boss et al., 2004; Matsoukas et al., 2012). A major age-dependent floral initiation gene family is the *SQUAMOSA* PROMOTER BINDING-LIKE (SPL) family, whose transcript levels increase as the plants age and are promoters of several floral pathway integrator genes (Chen et al., 2010).

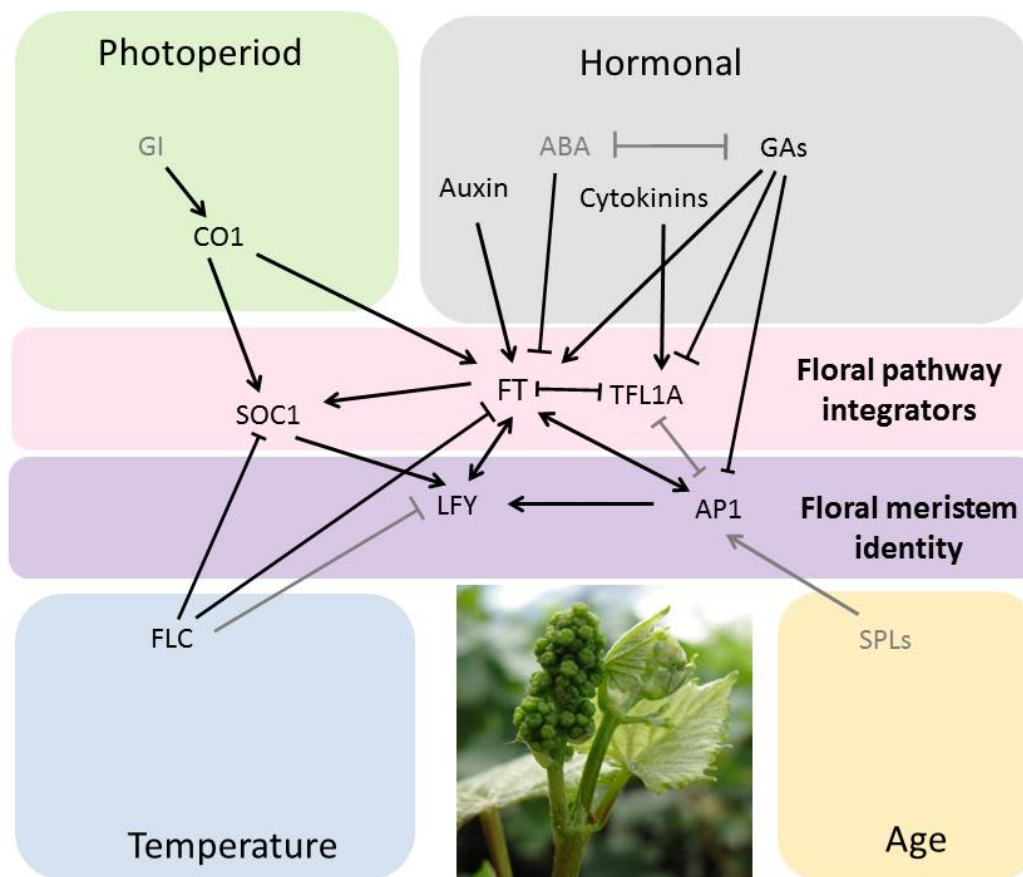


Figure 1.2 Genetic cues for floral development in grapevine.

Some of the major genes involved in each of the multiple pathways are shown. Floral promoter genes are indicated by arrowheads. Floral repressor genes are indicated by T-bars. Genes and interactions not yet investigated in grapevine are in grey.

1.1.3 Floral pathway integrator genes

FLOWERING LOCUS T/TERMINAL FLOWER (FT/TFL) genes

The FT/TFL gene family consists of genes that both promote and delay flowering. The FT gene promotes the transition to flowering in plants through both environmental and autonomous cues (Kobayashi et al., 1999). It is believed that FT promotes flowering by transportation of its translated product from leaves to the shoot meristem, which then activates flowering genes involved in inflorescence meristem identity and floral organ identity (Yoo et al., 2013). In contrast to FT, it is believed that TFL maintains the indeterminate status of the inflorescence by preventing terminal flower development at the apex of the meristem by repressing floral meristem identity genes such as LFY and AP1 (Ratcliffe et al., 1999; Boss et al., 2003). Besides having roles in protein trafficking (Sohn et al., 2007) and temperature signalling (Strasser et al., 2009), TFL1 is involved in the transition

from vegetative to reproductive phase and maintenance of inflorescence meristem indeterminacy (Shannon and Meeks-Wagner, 1991; Bradley et al., 1997). In addition, the interaction of floral promotor genes such as LFY with repressor genes like TFL1 are proposed to determine the inflorescence architecture of all flowering plants, with varying levels of each gene leading to alterations in the final inflorescence shape (Prusinkiewicz et al., 2007).

TFL1 levels have proven to be essential in determining inflorescence architecture in all model plants studied. Transgenic plants overexpressing the TFL1 gene or its homologues had inflorescences which developed secondary shoots along the peduncle, increased inflorescence density, and often have delayed flowering compared to wild type plants (Bradley et al., 1997; Ratcliffe et al., 1998; Nakagawa et al., 2002; Danilveskaya et al., 2010). Three TFL1 homologues have been identified in the grapevine genome- VvTFL1A, VvTFL1B, and VvTFL1C (Carmona et al., 2007). The grapevine TFL1 homologues have different expression patterns throughout the vine, indicating specialized roles in the development of the plant through the two year flowering cycle of the species (Carmona et al., 2007). TFL1 levels have been shown to affect inflorescence architecture in grapevine, with somatic mutants of 'Carignan' exhibiting inflorescences with increased branch numbers found to have high levels of TFL1A expression due to transposon-induced overexpression of the gene (Fernandez et al., 2010).

SUPPRESSOR OF CONSTANS1 (SOC1)

SOC1 is a MADS-domain family transcription factor that promotes flowering via the vernalization and photoperiod pathways (Lee et al., 2000). SOC1 is strictly regulated by other transcriptional regulators such as FLC (Hepworth et al., 2002) and APETALA2 (AP2) (Yant et al., 2010). Activation of SOC1 transcription in turn leads to up-regulation of the floral meristem identity gene LFY (Lee et al., 2000). In Arabidopsis, *soc1* mutants were found to flower earlier than wild type, caused by alterations in multiple pathways (Lee et al., 2000), however the mutant phenotype was alleviated by the activation of other flowering pathways (Hepworth et al., 2002). In grapevine, SOC1 was identified as VvMADS8 and was found to be most highly expressed during the period of inflorescence development in latent buds (Sreekantan and Thomas, 2006).

1.1.4 Flowering meristem identity genes

LEAFY (LFY)

LFY is a transcription factor that promotes both the timing of flowering and floral structures by activating the transcription of floral organ genes (Blazquez et al., 1997). As such, LFY expression increases as the plant transitions from a vegetative to a reproductive state (Blazquez et al., 1997).

The level of LFY expression is maintained by a positive feedback loop with floral organ genes such as AP1 (Blazquez et al., 2006). This loop in turn represses TFL1 expression, which allows flowering to occur (Ratcliffe et al., 1999).

In grapevine, a single LFY gene has been identified and found to be expressed in buds emerging from dormancy of the current year's growth, flowers, and tendrils (Carmona et al., 2008). Although the grapevine LFY gene (VFL) is believed to play a role in inflorescence development, it is not believed to be the only gene responsible for floral development in the species (Carmona et al., 2008). Instead, it is believed to play a role in maintaining the shoot apical meristem's indeterminacy and other floral initiation genes have a more important role in inflorescence development in grapevine.

APETELA1 (AP1)

AP1 is another MADS-domain transcription factor that promotes both floral meristem identity and floral differentiation via the ABC model of flower development (Blazquez et al., 2006; Benlloch et al., 2007). AP1 transcription is controlled by the direct binding of other transcription factors, notably LFY, FT, and SPL within its promoter region (Kaufmann et al., 2010). AP1 in turn represses flowering pathway integrator genes such as SOC1 and TFL1 (Liu et al., 2007), which leads to floral meristem and flower development in the inflorescence. AP1 has been shown to be repressed by gibberellins in grapevine (Zhang et al., 2008) but promoted by the hormone in other model species (Boss et al., 2004). In grapevine, VvAP1 is expressed at two time points, both during inflorescence meristem development and during flower differentiation (but not as part of the ABC model of flower development) the following spring (Calonje et al., 2004), as well as in tendrils. The expression of VvAP1 in tendrils led the researchers to hypothesize that this gene has another function other than flower development in the species.

In addition to the flowering pathway genes described above, genes involved in signalling pathways have also been identified as having a major role in inflorescence branching and architecture. The sugar signal trehalose-6-phosphate (T6P) has been implicated in inflorescence architecture based on mutant phenotypes observed in maize and Arabidopsis plants. This sugar is currently the focus of a lot of research, but to the best of our knowledge, no one is studying its effect on inflorescence architecture in grapevine. Similarly, an auxin signalling gene, BARREN STALK1/LAX PANICLE1 (BA1/LAX1) from maize is known to severely restrict branching in mutants, but little research is being done on this gene in any dicotyledonous species. As these genes have not yet been fully characterized in grapevine but are known to have a pronounced influence on inflorescence architecture in other plant species, they will be the main focus of this research.

1.1.5 Trehalose pathway genes

Trehalose is a disaccharide synthesized by many organisms which has gained much attention due to its ability to protect against abiotic stresses (Elbein et al., 2003). Derived from two glucose molecules through 5 possible pathways (Iturriaga et al., 2009), trehalose can constitute up to 15% of the dry weight of some organisms under stress conditions (Muller et al., 1995). Trehalose was initially believed to be synthesized only in desiccation-tolerant plants (Muller et al., 1995), but in 1998, publications identified genes responsible for trehalose synthesis in the model species *Arabidopsis thaliana* (Blazquez et al., 1998; Vogel et al., 1998). The identification of these genes in *Arabidopsis* has allowed the gene products and their function, as a signal molecule, to be further characterized (Kolbe et al., 2005; Harthill et al., 2006; Zhang et al., 2009). It is currently accepted that trehalose-6-phosphate (T6P) is integral for signalling various stress responses (Paul, 2007; Smith and Stitt, 2007), cytosolic sugar levels (Avonce et al., 2005; Lunn et al., 2006) and starch synthesis in plants (Kolbe et al., 2005; Lunn et al., 2006), although the exact pathways are unclear. It is believed that only one gene in each gene family encodes a functional enzyme and the other gene products within the family are likely involved in plant signalling rather than trehalose synthesis (Vandesteene et al., 2010) and as such are still under selective pressure (Avonce et al., 2006). Since their discovery in *Arabidopsis*, the genes responsible for trehalose synthesis have been identified in many other plant species (Müller et al., 1999; Wang et al., 2005; Kosmas et al., 2006; Satoh-Nagasawa et al., 2006; Wu et al., 2006; Lunn, 2007; Shima et al., 2007; Jiang et al., 2010), including recently in grapevine (this work; Fernandez et al., 2012).

By observing plants with mutated trehalose synthesis pathway genes, it was also determined that trehalose or its precursor, T6P, are also important for the transition to flowering and floral architecture in plants (Schluepmann et al., 2003; van Dijken et al., 2004; Satoh-Nagasawa et al., 2006; Chary et al., 2008). In maize plants with a mutant TREHALOSE-6-PHOSPHATE PHOSPHATASE (TPP) gene, which are then unable to process trehalose from T6P, the inflorescences had increased basal branching (Satoh-Nagasawa et al., 2006) and *Arabidopsis tpp* mutant plants had reduced flower development (van Dijken et al., 2004). In *Arabidopsis* plants overexpressing the TPP gene, inflorescence initiation was delayed by up to 3 weeks and had reduced branching (Schluepmann et al., 2003). In studies involving *Arabidopsis*, it was found that alterations of trehalose or T6P levels can alter flowering times and architectures of inflorescences independently of the major floral initiation genes, such as FLOWERING LOCUS T (FT) and LEAFY (LFY) (van Dijken et al., 2004; Wahl et al., 2013) via the age-dependant flowering pathway by altering expression of several SQUAMOSA PROMOTER LIKE (SPL) genes (Wahl et al., 2013). It was also found that TREHALOSE-6-PHOSPHATE SYNTHASE1 (TPS1) or T6P can significantly affect FT expression in *Arabidopsis* leaves, providing

evidence that members of the trehalose pathway are integral for signalling the carbohydrate status of the plant before the transition to flowering (Wahl et al., 2013). However, altered trehalose or T6P levels and the response of floral repressor genes such as TERMINAL FLOWER 1 (TFL1) have not yet been examined.

1.1.6 BARREN STALK1/LAX PANICLE1 (BA1/LAX1)

BA1/LAX1 is a member of a basic helix-loop-helix (bHLH) transcription factor family that has been shown to alter inflorescence morphology in model plants (Komatsu et al., 2003; Gallavotti et al., 2004; Yang et al., 2012). The BA1/LAX1 gene was shown to control sites of tissue divergence by limiting auxin transport into dividing cells (Gallavotti et al., 2008; Woods et al., 2011). The limitation of auxin into cells leads to drastic downstream effects, essentially arresting cell development from the divergence point (Gallavotti et al., 2008). As auxin and cytokinin are antagonistic to each other during meristem development (Müller and Leyser, 2011), limitation of auxin into cells leads to increased cytokinin concentrations, which can affect not only branching and differentiation, but also lead to programmed cell death (Kunikowska et al., 2013). While BA1/LAX1 is not the only gene responsible for auxin signalling in plants, this gene is of particular interest as it has been shown to have similar roles in auxin regulation in multiple species, indicating a widespread role throughout the plant kingdom (Woods et al., 2011).

Given its role as a regulator of branching, BA1/LAX1 could have a vital role in the development of grapevine inflorescence primordia. As described above, grapevine inflorescence primordia develop over two growing seasons, with initial inflorescence primordia forming during anthesis of the current year's growth (Morrison, 1991) and secondary and tertiary branching of the primordia occurring before dormancy (May, 2000). During budburst the following year, the inflorescence primordia undergo their final differentiation, driven by flowering cues such as FT and LFY (Carmona et al., 2008). Depending on the levels and timing of BA1/LAX1 expression, auxin-regulated branching can influence not only the size of the whole inflorescence, but also whether the primordia develops into an inflorescence or a tendril. In addition, given its specific expression at each branch point during differentiation (Gallavotti et al., 2008), BA1/LAX1 can also be the gene that drives differentiation of outer arm development into fruitfulness or tendrillness.

There are multiple pathways that lead to flowering in grapevine, and as such there are many factors that can affect not only the inflorescence primordia, but also the final differentiation of the primordia to affect the size of both the main branch and the outer arm. General flowering genes that are controlled by temperature and daylength, as well as some signalling genes are described

above, but another major factor that can affect flowering is the carbohydrate status of the plant during anlagen development and inflorescence primordia differentiation. The signalling of carbohydrate status during the flowering process is a major focus of this research.

1.1.7 Carbohydrate status of the plant

Carbohydrates formed via photosynthesis are either immediately used by grapevine as sources of energy or further processed into starch for storage (Zapata et al., 2004). In grapevine, starch levels and flowering are closely linked. Meiosis is the trigger for starch reserve accumulation in grapevine, indicating that flowering is a signal for the transition to dormancy (Zapata et al., 2004; Sreekantan et al., 2010). In addition, the amount of carbohydrates, specifically starch, within the grapevine correlates with the number of flowers that develop from a bud during both the current and the following growing season (Jackson, 1991; Lebon et al., 2004; Vasconcelos et al., 2009). Most grapevine starch reserves are stored in the root system (Zapata et al., 2004; Lebon et al., 2008). The levels of grapevine root starch reserves varies depending on variety and climate and is more sensitive to defoliation effects than trunk reserves (Bennett et al., 2005). In 'Pinot Noir', half of the root starch reserves built up from the previous season are lost from budbreak to flowering (Zapata et al., 2004). The root starch reserves are the primary energy source during the second phase of anlagen differentiation in early spring (Greer and Sicard, 2009), and as such have a major impact on the final development of the inflorescence (Lebon et al., 2008).

Limiting starch reserves in grapevine has been studied by numerous researchers using several different methods such as defoliation, girdling, and cropping levels (Hunter et al., 1995; Caspari et al., 1998; Bennett et al., 2005; Heazlewood et al., 2006). When flowering in the following years was examined, carbohydrate limitation led to reduced inflorescence formation and even decreased inflorescence branching (Bennett et al., 2005; Heazlewood et al., 2006), but long term multiyear studies have not yet been reported. The effects of limited starch reserves on flowering has been extensively studied in the field, but few researchers have looked at the effects of carbohydrates on flowering and inflorescence architecture at a molecular level.

The link between carbohydrates and flowering in grapevine indicates that molecular cues from both sugar signalling and flowering pathways must interact with a common messenger. As stated above, members of the trehalose pathway have been shown to have major roles in both carbohydrate signalling and the transition to flowering. In addition, the floral repressor gene TFL1 also has multiple roles in signalling, especially in response to temperature and floral transition cues. Many of the genes described above have only been studied in annual model species such as *Arabidopsis* and

maize. While the functions of these genes cannot be assumed to be the same in perennials, it is a valid starting point to study their role in grapevine. By studying genes that both promote and inhibit inflorescence development in annual model species, it is hoped that the roles of some of these genes in grapevine outer arm development can be elucidated. As carbohydrate status and its role in fruitfulness is an area of much research in the grapevine community, a molecular explanation incorporating both sugar signalling and flowering signalling into a single pathway would be of great value. It is hoped that findings from this research can be used to explain how fruitful outer arms, which have such an impact on the viticulture of red wine cultivars, are formed.

1.2 Preview of research done during this thesis

The following chapters are divided into groups depending on the types of analysis and gene families investigated. The first chapters describe the initial development of this research, such as method development and gene discovery. The following chapters describe the in-depth study of the gene families involved in the trehalose biosynthesis pathway and the BA1/LAX1 gene in grapevine. The final major chapter studies these genes and their correlation with the carbohydrate status of the plant during floral development.

1.2.1 Trehalose pathway genes in grapevine

When this research was initiated in 2009, no work on the trehalose pathway in grapevine was publicly available. To test the role of these genes in grapevine, the trehalose pathway genes first had to be identified. This was done *in silico* using the grapevine 'Pinot noir' sequenced genome (Jaillon et al., 2007) using trehalose pathway genes from Arabidopsis and maize as references. The results of this part of the study are described in Chapter 4. Once the putative grapevine trehalose pathway genes were identified, their functionality had to be tested. To test for functionality, yeast complementation experiments were done on the grapevine genes for both gene families using yeast mutants lacking functional trehalose pathway genes. To characterize the members of the trehalose pathway gene families, expression of the genes from both trehalose biosynthesis gene families was measured in grapevine tissue. This was done by screening the genes across several tissue types in a transcription assay experiment. The results of these experiments are described in Chapter 5.

1.2.2 The BA1/LAX1 gene in grapevine

As section 1.2.1, this hypothesis first began with *in silico* analysis to identify any putative BA1/LAX1 orthologues in grapevine. The results are described in Chapter 4. To test for functionality, a silencing experiment in grapevine was investigated but was not completed due to the length of time

needed for such an experiment in the perennial species. Instead, a transcription assay approach was taken in which expression of this gene was studied in nine different 'Pinot noir' tissue types. The results of these experiments are described in Chapter 6.

1.2.3 Carbohydrate status effect on outer arm development

To test whether the carbohydrate status of the plant contributes to the final structure of the outer arm, a single node cuttings experiment was performed using canes harvested from a pruning trial.

In another experiment, buds from canes of large or small diameter were harvested at different stages and used in a transcription assay experiment to test for differential expression of genes involved in the trehalose pathway, BA1/LAX1, and several flowering pathway genes. The results of these experiments are discussed in Chapter 7.

Chapter 2

Development of yeast expression plasmids for grapevine TPS and TPP complementation study

2.1 Introduction

Trehalose is a non-reducing disaccharide comprised of two glucose molecules joined via one of the several trehalose biosynthesis pathways present in all organisms except vertebrates (Paul, 2007). In plants, trehalose is synthesized by first forming trehalose-6-phosphate (T6P) from the enzymatic activity of TREHALOSE-6-PHOSPHATE SYNTHASE (TPS) on glucose-6-phosphate and UDP-glucose, followed by the dephosphorylation of T6P by TREHALOSE-6-PHOSPHATE PHOSPHATASE (TPP; Müller et al., 1999). The discovery of trehalose pathway genes in Arabidopsis (Blazquez et al., 1998; Vogel et al., 1998) has led to an explosion of research both within this model plant as well as other crop species.

As a result of gene and genome duplications during the evolutionary process (Avonce et al., 2004), plants have multiple copies of many genes which lead to the development of gene families. The trehalose pathway genes are no different- Arabidopsis, rice, maize, poplar, and *Selaginella* are all known to have multiple copies of TPS and TPP genes (Lunn, 2007). In Arabidopsis, there is only one TPS gene with trehalose biosynthesis capability (Vandesteene et al., 2010), whereas all TPP genes are capable of dephosphorylating T6P into trehalose (Vandesteene et al., 2012). Given the possibility of a large number of TPS and TPP genes in any plant species, a rapid screening method was developed for determining enzymatic functionality of the homologues in the model organism Baker's yeast (*Saccharomyces cerevisiae*).

In *S. cerevisiae*, trehalose is synthesized from glucose in a complex involving four enzymes, with TPS1 and TPS2 acting as the catalytic subunits of TPS and TPP respectively, and TREHALOSE SYNTHASE LARGE SUBUNIT1 (TSL1) and TREHALOSE-6-PHOSPHATE SYNTHASE3 (TPS3) having regulatory subunit roles (Bell et al., 1998). Knockout mutations for all subunits were developed by inserting an amino acid marker gene into the open reading frame of each gene to be altered, allowing for selection of mutants on media lacking the amino acids used for the mutation (Bell et al., 1998). The mutant genotypes showed phenotypes distinct from the wild type, making it easy to differentiate mutants from wild type. For example, *tps1Δ:TRP1* cannot synthesize glucose for glycosylation and so cannot grow on media containing this sugar (Blazquez et al., 1998) and *tps2Δ:LEU2* cannot grow at elevated temperatures due to the accumulation to toxic levels of T6P (Devirgilio et al., 1993). These mutant genotypes can be used to test the functionality of TPS and TPP homologues from other species by

transforming the yeast mutants with plasmids containing the homologues to look for recovery of the wild-type phenotype, and has been successfully tested using genes from species such as *Escherichia coli* (bacteria), *Magnaporthe oryzae* (fungus), *Oryza sativa* (monocotyledonous plant), and *Arabidopsis thaliana* (dicotyledonous plant) (Elbein et al., 2003; Li et al., 2008; Vandesteene et al., 2010; Schluepmann et al., 2012; Vandesteene et al., 2012). Yeast complementation studies are relatively quick as they can be completed in less than a week, with the transformation taking a day to perform and recovery of the wild-type phenotype seen within three days. In comparison, a complementation study using *Arabidopsis* mutants takes more than four weeks just to get the plants at the correct developmental stage to perform the transformation.

To test the functionality of the grapevine TPS and TPP homologues, complementation experiments using homologous recombination instead of plasmids was investigated but was abandoned due to the limited information regarding the genotype of the knockout strain and the large size of the oligonucleotides necessary for successful recombination (Wendland, 2003). Instead, focus turned to a plasmid-based complementation experiment. However, most yeast expression plasmids currently available use promoters that are either a toxic copper-inducible promoter or a galactose-inducible promoter to drive transcription of the cloned gene. The copper-inducible promoter requires varying concentrations of copper depending on the yeast genotype used (Romanos et al., 1992). Galactose is often used as the carbon source for growth of the mutant *tps1Δ:TRP1*, so no plasmids using the galactose-inducible promoter could be used to test the capability of grapevine TPS genes to complement the yeast mutant strain. It was also decided that using the yeast endogenous promoters for a complementation study would be more indicative of true complementation rather than using a constitutive promoter delivering high levels of transcriptional activation. Ultimately, it was decided that three different plasmids would be developed: 1) pYexTEF1-containing a constitutive promoter from the yeast transcriptional elongation factor EF1 α that was shown to be stably expressed when used as a plasmid promoter (Partow et al., 2010), 2) pYexTPS1- containing the yeast TPS1 promoter to study grapevine TPS functionality, and 3) pYexTPS2- containing the yeast TPS2 promoter to study grapevine TPP functionality.

2.2 Materials & methods

All enzymes used for this section were from Roche Diagnostics New Zealand Ltd. (NZ) unless otherwise stated. All primers and oligonucleotides used in this research were obtained from IDT (Custom Science, NZ).

2.2.1 Yeast mutant strains pedigree

The *S. cerevisiae* knockout strains used for this research were developed and kindly provided by the Hohmann lab (Bell et al., 1998). The wild type genotype is strain 6.106.-3A in W303-1A background (MAT α leu23/112 ura31 trp11 his311/15 ade21 can1100 GAL SUC2) from which all mutants were generated. The TPS1 mutant (*tps1 Δ :TRP1*) is strain 6.106.-1A (MAT α leu23/112 ura31 trp11 his311/15 ade21 can1100 GAL SUC2 *tps1D::TRP1*). The *tps1 Δ :TRP1* genotype has the auxotrophic marker gene TRYPTOPHAN1 (TRP1) inserted within the open reading frame (ORF) and is unable to synthesize glucose for glycosysis and so cannot grow on media containing this sugar (Blazquez et al., 1998). The TPS2 mutant (*tps2 Δ :LEU2*) is strain 6.106.-8C (MAT α leu23/112 ura31 trp11 his311/15 ade21 can1100 GAL SUC2 *tps2D::LEU2*). The *tps2 Δ :LEU2* genotype has the auxotrophic marker gene LEUCINE2 (LEU2) inserted within the ORF and cannot grow at higher temperatures (above 38°C) due to the accumulation of toxic T6P levels (Devirgilio et al., 1993).

2.2.2 Plasmid construction

Plasmid pedigree

The plasmid backbone used for development of the plasmids developed for this research is pYexBx, a discontinued plasmid from Clontech (Norrie Biotech, NZ). As shown in Figure 2.1(a), pYexBx is a 7.1Kbp plasmid that contains a 2 μ yeast origin of replication site, an ampicillin resistance gene for *E. coli* selection and the auxotrophic marker genes LEUCINE2 (LEU2) and URACIL3 (URA3) for yeast selection. The multiple cloning site contains only 6 restriction sites (SspI, BamHI, PvuII, SalI, PstI, EcoRI) immediately downstream of the copper-inducible promoter CUP1 (Butt et al., 1984), two of which (SspI, PvuII) are also present elsewhere on the plasmid.

Cloning of the promoters into pYexBx

The constitutive transcriptional elongation factor EF1 α (TEF1) promoter used for cloning into pYexBx was selected based on research done by Partow et al. (2010) that showed this promoter to be the most robust of the promoters tested, regardless of the carbon source. As described above, the promoters for ScTPS1 and ScTPS2 were selected as conditional promoters to test the complementation efficiency of the grapevine genes in a biologically relevant context. The promoters to replace CUP1 were PCR amplified from the wild-type yeast strain with HindIII and BamHI restriction sites as indicated in bold using the primers listed in Table 2.1.

Table 2.1 Primers used to amplify *S. cerevisiae* promoters for cloning into pYexBx to develop new plasmids for complementation experiments

Name	Forward Primer	Reverse Primer	Amplicon
TEF1	GACGAAAAGCTTCCTCCTCCAACGGT	CTCGTCGGATCCTTGTAATTAACCTTAGATT	439 bp
TPS1	GAGTACAAGCTTGTTTGTCAAGGGGTGATAG	CTCCTGGGATCCTAAGTCTGTATGTGAGTA	464 bp
TPS2	GACGAAAAGCTTCCTCCTCCAACGGT	CTGATCGGATCCTTCGGCACAGAAATAGT	439 bp

The PCR reaction was done as a “proofreading PCR” in three 50 µL volumes per promoter (Appendix A). The PCR products were gel purified using the Axygen® Axyprep™ DNA Gel Extraction Kit (Raylab, NZ) and 1 µg of the product and the pYexBx plasmid was digested with HindII and BamHI restriction enzymes in an overnight incubation with 1X BOVINE SERUM ALBUMIN (BSA) to increase enzyme stability. The digested plasmid and PCR products were again gel purified using the same kit as above and 50ng of digested plasmid was dephosphorylated using the Roche SHRIMP ALKALINE PHOSPHATASE (SAP) enzyme as per the manufacturer’s instructions. The dephosphorylated plasmid and digested PCR products were then ligated using TaKaRa Mighty Mix (Norrie Biotech, NZ) as per the manufacturer’s instructions using a 3:1 ratio of PCR product: plasmid using the following formula:

$$\frac{(ng \text{ plasmid} * \mu L \text{ plasmid used}) Kbp \text{ insert size}}{Kbp \text{ plasmid size}} * ratio \text{ insert: plasmid} = ng \text{ insert to add}$$

After ligation, 10µL of the reaction mixture was used to transform *E. coli* dH5α using the heat shock method (Sambrook and Russell, 2001) and the transformation mix was plated onto LB plates (Appendix C) containing 100mg/L ampicillin for selection of transformants. Transformed colonies were checked for the presence of the plasmid containing the promoters by PCR using the reagents and cycle described in Appendix A (Colony PCR) with the promoter specific forward primer and a pYexBx specific reverse primer (Appendix B). The PCR product was run on a 1% agarose gel and 3 positive colonies per plasmid were sequenced to ensure correct amplification of the promoter.

Cloning of the multiple cloning site (MCS) into pYexBx

As the pYexBx background had only 4 unique restriction sites in the multiple cloning site, a synthetic MCS was developed for cloning downstream of the promoter on each of the newly developed plasmids. The synthetic MCS was designed to have a total of 9 unique sites (5’ BamHI, SacII, NaeI, SacI, Sall, SmaI, XhoI, XbaI, EcoRI 3’) such that at least two of the restriction sites could be used to clone all of the TPS and TPP family genes to facilitate directional insertion. Two 60-bp oligonucleotides were designed containing the restriction sites listed above and 6 extra nucleotides on each end to allow for enzymatic digestion. The oligonucleotides were re-suspended to a final concentration of 100mM and hybridized by heating to 95°C for 5 minutes then annealed by decreasing the temperature by 1°C for 70 cycles in a Bio Rad iCycler™ thermocycler (Bio Rad

Laboratories Pty Ltd, NZ) as per a hybridization protocol by Hayworth (2009). The annealed primers were gel purified using the Axygen® Axyprep™ DNA Gel Extraction Kit (Raylab, NZ) and digested with BamHI and EcoRI in an overnight reaction as described above. After digestion, the synthetic MCS was cloned into digested pYexTEF1, pYexTPS1, and pYexTPS2 using TaKaRa Mighty Mix (Norrie Biotech, NZ) and transformed into *E.coli* as described above. Transformed colonies were checked for the presence of the plasmid containing the promoters and synthetic MCS by PCR using the reagents and cycle described in Appendix A (Colony PCR) with promoter specific forward primers and a pYexBx specific reverse primer (Appendix B). The PCR product was run on a 1% agarose gel and 3 positive colonies per plasmid were sequenced to ensure correct cloning of the MCS.

Cloning yeast TPS genes into the developed plasmids

To test promoter capability after cloning into the pYexBx backbone, the native yeast TPS genes were cloned into their respective plasmids and used to transform the mutant yeast strains. The *S. cerevisiae* TPS1 and TPS2 genes were PCR amplified (Whole gene PCR; Appendix A) from the wild-type strain listed above with Sall and PstI or NaeI and SmaI restriction sites for ScTPS1 or ScTPS2 respectively as indicated in bold using the primers listed in Table 2.2. The PCR product was purified and digested with the corresponding restriction enzymes as described above. Cloning and *E. coli* transformation were also as described above.

Table 2.2 Primers used to amplify *S. cerevisiae* TPS genes for cloning into pYexTEF1MCS, pYexTPS1MCS, or pYexTPS2MCS to test promoter function in the new plasmids developed for complementation experiments

Gene name	Forward primer	Reverse primer	Amplicon
ScTPS1	ACGGTT GTCGAC ATGACTACGGATAAC	AGTGTT CTGCAGT CAGTTTTTGGTGGC	1488 bp
ScTPS2	AATTAAG CCCGGC ATGACCACCACT	CGTTAA CCCGGGT CAAACCTTT	2691 bp

Yeast transformation

The three plasmids containing the endogenous yeast TPS1 or TPS2 gene as listed in Table 2.2 were transformed into the corresponding *S. cerevisiae* mutant genotype. Two plasmids (pYexTEF1MCS and pYexTPS1MCS) containing the ScTPS1 gene were transformed into the *tps1Δ:TRP1* genotype. The remaining plasmid (pYexTPS2MCS) containing the ScTPS2 gene was transformed into the *tps2Δ:LEU2* genotype. The transformations were performed as per a modified Geitz and Woods (2002) protocol, summarized here. Yeast cultures were inoculated in double strength YPD media (Appendix C) containing 4% galactose (for *tps1Δ:TRP1*) or 4% glucose (for *tps2Δ:LEU2*). The cultures were incubated at 28°C in an Infors HT Ecotron rotary incubator (Total Lab Systems, NZ) overnight at 200 rpm. The next day, the cultures were measured in a Bio Rad SmartSpec™3000 spectrophotometer

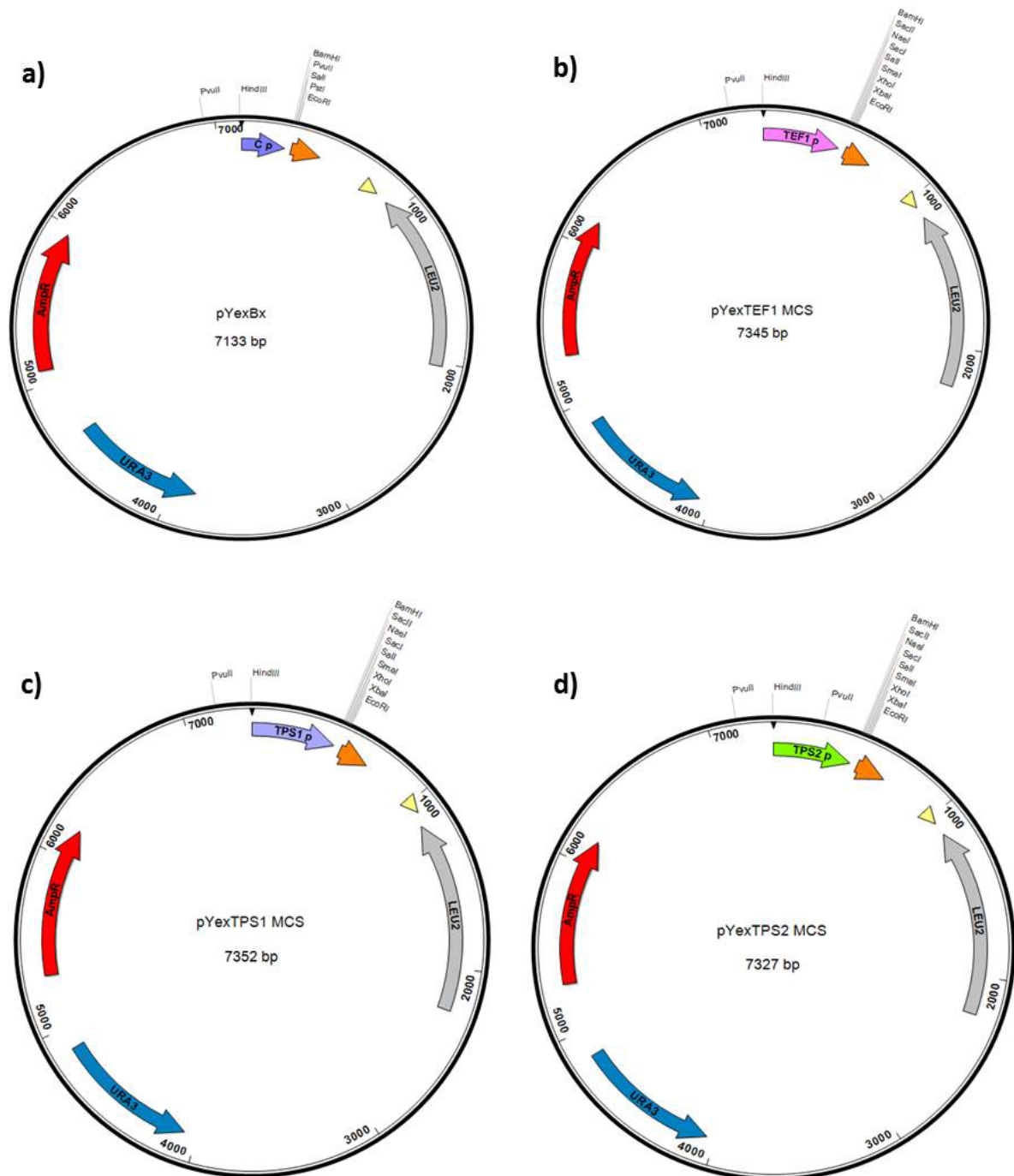
(Bio Rad Laboratories Pty Ltd, NZ) at OD₆₀₀ to determine total cell count. The cultures were then re-inoculated in 50mL fresh double strength YPD (Appendix C) with the corresponding carbohydrate source at a concentration of 5.0×10^8 cells. The culture was again incubated at 28°C in the rotary shaker for 4 hours at 200 rpm. After the second inoculation, the cell culture densities were again measured in the Bio Rad spectrophotometer at OD₆₀₀ to determine total cell count. The cells were then transferred to 50mL disposable tubes and harvested by centrifugation at 3000 x g for 5 minutes, washed in 25 mL sterile water and re-centrifuged 3000 x g for 5 minutes. The cells were then re-suspended in 1 mL sterile water and transferred to 1.7 mL disposable tubes and centrifuged at maximum speed for 30 seconds. The liquid was removed and the cells were diluted to 2×10^7 cells/mL. The cells were aliquoted into individual 1.7 mL disposable tubes to give 10^8 cells (100 µL) and spun down to remove the water. The tubes were then placed on ice for addition of the transformation mix.

The transformation mix consists of 240 µL 50%w/v PEG 3500 (Sigma Aldrich, NZ), 36 µL 1M LiAc (ThermoFischer Scientific NZ, Ltd.), 50 µL 2M denatured herring sperm DNA (Sigma Aldrich, NZ), 2000 ng of plasmid template, and sterile water to a final volume of 360 µL. The transformation mix ingredients were added to each tube individually and thoroughly mixed between each ingredient. The yeast cells were then transformed by heat shock by incubating at 42°C for 40 minutes. After the heat shock, the tubes were centrifuged at maximum speed for 30 seconds and the transformation mix removed from the cells. The transformed yeast was then given a recovery phase before plating by re-suspending in a 1:1 mix of 2M sorbitol (ThermoFischer Scientific NZ, Ltd.) and double strength minimal media lacking uracil (Appendix C) containing the correct carbohydrate source and incubating at room temperature overnight.

The transformed cultures were then plated on minimal media plates lacking uracil (Appendix C) for selection and complete rich and minimal media respectively for controls. The plates were incubated at 28 °C (for ScTPS1) or 38.6 °C (for ScTPS2) for up to 5 days to allow for transformed colony growth. After the colonies grew, four colonies from each transformation were selected to confirm transformation. Transformation confirmation was done by FTA card PCR as described in Appendix A. The primers used for the PCR reaction was specific for the promoter (forward) and the pYexBx plasmid backbone (reverse) as listed in Appendix B. 10 µL of the PCR products were run on a 1% agarose gel containing 2% ethidium bromide and visualized by UV light in a Bio Rad GelDoc apparatus (Bio Rad Laboratories Pty Ltd, NZ). The remaining PCR product (40 µL) was then purified using the Axygen® AxyPrep™ PCR Cleanup kit (Raylab, NZ) as per the manufacturer's protocol and submitted for sequencing to confirm the presence of the yeast TPS1 or TPS2 gene insert.

2.3 Results & discussion

A plasmid-based transformation protocol was selected to test grapevine trehalose biosynthetic candidate genes in yeast. Most of the plasmids currently available for yeast transformation utilize either a copper- or galactose-inducible promoter to drive transcription of the cloned gene. As galactose is used as the carbon source for growth of one of the yeast mutants used in this study and the concentration of copper required to activate the CUP1 promoter varies depending on genotype (Romanos et al., 1992), it was decided that new plasmids should be developed that can be used in all



◀ Figure 2.1 Plasmids developed for yeast transformation.

a) pYexBx plasmid as provided by the manufacturer (CloneTech, Norrie Biotech, NZ). The pYexBx plasmid contains the ampicillin resistance gene (red arrow) for bacterial selection and the leucine (LEU; grey arrow) and uracil (URA; dark blue arrow) auxotrophic marker genes for yeast selection. Gene expression is driven by the copper-inducible CUP1 promoter (light blue arrow) upstream of the multiple cloning site (MCS). Downstream of the MCS is the rest of the CUP1 gene (orange arrow). The yeast 2 μ origin of replication site (yellow triangle) is located just upstream of the URA gene. b) pYexTEF1MCS plasmid developed for this research. The constitutive TEF1 promoter (pink arrow) replaces the CUP1 promoter from pYexBx. A synthetic MCS containing 9 restriction sites were cloned into the original MCS. c) pYexTPS1MCS plasmid developed for this research. The yeast TPS1 promoter (purple arrow) replaces the CUP1 promoter from pYexBx upstream of the synthetic MCS. d) pYexTPS2MCS plasmid developed for this research. The yeast TPS2 promoter (green arrow) replaces the CUP1 promoter from pYexBx upstream of the synthetic MCS.

of the yeast strains to be tested. The yeast TPS1 and TPS2 promoters were selected for cloning into the plasmid, as using the endogenous promoters to test the functionality of the grapevine TPS and TPP genes would be more biologically relevant. A constitutive TEF1 promoter was also selected for cloning into the plasmid based on previous research that found it to be highly robust (Partow et al., 2010). Three plasmids were created using the discontinued commercial pYexBx yeast expression plasmid from CloneTech (Norrie Biotech, NZ) containing the three selected promoters (Fig 2.1). The multiple cloning site (MCS) from the pYexBx backbone was replaced with an expanded MCS that was synthetically produced and cloned into the backbone downstream of the promoters to allow for directional cloning of the large number of genes to be tested (Fig 2.1).

Colony PCR tests and sequencing of the plasmids showed that the three promoters and the MCS were successfully cloned into the pYexBx backbone (Appendix D). The yeast TPS1 and TPS2 promoters were identical matches to the promoter sequence from the yeast S288c reference genotype. The constitutive TEF1 promoter cloned into the pYexBx backbone had one insertion and one deletion of a nucleotide within the promoter when compared to the reference sequence (Appendix D). As this was present in all colonies tested, it was concluded that this is likely due to the different genotypes used to amplify the promoter (W303-1A) and used for the reference sequence (S288c). The MCS cloned into the three plasmids was an identical match to the synthesized reference sequence.

All three plasmids developed as part of this research were tested for promoter function by cloning the yeast trehalose pathway catalytic genes (ScTPS1 and ScTPS2) into the synthetic MCS downstream of the promoter. All three plasmids developed successfully complemented of the yeast *tps* mutants (Figure 2.2), indicating that the promoters are working. As shown in Figure 2.2 (b), the constitutive promoter TEF1 promoter is capable of driving transcription of the yeast TPS1 gene, leading to recovery of the wild-type phenotype when grown on glucose. A similar recovery of the wild-type phenotype is observed in Figure 2.2 (c), in which the endogenous yeast TPS1 promoter is driving

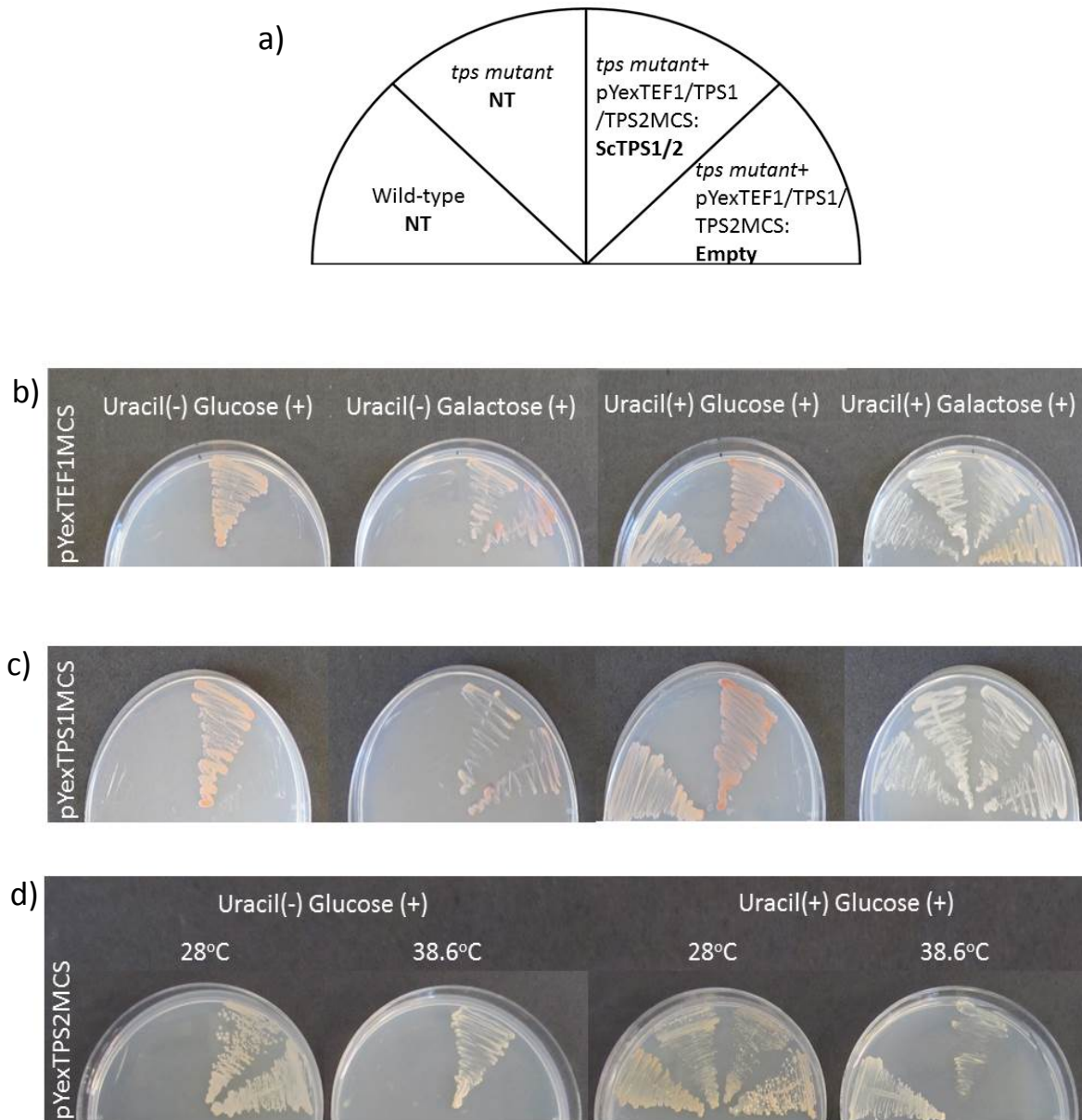


Figure 2.2 *S. cerevisiae* *tps* mutant strains transformed with three different plasmids containing the endogenous yeast *TPS1* or *TPS2* gene to test for promoter function.

a) Diagram showing the layout of the transformed yeast colonies on plates shown in (b-d). NT: Not transformed. b) Transformed *tps1Δ:TRP1* yeast strain grown at 28°C containing the pYexTEF1MCS plasmid that has the constitutive TEF1 promoter driving expression of the yeast *TPS1* gene growing on selection media lacking uracil with glucose or galactose as the carbohydrate source and on minimal media with glucose or galactose as the carbohydrate source. c) Transformed *tps1Δ:TRP1* yeast strain grown at 28°C containing the pYexTPS1MCS plasmid that has the endogenous *TPS1* promoter driving expression of the yeast *TPS1* gene growing on selection media lacking uracil with glucose or galactose as the carbohydrate source and on minimal media with glucose or galactose as the carbohydrate source. d) Transformed *tps2Δ:LEU2* yeast strain grown at 28°C or 38.6°C containing the pYexTPS2MCS plasmid that has the endogenous *TPS2* promoter driving expression of the yeast *TPS2* gene growing on selection media lacking uracil or minimal media containing uracil with glucose as the carbohydrate source.

transcription of the yeast TPS1 gene, allowing for growth of the *tps1Δ:TRP1* genotype on glucose. The yeast TPS2 promoter is also able to drive transcription of the yeast TPS2 gene, allowing for the recovery of the wild-type phenotype in the *tps2Δ:LEU2* genotype when grown at an elevated temperature (Figure 2.2 (d)). To the best of our knowledge, this is the first research to use endogenous promoters to test trehalose biosynthesis capability in yeast complementation experiments.

2.4 Conclusions and future prospects

To test the trehalose biosynthesis capability of the grapevine TPS and TPP genes, a complementation study using yeast trehalose pathway mutants was planned. Originally, the complementation in yeast was going to be done by homologous recombination, but the experiment was abandoned due to the lack of information regarding the location of the insertion used to develop the mutant genotypes. Instead, a plasmid-based complementation approach was designed. The majority of plasmids available for use in yeast utilize a galactose-inducible promoter, which cannot be used in one of the mutant genotypes because galactose is commonly used as is the carbon source necessary for survival of the mutant strain. Other yeast expression plasmids use the copper-inducible CUP1 promoter, which requires varying concentrations of copper to activate the promoter (Romanos et al., 1992). To overcome the challenges of using currently available yeast expression plasmids, three different plasmids were developed from the backbone of a discontinued commercially developed plasmid—one containing a constitutive promoter and two containing the endogenous promoter of the two trehalose biosynthesis catalytic genes. In addition to the promoters, an extended multiple cloning site (MCS) was added to each of the newly developed plasmids to allow for directional cloning of the grapevine trehalose pathway genes. To test the newly developed plasmids, the yeast TPS1 or TPS2 gene was cloned into the plasmids downstream of the promoters and transformed into the yeast *tps1* or *tps2* mutant strains. All three promoters successfully drove transcription of the yeast TPS1 or TPS2 gene, allowing for complementation of the mutant genotype. This indicates that all three promoters are sufficient to use in the testing of the grapevine trehalose biosynthetic pathway genes through complementation of the appropriate yeast *tps* mutant. This is the first experiment to use endogenous promoters to test trehalose biosynthesis genes for function in yeast complementation experiments.

After development and validation of the yeast expression plasmids, the grapevine TPS and TPP genes were cloned into the plasmids and transformed into the yeast mutant strains to test for complementation. The complementation of the yeast strains with the grapevine trehalose biosynthesis pathway genes is described in Chapter 5.

Chapter 3

Development of reference genes to use for transcriptional analysis in grapevine

3.1 Introduction

Quantitative reverse-transcription real time PCR (qRT-PCR) is a highly sensitive assay used to measure levels of gene transcription. The methodologies used in qRT-PCR were first conceptualized in the late 1980's (Wang et al., 1989). Over the past 30 years, qRT-PCR technology has increased in efficiency and sensitivity, allowing for more accurate measurements of transcription level to be carried out over shorter time points. During the development of qRT-PCR, it became apparent that variations in transcription expression measurement were occurring. These variations were a consequence of the assay itself, leading to inaccurate reporting of gene transcription in experiments. As a result of these erroneous reports, a standard for qRT-PCR was developed by several lead researchers in the field (Bustin et al., 2009). These standards, known as the Minimum Information for Publication of Quantitative Real-Time PCR Experiments (MIQE) guidelines, allowed for qRT-PCR experiments to be replicated consistently between laboratories. Therefore, assays that utilize the MIQE guidelines lead to greater confidence in the published results.

Within the MIQE guidelines, the necessity of normalization of the qRT-PCR results to reference genes is discussed. Unfortunately, many researchers still rely on “housekeeping genes” such as ACTIN (ACT) or UBITQUITIN (UBI) for use as reference genes for qRT-PCR normalization (Gutierrez et al., 2008), even though these genes are widely known to have variable expression in certain tissue types (Czechowski et al., 2005). As reagents and equipment utilized in qRT-PCR have become more sensitive and accurate, the reference genes used for gene transcription normalization have largely remained unchanged. In grapevine, the first list of reference genes for use in qRT-PCR was published by Reid et al. (2006) and is still the most popular reference gene source for the species. This paper lists 15 genes screened across nine tissue types. Some of the reference gene primers listed in this publication amplify multiple members of a gene family, which is not ideal for use as a normalization reference for a single gene of interest. In addition, most of the tissue samples screened were from a range of berries at different developmental stages (Reid et al., 2006), which is suitable for berry research but limits the paper's usefulness for assays utilizing other tissue types or developmental stages. Two other grapevine reference gene papers were published recently, identifying candidate reference genes to use for pathogen-related experiments (Gamm et al., 2011; Selim et al., 2012). Besides being specific for pathogen experiments, the major drawback for these grapevine reference

gene publications is the limited number of tissues screened in validating the reference genes. In addition, the amplicon length of many of the genes tested are much larger than the recommended size (75-150 bp) for SYBR-based qRT-PCR amplification in current protocols (Gunstream et al., 2011).

In this research, gene transcription assays were performed on a wide range of grapevine tissue types, with an emphasis on bud developmental stages. With the limited usefulness of the grapevine reference gene publications listed above, it was determined that development of a new suite of candidate reference genes was necessary before any qRT-PCR assays could be performed during the course of this research. Potential reference genes for screening in grapevine were identified from Arabidopsis homologues that were shown to be stably expressed in multiple microarray experiments (Czechowski et al., 2005) that were screened alongside the four reference genes currently used within the research group. The candidate reference genes were screened across 24 'Sauvignon blanc' tissue types and validated with three biological replicates of nine 'Pinot noir' tissue types to confirm stability across multiple samples and different grapevine cultivars. Data from the qRT-PCR assays were analysed using the geNorm Excel applet (Vandesompele et al., 2002) for both datasets described above. geNorm is a powerful tool to identify suitable reference genes due to its ability to handle non-normally distributed data and small data sets, a common occurrence in qRT-PCR assays (Vandesompele et al., 2002). The confirmation population was also analysed by ANOVA as described by Khanlou and Van Bockstaele (2012) to assess whether a simple statistical test is also sufficient in identifying the most stable reference genes across all the tissue types screened.

3.2 Materials & methods

3.2.1 Candidate reference gene identification

Based on results from analysis of Arabidopsis microarray databases (Czechowski et al., 2005) the 10 genes reported as being most stably expressed were selected for screening for use as potential reference genes in grapevine. The grapevine homologues were identified through BLAST (Basic Local Alignment Search Tool) searches (Altschul et al., 1990) performed on the NCBI website (www.ncbi.nlm.nih.gov) of the grapevine reference sequence (Jaillon et al., 2007). In the nucleotide BLAST suite, the reference RNA sequences (refseq_rna) database was selected and the organism was limited to *Vitis vinifera* (taxonomic id: 29760). The BLAST algorithm used was blastn (somewhat similar sequences) for nucleotide sequences (Altschul et al., 1990). Nucleotide sequences with greater than 70% identity were considered as homologues to the Arabidopsis reference genes and the sequences from those genes were used in this study.

3.2.2 Primer design

Primers for the grapevine putative reference gene sequences were developed using the Primer3 Plus program (www.bioinformatics.nl/cgi-bin/primer3plus/primer3plus.cgi/) for both qRT-PCR (Table 3.1) and for cloning a larger gene fragment (Appendix B) into Invitrogen's TOPO-TA cloning system (Invitrogen New Zealand Ltd., NZ) to use for a standard curve during qRT-PCR. The qRT-PCR primers were designed to amplify a 100-150 bp product using the default settings in Primer3Plus except as follows - General Settings: Primer size-Min, 20 Opt, 22 Max 26; Primer Tm: Min 60, Opt 63, Max 65; Advanced Settings: Max Self Complimentarity 5; Max 3' Self Complimentarity 2; Product size-Min, 80; Opt, 100; Max, 150 (Use Product Size Input and Ignore Product Size Range selected). The primers selected by Primer3 Plus were then checked on the reference sequence to see if they flank an intron for genomic DNA (gDNA) contamination control during qRT-PCR. The primers were then checked in the PrimerSelect program within the Lasergene 9 software suite (Burland, 2000) for dimerization and hairpin formation. Once the ideal primers were selected, they were tested for specificity on the NCBI website using the Primer BLAST algorithm against the Refseq mRNA database with the organism limited to *Vitis vinifera*. The cloning primers were designed in Primer3 Plus as described above with the exception of the selected Product size (Min, 200; Opt, 300; Max, 500). The selected cloning primers were quality checked as described above.

3.2.3 Plant material collected for qRT-PCR assays to test potential grapevine reference genes for stability across the samples tested

For the initial grapevine reference gene development, 'Sauvignon blanc' tissue was harvested from 2008-2011 from commercial vineyards in Marlborough, New Zealand. Whole berries collected over eight time points (from 20 days after anthesis to harvest) were collected from the Brancott Estate Booker vineyard during the 2008-2009 growing season (Podolyan et al., 2010). Seed from the final time point was collected independently at the same time as the whole berry sample. Leaf (~225 mm²), tendril (~20 mm), and root tip (~15mm) tissue was collected from shoots harvested from the Brancott Estate during dormancy in 2010 and grown as single node cuttings in the Lincoln University greenhouse in 2011. 'Sauvignon blanc' latent and dormant buds were collected from the Brancott Estate Booker vineyard during the 2010-2011 growing season from the basal (Nodes 1-4), mid (Nodes 5-8), and apical (Nodes 9-12) regions of the shoot. During the dormant period in 2011, shoots were collected from the vineyard and grown out as single node cuttings in the greenhouse at Lincoln University. From these cuttings, budswell and woolly buds were collected. All of the plant material described above was harvested in 2 mL disposable tubes and snap-frozen in liquid nitrogen on site. The frozen tissue was then transferred to -80°C for storage until ready for RNA extraction.

Table 3.1 Grapevine qRT-PCR reference gene primer sequences used to identify the most stably expressed genes in this study.

Gene symbol	Forward primer sequence (5' to 3')	Reverse primer sequence (5' to 3')	Amplicon	Source
ACT	CTTGCATCCCTCAGCACCTT	TCCTGTGGACAATGGATGGA	82 bp	Reid et al., 2006
AP2mu	GTCCCAACTTAAATCCCGTCCTG	CAATCTGGTGGCACA AAAACTGAC	129 bp	This work
EF1α	AAAATAAAGCGGACGATCTAT	GGAAGCCTCCTATCATCAAAA	85 bp	This work
GAPDH¹	TTCTCGTTGAGGGCTATTCCA	CCACAGACTTCATCGGTGACA	70 bp	Reid et al., 2006
HLK	TCATACAGCGAGAAAACACAACAGA	ATGGCACCCGCAGGATAAGT	116 bp	This work
HYP	AATATGCAGAGAAACCCAGACTAAA	AGAGACCCAGGGAACAAACAAT	98 bp	This work
N2227	GAAGATGAGGAGGCGGAAAGAC	TAGTTGAGATATGCGCTGATGATGC	104 bp	This work
PP2A	TGTTGAGCACGCGAATGTTCT	CCAATCCTGCATAACGACTCCA	102 bp	This work
SAND	CAACATCCTTTACCCATTGACAGA	GCATTTGATCCACTTGCAGATAAG	76 bp	Reid et al., 2006
TIP41	CTCGCAAGCGTTCCATTCTCAA	AAAAACCATCTCCGGCAAGTGTG	86 bp	This work
TRU5	CAATGTACGAGCTTTATGACCCATC	CAGTTGATCTTGTTGTTGTTTCCAG	100 bp	This work

¹GAPDH primers amplified multiple homologues in grapevine (Reid et al., 2006)

For grapevine reference gene validation, 'Pinot noir' tissue was harvested from the Lincoln University vineyard during the 2012-13 growing season. 'Pinot noir' clone 113 tissue was collected from nine plants pooled into three biological replicates (n=3). The tissue collected was as follows: latent bud, woolly bud, leaf (~225 mm²), tendril (~50mm), E-L stage 17 inflorescence (Coombe, 1995), post-anthesis flowers, pre-veraison berry (3.7 °Brix at 25.0°C), veraison berry (11.5 °Brix at 21.6 °C), and late veraison berry (16.1 °Brix at 22.1 °C). The tissue was collected in 2mL disposable tubes and snap-frozen in liquid nitrogen on site. The frozen tissue was then transferred to -80°C for storage until ready for RNA extraction.

3.2.4 RNA extraction and cDNA synthesis

The tissue types described above were ground in liquid nitrogen and ~100 mg was aliquoted in 2mL microcentrifuge tubes. Surplus ground material was returned to -80°C for long-term storage. RNA was extracted from each of the samples using the Sigma Spectrum™ Plant Total RNA kit (Sigma-Aldrich, NZ) with the On-Column DNaseI treatment protocol. The extracted RNA was quantified using an Invitrogen Qubit® fluorometer with the Qubit® RNA buffer and dye (Life Technologies, NZ) and calibrated with the supplied standards. RNA quality was checked on a 1.5% denaturing agarose gel (Sambrook and Russell, 2001) and visualized by UV excitation of ethidium bromide on a BioRad GelDoc apparatus (Bio Rad Laboratories Pty Ltd, NZ). Contamination of RNA with proteins or extraction reagents was measured on a Nanodrop™ 1000 spectrophotometer (ThermoFisher Scientific, NZ). Good quality, pure RNA was used to synthesize complementary DNA (cDNA) using the TaKaRa BluePrint™ RT-PCR kit (Norrie Biotech, NZ). 300ng of RNA was used in a 10µL reaction with oligo dTs provided by the manufacturer. The cDNA was synthesized according to the kit's protocol and subsequently diluted 20-fold with sterile water. The synthesized cDNA was checked for amplification and lack of genomic DNA (gDNA) contamination by PCR (cDNA check PCR; Appendix A).

3.2.5 qRT-PCR assays

Reference gene development

qRT-PCR was performed on cDNA synthesized from the 24 'Sauvignon blanc' tissue types tissues described above using TaKaRa SYBR® Premix ExTaq™ II PCR reagents (Norrie Biotech, NZ). The relative expression assays were run on the Illumina Eco™ Real Time PCR System (dnature, NZ) with the tissue types repeated in triplicate spread across 2x 48-well plates. For the assays, a master mix containing the reagents and the qRT-PCR primers (Table 3.1) was made and the cDNA template and master mix was aliquoted into the qRT-PCR plates using an Eppendorf epMotion 5070 liquid handling robot (Eppendorf, NZ) to reduce any pipetting error. In addition to the test samples, each plate contained a plate control sample of woolly bud cDNA amplifying a fragment of the Actin gene with qRT-PCR ACT primers (Table 3.1) repeated in triplicate to normalize any plate variation. For each

assay, linearized plasmid containing the cloned reference gene fragment was used to create a five-point standard curve of 10-fold dilutions, of which the concentrations 1×10^{-2} , 1×10^{-4} , 1×10^{-6} , 1×10^{-7} and 1×10^{-8} (ng/ μ L) were used as both an internal positive control for the assay and to determine the PCR efficiency of the reactions. Molecular biology grade sterile water was used in place of cDNA in the same reaction mix for a non-template control to check for contamination in the assay. Both the standard curve and water samples were repeated in triplicate. The qRT-PCR reaction is described in Appendix A.

Reference gene validation using a different population and variety

As described in the Results & Discussion section below, after the reference genes were found to be stably expressed in the 24 'Sauvignon blanc' tissue types described above, validation of the results was performed by qRT-PCR on cDNA synthesized from three biological replicates of the nine 'Pinot noir' tissue types tissues described above using the same reagents and equipment. In addition to the test samples, each plate contained a plate control sample of woolly bud from replicate 2 cDNA amplifying a fragment of the Actin gene with qRT-PCR ACT primers (Table 3.1) repeated in triplicate to normalize any plate variation. For each assay, a five-point standard curve and non-template control was included as described above. The qRT-PCR reaction is described in Appendix A.

Raw data from the qRT-PCR assays described above were entered into the Illumina EcoStudy 4.0 software for plate normalization. The PCR efficiencies for each assay were entered into the software and the efficiency-adjusted data was exported into Excel for normalization and statistical analysis.

3.2.6 Statistical analysis

Reference gene development

The stability of potential reference genes was determined using the geNorm version 3.4 Excel applet (Vandesompele et al., 2002). First, EcoStudy plate-normalized qRT-PCR quantification cycle (C_q) data was used to determine the Q value, by the delta- C_t method (Vandesompele et al., 2002). The Q value was then uploaded into the geNorm applet to calculate the pairwise stability value of each gene when compared to all other genes (M value), and the recommended number of reference genes to use on this particular sample set (indicated by the CV value). Graphs derived from the geNorm applet were re-drawn using Excel. The entire dataset was analysed first, then by including only the berry tissue types, and finally by including only the bud tissue types. Boxplots of the C_q range for each gene was developed using the GenStat 15 software package (VSN International, Ltd.).

Reference gene validation

The stability of the reference genes screened across the confirmation population of nine 'Pinot noir' tissue types from three biological replicates was determined using the geNorm version 3.4 Excel

applet (Vandesompele et al., 2002) as described above. These samples were analysed as an entire dataset, since there were only nine tissue types. As an alternative method to determine the stability of the reference genes tested, ANOVA of the log₁₀ transformed *Q* values was performed using the GenStat 15 software package (VSN International, Ltd.) and an Excel application developed by McDonald (2009) as per Khanlou and Van Bockstaele (2012).

3.3 Results & discussion

A total of 11 candidate reference genes (Table 3.2) were screened across 24 ‘Sauvignon blanc’ and nine ‘Pinot noir’ tissue types to determine the most stable genes to use for normalization during qRT-PCR. Ten putative reference genes were identified from the Czechowski et al. (2005) publication as being the most stably expressed genes across Arabidopsis microarray datasets. One of the Arabidopsis genes (AT1G59830) was orthologous to multiple genes in grapevine, so was not included. Another Arabidopsis gene (AT5G08290) did not match any grapevine genes within the parameters used for homologue selection as listed in Section 3.2.1, and was also excluded. A third Arabidopsis gene (AT2G28390) was already being used within the research group. This gene encodes a SAND family gene and was previously identified as being stably expressed in grapevine (Reid et al., 2006). This left a total of seven new candidate reference genes identified for possible use in qRT-PCR. The remaining candidate reference genes currently being used within the research group were sourced from Reid et al. (2006). Two of the genes, EF1 α and GAPDH were designed by Reid et al. (2006) to amplify multiple homologues in grapevine. Primers specific to a single EF1 α gene were designed for this research, but primers for amplification of a single GAPDH gene could not be identified.

Initial screening of the 11 candidate reference genes was performed on 24 ‘Sauvignon blanc’ tissue types. The amplification range (Figure 3.1) of the genes varied, with GAPDH having the earliest amplification range (Cycles 10-18) and HLK having the latest amplification range (cycles 23-28). HLK and HYP amplified a sample outside of the 3rd + 1.5 interquartile range (Figure 3.1). These outliers were from a dormant bud sample, and are likely more indicative of the low transcription rate of these genes during dormancy. When developing the geNorm applet, Vandesompele et al. (2002) developed a measurement termed the *M* value that described the stability of a given gene to all other genes being tested. An *M* value below 1.5 is suitable for reference genes in qRT-PCR (Vandesompele et al., 2002). As shown in Figure 3.2(a), all 11 genes are stably expressed in the 24 tissues screened, as indicated by the *M* value being below 1.5 for each of the genes. When all 24 tissue types were analysed, ACT, TRU5, and AP2mu were the three most stable reference genes. When the tissue types were limited to either berries (Figure 3.2 (b)) or buds (Figure 3.2 (c)), the *M*

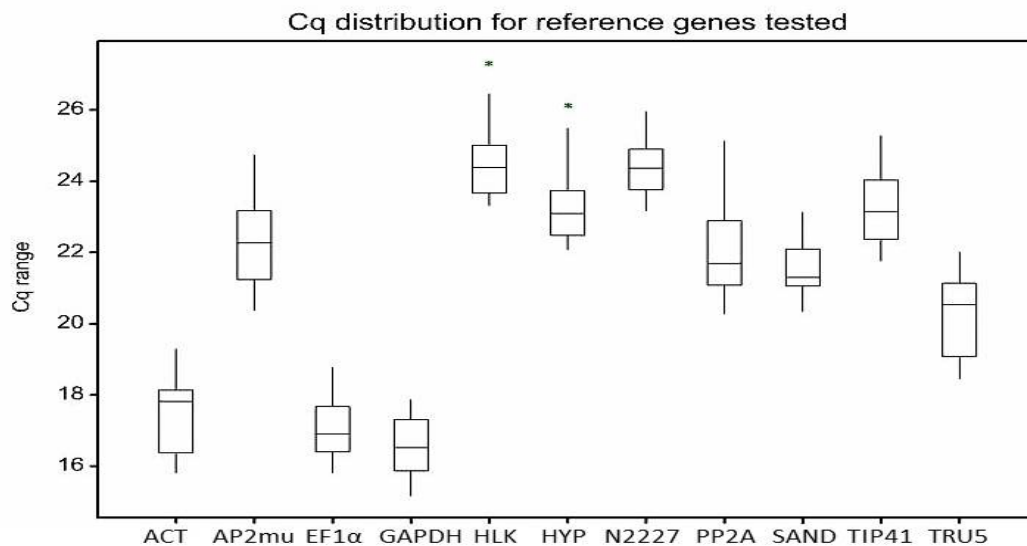


Figure 3.1 Box and whisker plot showing the C_q range of the reference genes tested across 24 'Sauvignon blanc' tissue types.

Reference gene names are as listed in Table 3.1. The box covers the first to third interquartile range, with the median C_q value indicated by the line. Whiskers extend a further 1.5 interquartile range above and below the first and third interquartile range. Outliers are indicated by an asterisk (*).

value decreased to around or below 0.5 for the 11 genes, which is the M value of most commonly used reference genes (Czechowski et al., 2005). In the berries only dataset, AP2mu, PP2A, and TIP41 are the three most stable reference genes (Figure 3.2 (b)). In the buds only dataset, TIP41, TRU5, and AP2mu are the three most stable reference genes (Figure 3.2 (c)). It is worth noting that although all 11 genes were stably expressed in the different datasets, the ranking of most stable to least stable genes was altered (Table 3.3). This highlights the necessity of screening multiple reference genes to identify the best genes to use for each experiment.

In the confirmation population, all 11 reference genes are again stably expressed, with the M values for the genes well below the recommended 1.5 cut-off value (Vandesompele et al., 2002). This indicates that the reference genes are suitable to test in different grapevine varieties, as the genes were stable in both 'Sauvignon blanc' and 'Pinot noir.' For the confirmation population, the geNorm applet found HLK, SAND, and TRU5 to be the three most stable reference genes (Figure 3.3). As an alternative method to identifying stable reference genes, and to confirm the validity of the reference genes ranking as determined by the geNorm applet, an analysis of variance (ANOVA) was carried out using data from the confirmation population of 'Pinot noir' tissue types. As discussed by Khanlou and Van Bockstaele (2012), one of the major drawbacks to geNorm for reference gene stability identification is that genes that have the same expression profile (i.e. involved in the same biological pathway) are ranked as having a low inter-gene variance, regardless of the stability of the gene across all tissues.

Table 3.2 **Reference genes screened for stability in this study.**

Gene symbol	Gene name	Function	Gene database and locus ID		
			Arabidopsis TAIR	Vitis NCBI	Vitis Genoscope
ACT	Actin 1	Cytoskeleton, root hair elongation	AT2G37620	XM_002282480	GSVIVT00034893001
AP2mu	AP-2 complex subunit mu-1	Intracellular protein transport, vesicle mediated transport	AT5G46630	XM_002281261	GSVIVT00015802001
EF1α	Elongation factor 1-alpha	Translation, RNA transport	AT1G07920	XM_002284888	GSVIVT01008382001
GAPDH	Glyceraldehyde-3-phosphate dehydrogenase	Glycolysis, gluconeogenesis	AT1G13440	Multiple	Multiple
HLK	Helicase	Nucleic acid binding	AT1G58050	XM_002263853	GSVIVT01023271001
HYP	Hypothetical protein	Unknown	AT4G33380	XM_002284574	GSVIVT01009523001
N2227	N2227-like domain-containing protein	Nucleotide biosynthesis	AT2G32170	XM_003634568	GSVIVT01026115001
PP2A	Serine/threonine-protein phosphatase 2A	Phosphorylation regulation	AT1G13320	XM_002276144	GSVIVT00017658001
SAND	SAND family protein	Calcium ion transport, zinc ion homeostasis, nematode response	AT2G28390	XM_002285134	GSVIVT01025191001
TIP41	TIP41-like protein	TOR signaling	AT4G34270	XM_002270674	GSVIVT01037896001
TRU5	Thioredoxin-like U5 snRNP	mRNA splicing	AT5G08290	XM_002283586	GSVIVT00020074001

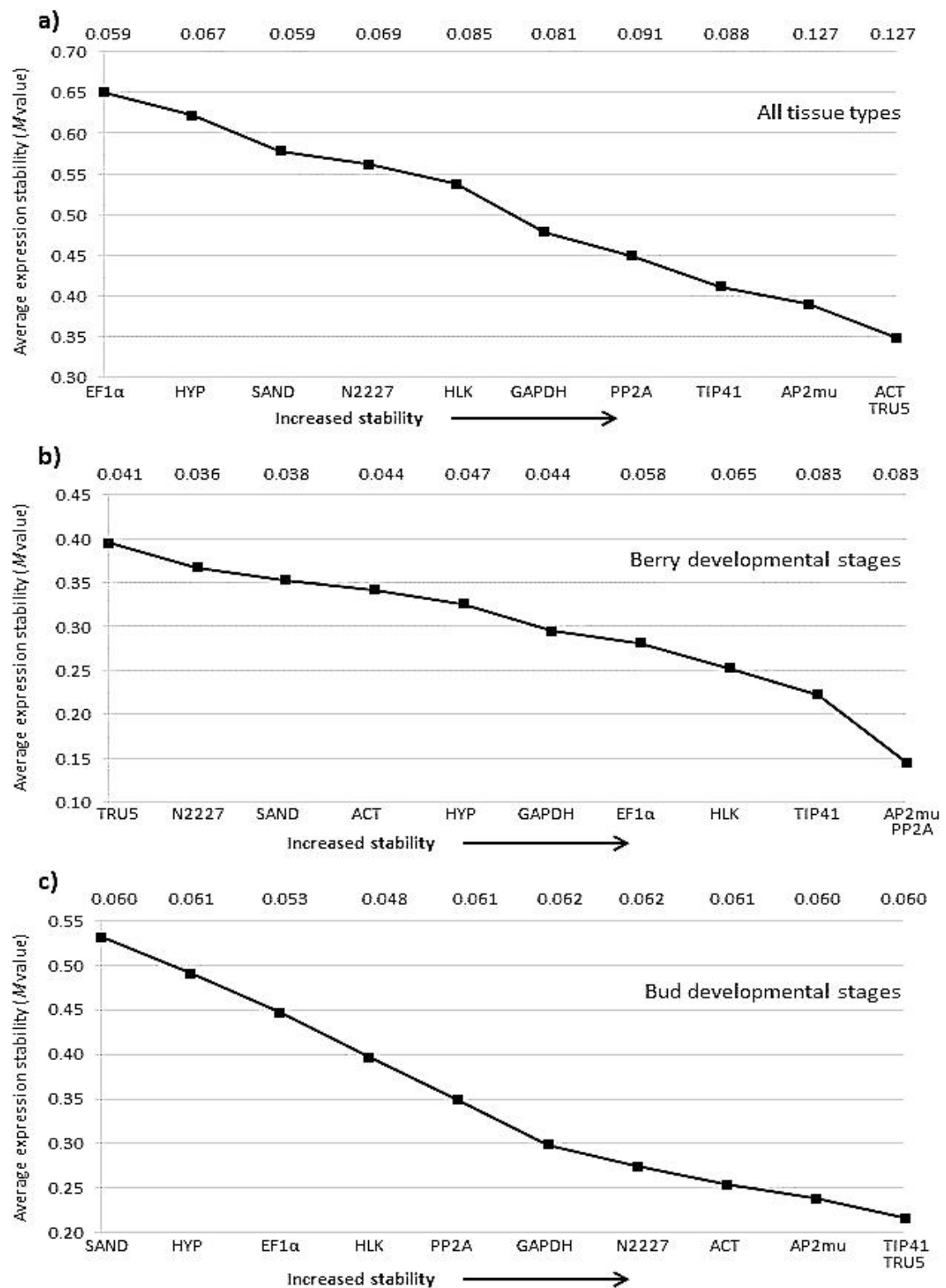


Figure 3.2 Stability of the reference genes tested on 24 ‘Sauvignon blanc’ tissues as determined by geNorm (Vandesompele et al., 2002).

Genes are listed left to right as least stable to most stable, based on the tissues used in the analysis. Values on the y-axis are the range of *M* values determined for each dataset. Values across the top of each chart are the pairwise variation (CV) values determined for each gene pair. a) Stability of the reference genes tested across all tissue types. b) Stability of the reference genes tested across eight berry stages. c) Stability of the reference genes tested across 12 bud tissue types.

Table 3.3 Ranking of reference genes screened for stability in ‘Sauvignon blanc’ tissue based on geNorm analysis (Vandesompele et al., 2002) and the tissue types used in each dataset.

Rank for all samples tested	<i>M</i> value	Rank for berry stages tested	<i>M</i> value	Rank for bud stages tested	<i>M</i> value
1. ACT & TRU5	0.349	1. AP2mu & PP2A	0.145	1. TIP41 & TRU5	0.216
3. AP2mu	0.390	3. TIP41	0.222	3. AP2mu	0.238
4. TIP41	0.411	4. HLK	0.253	4. ACT	0.254
5. PP2A	0.449	5. EF1 α	0.281	5. N2227	0.273
6. GAPDH	0.478	6. GAPDH	0.295	6. GAPDH	0.299
7. HLK	0.538	7. HYP	0.326	7. PP2A	0.349
8. N2227	0.562	8. ACT	0.342	8. HLK	0.397
9. SAND	0.578	9. SAND	0.353	9. EF1 α	0.447
10. HYP	0.622	10. N2227	0.367	10. HYP	0.491
11. EF1 α	0.650	11. TRU5	0.395	11. SAND	0.544

When genes that have the same expression profile are used as reference genes, artificially lowered *M* values are calculated, leading to higher gene rankings. To avoid falsely listing a reference gene as stable due to bias, the authors suggested a novel ANOVA-based method that uses log-transformed *Q* values similar to geNorm (Khanlou and Van Bockstaele, 2012). As shown in Table 3.4 and Appendix F, the ANOVA analysis is a powerful tool that indicates not only the overall stability of the genes, but also the sources of large variance (i.e. different samples). The results of the ANOVA indicate that there is very low within group variance (0.1858-0.4206), as should be expected since the three biological replicates were harvested at the same time from clonally propagated material. The between group variance ranges between 0.5544-2.4101, which again is expected given the wide range of tissue types tested in this study. Based on the stability value computed as per both the geNorm applet (Vandesompele et al., 2002) and Khanlou and Van Bockstaele (2012), the ranking of reference genes from most to least stable is listed in Table 3.5.

Overall, the stability of the reference genes is similar for the two methods tested. This may be due to the varied biological pathways in which the 11 reference genes are involved (Table 3.2). The major exception is HLK, which is listed as one of the two most stable genes by geNorm, but is ranked as the 6th most stable by the ANOVA method. This may be due to similar expression profiles of SAND and HLK in the tissue samples tested, or the two genes may be involved in the same pathway which, to the best of our knowledge, has not yet been identified. It is important to note that the rankings of the stability of the reference genes, regardless of the method used, is dependent on the tissue samples tested and the experiment itself.

Table 3.4 ANOVA testing of candidate reference genes to determine the stability value for each gene from three biological replicates of nine 'Pinot noir' tissue types (Khanlou and Van Bockstaele, 2012).

Gene Symbol	Sum Squares of Variance		F value	Significance	Mean Variance ¹ (-1/ \bar{X})	V _W (SS _W /MV)	V _B (SS _B /MV)	Stability value ² (V _W *V _B)
	Within Group (SS _W)	Between Group (SS _B)						
ACT	0.2334	0.9397	7.6064	0.0002	3.4733	0.0672	0.2706	0.0182
AP2mu	0.2971	0.7714	5.8419	0.0009	2.3362	0.1272	0.3302	0.0420
EF1a	0.2838	1.0237	8.1160	0.0001	2.5801	0.1100	0.3967	0.0436
GAPDH	0.2325	0.7074	6.8460	0.0004	3.8957	0.0597	0.1816	0.0108
HLK	0.4017	0.8021	4.4930	0.0039	3.4336	0.1170	0.2336	0.0273
HYP	0.4206	2.4101	12.8930	0.0000	2.3788	0.1768	1.0132	0.1791
N2227	0.2011	0.5580	6.2440	0.0006	3.0148	0.0667	0.1851	0.0123
PP2A	0.3171	1.0017	7.1080	0.0003	2.5739	0.1232	0.3892	0.0479
SAND	0.1858	0.9512	11.5180	0.0000	4.8766	0.0381	0.1951	0.0074
TIP41	0.3202	0.7307	5.1340	0.0019	2.1244	0.1507	0.3440	0.0519
TRU5	0.2632	0.5544	4.7380	0.0029	3.3696	0.0781	0.1645	0.0129

¹ Mean variance determined by dividing -1 by the average of the log10 transformed Cq values.

² Lower stability values indicate a higher stability for the gene.

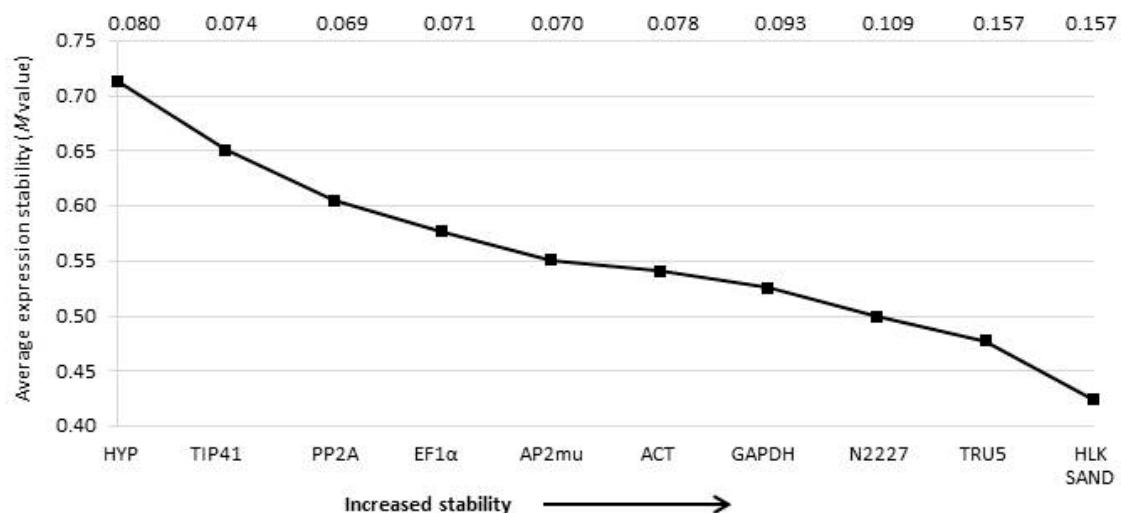


Figure 3.3 Stability of the reference genes tested on three biological replicates of 'Pinot noir' as determined by geNorm (Vandesompele et al., 2002).

Genes are listed left to right as least stable to most stable. Values on the y-axis are the range of *M* values determined for each gene. Values across the top of each chart are the pairwise variation (CV) values determined for each gene pair.

Table 3.5 Ranking of reference genes screened for stability in three biological replicates of 'Pinot noir' based on geNorm (Vandesompele et al., 2002) and ANOVA (Khanlou and Van Bockstaele, 2012) analysis.

geNorm rank	<i>M</i> value	ANOVA rank	Stability index
1. HLK & SAND	0.424	1. SAND	0.007
		2. GAPDH	0.011
3. TRU5	0.478	3. N2227	0.012
4. N2227	0.500	4. TRU5	0.013
5. GAPDH	0.526	5. ACT	0.018
6. ACT	0.542	6. HLK	0.027
7. AP2mu	0.551	7. AP2mu	0.042
8. EF1a	0.577	8. EF1a	0.044
9. PP2A	0.605	9. PP2A	0.048
10. TIP41	0.651	10. TIP41	0.052
11. HYP	0.714	11. HYP	0.179

For this particular experimental set, the three reference genes suggested for use in qRT-PCR assays with primers that amplify a single product are: SAND, TRU5, and N227. These three genes are the most stable across both analysis methods (Table 3.5) and do not amplify multiple genes (unlike GAPDH) or have a notable change in stability ranking across both analysis methods (unlike HLK). Whichever reference gene stability test method is adopted by the researcher, the experimental samples must be tested using multiple reference genes to determine the most stable genes for the experiment.

3.4 Conclusions and future prospects

To measure the amount of gene transcription occurring with the trehalose biosynthesis and VvBA1/LAX1 genes of interest for this research, a series of qRT-PCR experiments was planned. The reference genes previously being used by researchers in the grapevine community were limited in the range of tissues upon which they were tested and lacked the standards currently accepted by many researchers for qRT-PCR experiments. To provide an expanded list of potential reference genes for use in qRT-PCR in grapevine, a new group of possible reference gene candidates was identified from a study of microarray data in the heterologous species *Arabidopsis*, which showed stable expression of several genes suitable for use as reference genes in the species (Czechowski et al., 2005). Ten genes identified from this work as being the most stable across all experiments studied were selected for development as possible reference genes in grapevine. Of those ten genes, seven novel genes were identified and one was currently in use within the research group. The seven novel genes and the four genes already being used as reference genes within the research group were screened on 24 'Sauvignon blanc' tissue types, ranging from root tips to ripe seed. The genes were tested for stability in the geNorm applet for Excel (Vandesompele et al., 2002) and all 11 genes were found to be stably expressed. Although all 11 genes were found to be stable, the stability and ranking of the genes changed when the tissue types were limited to berry samples or bud samples. To confirm the stability of the reference genes and to test the reference genes for stability across a different grapevine variety and with a different analysis tool, the 11 genes were again screened on three biological replicates of nine 'Pinot noir' tissue types, ranging from buds to late veraison berries. The genes were tested for stability in the confirmation population using both the geNorm applet and ANOVA analysis (Khanlou and Van Bockstaele, 2012). Again, all 11 genes were found to be stably expressed within the different tissue types, but the stability and ranking of the genes changed when compared to the results in 'Sauvignon blanc' and type of analysis performed. This highlights the necessity of testing multiple reference genes for stability across every qRT-PCR experiment to determine the optimal genes to use for normalization of the data. It cannot be stressed enough how important the selection of suitable reference genes are for any qRT-PCR experiment before any inferences from the data can be done.

Chapter 4

***In silico* identification of grapevine genes encoding trehalose biosynthetic enzymes and homologues of the transcription factor BARREN STALK1/LAX PANICLE1 (BA1/LAX1)**

4.1 Introduction

There are numerous overlapping pathways involved in inflorescence development in all angiosperms (for review see Chapter 1). Grapevine, a perennial vine, relies on cues such as photoperiod, carbohydrate status, and age to determine not only when to flower but also the size of inflorescences to develop. Much research has already been done on the major floral pathway integrator and meristem identity genes in grapevine (Calonje et al., 2004; Sreekantan and Thomas, 2006; Carmona et al., 2007; Almada et al., 2009), but little work has been done on the numerous pathways upstream of these genes. Based on work done in maize, two pathways of particular interest for this research into outer arm development were the age-dependent pathway, in which the carbohydrate status of the plant regulates floral development (Satoh-Nagasawa et al., 2006; Wahl et al., 2013), and the hormonal pathway, in which competing hormone levels regulate the development and differentiation of inflorescences (Gallavotti et al., 2008; Matsoukas et al., 2012). Two maize mutants led us to focus on the age-dependant and hormone signalling pathways during the course of this research. In maize, the classic *ramosa3* mutant is characterized by increased basal branching in the inflorescence, which was found to be caused by a mutation of a TREHALOSE-6-PHOSPHATE PHOSPHATASE (TPP) gene (Satoh-Nagasawa et al., 2006). As described below, this gene is part of the trehalose biosynthesis pathway, which is involved in signalling the carbohydrate status of the plant, among other roles. The other maize mutant of interest is the *barren stalk1* mutant, which is characterized by a complete lack of inflorescence branching caused by auxin exclusion in the inflorescence primordia during differentiation (Gallavotti et al., 2004).

The trehalose biosynthetic pathway has gained much attention from researchers due to its association with abiotic stress resistance (Muller et al., 1995; Goddijn and van Dun, 1999) and its role in sugar signalling (Thevelein and Hohmann, 1995; Schluepmann et al., 2012). In plants, trehalose is synthesized from glucose-6-phosphate (G6P) and UDP-glucose via TREHALOSE-6-PHOSPHATE SYNTHASE (TPS), forming the intermediate trehalose-6-phosphate (T6P) which is subsequently dephosphorylated by TREHALOSE-6-PHOSPHATE PHOSPHATASE (TPP) to form trehalose (Muller et al., 1995). The discovery of trehalose pathway genes in the model plant species *Arabidopsis* (Blazquez et al., 1998; Vogel et al., 1998) has opened up investigations into homologous trehalose

pathway genes in other plant species. Subsequent research has found multiple genes for each step in the pathway- forming TPS and TPP gene families in all plant species studied (Leyman et al., 2001; Satoh-Nagasawa et al., 2006; Lunn, 2007; Li et al., 2008). Of particular interest to this research is the purported role of trehalose, or its precursor T6P, in inflorescence branching as seen in Arabidopsis mutants (Schluepmann et al., 2003; van Dijken et al., 2004) and quite strikingly in the maize *ramosa3* mutant (Satoh-Nagasawa et al., 2006). By using the already characterized TPS and TPP gene sequences from these species, the grapevine genome can be screened to determine whether these genes are also present, and if so, whether there are multiple genes forming gene families for each step in the trehalose pathway.

The basic helix-loop-helix (bHLH) transcription factor BARREN STALK1/LAX PANICLE1 (BA1/LAX1) is involved in regulating axillary meristems by auxin signalling (Gallavotti et al., 2008) and has also been shown to affect inflorescence architecture and leaf shape (Gallavotti et al., 2011; Woods et al., 2011). The Arabidopsis BA1/LAX1 homologue, REGULATOR OF AXILLARY MERISTEM FORMATION (AtROX) also controls axillary meristem development, however the role of auxin regulation was not investigated (Yang et al., 2012). In both maize and Arabidopsis, BA1/LAX1 was found to be a single copy gene (Woods et al., 2011), although the bHLH transcription factor family is quite large (over 100 genes) in all plant species studied (Carretero-Paulet et al., 2010). During the discovery and characterization of AtROX, the gene was found to be incorrectly annotated in the Arabidopsis reference genome as being part of the APRATAXIN (APT) gene (Woods et al., 2011).

To characterize the trehalose biosynthesis pathway and the BA1/LAX1 homologues in grapevine, the genes first must be identified. The published sequences for the TPS and TPP genes from Arabidopsis were used as a starting point for identifying homologues in grapevine, while the maize BA1 gene initiated the search for a grapevine BA1/LAX1 homologue. The publication of the 'Pinot Noir' grapevine genome sequence (Jaillon et al., 2007) allows for genes from other species to be quickly identified as putative homologues within grapevine. However, the genotype that was sequenced was selfed over several generations, leading to a highly homozygous genome (Jaillon et al., 2007), that likely differs from the commercial varieties. Nonetheless, the reference genome allows for a starting point in screening grapevine for genes of interest for researchers wanting to do reverse genetics studies in this species.

4.2 Materials & methods

4.2.1 Gene identification and annotation

Grapevine TPS and TPP homologue identification

To identify putative TPS or TPP homologues, BLAST (Basic Local Alignment Search Tool) searches were performed on the NCBI website (Altschul et al., 1990). Arabidopsis TPS and TPP nucleotide sequences were first identified using a text search tool on the NCBI Entrez webpage based on the known number of genes per family. From each of the Arabidopsis TPS and TPP genes' webpage, BLAST searches of the nucleotide sequence were performed to identify grapevine homologues for the TPS and TPP genes. In the nucleotide BLAST suite, the reference RNA sequences (refseq_rna) database was selected and the organism was limited to *Vitis vinifera* (taxonomic id: 29760). The BLAST algorithm used was blastn (somewhat similar sequences). Nucleotide sequences with greater than 70% identity were considered as homologues to the Arabidopsis TPS/TPP genes and the sequences from those genes were used in this study.

Grapevine BA1/LAX1 homologue identification

The work by Woods et al. (2011) on BA1/LAX1 expression clearly showed that there was only one homologue in grapevine. However, the locus identifier used in their work was no longer in use on the NCBI or the Genoscope Grape Genome Browser database (www.genoscope.cns.fr). The grapevine BA1/LAX1 sequence was kindly provided by the BA1/LAX1 researchers (Woods et al., 2011), which was saved as a file in the SeqBuilder program from the Lasergene 8 software suite (Burland, 2000). The sequence was confirmed as the only homologue in grapevine by using the supplied sequence as a reference to BLAST the NCBI database as described above.

4.2.2 Phylogenetic tree development

Multiple alignments and phylogenetic trees of the TPS, TPP, and BA1/LAX1 gene families were generated using the software program MEGA version 5 (Tamura et al., 2011). For the TPS and TPP gene families, protein sequences from *Arabidopsis thaliana*, *Escherichia coli*, *Saccharomyces cerevisiae*, *Solanum lycopersicum*, *Vitis vinifera* and *Zea mays* (TPP genes only) were collected from the NCBI database. Protein sequences from *Oryza sativa*, *Populus trichocarpa*, *Selaginella moellendorffii*, and *Zea mays* (TPS genes only) were obtained from Lunn's (2007) supplementary material. Sequences from the species listed above were used in the alignment of the gene families and development of the TPS and TPP phylogenetic trees. The BA1/LAX1 gene family was aligned and a phylogenetic tree was generated using the grapevine BA1/LAX1 protein sequence provided by Woods et al. (2011) as well as *Arabidopsis thaliana*, *Medicago truncatula*, *Oryza sativa*, *Populus trichocarpa*, and *Zea mays* homologues collected from the NCBI database. For phylogenetic tree construction, the protein sequences for each gene family were first uploaded into the MEGA

software and aligned using the MUSCLE algorithm (Edgar, 2004). After alignment, the characteristic domain of each gene family was selected from each sequence and used for developing the trees. Once the domains were selected, pairwise distances for each sequence were calculated using the default parameters to check for outliers. The outliers were removed from analysis before continuing to the tree. Phylogenetic trees for the gene families were drawn using the maximum likelihood method based on the JTT-matrix model (Jones et al., 1992). Consensus trees were developed using a bootstrapping method with 1000 replicates (Felsenstein, 1985). Branches of the consensus tree with replicate values less than 50% were collapsed into the neighbouring branch. The resulting trees were then copied into a Word document and formatted for ease of viewing.

4.2.3 Karyotype development

The chromosomal locations of the VvTPS and VvTPP gene families were written in the BED data file format using only the 3 required columns (chromosome number, start position, stop position) in Notepad and uploaded into the Ensembl Plants *Vitis vinifera* karyotype website (plants.ensembl.org/Vitis_vinifera/Location/Genome). The output from the Ensembl website was then copied into PowerPoint and formatted for ease of viewing.

4.3 Results & discussion

4.3.1 Grapevine trehalose pathway genes

As shown in Table 4.1, seven TPS and seven TPP genes were identified in grapevine. The seven TPS genes are located on six of the 19 chromosomes in grapevine (Figure 4.1), with chromosome 1 containing VvTPS2 and VvTPS5. The seven TPP genes are located on five of the grapevine chromosomes (Figure 4.1). Two chromosomes have multiple VvTPP genes –chromosome 2 has VvTPPC and VvTPPG while VvTPPA and VvTPPF are located on chromosome 16. One of the grapevine TPP genes, VvTPPG is unique to this work. The number of genes for each gene family is similar to the number of genes found in other species in which the trehalose biosynthesis pathway was studied (Lunn, 2007). In other species, there appears to be a nearly equal number of genes for each gene family with the number of genes per family ranging from 6-8 homologues (Lunn, 2007), except in Arabidopsis where there are 10 TPS and 11 TPP homologues, respectively (Li et al., 2008).

Grapevine TPS gene family

In plants, the TPS gene family is divided into two classes (Leyman et al., 2001). Class I TPS genes are characterized by an N-terminal extension of about 30 amino acids upstream of the glycosyltransferase-like domain responsible for T6P synthesis (Lunn, 2007). As shown in Figure 4.2, the glycosyltransferase-like domain in the TPS gene family contains the conserved residues of Arg9, Trp40, Tyr76, Trp85 for glucose-6-phosphate binding and Gly22, Asp130, His154, Arg262,

Asp361, Glu369 for UDP-glucose binding (Avonce et al., 2004). To date, only one Class I TPS gene from all species studied has been shown to be active in trehalose biosynthesis, and only *Arabidopsis* is known to have multiple orthologues in this class of TPS genes (Vandesteene et al., 2010; Zang et al., 2011). Class II TPS genes (Appendix D) also contain the glycosyltransferase-like domain, lack the N-terminal extension, and have a C-terminal extension containing a L-2-haloacid dehalogenase (HAD) domain that is characteristic of the TPP gene family (Lunn, 2007). In Class II TPS genes, neither the glycosyltransferase nor the HAD domain is biosynthetically active (Vogel et al., 2001; Ramon et al., 2009). Class II TPS genes are not involved in trehalose biosynthesis and their role is not yet known in plants (Vandesteene et al., 2010). In grapevine, only one TPS gene (VvTPS1) clusters with Class I TPS genes from other species (Figure 4.3). The remaining grapevine TPS genes (VvTPS2-VvTPS7) cluster with Class II TPS genes from the other plant species tested (Figure 4.3). The results of the TPS gene family phylogenetic tree indicate that of the 7 grapevine TPS genes, there is one Class I TPS gene (VvTPS1) that may be biosynthetically active and the remaining 6 grapevine TPS genes (VvTPS2-VvTPS7) belong to the Class II TPS gene family whose function is not yet known.

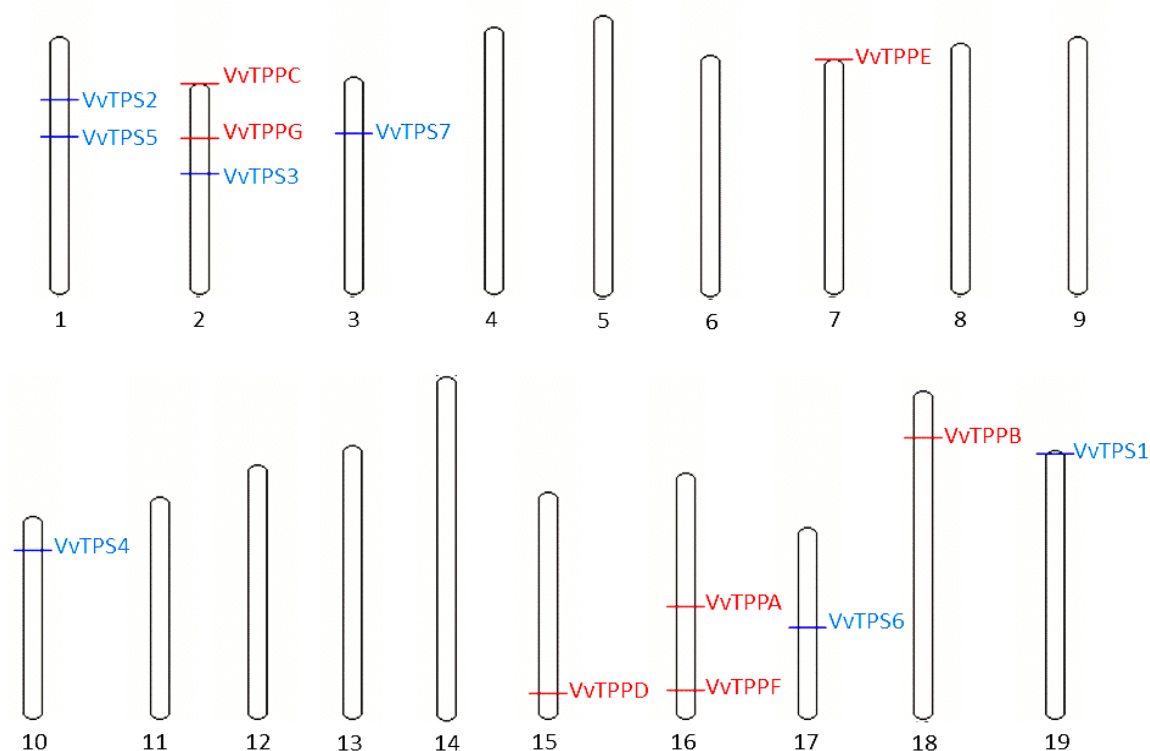


Figure 4.1 Grapevine karyotype showing the locations of the VvTPS and VvTPP genes.

Karyotype was generated on the Ensembl website using the sequence locations for each gene collected from the NCBI database as described in Section 4.2.1. The TPS family genes are in blue while the TPP family genes are in red.

Table 4.1 Grapevine trehalose pathway genes

Name ¹	Chromosome	Nucleotide			Protein	
		Accession number	Length	Exon number	Accession number	Length
TREHALOSE-6-PHOSPHATE SYNTHASE (TPS)						
VvTPS1	19	XM_002285596	2784 bp	17	XP_002285632	927 aa
VvTPS2	1	XM_002284936	2565 bp	3	XP_002284972	865 aa
VvTPS3	2	XM_002277467	2604 bp ²	3	XP_002277503	868 aa ²
VvTPS4	10	XM_002268138	2566 bp	3	XP_002268174	853 aa
VvTPS5	1	XM_002264837	2583 bp	4	XP_002264873	860 aa
VvTPS6	17	XM_002283179	2589 bp	3	XP_002283215	862 aa
VvTPS7	3	XM_002281350	2122 bp	1	XP_002281386	705 aa
TREHALOSE-6-PHOSPHATE PHOSPHATASE (TPP)						
VvTPPA	16	XM_002265643	1158 bp	12	XP_002265679	373 aa
VvTPPB	18	XM_002284165	1128 bp	11	XP_002284201	375 aa
VvTPPC	2	XM_002264435	1182 bp	11	XP_002264471	393 aa
VvTPPD	15	XM_002277126	948 bp	9	XP_002277162	315 aa
VvTPPE	7	XM_002263042	1098 bp	11	XP_002263078	365 aa
VvTPPF	16	XM_002267971	1242 bp	11	XP_002268007	413 aa
VvTPPG	2	XM_003631399	1182 bp	11	XP_003631447	393 aa

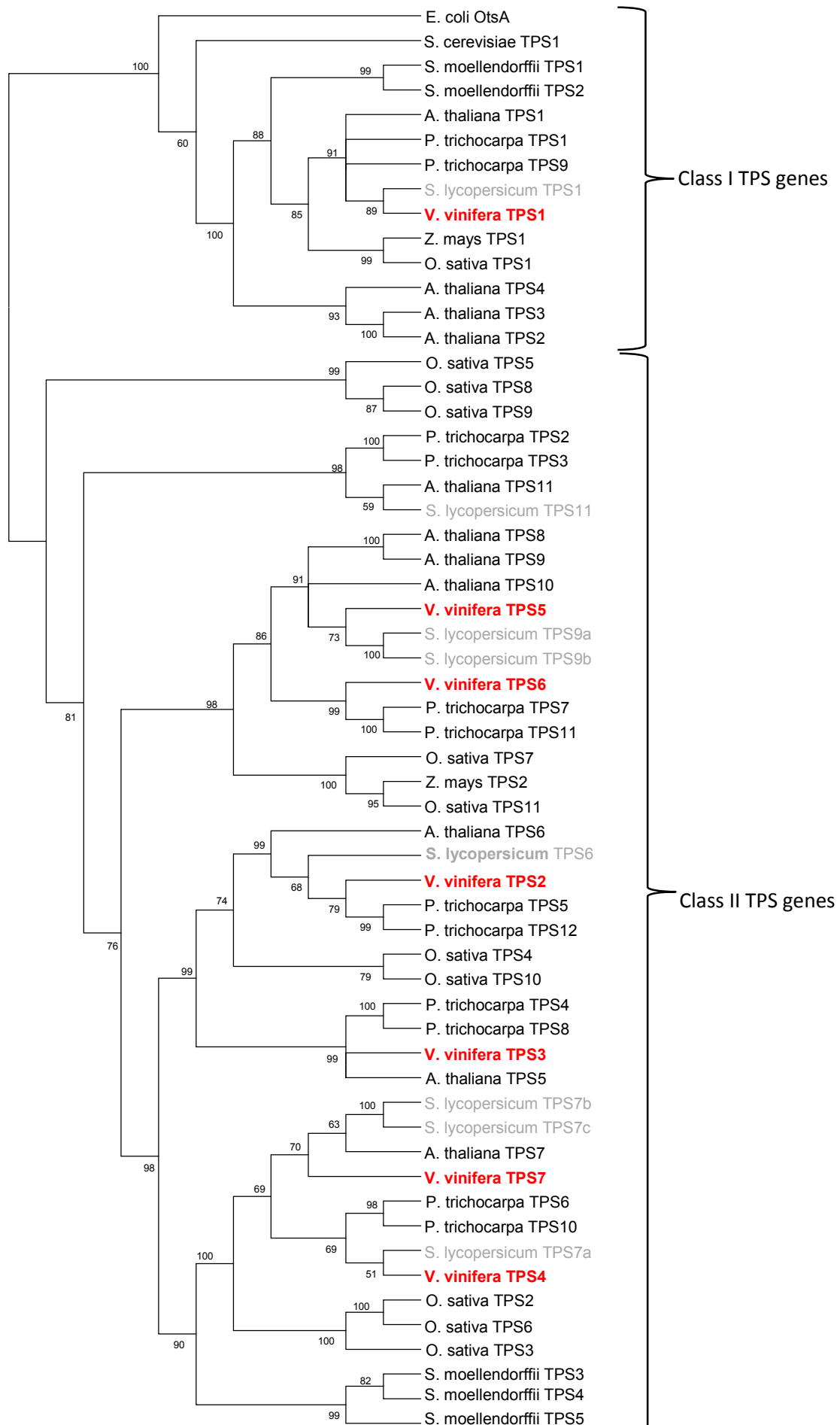
¹ Gene names are as published by Fernandez et al. (2012) with the exception of VvTPPG, which is original to this work.

² The length of VvTPS3 differs from the NCBI database due to an additional 81bp found in all samples tested while screening the gene with RT-PCR.

EcOtsA	M	S	R	L	V	V	V	S	N	R	I	A	P	-	-	-	-	-	-	-	P	D	E	H	A	A	S	A	G	G	L	A	V	G	I	L	G	A	L	K	A	A	G	G	L	W	F	G				
ScTPS1	-	-	-	I	I	V	V	S	N	R	L	P	V	T	-	I	T	K	N	S	S	T	G	Q	Y	E	Y	A	M	S	S	G	G	L	V	T	A	L	E	G	A	L	K	K	T	Y	T	F	K	W	F	G
SmTPS1	K	Q	R	L	L	V	V	A	N	R	L	P	V	S	A	T	R	R	K	G	D	T	-	Q	W	S	L	E	V	S	A	G	G	L	V	S	A	L	L	G	V	K	Q	-	F	Q	V	I	W	I	G	
AtTPS1	R	Q	R	L	L	V	V	A	N	R	L	P	V	S	A	V	R	R	G	G	E	D	-	S	W	S	L	E	I	S	A	G	G	L	V	S	A	L	L	G	V	K	E	-	F	E	A	R	W	I	G	
VvTPS1	R	Q	R	L	L	V	V	A	N	R	L	P	V	S	A	I	R	R	G	E	E	-	S	W	S	L	E	I	S	A	G	G	L	V	S	A	L	L	G	V	K	E	-	F	E	A	R	W	I	G		
EcOtsA	W	S	G	E	T	G	N	E	D	Q	P	L	K	K	V	K	K	-	-	G	N	I	T	W	A	S	F	N	L	S	E	Q	D	L	D	E	Y	Y	N	Q	F	S	N	A	V	L	W	P	A	F		
ScTPS1	W	P	G	L	E	I	P	D	D	E	K	D	Q	V	R	K	D	L	L	E	K	F	N	A	V	P	I	F	L	S	D	E	I	A	D	L	H	Y	N	G	F	S	N	S	I	L	W	P	L	F		
SmTPS1	W	P	G	V	Y	V	Q	D	D	V	G	R	Q	S	L	A	Q	A	L	E	E	K	G	F	V	G	V	L	L	D	E	A	T	V	D	Q	Y	Y	N	G	Y	C	N	N	V	L	W	P	L	F		
AtTPS1	W	A	G	V	N	V	P	D	E	V	G	Q	K	A	L	S	K	A	L	A	E	K	R	C	I	P	V	F	L	D	E	E	I	V	H	Q	Y	Y	N	G	Y	C	N	N	I	L	W	P	L	F		
VvTPS1	W	A	G	V	N	V	P	D	E	A	G	Q	R	A	L	T	K	A	L	A	E	K	M	C	I	P	V	F	L	D	E	D	I	V	H	Q	Y	Y	N	G	Y	C	N	N	I	L	W	P	L	F		
EcOtsA	H	Y	-	-	-	-	-	-	R	L	D	L	V	Q	F	Q	R	P	A	W	D	G	Y	L	R	V	N	A	L	L	A	D	K	L	L	P	L	L	Q	D	D	D	I	I	W	I	H	D	D	D		
ScTPS1	H	Y	-	-	-	-	-	-	H	P	G	E	I	N	F	D	E	N	A	W	L	A	Y	N	E	A	N	Q	T	F	T	N	E	I	A	K	T	M	N	H	N	D	L	I	W	V	H	D	D	D		
SmTPS1	H	Y	I	G	L	R	Q	E	D	R	L	A	A	T	R	S	L	Q	S	Q	F	N	A	Y	K	R	A	N	Q	L	F	A	D	A	V	I	K	N	Y	Q	E	G	D	F	V	W	C	H	D	D		
AtTPS1	H	Y	L	G	L	P	Q	E	D	R	L	A	T	T	R	S	F	Q	S	Q	F	A	A	Y	K	K	A	N	Q	M	F	A	D	V	V	N	E	H	Y	E	E	G	D	V	V	W	C	H	D	D		
VvTPS1	H	Y	L	G	L	P	Q	E	D	R	L	A	T	T	R	S	F	Q	S	Q	F	A	A	Y	K	K	A	N	Q	M	F	A	D	V	V	N	K	H	Y	E	E	G	D	V	V	W	C	H	D	D		
EcOtsA	H	L	L	P	F	A	H	E	L	R	-	-	-	-	-	K	R	G	V	N	N	R	I	G	F	F	L	H	I	P	F	P	T	P	E	I	F	N	A	L	P	T	Y	D	T	L	L	E	Q	L		
ScTPS1	H	L	M	V	L	P	S	Y	L	K	-	-	-	-	-	E	Y	N	S	H	M	K	V	G	W	F	L	H	T	P	F	P	S	S	E	I	Y	R	T	L	P	L	R	A	E	L	L	Q	G	V		
SmTPS1	H	L	M	V	L	P	S	Y	L	K	-	-	-	-	-	E	Y	N	S	H	M	K	V	G	W	F	L	H	T	P	F	P	S	S	E	I	Y	R	T	L	P	L	R	A	E	L	L	Q	G	V		
AtTPS1	H	L	M	F	L	P	K	C	L	K	-	-	-	-	-	E	Y	N	S	K	M	K	V	G	W	F	L	H	T	P	F	P	S	S	E	I	H	R	T	L	P	S	R	S	E	L	L	R	S	V		
VvTPS1	H	L	M	F	L	P	K	C	L	K	-	-	-	-	-	K	Y	N	S	E	M	K	V	G	W	F	L	H	T	P	F	P	S	S	E	I	H	R	T	L	P	S	R	S	E	L	L	H	S	V		
EcOtsA	C	D	Y	D	L	L	G	F	Q	T	E	N	D	R	L	A	F	L	D	C	L	S	N	L	T	R	V	T	T	R	S	A	K	S	H	T	A	W	G	K	A	F	R	T	E	V	Y	P	I	G		
ScTPS1	L	S	C	D	L	V	G	F	H	T	Y	D	Y	A	R	H	F	L	S	S	V	Q	R	V	L	N	V	N	T	L	P	N	G	V	E	Y	Q	-	G	R	F	V	N	V	G	A	F	P	I	G		
SmTPS1	L	A	A	D	L	V	G	F	H	T	Y	D	Y	A	R	H	F	V	S	A	C	T	R	I	L	G	L	E	G	T	P	E	G	V	E	D	Q	-	G	K	I	T	R	V	A	A	F	P	I	G		
AtTPS1	L	A	A	D	L	V	G	F	H	T	Y	D	Y	A	R	H	F	V	S	A	C	T	R	I	L	G	L	E	G	T	P	E	G	V	E	D	Q	-	G	R	L	T	R	V	A	A	F	P	I	G		
VvTPS1	L	A	A	D	L	V	G	F	H	T	Y	D	Y	A	R	H	F	V	S	A	C	T	R	I	L	G	L	E	G	T	P	E	G	V	E	D	Q	-	G	R	L	T	R	V	A	A	F	P	I	G		
EcOtsA	I	E	P	K	E	I	A	K	Q	A	A	G	P	-	L	P	P	K	L	A	Q	L	K	A	E	L	K	N	V	Q	N	I	F	S	V	E	R	L	D	Y	S	K	G	L	P	E	R	F	L	A		
ScTPS1	I	D	V	D	K	F	T	D	G	L	K	K	E	S	V	Q	K	R	I	Q	Q	L	K	E	T	F	K	G	C	K	I	I	V	G	V	D	R	L	D	Y	I	K	G	V	P	Q	K	L	H	A		
SmTPS1	I	D	S	E	R	F	T	H	A	V	E	T	E	A	V	K	Q	H	I	Q	E	L	S	A	R	F	A	G	R	K	V	M	L	G	V	D	R	L	D	M	I	K	G	I	P	Q	K	L	L	A		
AtTPS1	I	D	S	D	R	F	I	R	A	L	E	V	P	E	V	I	Q	H	M	K	E	L	K	E	R	F	A	G	R	K	V	M	L	G	V	D	R	L	D	M	I	K	G	I	P	Q	K	I	L	A		
VvTPS1	I	D	S	H	R	F	I	R	A	L	D	A	P	Q	V	Q	D	R	I	N	E	L	K	R	T	F	T	G	R	K	V	M	L	G	V	D	R	L	D	M	I	K	G	I	P	Q	K	I	L	A		
EcOtsA	Y	E	A	L	L	E	K	Y	P	Q	H	H	G	K	I	R	Y	T	Q	I	A	P	T	S	R	G	D	V	Q	A	Y	Q	D	I	R	H	Q	L	E	N	E	A	G	R	I	N	G	K	Y	G		
ScTPS1	M	E	V	F	L	N	E	H	P	E	W	R	G	K	V	V	L	V	Q	V	A	V	P	S	R	G	D	V	E	E	Y	Q	Y	L	R	S	V	V	N	E	L	V	G	R	I	N	G	Q	F	G		
SmTPS1	F	E	K	F	L	E	E	N	P	E	W	R	D	K	V	I	L	V	Q	I	A	V	P	T	R	T	D	V	L	E	Y	Q	K	L	A	S	Q	V	H	E	I	V	G	R	I	N	G	R	Y	G		
AtTPS1	F	E	K	F	L	E	E	N	A	N	W	R	D	K	V	V	L	L	Q	I	A	V	P	T	R	T	D	V	P	E	Y	Q	K	L	T	S	Q	V	H	E	I	V	G	R	I	N	G	R	F	G		
VvTPS1	F	E	K	F	L	E	E	N	S	E	W	Q	Q	K	V	V	L	L	Q	I	A	V	P	T	R	T	D	V	P	E	Y	Q	K	L	T	S	Q	V	H	E	I	V	G	R	I	N	G	R	F	G		
EcOtsA	Q	L	G	W	T	P	L	Y	Y	L	N	Q	H	F	D	R	K	L	L	M	K	I	F	R	Y	S	D	V	G	L	V	T	P	L	R	D	G	M	N	L	V	A	K	E	Y	V	A	A	Q	D		
ScTPS1	T	V	E	F	V	P	I	H	F	M	H	K	S	I	P	F	E	E	L	I	S	L	Y	A	V	S	D	V	C	L	V	T	S	L	R	D	G	M	N	L	V	S	Y	E	F	V	A	C	Q	E		
SmTPS1	S	L	T	T	V	P	I	H	H	L	D	R	S	M	K	F	P	E	L	C	A	L	Y	A	I	T	D	V	L	L	V	T	S	L	R	D	G	M	N	L	V	S	Y	E	F	V	A	C	Q	N		
AtTPS1	T	L	T	A	V	P	I	H	H	L	D	R	S	L	D	F	H	A	L	C	A	L	Y	A	V	T	D	V	A	L	V	T	S	L	R	D	G	M	N	L	V	S	Y	E	F	V	A	C	Q	E		
VvTPS1	T	L	T	A	V	P	I	H	H	L	D	R	S	L	D	F	Y	A	L	C	A	L	Y	A	V	T	D	V	A	L	V	T	S	L	R	D	G	M	N	L	V	S	Y	E	F	V	A	C	Q	E		

Figure 4.2 Sequence alignment of the glycosyltransferase region of Class I TPS genes.

Sequences used for alignment of the glycosyltransferase region of Class I TPS genes were retrieved from sources as described in Section 4.2.2. Sequences were aligned in the MEGA software (Tamura et al., 2011) using the MUSCLE alignment algorithm (Edgar, 2004) as described in Section 4.2.2. Conserved residues for glucose-6-phosphate binding are highlighted in yellow. Conserved regions for UDP-glucose binding are highlighted in blue.



◀ Figure 4.3 Phylogenetic tree of TPS genes.

The phylogenetic tree was drawn using a bootstrapped maximum likelihood method. Numbers indicate percentage of bootstraps in which the genes within the branches clustered together (1000 replicates). Branches with less than 50% likelihood difference are collapsed. Grapevine TPS genes are in red. TPS genes from previously uncharacterised species used in this analysis are in grey.

Grapevine TPP gene family

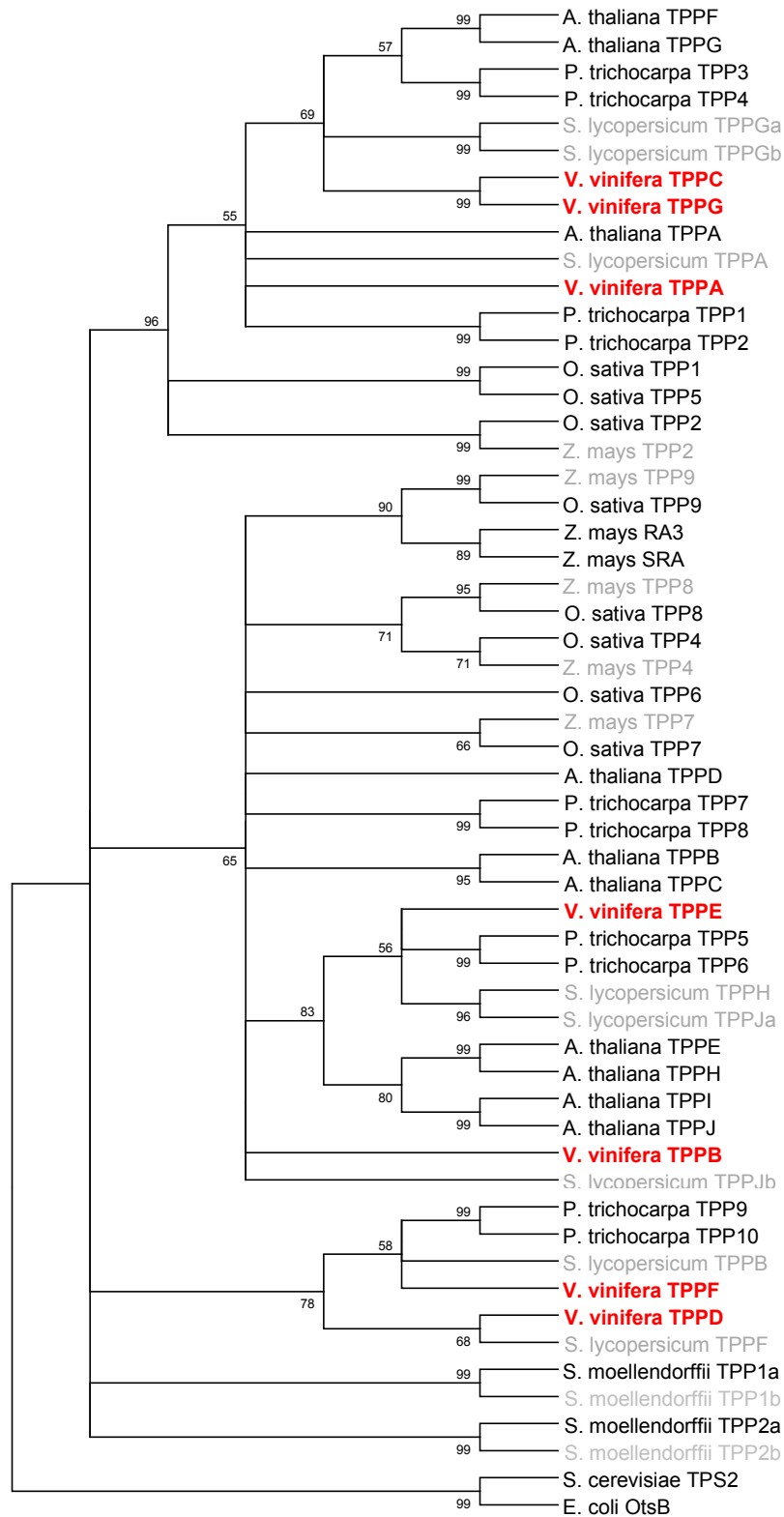
The TPP gene family is characterized by having biosynthetically active HAD domains. As shown in Figure 4.4, HAD domains have 3 conserved motifs-motif I consists of DXDX(T/Y), motif II is a hydrophobic Ser/Thr, and motif III is KX₁₈₋₃₀(G/S)(D/S)X₃(D/N) (Avonce et al., 2004). In Arabidopsis, all TPP genes have been shown to be biosynthetically active, with highly specific expression patterns (Vandesteene et al., 2012). AtTPPB is believed to be the only Arabidopsis gene involved in trehalose biosynthesis, with the other TPP genes predicted to be involved in various processes from pathogen response to metabolite synthesis (Li et al., 2008; Nunes et al., 2013). As seen in Figure 4.5, the 7 grapevine TPP genes tend to cluster with other TPP homologues in 3 groups. VvTPPC and VvTPPG cluster with other genes that appear to have remained highly similar over evolutionary time, as observed by the high frequency of association amongst the branches of tomato TPPG (a and b), Arabidopsis TPPF/G and poplar TPP3/4 groups. This observation is supported by VvTPPC and VvTPPG having a highly similar sequence, as shown in Figure 4.4. VvTPPB and VvTPPE cluster with TPP genes that make up the majority of the group. This group contains 7 of the Arabidopsis TPP genes (including the trehalose biosynthesis gene AtTPPB) and all but one of the maize TPP genes (Figure 4.5). Included in this group is the ZmRA3 gene, whose mutation causes the *ramosa3* phenotype in maize, characterized by increased branching in inflorescences and is of interest to this work. VvTPPA clusters with the remaining maize TPP gene and is highly similar to the tomato TPPA and Arabidopsis TPPA homologues. VvTPPD and VvTPPF group with tomato TPPF and TPPB and the poplar genes TPP9 and TPP10, respectively. It should be noted that the last group does not contain any TPP genes from monocots or Arabidopsis, perhaps indicating a TPP gene clade that was lost over evolutionary time.

EcOtsB	H	Y	R	Q	A	P	Q	H	E	-	D	A	L	M	T	L	A	Q	R	I	T	Q	I	W	P	-	-	-	Q	M	A	L	Q	Q	G	K	C	V	V	E	I	K	P	R	G	T	-	S	K	G
ScTPS2	H	Y	R	R	T	V	P	E	L	G	E	F	H	A	K	E	L	K	E	K	L	L	S	F	T	D	D	F	D	L	E	V	M	D	G	K	A	N	I	E	V	R	P	R	F	V	-	N	K	G
SmTPP1a	H	F	R	Q	V	R	E	Q	D	W	Q	F	L	A	Q	E	V	Q	S	V	L	K	R	Y	P	-	-	-	E	L	S	I	T	H	G	R	K	V	L	E	I	R	P	S	I	K	W	D	K	G
AtTPPB	H	F	R	R	V	D	E	K	R	W	P	A	L	A	E	V	V	K	S	V	L	I	D	Y	P	-	-	-	K	L	K	L	T	Q	G	R	K	V	L	E	I	R	P	T	I	K	W	D	K	G
ZmRA3	H	F	R	C	V	R	E	E	E	W	N	A	V	N	E	E	V	R	S	V	L	R	E	Y	P	-	-	-	N	L	K	L	T	H	G	R	K	V	L	E	I	R	P	S	I	K	W	D	K	G
VvTPPA	H	Y	R	N	V	D	E	K	Y	W	K	T	I	A	Q	C	V	D	D	I	L	K	D	Y	P	-	-	-	R	L	R	L	T	H	G	R	K	V	L	E	V	R	P	V	I	D	W	D	K	G
VvTPPB	H	F	R	C	V	D	E	Q	R	W	T	A	L	A	E	Q	V	R	L	V	L	N	Q	Y	P	-	-	-	K	L	R	L	T	Q	G	R	K	V	L	E	I	R	P	T	I	K	W	D	K	G
VvTPPC	H	Y	R	N	V	D	E	N	S	W	S	T	I	A	Q	Y	V	H	D	V	L	K	D	Y	P	-	-	-	R	L	R	L	T	H	G	R	K	V	L	E	V	R	P	V	I	D	W	N	K	G
VvTPPD	H	F	R	C	V	H	E	K	D	T	N	A	L	K	E	V	V	E	S	V	L	E	D	Y	P	-	-	-	D	F	R	V	T	R	G	K	K	V	L	E	V	R	P	L	I	E	W	D	K	G
VvTPPE	H	Y	R	C	V	D	E	K	K	W	S	I	L	A	Q	Q	V	R	S	V	L	Q	Q	Y	P	-	-	-	K	L	R	L	T	Q	G	R	K	V	L	E	I	R	P	T	I	K	W	D	K	G
VvTPPF	H	F	R	R	V	H	E	K	D	Y	D	T	L	E	E	K	V	K	S	V	V	K	N	Y	P	-	-	-	E	F	R	L	T	S	G	K	K	V	M	E	I	R	P	S	I	K	W	D	K	G
VvTPPG	H	Y	R	N	V	D	E	N	S	W	S	T	I	A	Q	Y	V	H	D	V	L	K	D	Y	P	-	-	-	R	L	R	L	T	H	G	R	K	V	L	E	V	R	P	V	I	D	W	N	K	G

EcOtsB	E	A	I	A	A	F	M	-	Q	E	A	P	F	I	G	R	-	-	-	-	-	-	-	-	-	-	-	-	-	T	P	V	F	L	-	-	-	G	D	D	L	T	D	E	S	G	F	A	V	V
ScTPS2	E	I	V	K	R	L	V	W	H	Q	H	G	K	P	Q	D	M	L	K	G	I	S	E	K	L	P	K	D	E	M	P	D	F	V	L	C	L	G	D	D	F	T	D	E	D	M	F	R	Q	L
SmTPP1a	K	A	V	E	Y	L	L	-	E	A	L	G	L	-	G	D	-	-	-	-	-	-	-	-	S	R	D	V	L	P	V	Y	I	-	-	-	G	D	D	R	T	D	E	D	A	F	E	I	L	
AtTPPB	Q	A	L	N	F	L	L	-	K	S	L	G	Y	-	E	N	-	-	-	-	-	-	-	-	S	D	D	V	V	P	V	Y	I	-	-	-	G	D	D	R	T	D	E	D	A	F	K	V	L	
ZmRA3	K	A	L	E	F	L	L	-	K	S	L	G	Y	-	A	G	-	-	-	-	-	-	-	-	R	N	D	V	F	P	I	Y	I	-	-	-	G	D	D	R	T	D	E	D	A	F	K	V	L	
VvTPPA	K	A	V	E	F	L	L	-	E	S	L	G	L	-	N	N	-	-	-	-	-	-	-	-	S	D	D	V	L	P	I	Y	V	-	-	-	G	D	D	R	T	D	E	D	A	F	K	F	L	
VvTPPB	N	A	L	E	F	L	L	-	E	S	L	G	Y	-	A	N	-	-	-	-	-	-	-	-	S	N	D	V	F	P	I	Y	I	-	-	-	G	D	D	R	T	D	E	D	A	F	K	V	L	
VvTPPC	K	A	V	E	F	L	L	-	E	S	L	G	L	-	T	N	-	-	-	-	-	-	-	-	S	E	D	V	L	P	I	Y	I	-	-	-	G	D	D	R	T	D	E	D	A	F	K	V	L	
VvTPPD	H	A	L	E	Y	L	L	-	D	T	L	G	F	-	D	-	-	-	-	-	-	-	-	-	S	S	D	V	V	P	I	Y	L	-	-	-	G	D	D	R	T	D	E	D	A	F	K	M	I	
VvTPPE	K	A	L	E	F	L	L	-	E	S	L	G	F	-	G	N	-	-	-	-	-	-	-	-	C	T	D	V	F	P	V	Y	I	-	-	-	G	D	D	R	T	D	E	D	A	F	K	I	L	
VvTPPF	C	A	L	E	Y	L	L	-	D	T	L	G	F	-	S	D	-	-	-	-	-	-	-	-	S	S	D	V	L	P	L	Y	I	-	-	-	G	D	D	R	T	D	E	D	A	F	K	V	I	
VvTPPG	K	A	V	E	F	L	L	-	E	S	L	G	L	-	T	N	-	-	-	-	-	-	-	-	S	E	D	V	L	P	I	Y	I	-	-	-	G	D	D	R	T	D	E	D	A	F	K	V	L	

Figure 4.4 Sequence alignment of the phosphatase region of TPP genes.

Sequences used for alignment of the phosphatase region of TPP genes were retrieved from sources as described in Section 4.2.2. Sequences were aligned in the MEGA software (Tamura et al., 2011) using the MUSCLE alignment algorithm (Edgar, 2004) as described in Section 4.2.2. Conserved residues for the HAD binding are highlighted in green. The highly similar sequences of VvTPPC and VvTPPG are highlighted in grey.



◀ Figure 4.5 **Phylogenetic tree of TPP genes.**

The tree was drawn using a bootstrapped maximum likelihood method. Numbers indicate percentage of bootstraps in which the genes within the branches clustered together (1000 replicates). Branches with less than 50% likelihood difference are collapsed. Grapevine TPP genes are in red. TPS genes from previously uncharacterised species used in this analysis are in grey.

4.3.2 Grapevine BA1/LAX1

The grapevine BA1/LAX1 sequence consists of 486 base pairs encoding a polypeptide of 162 amino acids (Table 4.2). The nucleotide sequence is not recognized as encoding a predicted gene on the NCBI website's 12X coverage of the grapevine genome. The NCBI accession number provided by Woods et al. (2011) leads to a discontinued record (XM_002268833.1) from the original 8X coverage of the reference genome. However, both the 8X and 12X coverage of the grapevine reference sequence in the Genoscope browser (www.genoscope.cns.fr/externe/GenomeBrowser/Vitis/) recognizes the sequence as a functional hypothetical protein (GSVIVT01030333001; 12X coverage) that encodes a BA1/LAX1 orthologue. The BA1/LAX1 clade of the bHLH transcription factor family is characterized by having an Ala9 replacing Glu9 in the E-box DNA binding site (Gallavotti et al., 2004). As seen in Figure 4.6, the grapevine VvBA1 also contains this amino acid, indicating that it is indeed a member of the BA1/LAX1 bHLH gene clade. The grapevine BA1/LAX1 gene clusters with poplar BA1/LAX1 homologues within the BA1/LAX1 clade as seen in Figure 4.7. The results of the phylogenetic tree and sequence analysis indicates that grapevine has one BA1 gene, named VvBA1/LAX1 that is similar in structure to the maize BA1 gene.

The Medicago BA1/LAX1 and the Arabidopsis BA1/LAX1 (AtROX) homologues, however, do not align with any other bHLH genes used in the development of this phylogenetic tree (Figure 4.6), although these genes were found to group with the BA1/LAX1 clade by other researchers (Woods et al., 2011; Yang et al., 2012). The difference in the placement of MtBA1/LAX1 and AtROX in the trees may be due to the different phylogenetic analyses used, the region of the genes used to form the trees, the species of organisms used to develop the trees, or the rooting of the phylogenetic trees by the other researchers. As seen in Figure 4.7, the bHLH regions of MtBA1/LAX1 and AtROX do appear to have a more divergent sequence than the genes from other species. This indicates that the MtBA1/LAX1 and AtROX genes may not be a member of the BA1/LAX1 clade of the bHLH gene family but rather members of a closely related clade within the large gene family of this transcription factor.

Table 4.2 Grapevine BARREN STALK1/LAX PANICLE1 (BA1/LAX1) gene

Name	Chromosome	Nucleotide accession number			Exon number	Protein accession number		
		NCBI	Genoscope	Length		NCBI	Genoscope	Length
VvBA1/ LAX1	8	XM_002268833	GSVIVT00001325001 (8X)	441 bp	1	XP_002268869	GSVIVP00001325001 (8X)	147 aa
			GSVIVT01030333001 (12X)	486 bp			GSVIVT01030333001 (12X)	162 aa

```

ZmBA1      S T D P - - - - Q S V A A R E R R H R I S D R F R V L R S L V P G - - - - - G S K M - -
OsLAX1     S T D P - - - - Q S V A A R E R R H R I S D R F R V L R S L V P G - - - - - G S K M - -
AtROX      V S D S G E D I K E D S E R N K K Y K G S Q D K A V T N N L E S E S L E D T R G S G K K M S K
VvBA1/LAX1 S T D P - - - - Q S V A A R E R R H R I S D R F K I L Q S L V P G - - - - - G T K M - -

```



```

ZmBA1      - - - - - - - - - - - - - - - - - - - - - - - - D T V S M L E Q - - - - - A I H Y V K F L
OsLAX1     - - - - - - - - - - - - - - - - - - - - - - - - D T V S M L E Q - - - - - A I H Y V K F L
AtROX      G W N T W A L A L H S I A M H P E R H E N V V L E Y L D N I V V I N D Q Y P K A R K H V L V L
VvBA1/LAX1 - - - - - - - - - - - - - - - - - - - - - - - - D T V S M L E E - - - - - A I H Y V K Y L

```

Figure 4.6 Sequence alignment of the BA1/LAX1 clade of bHLH genes.

Sequences used for alignment of the bHLH region of BA1/LAX1 genes were retrieved from sources as described in Section 4.2.2. Sequences were aligned in the MEGA software (Tamura et al., 2011) using the MUSCLE alignment algorithm (Edgar, 2004) as described in Section 4.2.2. The characteristic residue for the BA1/LAX1 clade is highlighted in yellow.

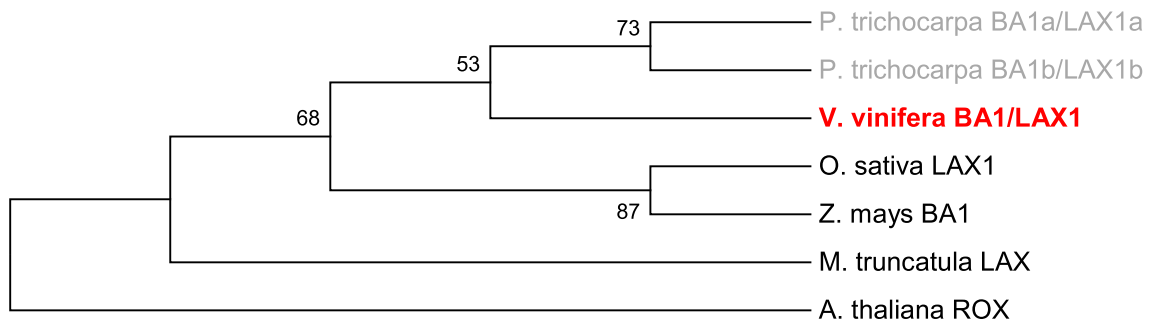


Figure 4.7 Phylogenetic tree of the BA1/LAX1 clade of bHLH genes.

The tree was drawn using a bootstrapped maximum likelihood method. Numbers indicate percentage of bootstraps in which the genes within the branches clustered together (1000 replicates). The grapevine BA1/LAX1 gene is in red. BA1/LAX1 genes from previously uncharacterised species used in this analysis are in grey.

To see if there is a grapevine gene similar to AtROX, a search for a ROX homologue in grapevine was done using the annotated APTX gene that contains the AtROX open reading frame. A grapevine ROX homologue was identified by a BLAST search (Altschul et al., 1990) of the NCBI database. The grapevine ROX homologue, however, does not contain a bHLH region (data not shown). This indicates that VvROX is more similar to the APRATAXIN (APTX) gene that is tightly linked to the bHLH protein in Arabidopsis. This also suggests that AtROX is likely to have diverged from the other BA1/LAX1 genes due to the tight linkage of the bHLH with APTX. This hypothesis is supported by both the sequence data as shown in Figure 4.6, in which the characteristic Arg9 protein that identifies the BA1/LAX1 clade (Gallavotti et al., 2004) is lacking in AtROX, as well as the results of the bootstrapped phylogenetic tree (Figure 4.7) that shows the gene to be highly divergent from the main BA1/LAX1 clade. Based on the results shown here, the Arabidopsis AtROX gene is not a member of the BA1/LAX1 clade of the bHLH transcription factor family.

4.4 Conclusions and future prospects

In silico analysis of the trehalose pathway genes and the BA1/LAX1 gene families in grapevine indicate the presence of gene families for TPS and TPP and only a single gene present for BA1/LAX1. The grapevine TPS gene family consists of seven genes (VvTPS1-7), in agreement with the findings of recently published reports (Fernandez et al., 2012). The grapevine TPS gene family has a single Class I TPS gene (VvTPS1) which may be involved in trehalose biosynthesis. The remaining grapevine TPS genes (VvTPS2-VvTPS7) are members of the Class II TPS genes that have as yet unknown functions (Vandesteene et al., 2010). The grapevine TPP gene family also consists of seven genes (VvTPPA-G). Previous publications identified only six VvTPP genes (Fernandez et al., 2012). VvTPPG is novel to this research and is likely a highly conserved duplication of VvTPPC as indicated by both genes having

nearly identical sequence. Similar to results found in Arabidopsis (Vandesteene et al., 2012), all VvTPP genes are predicted to be biosynthetically active, with two grapevine TPP genes (VvTPPB & VvTPPE) closest in similarity to the Arabidopsis TPP gene (AtTPPB) involved in trehalose synthesis (Li et al., 2008; Nunes et al., 2013). Besides being potentially involved in the trehalose synthesis pathway, these two genes are also of particular interest to this research due to their similarity with ZmRA3, a TPP gene known to affect inflorescence architecture in maize. Further research on these genes will be carried out in the following chapters to elucidate their role in grapevine, with particular emphasis on potential roles in inflorescence architecture and outer arm development.

Another gene of interest to this research due to its known effect on inflorescence architecture in maize is the BA1 gene. A single grapevine BA1/LAX1 gene was identified by previous researchers (Woods et al., 2011) on the original 8X grapevine genome. The putative gene was later removed from the 12X genome by the NCBI gene prediction software, but remained listed as a hypothetical gene on the Genoscope database. The VvBA1/LAX1 gene is highly similar to the maize and rice BA1 and LAX1 genes, respectively- unlike the Arabidopsis ROX gene. The MtBA1/LAX1 and AtROX genes have been previously shown to align with the BA1/LAX gene family by other researchers (Woods et al., 2011; Yang et al., 2012), but this work was unable to group the genes in the BA1/LAX1 clade. Based on the results of the data collected as part of this research, the AtROX gene is not part of the BA1/LAX1 clade. Further research on the grapevine VvBA1/LAX1 gene will be carried out in the following chapters to not only confirm its presence as a functional gene in grapevine, but also to determine this gene's potential role in influencing inflorescence architecture and outer arm development.

Chapter 5

Characterization of the TPS/TPP gene family in grapevine

5.1 Introduction

Trehalose is a disaccharide synthesized by many organisms which has gained much attention due to its ability to protect against abiotic stresses (Elbein et al., 2003). Derived from two glucose molecules through 5 possible pathways (Iturriaga et al., 2009), trehalose can constitute up to 15% of the dry weight of some organisms under stress conditions (Muller et al., 1995). In plants, trehalose is synthesized by first forming trehalose-6-phosphate (T6P) from the enzymatic activity of TREHALOSE-6-PHOSPHATE SYNTHASE (TPS) on glucose-6-phosphate and UDP-glucose, followed by the dephosphorylation of T6P by TREHALOSE-6-PHOSPHATE PHOSPHATASE (TPP) (Figure 5.1; Müller et al., 1999). Trehalose was initially believed to be synthesized only in desiccation-tolerant plants (Muller et al., 1995), but in 1998 publications identified genes responsible for trehalose synthesis in the model species *Arabidopsis thaliana* (Blazquez et al., 1998; Vogel et al., 1998). The identification of these genes in *Arabidopsis* has allowed the gene products and their function, as a signal molecule, to be further characterized (Kolbe et al., 2005; Harthill et al., 2006; Zhang et al., 2009). It is currently accepted that trehalose-6-phosphate (T6P) is integral for signalling various stress responses (Paul, 2007; Smith and Stitt, 2007), cytosolic sugar levels (Avonce et al., 2005; Lunn et al., 2006) and starch synthesis in plants (Kolbe et al., 2005; Lunn et al., 2006), although the exact pathways are unclear. It is believed that only one gene in each gene family encodes a functional enzyme and the other gene products within the family are likely involved in plant signalling rather than trehalose synthesis (Vandesteene et al., 2010) and as such are still under selective pressure to remain as active genes (Avonce et al., 2006). Since their discovery in *Arabidopsis*, the genes responsible for trehalose synthesis have been identified in many other plant species (Müller et al., 1999; Wang et al., 2005; Kosmas et al., 2006; Satoh-Nagasawa et al., 2006; Wu et al., 2006; Lunn, 2007; Shima et al., 2007; Jiang et al., 2010), including recently in grapevine (this work; Fernandez et al., 2012).

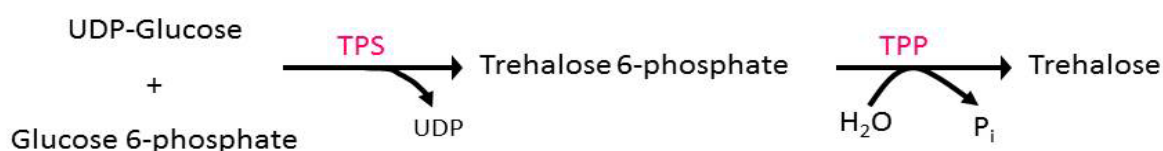


Figure 5.1 The trehalose biosynthesis pathway in plants.

The enzymes involved in trehalose biosynthesis are in pink. TPS: TREHALOSE-6-PHOSPHATE SYNTHASE, TPP: TREHALOSE-6-PHOSPHATE PHOSPHATASE.

5.1.1 Trehalose-6-phosphate (T6P) in carbohydrate synthesis

The role of the T6P in sugar metabolism was first identified in yeast, with *S. cerevisiae tps1* mutants unable to synthesize glucose for glycolysis due to the unrestricted loading of glucose into the pathway (Blazquez et al., 1993). This leads to an increase in hexose phosphate molecules within the system overloading the glycolysis pathway, resulting in a deficit of ATP and P_i (Teusink et al., 1998). In plants, energy from the sun is converted into carbohydrates via photosynthesis. This set of reactions allows the plant to store the sun's energy for its own energy source during times of reduced light. The carbohydrates formed via photosynthesis are many and varied, with starch composing up to 50% of the plant's supply of stored energy (Stitt and Zeeman, 2012). Starch is synthesized in chloroplasts during the day after products from the Calvin-Benson cycle reach a surplus (Kolbe et al., 2005; Stitt and Zeeman, 2012). The enzyme ADP-GLUCOSE PYROPHOSPHORYLASE (AGPase) is responsible for the first step in the starch synthesis pathway. AGPase is a heterodimer comprising two large and two smaller subunits (Okita et al., 1990). This enzyme is regulated by post-translational modification of the smaller subunits into either an inactive oxidized dimer or an active reduced monomer (Kolbe et al., 2005). In Arabidopsis and potato, trehalose was found to reduce the AGPase small subunit, which in turn activated the starch biosynthesis pathway (Kolbe et al., 2005). Upon closer inspection, it was found that the trehalose intermediate molecule, trehalose-6-phosphate (T6P), was the molecule capable of AGPase small subunit reduction in chloroplasts via a SNF1-RELATED PROTEIN KINASE1 (SnRK1) signalling pathway (Kolbe et al., 2005). The inclusion of T6P in the starch synthesis as well as the SnRK1 pathway allows for a carbohydrate component to be incorporated into a signalling network. SnRK1 signalling is involved in numerous pathways, as described below.

5.1.2 Trehalose-6-phosphate (T6P) as a signal molecule

Trehalose in plants was initially an area of much interest to researchers due to its purported role in abiotic stress defence (Goddijn and van Dun, 1999). Further work on the molecule showed that its precursor, trehalose-6-phosphate (T6P), was also an important molecule for signalling the carbohydrate status of the plant for various developmental processes, such as starch metabolism as described above. While many researchers recognized the importance of T6P in signalling, the mechanism by which T6P could be used as a signal was unclear (Schluepmann et al., 2003; Avonce et al., 2004; Avonce et al., 2005). The discovery of trehalose-6-phosphate acting in the SNF1-related protein kinase1 (SnRK1) signalling pathway (Schluepmann et al., 2004; Kolbe et al., 2005; Zhang et al., 2009) explains how T6P can be involved in the many diverse signalling roles in which it is active.

The SnRK1 signalling pathway is controlled by a family of serine-threonine protein kinases whose role in cells is to restrict metabolism during times of limited energy supply by pre-transcriptional

modification (Baena-Gonzalez et al., 2007) via phosphorylation of transcription factors (Robaglia et al., 2012) or to promote cell division and catabolism during times of plenty by inhibition of transcription factor inhibitors (Guerinier et al., 2013). This pathway is found in all eukaryotes, with the regulatory SnRK1 complex comprising a heterotrimer (Smeekens et al., 2010; Robaglia et al., 2012). In Arabidopsis, the catalytic α -subunit of the SnRK1 enzyme is encoded by two homologues, ARABIDOPSIS SNF1 KINASE HOMOLOGUE10/11 (AKIN10/11), which have been shown to repress gene activity based on the energy status of the plant (Baena-Gonzalez et al., 2007). The SnRK1 signalling pathway is the focus of much research in the plant community due to its role as an integrator of energy and stress signals in the control of basic metabolism and development (Sheen et al., 1999; Baena-Gonzalez et al., 2007; Jossier et al., 2009; Cho et al., 2012; Tsai and Gazzarrini, 2012). The SnRK1 pathway is able to regulate over 1000 genes during periods of low energy or stress, mainly by increasing transcription for degradation and catabolism genes or repressing genes involved in protein synthesis or anabolism (Baena-Gonzalez et al., 2007). It was therefore determined that this pathway is key to controlling not only stress response in plants by limiting gene transcription, but also the overall development of plants as they age (Baena-Gonzalez et al., 2007; Cho et al., 2012; Tsai and Gazzarrini, 2012).

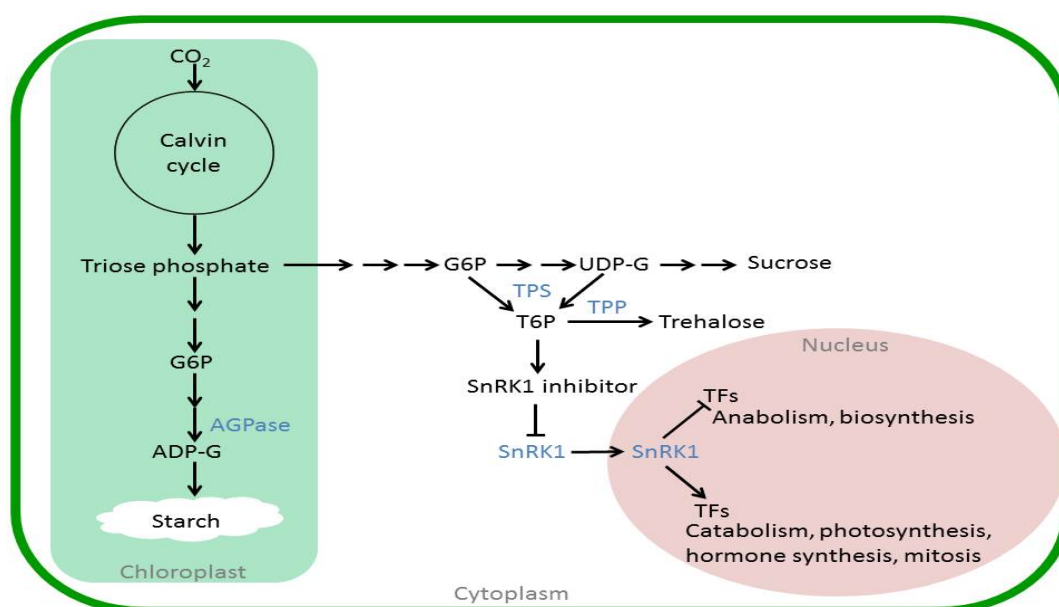


Figure 5.2 Simplified diagram of SnRK1 signalling in plant cells.

The diagram incorporates both sucrose and starch synthesis pathways while showing the role of T6P in signalling carbohydrate status to the SnRK1 signal cascade in the nucleus. The enzymes of note in the diagram are in blue. AGPase: ADP-GLUCOSE PYROPHOSPHORYLASE, SnRK1: SNF1-RELATED PROTEIN KINASE1, TPS: TREHALOSE-6-PHOSPHATE SYNTHASE, TPP: TREHALOSE-6-PHOSPHATE PHOSPHATASE.

T6P interacts in the SnRK1 signalling pathway as an indicator of carbohydrate supply within the system. During times of plentiful carbohydrate (i.e. daytime, vegetative growth period), T6P levels increase as the products of the Calvin-Benson cycle (ultimately UDP-Glucose & Glucose-6-phosphate) are being converted into other sugar molecules (Rolland et al., 2006). As shown in Figure 5.2, when T6P levels increase, they can act as analogues of sucrose in signalling cascades to indicate sucrose levels in the system (O'Hara et al., 2013), thereby inhibiting the SnRK1 signalling cascade and activating AGPase for starch synthesis during times of high carbohydrate availability (Zhang et al., 2009; Schluepmann et al., 2012). In young Arabidopsis leaves, T6P inhibition of the SnRK1 enzyme occurs through a yet unknown intermediate protein/enzyme that is lost as the plant matures (Zhang et al., 2009). Recently, T6P inhibition of the SnRK1 signalling cascade was suggested to act in a “partial non-competitive model”, in which T6P converts the inhibitor into a modified enzyme that binds to SnRK1 at a different site than the substrate thereby inhibiting SnRK1 activity without blocking the catalytic site of the enzyme (Nunes et al., 2013). The researchers also found that SnRK1 inhibition by the unknown intermediate can also occur using glucose-1-phosphate (G1P) or glucose-6-phosphate (G6P) as the indicator sugar, with the different sugars leading to inhibition of SnRK1 at different binding sites, leading to an additive inhibition effect when multiple sugars are present (Nunes et al., 2013). The identification of T6P aiding in the inhibition of the SnRK1 signalling cascade explains how this seemingly innocuous molecule can affect so many different major developmental pathways in plants.

5.1.3 Trehalose-6-phosphate (T6P) in inflorescence architecture

By observing plants with mutated trehalose synthesis pathway genes, it was also determined that trehalose or its precursor, T6P, are also important for the transition to flowering and floral architecture in plants (Schluepmann et al., 2003; van Dijken et al., 2004; Satoh-Nagasawa et al., 2006; Chary et al., 2008). In plants with a mutant TREHALOSE-6-PHOSPHATE PHOSPHATASE (TPP) gene, which are then unable to process trehalose from T6P, the inflorescences had increased basal branching (Satoh-Nagasawa et al., 2006) and reduced flower development (van Dijken et al., 2004). In Arabidopsis plants overexpressing the TPP gene, inflorescence initiation was delayed by up to 3 weeks and had reduced branching (Schluepmann et al., 2003). In other Arabidopsis studies, it was found that alterations of trehalose or T6P levels can alter flowering times and architectures of inflorescences independently of the major floral initiation genes, such as FLOWERING LOCUS T (FT) and LEAFY (LFY) (van Dijken et al., 2004; Wahl et al., 2013) via the age-dependant flowering pathway by altering expression of several SQUAMOSA PROMOTER LIKE (SPL) genes (Wahl et al., 2013). It was also found that TREHALOSE-6-PHOSPHATE SYNTHASE1 (TPS1) or T6P can significantly affect FT expression in Arabidopsis leaves, providing evidence that members of the trehalose pathway are

integral for signalling the carbohydrate status of the plant before the transition to flowering (Wahl et al., 2013).

The discovery that the SnRK1 signalling pathway can affect the developmental stages in plants suggests a possible route by which T6P can affect inflorescence architecture. In *Arabidopsis*, the SnRK1 homologue (AKIN10) was shown to affect the transition to a reproductive state, with overexpression of the gene leading to severely delayed flowering (Baena-Gonzalez et al., 2007) and a repression of the B3 domain transcription factor FUSCA3, that in turn leads to altered lateral organ development and phyllotaxy (Tsai and Gazzarrini, 2012). As seen in maize, overexpression of T6P leads to increased inflorescence branching (Sato-Nagasawa et al., 2006), which in theory is due to inhibition of the SnRK1 pathway, which in turn leads to increased cell division. Alternatively, the decrease of T6P can lead to activation of the SnRK1 pathway, which causes delays in inflorescence primordia branching and development, as observed in *Arabidopsis* (Schluepmann et al., 2003; Baena-Gonzalez et al., 2007). By utilizing T6P to indicate the overall carbohydrate status of the plant, the SnRK1 pathway can regulate not only when the plant is ready for the reproductive phase but also how fruitful the plant should be. In this way, high T6P levels within the plant represent a surplus of stored energy, which in turn signals the ability for the plant to produce more or larger inflorescences once it reaches its reproductive stage.

To test if trehalose pathway enzymes or molecules are involved in grapevine inflorescence architecture and differentiation in a similar manner as observed in other model species, the identification and characterization of the genes involved in the pathway in grapevine was initiated. As described in Chapter 4, seven TPS and seven TPP gene homologues were identified in grapevine. To further characterize the expression of these genes, a series of experiments were conducted to identify where in the plant the genes are expressed as well as which of the genes, if any, are biosynthetically active. The results from these experiments indicates not only which TPS and TPP genes are capable of synthesizing trehalose in grapevine, but also gives clues as to the possible role of T6P in signalling for carbohydrate status and inflorescence development, as seen in *Arabidopsis*.

5.2 Materials & Methods

5.2.1 Cloning of VvTPS and VvTPP genes

VvTPS and VvTPP expression was verified in grapevine by RT-PCR as described in Appendix E, and then the whole gene was amplified from the cDNA sample showing the strongest expression using TaKaRa PrimeStar™ reagents (Norrie Biotech, NZ). The reaction was set up as a “proofreading PCR” as described in Appendix A using the VvTPS or VvTPP primers to amplify the whole gene (Appendix B) containing the CACC leader sequence on the forward primer for topoisomerase cloning in the

Invitrogen pENTR™/D-TOPO® cloning kit (Invitrogen, NZ). The PCR product was run on a 1% agarose gel and excised for purification. The PCR products were gel purified using the Axygen® Axyprep™ DNA Gel Extraction Kit (Raylab, NZ). The purified PCR product was cloned into the Invitrogen pENTR™/D-TOPO® cloning kit (Invitrogen, NZ) as per the manufacturer's instructions. The cloned plasmid was then transformed into *E. coli* DH5α competent cells by heat shock as per the kit's protocol and plated onto LB plates (Appendix C) containing 50mg/L kanamycin. Transformed colonies were checked for the presence of the plasmid containing the VvTPS or VvTPP gene by PCR (Appendix A-Colony PCR) using the reagents and cycle described in Appendix A with M13 primers (Appendix B) that amplify a region of the plasmid flanking the insertion site. The PCR product was run on a 1% agarose gel and 2-3 positive colonies were sequenced to ensure correct amplification of the gene.

5.2.2 Yeast complementation

The grapevine TPS and TPP genes cloned into pENTR™/D-TOPO® were PCR amplified by "proofreading PCR" as described in Appendix A using the primers listed in Table 5.1 containing restriction enzyme recognition sites for cloning into the yeast expression plasmids developed in Chapter 2. The PCR products were gel purified using the Axygen® Axyprep™ DNA Gel Extraction Kit (Raylab, NZ) and 1 µg of the product and the plasmids developed in Chapter 2 were digested with the restriction enzymes listed in Table 5.1 in an overnight incubation with 1X BOVINE SERUM ALBUMIN (BSA) to increase enzyme stability. The restriction enzymes and BSA were supplied by Roche (Roche Diagnostics New Zealand Ltd.). The digested plasmid and PCR products were again gel purified using the same kit as above and 50ng of digested plasmid was dephosphorylated using the Roche SHRIMP ALKALINE PHOSPHATASE (SAP) enzyme (Roche Diagnostics New Zealand Ltd.) as per the manufacturer's instructions. The dephosphorylated plasmid and digested PCR products were then ligated using TaKaRa Mighty Mix™ ligation mix (Norrie Biotech, NZ) as per the manufacturer's instructions using a 3:1 ratio of PCR product: plasmid. After ligation, 10µL of the reaction mixture was used to transform *E. coli* DH5α using the heat shock method (Sambrook and Russell, 2001) and the transformation mix was plated onto LB plates containing 100mg/L ampicillin for selection of transformants. Transformed colonies were checked for the presence of the plasmid containing the genes by PCR using the reagents and cycle described in Appendix A (Colony PCR) with the gene specific forward primer and a pYexBx specific reverse primer (Appendix B). The PCR product was run on a 1% agarose gel and 3 positive colonies per plasmid were sequenced to ensure correct amplification of the gene.

The pYexTEF1MCS and pYexTPS1MCS plasmids containing the TPS family genes listed in Table 5.1 were transformed into the yeast *tps1Δ:TRP1* genotype. The pYexTPS2MCS plasmid containing the

TPP family genes listed in Table 5.1 were transformed into the yeast *tps2Δ:LEU2* genotype. For the TPP family genes, the plasmid containing the yeast TPS2 promoter was screened first for the complementation study as previous work in Arabidopsis showed that all AtTPP genes were able to complement the mutant yeast strain (Vandesteene et al., 2012). The transformations were performed as per a modified Geitz and Woods protocol (2002), as summarized in Chapter 2.

The transformed cultures were then plated on selection media plates (Appendix C) containing either galactose (for the *tps1Δ:TRP1* mutant) or glucose (for the *tps2Δ:LEU2* mutant) and lacking uracil for selection as well as complete rich and minimal media (Appendix C) with the associated carbohydrate source for controls. The plates were incubated at 28 °C (for *tps1Δ:TRP1*) or 28 °C and 38.6 °C (for *tps2Δ:LEU2*) for up to 5 days to allow for transformed colony growth. After the colonies grew, four colonies from each transformation were selected to confirm transformation. Transformation confirmation was done by “FTA card PCR” as described in Appendix A. The primers used for the PCR reaction were specific for the promoter (forward) and the pYexBx plasmid backbone (reverse) as listed in Appendix B. 10μL of the PCR products were run on a 1% agarose gel containing 2% ethidium bromide and visualized by UV light in a Bio Rad GelDoc apparatus (Bio Rad Laboratories Pty Ltd, NZ). Two or three colony PCR products per transformed gene, indicating the presence of the correct insert, were sent for sequencing after the remaining PCR product (40μL) was purified using the Axygen® AxyPrep™ PCR Cleanup kit (Raylab, NZ) as per the manufacturer’s protocol.

Table 5.1 Primers used to clone TPS and TPP genes into pYexTEF1/TPS1/TPS2 plasmids for yeast complementation.

The restriction enzyme recognition sites are highlighted in bold within the primer sequence.

Gene	Primer		Restriction Enzyme	
	Forward	Reverse	5' end	3' end
TPS genes				
ScTPS1	GGTT GTCGAC ATGACTACGGATAAC	AGTGTT CTGCAGT CAGTTTTTGGTGGC	Sall	PstI
AtTPS1	AATTA ACCGCGG ATGCCTGGAATA	GGTTGGT CTAGAT TAAGGTGAGGAAGTG	SacII	XbaI
VvTPS1	AATAAT GGATCC ATGCCCGGAACAAGT	GAAAGG CTCGAG TTAAAAAGAAGACTT	BamHI	XhoI
VvTPS2	AATT GAGCTC ATGGTGTGAGATCGTA	AATT CCCGGGT TATTCTCTCTCTCTCT	SacI	SmaI
VvTPS3	TTCAG GATCC ATGGTCTCAAGGTC	AATT CCCGGGT TACTCTCTGTCT	BamHI	SmaI
VvTPS4	AATT GCCGGC ATGATGTCAAGAT	AAT CCCGGGT CAAGGAGAGC	NaeI	SmaI
VvTPS5	AATT CCGCGG ATGGCCTCAAGAT	AATTT CTAGAT CATATCCGCAACAAGC	SacII	XbaI
VvTPS6	AATT CCGCGG ATGGTGTCAAGAT	GGGGT CTAGAT CAAGCAACACTTTC	SacII	XbaI
VvTPS7 ¹	N/A			
TPP genes				
ScTPS2	AATTAAG CCGGC ATGACCACCACT	CGTTAA CCCGGGT CAAACCTTT	NaeI	SmaI
AtTPPB	AATTAAG CCGGC ATGACTAACCAG	AATTAAG AATTCT CACTCTTCTCCCACTG	NaeI	EcoRI
VvTPPA	AATAAT GGATCC ATGGATCTGAAGTC	CATAAT GAATTCT TATAGTCACTTGACT	BamHI	EcoRI
VvTPPB	AATAAC GATCC ATGACCAACCAG	CCTAATT CTAGAT CAGTCTCTACTCAATATA	BamHI	XbaI
VvTPPC ²	N/A			
VvTPPD	AATAA CCCGCGG ATGGACAGG	AATAAT GAATTCT CATGAATTTCCAGC	SacII	EcoRI
VvTPPE	TTA GTCGAC ATGACGAGGCAGAATGTA	CCC ACTGCAGT TACACCCTGTATTG	Sall	PstI
VvTPPF ¹	N/A			
VvTPPG	AATCAT GGATCC ATGGATTGAAGT	CATAAC GAATTC CTATGCTCCTCTT	BamHI	EcoRI

5.2.3 Quantitative gene expression assays in grapevine tissue by qRT-PCR

To accurately measure the amount of VvTPS and VvTPP expression within the tissue types identified from the RT-PCR experiment (Appendix E), 'Pinot noir' tissue was collected from the Lincoln University vineyard during the 2012-13 growing season for qRT-PCR assays. 'Pinot noir' clone 113 tissue was collected from nine plants pooled into three biological replicates (n=3). The tissue collected was as follows: latent bud, woolly bud, leaf (~225 mm²), tendril (~50mm), E-L stage 17 inflorescence (Coombe, 1995), post-anthesis flowers, pre-veraison berry (3.7 °Brix at 25.0°C), veraison berry (11.5 °Brix at 21.6 °C) and late veraison berry (16.1 °Brix at 22.1 °C). Representative images of the tissue types collected are in Figure 5.6. The tissue was collected in 2mL microcentrifuge tubes and snap-frozen in liquid nitrogen on site. The frozen tissue was then transferred to -80°C for storage until ready for RNA extraction.

RNA extraction and cDNA synthesis

RNA from the tissue types described above was extracted and quality checked as described in 3.2.4. For cDNA synthesis, 300ng of RNA was used in a 10µL reaction with oligo dTs provided by the manufacturer. The cDNA was synthesized according to protocol and subsequently diluted 20-fold with sterile water. The synthesized cDNA was checked for amplification and lack of genomic DNA (gDNA) contamination by PCR (cDNA check PCR; Appendix A).

qRT-PCR assays

qRT-PCR assays were performed on the cDNA synthesized from the tissues described above using TaKaRa SYBR® Premix ExTaq™ II PCR reagents (Norrie Biotech, NZ). The assays were done using the Illumina Eco™ Real Time PCR System (dnature, NZ) with the nine tissue types from three biological replicates (27 samples total) repeated in triplicate spread across two 48-well plates. For the assays, a master mix containing the reagents and the qRT-PCR primers (Appendix B) was made and the cDNA template and master mix was aliquoted into the qRT-PCR plates using an Eppendorf epMotion 5070 liquid handling robot (Eppendorf, NZ) to reduce any pipetting error. In addition to the test samples, each plate contained a plate control sample of woolly bud from replicate two cDNA amplifying a fragment of the Actin gene with qRT ACT primers (Table 3.1, page 26) repeated in triplicate to normalize any plate variation. For each assay, digested plasmid containing the cloned VvTPS or VvTPP gene was used to create a 5-point standard curve of 10-fold dilutions, of which the concentrations 1x10⁻², 1x10⁻⁴, 1x10⁻⁶, 1x10⁻⁷ and 1x10⁻⁸ (ng/µL) were used as both an internal positive control for the assay and to determine the PCR efficiency of the reactions. Sterile water was used in place of cDNA in the same reaction mix for a non-template control to check for contamination of the reagents. Both the standard curve and water samples were repeated in triplicate. The qRT-PCR reaction is described in Appendix A.

Raw data from the qRT-PCR assays were entered into the Illumina EcoStudy 4.0 software (dnature, NZ) for plate normalization. The plate-normalized data was then exported to Excel and the average quantification cycle (C_q) and standard deviation for each tissue type was calculated from the three biological replicates. The averaged C_q and standard deviation values for the pooled replicates was normalized to the geometric mean of three reference genes (N2227, SAND, TRU5) that were found to be the most stable reference genes for this experimental set as described in Chapter 3. The average relative expression of the tissues was compared to the pooled veraison berry sample in Excel by the Pfaffl method as described in Vandesompele et al. (2002) and Appendix A. Bar graphs of the normalized relative average expression of the tissue types were generated in Excel.

Statistical analysis

Post-hoc analysis of the normalized average relative expression of the VvTPS and VvTPP genes in the tissue types tested was performed by the Tukey-Kramer test after ANOVA using the GenStat 15 software package (VSN International, Ltd.). Means significantly different at $\alpha=0.05$ are indicated by different letters on the bar graphs for each gene assayed.

5.3 Results & discussion

5.3.1 Complementation assays for grapevine TPS and TPP gene function in mutant strains of *Saccharomyces cerevisiae*

Once TPS and TPP genes were identified in grapevine as described in Chapter 4, the next objective was to test the capability of the grapevine TPS and TPP genes for trehalose biosynthesis. The model organism *Saccharomyces cerevisiae* (Baker's yeast) was utilized to explore VvTPS and VvTPP functionality as a strain of this species was used to develop mutants that lacked TPS and TPP activity (Bell et al., 1998). A modified heat shock protocol as described by Geitz and Woods (2002) was utilized to transform the yeast *tps1Δ:TRP1* (TPS mutant) or *tps2Δ:LEU2* (TPP mutant) genotypes with plasmids developed in Chapter 2 containing the grapevine TPS or TPP genes, respectively. For the grapevine TPS gene family experiment, the identification of transformed yeast colonies was done on selection media containing glucose, as the non-transformed *tps1Δ:TRP1* genotype is unable to utilize glucose for glycolysis (Teusink et al., 1998), and lacking uracil for selection of transformed colonies containing the plasmid, which has the auxotrophic marker uracil. As controls, all cultures were also grown on complete rich and minimal media as well as selection media lacking uracil utilizing galactose as the carbon source. In addition, the endogenous yeast TPS gene (ScTPS1) and the Arabidopsis TPS1 gene (AtTPS1; Blazquez et al., 1998) were also used to transform the yeast *tps1Δ:TRP1* genotype as controls for the transformation experiment, as these genes have already been used to transform this yeast strain. VvTPS7 could not be isolated in its entirety, and so was not studied in this experiment. As shown in Figure 5.3, the only grapevine TPS gene that was able to

complement the yeast *tps1Δ* mutation was the Class I TPS family gene VvTPS1. This is the first study to identify a biosynthetically functional TPS gene from grapevine.

Both the Arabidopsis and grapevine TPS1 genes transformed into the yeast *tps1Δ*:TRP1 mutant contain an N-terminal leader sequence not found in the yeast TPS1 gene. The successful complementation of the yeast *tps1Δ*:TRP1 mutant with both plant TPS1 genes indicates that the leader sequence is not sufficient to inhibit the formation of the trehalose synthase enzyme complex that occurs in yeast (Bell et al., 1998).

The results observed here are similar to results previously published in the Arabidopsis TPS gene family (Vandesteene et al., 2010), in which the only biosynthetically active TPS gene was the Arabidopsis Class I TPS family gene, AtTPS1. As discussed by Vandesteene et al. (2010), although the remaining TPS genes cannot synthesize T6P, their enzymes may still be able to bind to substrates and act as localized signals of as yet unknown function. This hypothesis is backed by the finding of other researchers, who found that the VvTPS5 protein binds to the T6P substrate UDP-glucose (Harthill et al., 2006). This suggests that the remaining grapevine Class II TPS genes (VvTPS2-7) may have similar functions in grapevine as those predicted for the Class II Arabidopsis TPS genes-namely regulating T6P synthesis by substrate binding in localized tissue.

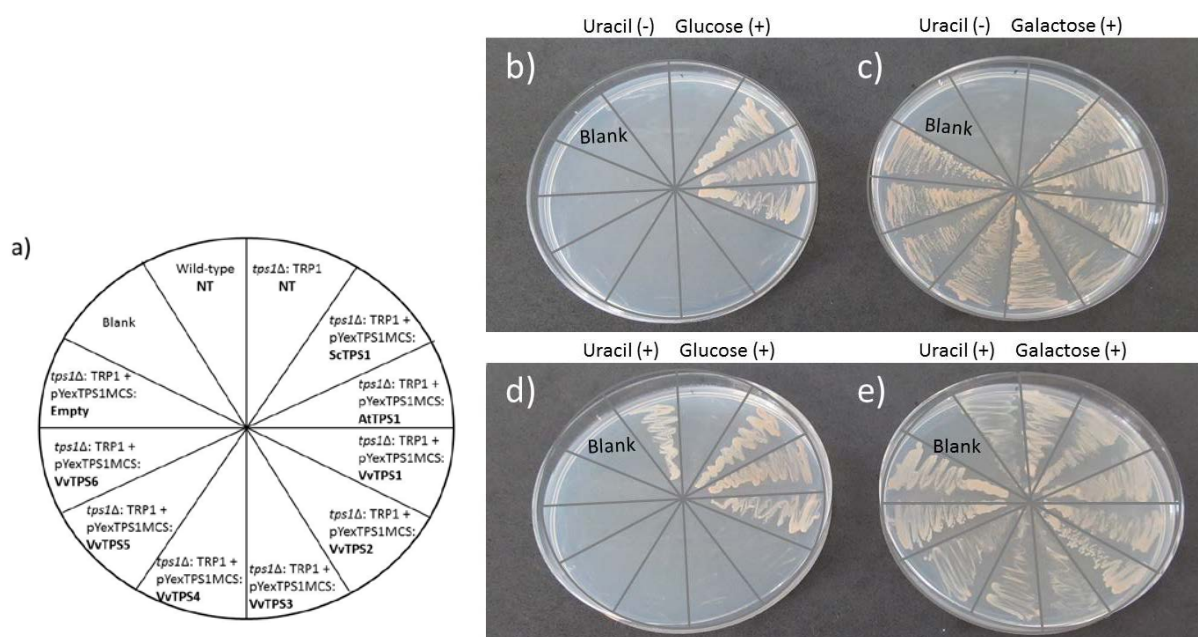


Figure 5.3 Complementation of the yeast *tps1Δ*:TRP1 genotype with grapevine TPS gene family genes using the endogenous yeast TPS1 promoter.

◀ The yeast genotype was transformed as described in Section 5.2.2 using plasmids containing the native yeast TPS1 promoter to drive transcription of the cloned genes. a) Diagram showing the layout of the transformed yeast colonies on plates shown in (b-e). NT: Not transformed. b) Transformed *tps1Δ:TRP1* genotypes containing the cloned genes as listed in (a) growing on selection media lacking uracil with glucose as the carbohydrate source. c) Transformed *tps1Δ:TRP1* genotypes containing the cloned genes as listed in (a) growing on selection media lacking uracil with galactose as the carbohydrate source. d) Transformed *tps1Δ:TRP1* genotypes containing the cloned genes as listed in (a) growing on complete minimal media with glucose as the carbohydrate source. e) Transformed *tps1Δ:TRP1* genotypes containing the cloned genes as listed in (a) growing on complete minimal media with galactose as the carbohydrate source.

To test if the lack of TPS activity for the grapevine Class II TPS genes was due to the type of promoter used to drive VvTPS gene expression in yeast, both the endogenous yeast TPS1 promoter and a constitutive yeast promoter from the transcriptional elongation factor EF1 α (TEF1) gene were used for the complementation study. As shown in Figures 5.3 and 5.4, the TPS1 genes from both grapevine and Arabidopsis were able to complement the yeast mutant using either the endogenous ScTPS1 promoter or the constitutive ScTEF1 promoter. To the best of our knowledge, this is the first study to investigate using the endogenous ScTPS1 promoter to drive plant TPS1 transcription in yeast complementation experiments. Our results indicate that, for TPS1, using the endogenous promoter in plant TPS1 complementation studies is just as successful as using a constitutive promoter.

As shown in Figure 5.4, no grapevine Class II TPS genes were able to complement the yeast *tps1Δ:TRP1* mutant using the constitutive ScTEF1 promoter. This indicates that the grapevine Class II TPS genes are either too disparate structurally from the yeast TPS1 gene or the TPS region of these genes is no longer catalytically active. As shown in Figure 4.3 (page 44), the grapevine Class II TPS genes have different amino acids at catalytic sites for both glucose-6-phosphate and UDP-glucose binding in the glycosyltransferase region of the enzyme, suggesting that loss of catalytic function is the reason why the VvTPS2-6 genes are unable to complement the yeast *tps1Δ:TRP1* mutant. As discussed above, this suggests that the grapevine Class II TPS genes may be involved in localized regulation of T6P synthesis by substrate binding or have another function that has not yet been determined.

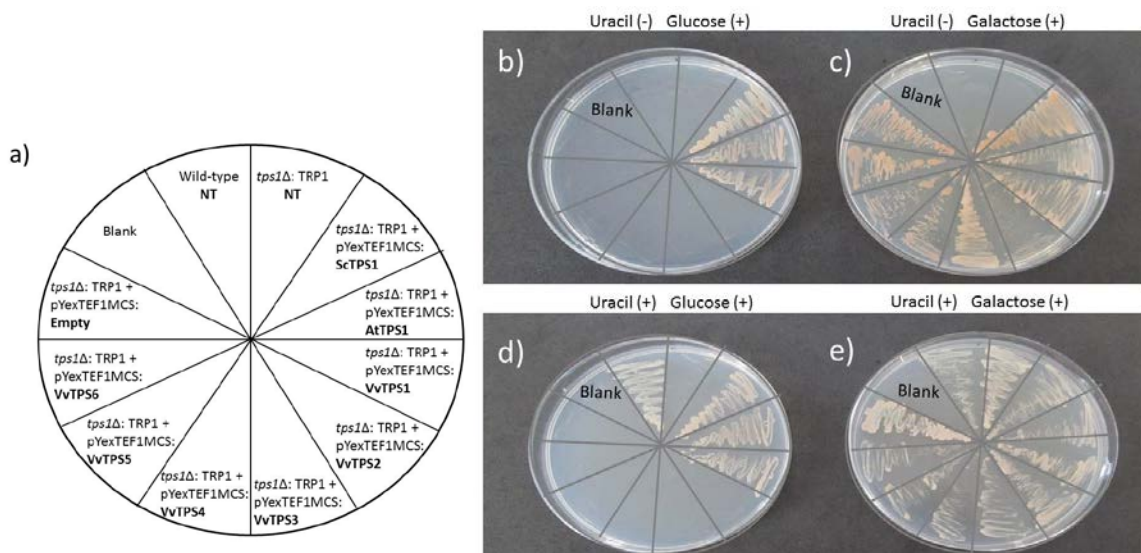


Figure 5.4 Complementation of the yeast *tps1Δ*:TRP1 genotype with grapevine TPS gene family genes using the constitutive yeast TEF1 promoter.

The yeast genotype was transformed as described in Section 5.2.2 using plasmids containing the constitutive yeast TEF1 promoter to drive transcription of the cloned genes. a) Diagram showing the layout of the transformed yeast colonies on plates shown in (b-e). NT: Not transformed. b) Transformed *tps1Δ*:TRP1 genotypes containing the cloned genes as listed in (a) growing on selection media lacking uracil with glucose as the carbohydrate source. c) Transformed *tps1Δ*:TRP1 genotypes containing the cloned genes as listed in (a) growing on selection media lacking uracil with galactose as the carbohydrate source. d) Transformed *tps1Δ*:TRP1 genotypes containing the cloned genes as listed in (a) growing on complete minimal media with glucose as the carbohydrate source. e) Transformed *tps1Δ*:TRP1 genotypes containing the cloned genes as listed in (a) growing on complete minimal media with galactose as the carbohydrate source.

To test for complementation of the yeast *tps2Δ*:LEU2 mutant genotype with members of the grapevine TPP gene family, the transformed yeast culture was grown on complete or selection media at 38.6°C or at 28°C as a control, as the yeast TPP mutant cannot grow at high temperatures due to an accumulation of T6P (Vogel et al., 1998). The selection media used glucose as the carbohydrate source and lacked uracil for selection of transformed colonies containing the plasmid, which has the auxotrophic marker uracil. In addition, the endogenous yeast TPP gene (ScTPS2) and the previously tested Arabidopsis TPPB gene (AtTPPB; Vogel et al., 1998) were also used to transform the yeast *tps2Δ*:LEU2 mutant. For this research, the Arabidopsis TPPB gene was used as a plant-based TPP family gene control rather than AtTPPA as previous work in Arabidopsis has shown that AtTPPB is likely to be the biosynthetically active TPP gene in this species (Nunes et al., 2013) even though the other Arabidopsis TPP gene members are able to complement the yeast *tps2Δ* mutation (Vandesteene et al., 2012). Previous work in grapevine had identified six TPP gene family genes, but complementation studies were conducted on only one of these genes (VvTPPA; Fernandez et al., 2012). In an attempt to completely study the TPP gene family, this study performed complementation experiments on all available members of the family, including a novel grapevine TPP family gene (VvTPPG) that was identified during the course of this research (Section 4.3.1,

Chapter 4). VvTPPF could not be isolated in its entirety, and so was not studied in this experiment. As shown in Figure 5.5, all grapevine TPP gene family genes tested were able to complement the yeast *tps2Δ* mutation. This result confirms previously published results shown in grapevine for VvTPPA (Fernandez et al., 2012) and is similar to results previously published in the Arabidopsis TPP gene family (Vandesteene et al., 2012).

All of the grapevine TPP genes tested successfully complemented the yeast *tps2Δ* mutant phenotype, indicating that they are able to integrate into the yeast trehalose enzyme complex. Why there are so many seemingly redundant genes within this family is unclear. As indicated by the gene transcript assays discussed below in Section 5.3.2, there is differential expression of many of the VvTPP genes within different grapevine tissue types. This may indicate a localized function for the VvTPP genes within different tissues. In Arabidopsis, a similar localization of the AtTPP genes was observed (Li et al., 2008; Vandesteene et al., 2012).

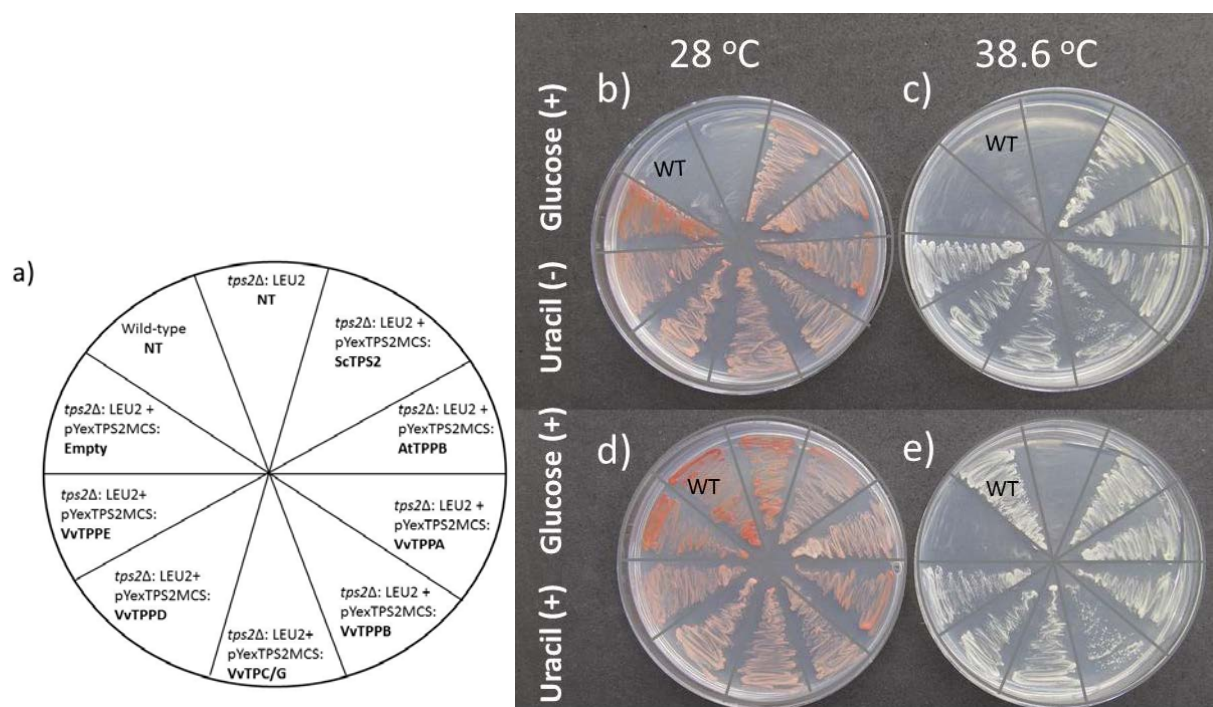


Figure 5.5 Complementation of the yeast *tps2Δ*:*LEU2* genotype with grapevine TPP gene family genes using the endogenous yeast TPS2 promoter.

The yeast genotype was transformed as described in Section 5.2.2 using plasmids containing the native yeast TPS2 promoter to drive transcription of the cloned genes. a) Diagram showing the layout of the transformed yeast colonies on plates shown in (b-e). NT: Not transformed. b) Transformed *tps2Δ*:*LEU2* genotypes containing the cloned genes as listed in (a) growing on selection media after incubation at 28°C. c) Transformed *tps2Δ*:*LEU2* genotypes containing the cloned genes as listed in (a) growing on selection media after incubation at 38.6°C. d) Transformed *tps2Δ*:*LEU2* genotypes containing the cloned genes as listed in (a) growing on complete minimal media after incubation at 28°C. e) Transformed *tps2Δ*:*LEU2* genotypes containing the cloned genes as listed in (a) growing on complete minimal media after incubation at 38.6°C.

Similar to results observed in the grapevine TPS family yeast complementation study, the endogenous ScTPS2 promoter was successful in driving transcription of the VvTPP genes. As complementation of the yeast *tps2Δ* mutation occurred using all of the grapevine TPP genes tested, yeast complementation experiments using plasmids containing the constitutive ScTEF1 promoter were not performed.

5.3.2 Quantitative assays for TPS and TPP gene expression in grapevine tissues by qRT-PCR

To accurately measure TPS and TPP gene expression in grapevine, qRT-PCR assays were done on the tissue types shown in Figure 5.6. Three biological replicates of the nine tissue types were collected from the Lincoln University vineyard and run as described in Section 5.2.3. The raw data was normalized to the geometric mean of the three reference genes found to be most stably expressed in this experimental set as described in Chapter 3 (N2227, SAND, TRU5) and the relative expression of the genes in each tissue type was compared to the expression level of the same gene in veraison berry tissue. After normalization, the relative expression levels of the three biological replicates was tested for differences between the tissue types by analysis of variance (ANOVA) and significant differences between the tissues were tested by the Tukey-Kramer test ($p < 0.5$).

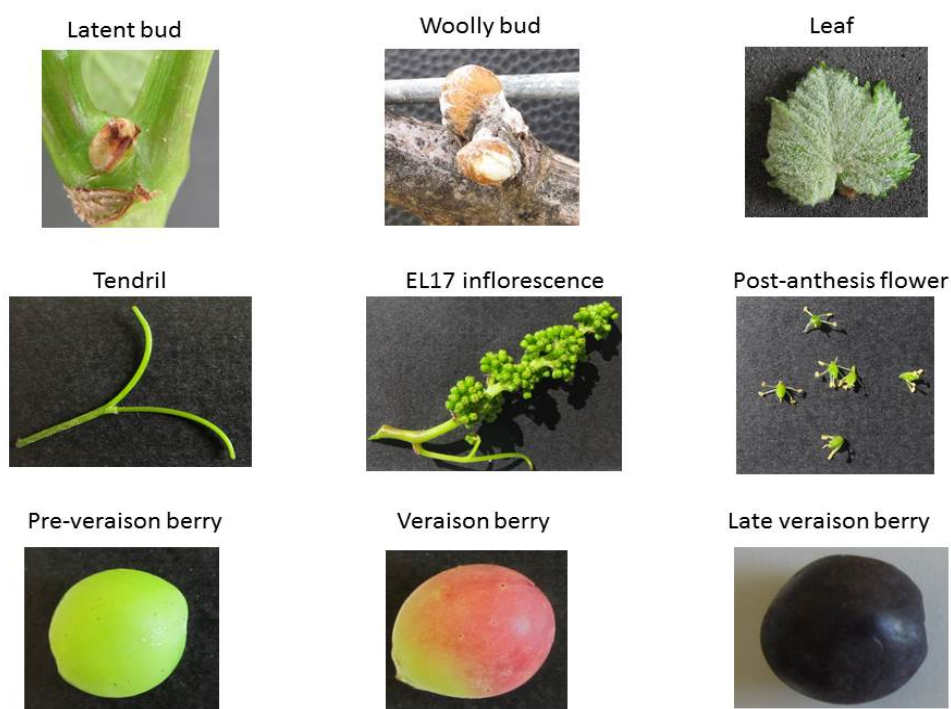


Figure 5.6 Grapevine 'Pinot noir' tissue types used to quantify VvTPS and VvTPP transcript activity by qRT-PCR.

Quantification of VvTPS gene family relative expression in grapevine tissue by qRT-PCR

As shown in Figure 5.7, VvTPS1 had the highest mean expression in woolly buds. As shown by the yeast complementation results discussed in Section 5.3.1 of this Chapter, VvTPS1 is hypothesized to be the only biosynthetically active TPS gene in grapevine. The high expression of VvTPS1 in woolly buds may indicate the increased synthesis of the signal molecule trehalose-6-phosphate (T6P) as the starch reserves within the plant are being broken down into simpler sugars such as sucrose during the transition from dormancy to active growth (Zapata et al., 2004). An alternative reason for increased VvTPS1 expression during this bud developmental stage may be due to the role of T6P in inflorescence architecture (Satoh-Nagasawa et al., 2006). In maize, T6P is believed to regulate determinacy in inflorescences, so the increased VvTPS1 expression in woolly buds may indicate that T6P is also required in grapevine inflorescences to regulate inflorescence differentiation and determinacy as the inflorescence primordia within the woolly buds undergo the final rounds of division and differentiation.

The tissue type with the next highest relative expression of VvTPS1 was post-anthesis flowers (Figure 5.7). This result is similar to transcript experiments performed in *Arabidopsis*, in which AtTPS1 also had high relative expression in flowers (van Dijken et al., 2004). In *Arabidopsis*, it was found that trehalose was necessary for fertile pollen development (Munoz-Bertomeu et al., 2010), so high expression of VvTPS1 in post-anthesis flowers may suggest that a similar trehalose requirement is also involved in grapevine pollen development.

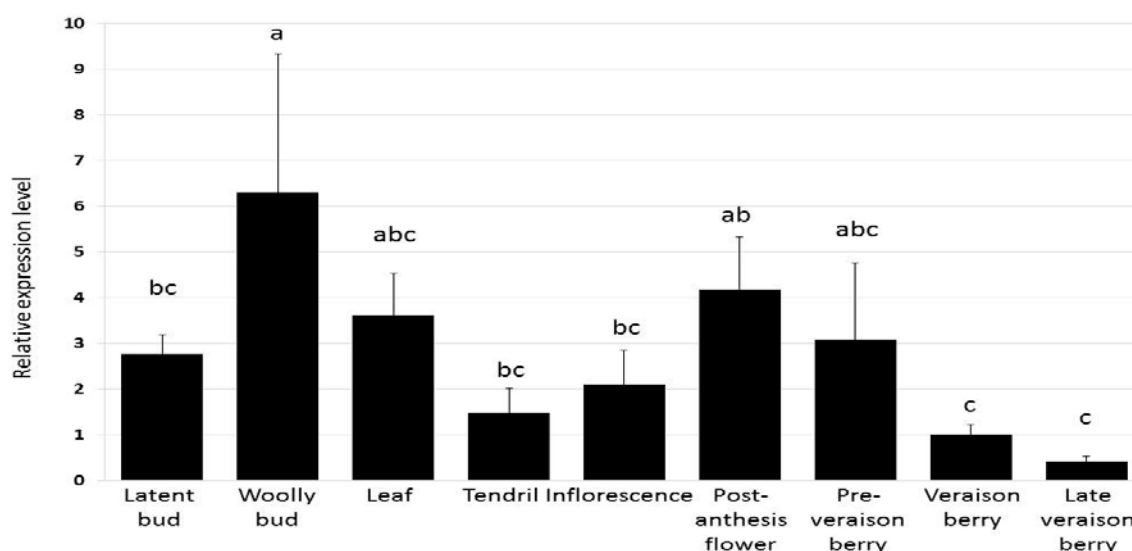


Figure 5.7 Relative expression of VvTPS1 assayed across nine ‘Pinot noir’ tissue types.

The tissues listed below the charts were collected from the Lincoln University vineyard as described in Section 5.2.3. Bars represent the mean of the three biological replicates of each tissue type relative to the veraison berry tissue. Standard deviations of the means are represented by vertical lines above the bars. Tissues with the same letter above the bars indicates the means are not significantly different ($p < 0.05$) as determined by the Tukey-Kramer test after ANOVA.

VvTPS1 was expressed over three times higher in leaves than in the veraison berry reference sample (Figure 5.7). This result is similar to published results in Arabidopsis of AtTPS1 expression, in which young leaves (such as those used in this research) have high relative gene expression (van Dijken et al., 2004; Vandesteene et al., 2010). In addition, AtTPS1 expression in leaves showed a diurnal expression pattern, similar to that of the photoperiod responsive-gene CO1, and Arabidopsis *tps1* mutants have no expression of the floral pathway integrator gene FT (Wahl et al., 2013), indicating that AtTPS1 expression in leaves is necessary for FT floral initiation. A study to determine if VvTPS1 also interacts with flowering pathway genes is discussed in Chapter 7.

There is also somewhat high relative expression of VvTPS1 in latent buds (Figure 5.7). This may suggest that VvTPS1 expression is required in this tissue during the period of inflorescence primordia initiation in grapevine. If so, then variable expression of VvTPS1 in latent buds may suggest a method for inflorescence plasticity and fruitful outer arm development in grapevine. As discussed above, TPS1 expression has been shown to regulate expression of the flowering pathway integrator FT. By altering the timing of FT expression, VvTPS1 may dictate not only the number of inflorescence primordia that develop within a latent bud, but also the size of the primordia that develops before dormancy.

All of the tissues described above are undergoing rapid growth. As such, these tissues would have rapidly dividing cells that would require a lot of energy. The SnRK1 signalling pathway is known for regulating gene transcription based on energy supply (Baena-Gonzalez et al., 2007; Guerinier et al., 2013). The trehalose intermediary molecule T6P has been shown to signal carbohydrate status to the SnRK1 pathway (Zhang et al., 2009). The high levels of VvTPS1 gene expression in rapidly growing tissues suggests that T6P is signalling the carbohydrate status of the plant to the SnRK1 pathway while these tissues develop.

The relative expression of VvTPS1 decreased in the different stages of berries tested. Supplementary material from a recent grapevine berry GeneChip® (Affymetrix, Santa Clara, USA) microarray study, indicated that VvTPS1 decreased at least two-fold in grape berries as they ripened (Lijavetzky et al., 2012). This suggests that the products of the trehalose biosynthesis pathway are not required during the ripening process of grape berries.

VvTPS2 had the highest relative expression in woolly buds, with the mean expression about 3.5 times higher than in the veraison berry reference sample (Figure 5.8). There was also relatively high VvTPS2 expression in latent buds. The high relative expression in the bud developmental stages is quite interesting, and may suggest a role for VvTPS2 in localized signalling within buds. The results from the yeast complementation study described in Section 5.3.1 of this chapter indicate that VvTPS2 is not capable of trehalose biosynthesis. As shown in Figure 4.3 of Chapter 4 (page 44), VvTPS2 has the closest sequence similarity to the Arabidopsis Class II TPS gene AtTPS6. Based on microarray data, AtTPS6 is relatively constitutively expressed during the life cycle, with high expression during the last 5 days of growth (Avonce et al., 2006). These researchers also found AtTPS6 to have specific expression in calli, petals, and embryos (Avonce et al., 2006). The specific expression in calli and embryo tissue of Arabidopsis may suggest a role for AtTPS6 in cell differentiation, which may also infer a role for VvTPS2 in cell differentiation within the bud tissue.

Contrary to the observations of AtTPS6, VvTPS2 did not have significantly higher expression in inflorescences. This suggests that either VvTPS2 is not expressed in petals or it may indicate that the gene is highly specific in petal expression, and the expression of VvTPS2 in petals was overwhelmed by the transcription of other genes in the whole inflorescence examined in this research. The high relative expression of AtTPS6 during the last days of the Arabidopsis life cycle suggests a role for the gene in seed maturation. VvTPS2 relative expression appears to be decreasing during berry development, which is different than the expression pattern of AtTPS6. This may be due to the berry tissue not being late enough during seed development to show an increased expression for VvTPS2. It could also mean that VvTPS2 and AtTPS6 are not involved in seed maturation, but instead are involved in other biological processes that would be occurring during the last days of a plant's life cycle, such as senescence.

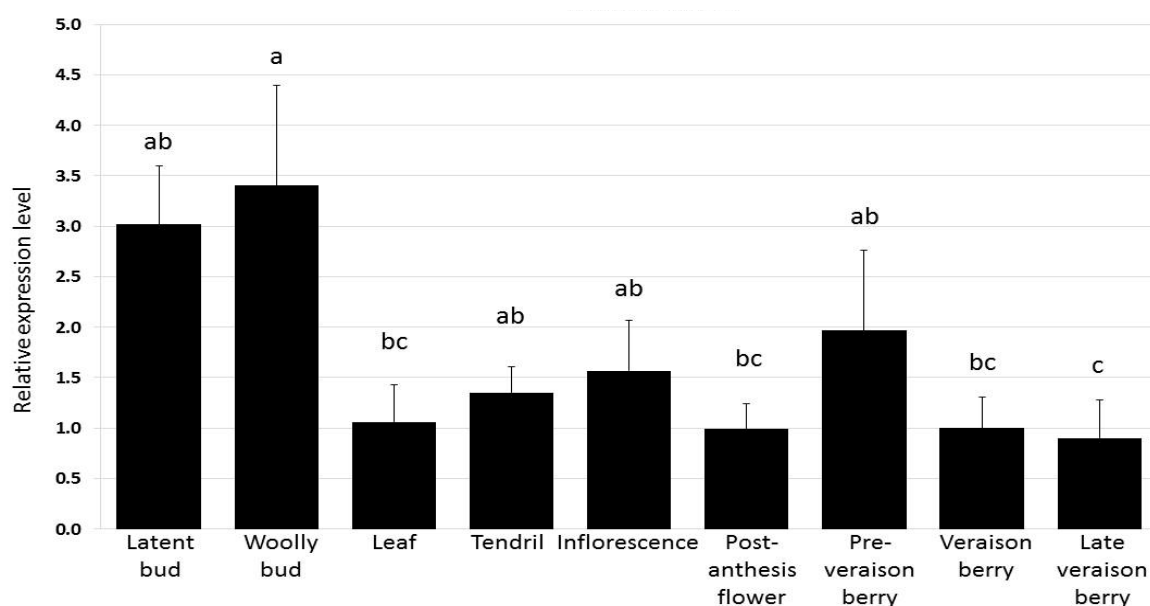


Figure 5.8 Relative expression of VvTPS2 assayed across nine ‘Pinot noir’ tissue types.

The tissues listed below the charts were collected from the Lincoln University vineyard as described in Section 5.2.3. Bars represent the mean of the three biological replicates of each tissue type relative to the veraison berry tissue. Standard deviations of the means are represented by vertical lines above the bars. Tissues with the same letter above the bars indicates the means are not significantly different ($p < 0.5$) as determined by the Tukey-Kramer test after ANOVA.

As shown in Figure 4.3 of Chapter 4 (page 44), VvTPS3 is closest in sequence similarity to the Arabidopsis Class II TPS gene AtTPS5. Microarray data of the Arabidopsis TPS gene family show that AtTPS5 is relatively constitutively expressed, with the highest expression during the early seed development stage (Days 36-44.9) of the life cycle of the plant, and specific expression only in embryos (Avonce et al., 2006). VvTPS3 does appear to be relatively constitutively expressed, with the highest expression in tendril tissues being about 2.5 times higher than veraison berry reference tissue expression and the lowest VvTPS3 expression in late veraison berries being only two-thirds that of the veraison berry reference sample (Figure 5.9). VvTPS3 had relatively high expression in inflorescence and post-anthesis flowers (Figure 5.9), indicating a possible role in inflorescence expression after differentiation of the primordia into the final tissue type. The AtTPS5 protein was found to be able to bind to the T6P substrate UDP-glucose, indicating that it may be involved in localized signalling of trehalose biosynthesis (Harthill et al., 2006). These researchers also found that AtTPS5 is activated by the SnRK1 pathway, indicating that this gene may be involved in downstream signalling within the pathway (Harthill et al., 2006). It would be interesting to determine if VvTPS3 is also regulated by the SnRK1 pathway. A decreasing expression pattern is seen in the berry stages with the VvTPS3 assay (Figure 5.9), with veraison and late veraison berries having significantly lower relative expression than the pre-veraison berry. This suggests that VvTPS3 does not play a role in berry ripening and may indicate regulation of the gene during the ripening process.

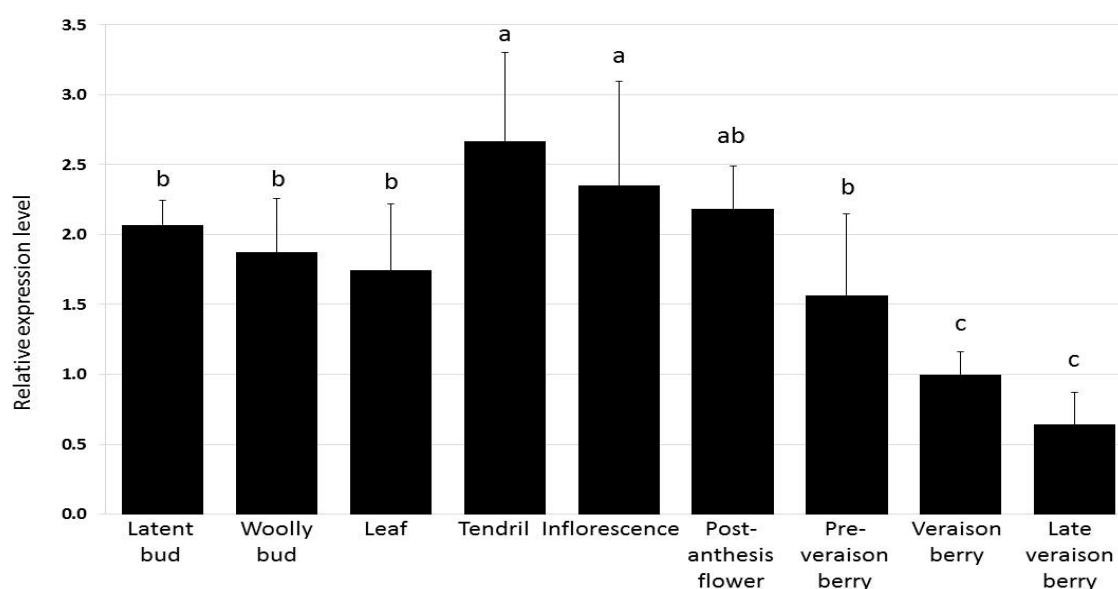


Figure 5.9 Relative expression of VvTPS3 assayed across nine 'Pinot noir' tissue types.

The tissues listed below the charts were collected from the Lincoln University vineyard as described in Section 5.2.3. Bars represent the mean of the three biological replicates of each tissue type relative to the veraison berry tissue. Standard deviations of the means are represented by vertical lines above the bars. Tissues with the same letter above the bars indicates the means are not significantly different ($p < 0.5$) as determined by the Tukey-Kramer test after ANOVA.

VvTPS4 had relatively stable expression across all of the tissue types tested (Figure 5.10), with the difference in expression being only about two-fold between the tissue with the highest relative expression (woolly bud) and the reference sample (veraison berry). As shown in Figure 4.3 of Chapter 4 (page 44), VvTPS4 has the most sequence similarity to the Arabidopsis Class II TPS gene AtTPS7. Microarray data from Arabidopsis found that AtTPS7 had the highest relative expression in the middle of the life cycle of the plant (Days 14-28.9), with specific expression in roots, cauline leaves, petals, and sepals (Avonce et al., 2006). VvTPS4 did not have significantly higher relative expression in inflorescence tissue (which includes petals and sepals). This indicates that either VvTPS4 does not have a similar expression pattern to AtTPS7, or that the expression is so specific in petals and sepals that the transcript signal is overwhelmed by transcript from the rest of the tissue. Based on the results of this research, VvTPS4 appears to have more specificity in bud tissue (latent and woolly) (Figure 5.10). The results from the yeast complementation study described in Section 5.3.1 of this chapter indicate that VvTPS4 is not capable of trehalose biosynthesis, so a more localized signalling role is suggested for this gene. There was slightly less expression of VvTPS4 in tendrils when compared to the expression in inflorescences, although the difference is not significant.

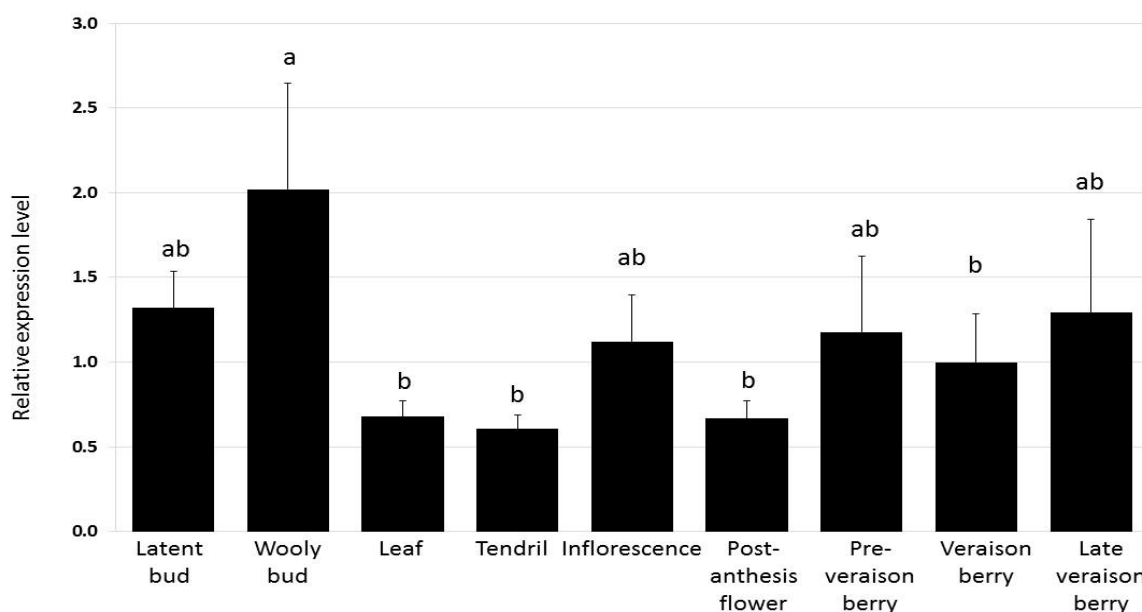


Figure 5.10 Relative expression of VvTPS4 assayed in nine ‘Pinot noir’ tissue types.

The tissues listed below the charts were collected from the Lincoln University vineyard as described in Section 5.2.3. Bars represent the mean of the three biological replicates of each tissue type relative to the veraison berry tissue. Standard deviations of the means are represented by vertical lines above the bars. Tissues with the same letter above the bars indicates the means are not significantly different ($p < 0.5$) as determined by the Tukey-Kramer test after ANOVA.

VvTPS5 had about 2 to 2.5 times the relative expression levels in latent and woolly buds to the veraison berry reference sample (Figure 5.11). This may indicate that VvTPS5 is involved in inflorescence initiation and development in grapevine buds. Further work to examine the role in VvTPS5 during bud development is described in Chapter 7. As shown in Figure 4.3 of Chapter 4 (page 44), VvTPS5 is closest in sequence similarity to the Arabidopsis Class II TPS genes AtTPS 8-10. AtTPS9 and AtTPS10 have 14-3-3 protein phosphorylation sites, indicating that they may be regulated by a signalling cascade (Harthill et al., 2006). It would be interesting to see if VvTPS5 is also regulated by the 14-3-3 signalling cascade. Microarray data in Arabidopsis shows that these three Arabidopsis TPS genes have the highest relative expression early in the life cycle of the plant (Days 1-20.9), with quite similar specific expression patterns for AtTPS9 and AtTPS10 in root tissues (Avonce et al., 2006). The expression of AtTPS9-10 early in the Arabidopsis life cycle and the high relative expression of VvTPS5 in bud tissues suggest that VvTPS5 may have a similar role in grapevine organ differentiation and development. Meanwhile, AtTPS8 expression was more specific to the stem regions in Arabidopsis (Avonce et al., 2006). Neither roots nor stems was analysed in this transcript assay experiment, so similar expression patterns of VvTPS5 to AtTPS8-10 in these tissue types cannot be inferred. The relative expression of VvTPS5 appears to be increasing during the berry ripening process in grapevine, although the differences in expression are not significant.

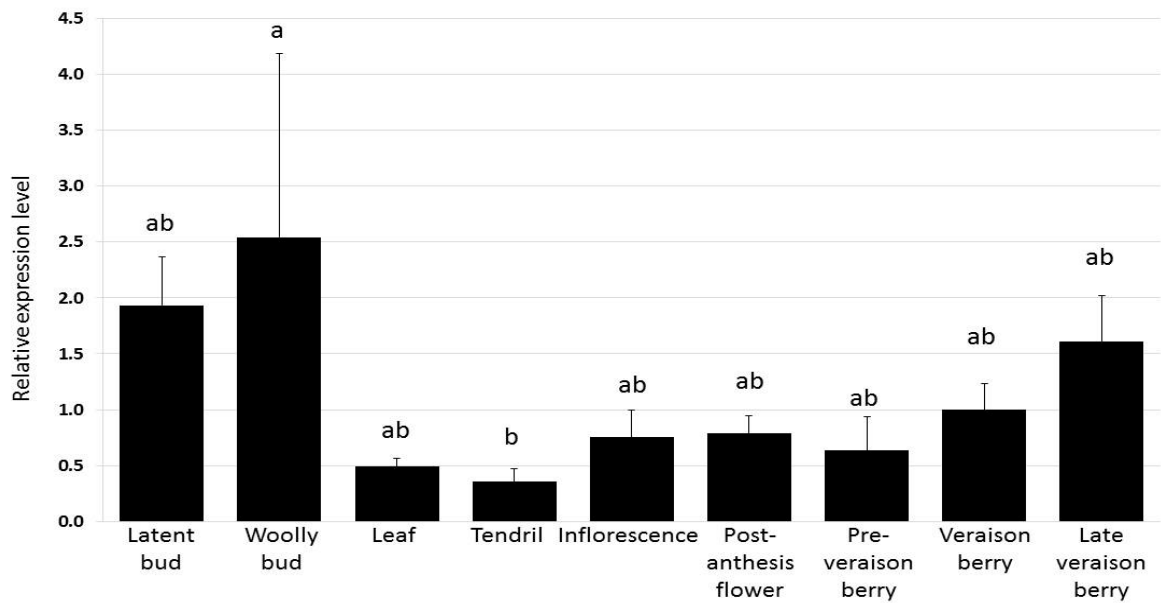


Figure 5.11 Relative expression of VvTPS5 assayed in nine 'Pinot noir' tissue types.

The tissues listed below the charts were collected from the Lincoln University vineyard as described in Section 5.2.3. Bars represent the mean of the three biological replicates of each tissue type relative to the veraison berry tissue. Standard deviations of the means are represented by vertical lines above the bars. Tissues with the same letter above the bars indicates the means are not significantly different ($p < 0.5$) as determined by the Tukey-Kramer test after ANOVA.

VvTPS6 had a high relative expression in woolly bud tissue, but one of the biological replicates had an unusually high level of expression, leading to a very large standard deviation for this tissue type (Figure 5.12). The large standard deviation is observed in many of the woolly bud assays, and is likely due to the large amount of changes that are occurring transcriptionally within this rapidly developing tissue type that cannot be observed physiologically. Nonetheless, the mean relative expression of VvTPS6 in woolly buds was nearly 5 times higher than that of the veraison berry reference sample. As shown in Figure 4.3 of Chapter 4 (page 44), VvTPS6 has the closest sequence similarity to the Arabidopsis Class II TPS genes AtTPS8-10, although the gene was closest in similarity to the Poplar TPS genes PtTPS7 and PtTPS11. No research into the TPS family has been done in poplar. The expression patterns of AtTPS8-10 are described above with VvTPS5. As described above with VvTPS5, the Arabidopsis genes AtTPS9 and AtTPS10 had 14-3-3 protein phosphorylation sites (Harthill et al., 2006). VvTPS6 also had relatively high expression in post-anthesis flowers (Figure 5.12), suggesting a possible role for localized signalling within the mature flower structure. The remaining tissue types used in this transcript experiment showed little difference in VvTPS6 expression. This suggests that either VvTPS6 is fairly constitutively expressed, or that this gene has a more specific expression pattern in woolly buds and mature flowers.

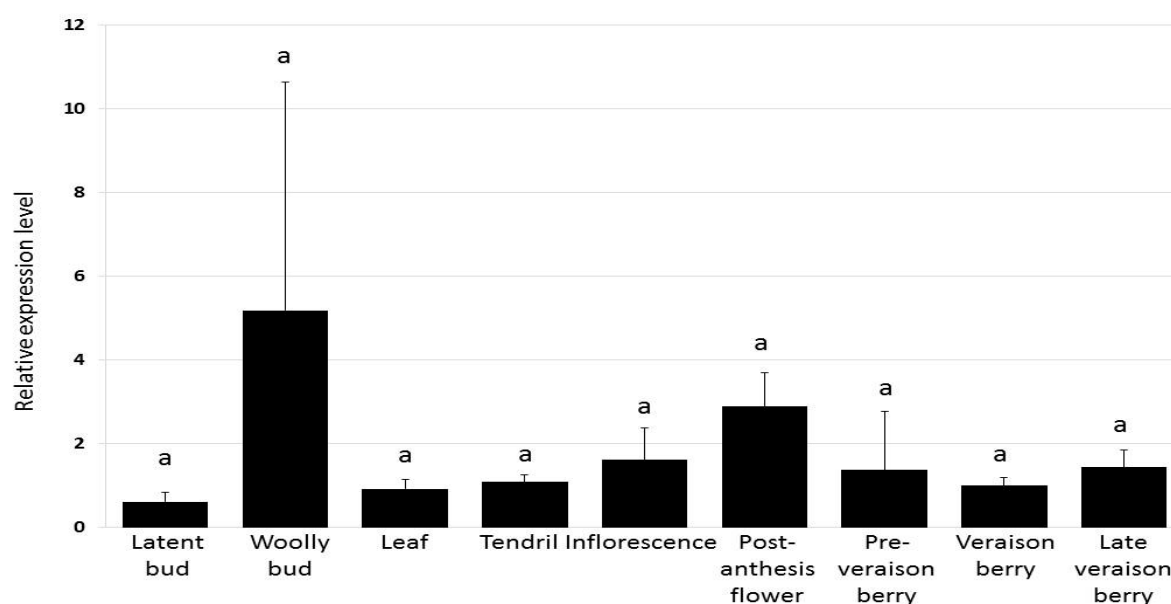


Figure 5.12 Relative expression of VvTPS6 assayed in nine ‘Pinot noir’ tissue types.

The tissues listed below the charts were collected from the Lincoln University vineyard as described in Section 5.2.3. Bars represent the mean of the three biological replicates of each tissue type relative to the veraison berry tissue. Standard deviations of the means are represented by vertical lines above the bars. Tissues with the same letter above the bars indicates the means are not significantly different ($p < 0.5$) as determined by the Tukey-Kramer test after ANOVA.

As noted in Table 5.1 (page 60), the VvTPS7 gene could not be isolated in its entirety from any of the grapevine tissues screened. As shown in Appendix E, the only tissues that amplified a VvTPS7 fragment by RT-PCR were the same tissues in which the closest grapevine homologue (VvTPS4) had the greatest amplification. This suggests that the bands observed for the VvTPS7 could be due to non-specific amplification of VvTPS4 using the VvTPS7 primers. The limited success in identifying VvTPS7 expression in grapevine tissue and the inability to amplify the whole gene made characterization of the gene difficult. As many of the tissue types used to screen for VvTPS7 expression by RT-PCR were also used in this experiment, the gene was not studied in this assay.

The results of the transcriptome assay discussed here show that many of the grapevine TPS family genes have high expression in the same tissues. Many of the VvTPS genes had high relative expression in bud tissues, indicating a possible signalling role for these genes during the development of inflorescences in grapevine. Some of the genes showing high relative expression in bud tissues are investigated further in Chapter 7. The reason for such overlapping expression of genes from the same gene family is perplexing, especially given that only one of these genes (VvTPS1) is biosynthetically active. In rice, it was found that some Class II TPS genes interact with the single rice Class I TPS1 gene (OsTPS1) to form a multi-subunit complex (Zang et al., 2011). A similar TPS complex may occur in grapevine, which would explain the seemingly redundant expression patterns of so many TPS family genes in the species. As described above, the closest VvTPS3

homologue in Arabidopsis (AtTPS5) was shown to be activated by the SnRK1 signalling cascade (Harthill et al., 2006). This may indicate that some Class II grapevine TPS genes may also act downstream of the SnRK1 cascade in regulating plant development. In addition, VvTPS5 and VvTPS6 are highly similar in sequence to Arabidopsis genes that show regulation by the 14-3-3 signal cascade. It would be interesting to determine if the grapevine Class II TPS genes are also controlled by 14-3-3 regulation, as shown for the closest Arabidopsis homologues (AtTPS9-10) (Harthill et al., 2006). Further work into transcript regulation of the grapevine TPS gene family needs to be done to determine whether or not they are involved in signalling cascades.

Quantification of VvTPP gene family relative expression in grapevine tissue by qRT-PCR

As shown in Figure 5.13, the highest mean relative expression of VvTPPA was in woolly bud tissue and the veraison berry reference gene sample. The lowest mean relative expression of VvTPPA was in tendril tissue, which was about ten times lower than the veraison berry reference sample. In grapevine, VvTPPA was previously shown to have high expression in roots and stems, with fairly low expression in leaves (Fernandez et al., 2012). The low expression of VvTPPA in leaves was also observed in this research. In addition, the wider range of tissues examined in this experimental dataset shows the high relative expression of this gene in woolly buds and berries throughout the ripening process (Figure 5.13).

As shown in Figure 4.5 of Chapter 4 (page 48), VvTPPA groups weakly with the Arabidopsis homologue AtTPPA, which is predicted to have roles in wound response, disease resistance, and RNA binding among others (Li et al., 2008), and has a diurnal expression profile (Lunn, 2007). Microarray data of Arabidopsis TPPA gene expression shows relatively high expression patterns during the juvenile stage of the plant's life cycle (Days 14-17.9) with little specific tissue expression except in pollen (Li et al., 2008). The gene specificity of AtTPPA in pollen was not seen in VvTPPA gene expression, as the tissue sample containing pollen grains (post-anthesis flowers) had about three times less expression than the veraison berry reference sample (Figure 5.13). This may reflect a different specificity of VvTPPA gene expression in grapevine or the expression of VvTPPA in pollen grains is so specific that its expression was lost in the transcript pool of the entire mature flower. GUS assays of AtTPPA found the gene to be strongly expressed in young tissues such as root tips, leaf primordia and cotyledons (Vandesteene et al., 2012). The high relative expression of VvTPPA in woolly buds, in which primordia are undergoing rapid development before budburst, suggests that this gene may have a role similar to AtTPPA in grapevine.

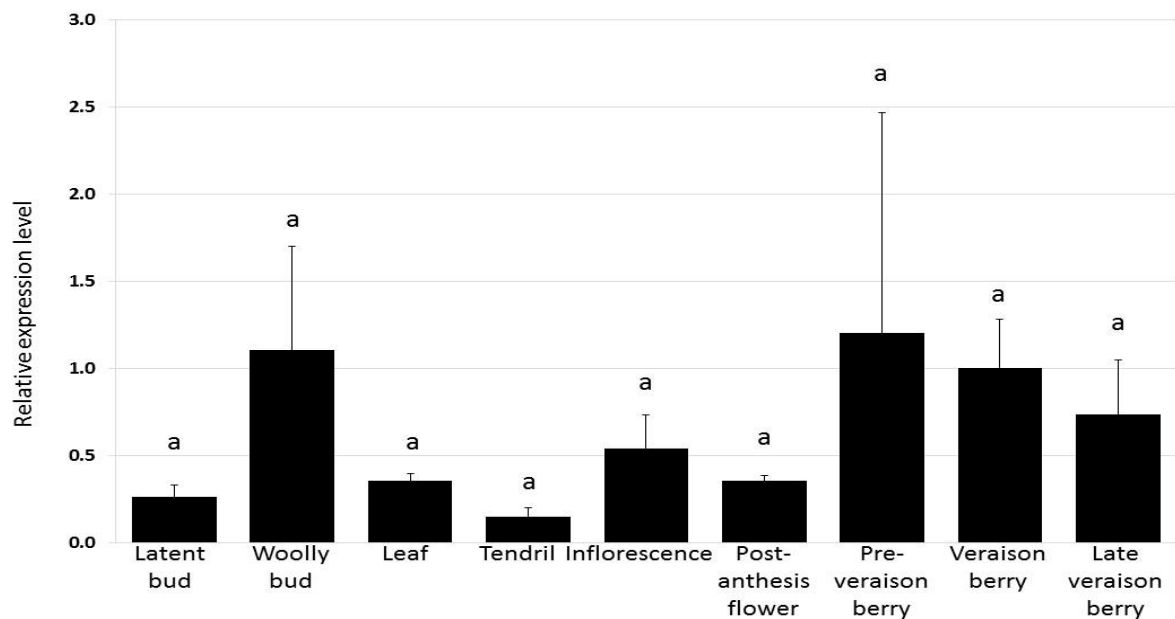


Figure 5.13 Relative expression of VvTPPA assayed in nine ‘Pinot noir’ tissue types.

The tissues listed below the charts were collected from the Lincoln University vineyard as described in Section 5.2.3. Bars represent the mean of the three biological replicates of each tissue type relative to the veraison berry tissue. Standard deviations of the means are represented by lines above the bars. Tissues with the same letter above the bars indicates the means are not significantly different ($p < 0.5$) as determined by the Tukey-Kramer test after ANOVA.

There was a four-fold difference in the expression of VvTPPA between tendrils and inflorescences (Figure 5.13). Although the difference was not significant, it may suggest preferential expression of VvTPPA in fruitful inflorescences when compared to the non-fruitful tendril derived from the same primordia. As discussed in Section 5.3.1 of this chapter, all grapevine TPP genes were capable of complementing the yeast mutant strain lacking TPP activity, indicating that VvTPPA may be involved in T6P phosphorylation.

VvTPPB has significantly higher expression in post-anthesis flowers than the other tissue types tested (Figure 5.14). The high relative expression of VvTPPB in this tissue type may indicate a role for the gene in pollen or ovule development in grapevine. In Arabidopsis, it was found that trehalose was required for viable pollen development (Munoz-Bertomeu et al., 2010), and a similar requirement may be involved in grapevine fertility. VvTPPB also had nearly three times higher expression in EL-17 stage inflorescences (Coombe, 1995) than the veraison berry reference sample (Figure 5.14). As shown in Figure 4.5 of Chapter 4 (page 48), VvTPPB is closest in sequence similarity to the Arabidopsis TPP genes AtTPPB-D. The Arabidopsis gene AtTPPB is believed to be the only gene involved in trehalose biosynthesis (Nunes et al., 2013). Microarray data of AtTPPB-D gene expression shows that AtTPPB-D has the highest relative expression during the juvenile stage of the plant life cycle (Days 14-17.9), with AtTPPB also showing high relative expression during the flowering and seed development stages (Days 29-50) (Li et al., 2008). The Arabidopsis TPP genes closest in

sequence similarity to VvTPPB had specific expression in root tissue (AtTPPB), vascular tissue and seed developmental tissue (AtTPPC), and cells grown in liquid culture (AtTPPD) (Li et al., 2008). VvTPPB did not show increased expression in the berry developmental stages tested here (which would contain the seed tissue), so either VvTPPB is not involved in seed development or the transcript signal was not detectable in the transcript pool for this tissue type. GUS expression assays in *Arabidopsis* found that AtTPPB was expressed in new leaves and root tissue, AtTPPC was weakly expressed at the hypocotyl-root junction, and AtTPPD was expressed at the hypocotyl-root junction and root meristems (Vandesteene et al., 2012). The high expression of AtTPPB in young leaves is not reflected in VvTPPB expression in grapevine leaves, as VvTPPB had the lowest relative expression in this tissue type (Figure 5.14). In grapevine, VvTPPB was previously found to have the highest relative expression in root tissue and low relative expression in stem and leaf tissue (Fernandez et al., 2012). The low relative expression of VvTPPB in leaves found by Fernandez et al. (2012) is confirmed in this research. In addition, the wider range of tissues examined in this experimental dataset shows the high relative expression of this gene in floral structures, particularly post-anthesis flowers (Figure 5.14)

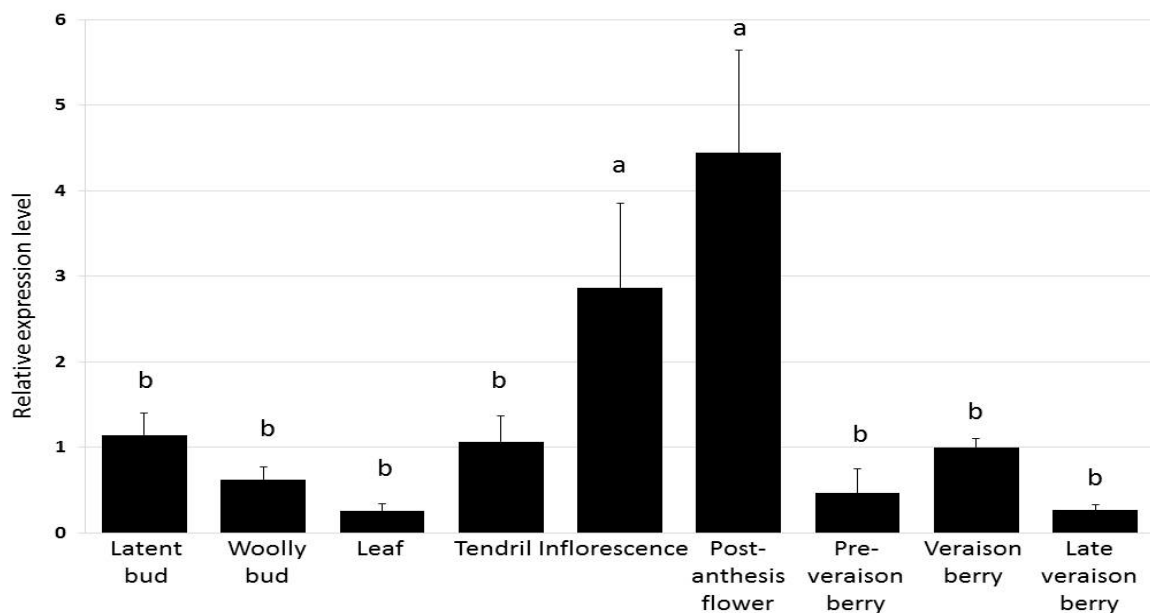


Figure 5.14 Relative expression of VvTPPB assayed in nine ‘Pinot noir’ tissue types.

The tissues listed below the charts were collected from the Lincoln University vineyard as described in Section 5.2.3. Bars represent the mean of the three biological replicates of each tissue type relative to the veraison berry tissue. Standard deviations of the means are represented by lines above the bars. Tissues with the same letter above the bars indicates the means are not significantly different ($p < 0.5$) as determined by the Tukey-Kramer test after ANOVA.

The VvTPPB sequence clusters with the maize RA3 gene (Figure 4.5, page 48), which is of particular interest to this research given its role in regulating inflorescence architecture in maize (Satoh-Nagasawa et al., 2006). The maize RA3 gene encodes a functional TPP gene, as shown by yeast complementation of a strain lacking TPP function (Satoh-Nagasawa et al., 2006). As shown in Section 5.3.1 of this chapter, all grapevine TPP genes are capable of complementing the yeast TPP mutant strain. This suggests that VvTPPB may have a similar function in inflorescence architecture as ZmRA3 gene has in maize. Further investigations into the possible role of VvTPPB expression during inflorescence initiation and differentiation are discussed in Chapter 7.

As shown in Figure 4.5 of Chapter 4 (page 48), VvTPPC and VvTPPG have highly similar sequences, and primers for exclusive amplification of each gene could be developed. VvTPPC and VvTPPG are closest in sequence similarity to the Arabidopsis genes AtTPPF and AtTPPG, which are also likely paralogs (Figure 4.5, page 48). Microarray data of AtTPPF and AtTPPG expression in Arabidopsis shows high relative expression during the seed development stage (Days 36-50) of the life cycle of the plant, with specific expression of both genes in pollen (Li et al., 2008). There is a similar expression pattern of VvTPPC/G specificity observed in both post-anthesis flowers (containing pollen grains) as well as the berry developmental stages used in this research, with VvTPPC/G expression rising to nearly four times higher in late veraison berries than the expression of the gene(s) in veraison berries (Figure 5.15). This suggests that one or both VvTPPC/G genes have similar functions in grapevine as AtTPPF/G has in Arabidopsis; they may be involved in both grapevine fertility and seed development. Gus expression assays in Arabidopsis show specific expression of AtTPPF in anthers and of AtTPPG in root tissue, leaf primordia, and trichomes (Vandesteene et al., 2012). The high relative expression of VvTPPC/G in post-anthesis flowers agrees with the expression pattern observed for AtTPPF in Arabidopsis anthers and suggests that at least one of these genes is involved in pollen development.

As shown in Section 5.3.1 of this chapter, all grapevine TPP genes are capable of complementing the yeast TPP mutant strain. However, only a single grapevine TPP gene is hypothesized to be involved in trehalose biosynthesis. The high relative expression of VvTPPC/G in floral tissue and ripening berries may indicate that this gene is involved in regulation of the signal molecule T6P during these important developmental stages.

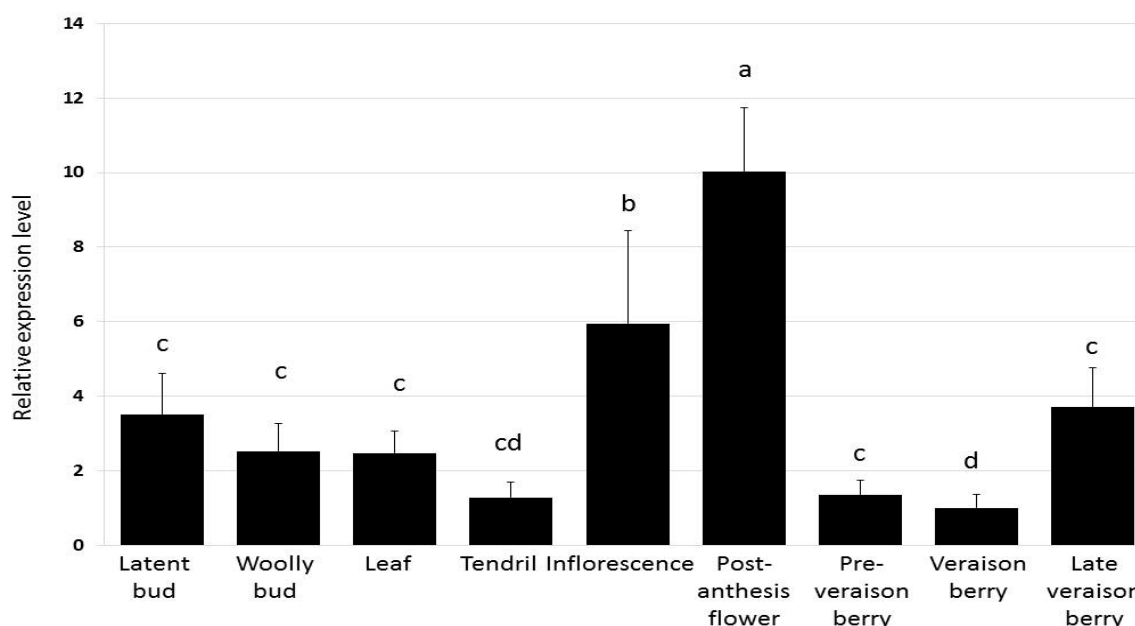


Figure 5.15 Relative expression of VvTPPC/G assayed in nine ‘Pinot noir’ tissue types.

The tissues listed below the charts were collected from the Lincoln University vineyard as described in Section 5.2.3. Bars represent the mean of the three biological replicates of each tissue type relative to the veraison berry tissue. Standard deviations of the means are represented by lines above the bars. Tissues with the same letter above the bars indicates the means are not significantly different ($p < 0.5$) as determined by the Tukey-Kramer test after ANOVA.

In grapevine, VvTPPC expression was previously screened across root, stem, and leaf tissue; it was found to be only expressed in leaf tissue (Fernandez et al., 2012). As shown in Figure 5.15, VvTPPC/G expression in leaves was found to be about two times higher than the reference sample, in agreement with the findings of the previous work (Fernandez et al., 2012). In addition, the wider range of tissues examined in this experimental dataset shows the high relative expression of this gene in many more tissue types, particularly floral tissues and late veraison berries (Figure 5.15).

Figure 5.16 shows very high expression of VvTPPD in post-anthesis flowers (over 100 times higher than the veraison berry reference sample). The other tissues used in the assay show very similar expression patterns to the reference sample. This indicates that VvTPPD is specifically expressed in mature flowers and suggests a role for this gene in grapevine fertility. In grapevine, VvTPPD was previously found to only be expressed in stems (Fernandez et al., 2012). Grapevine stems were not examined in this research, so confirmation of previous expression findings of VvTPPD in grapevine cannot be done. However, the wider range of tissues examined in this experimental dataset allows for the identification of the highly specific relative expression of this gene in post-anthesis flowers (Figure 5.16). VvTPPD does not show sequence similarity to any of the monocot or Arabidopsis TPP genes (Figure 4.5 page 48). Instead, VvTPPD groups with TPP genes from poplar and tomato.

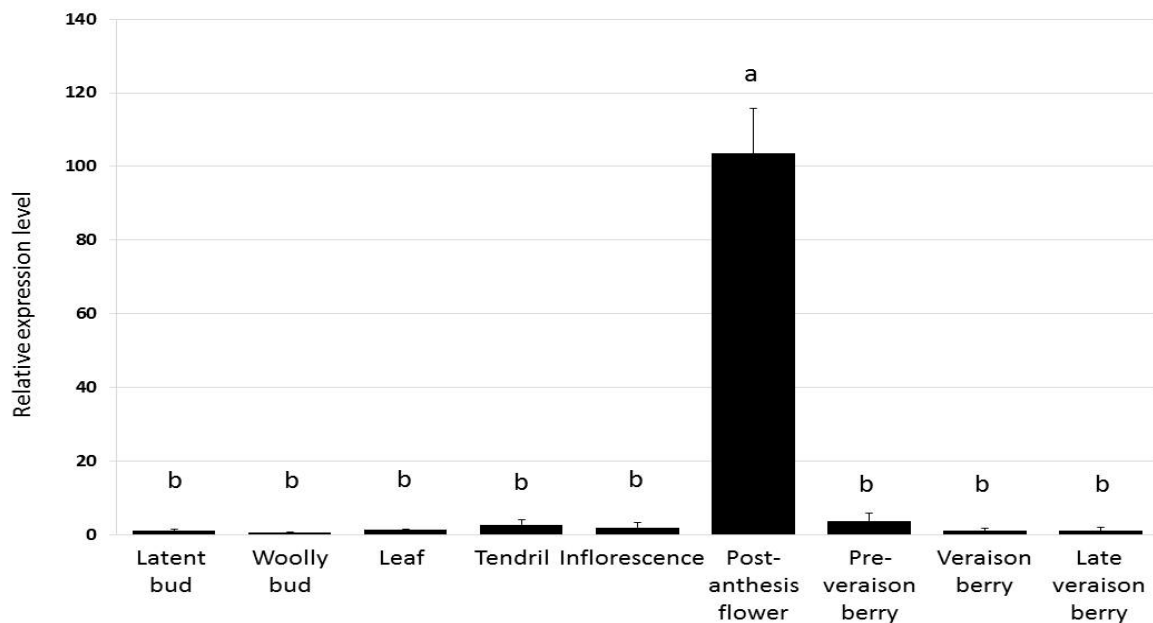


Figure 5.16 Relative expression of VvTPPD assayed in nine ‘Pinot noir’ tissue types.

The tissues listed below the charts were collected from the Lincoln University vineyard as described in Section 5.2.3. Bars represent the mean of the three biological replicates of each tissue type relative to the veraison berry tissue. Standard deviations of the means are represented by lines above the bars. Tissues with the same letter above the bars indicates the means are not significantly different ($p < 0.5$) as determined by the Tukey-Kramer test after ANOVA.

Unfortunately, no research into the TPP gene family has been done in either of these species. As discussed in Section 4.3.1, this suggests this clade of TPP genes may have been lost over evolutionary time. Therefore, the function of VvTPPD in grapevine cannot be inferred from research done in other model plant species. Given the high relative expression in post-anthesis flowers, however, it is clear that VvTPPD is involved in the sexual reproduction of grapevine. As many of the grapevine TPP genes are also highly expressed in post-anthesis flowers, it would be interesting to study further the potential role for this gene family in reproductive fitness in grapevine.

VvTPPE has quite high relative expression in all tissue types tested except for the veraison berry reference tissue and late veraison berry (Figure 5.17). The highest relative expression is in post-anthesis flowers, similar to the high expression pattern of many grapevine TPP genes in this tissue type. In bud tissues, VvTPPE has about 35 times higher relative expression in latent buds and about 25 times higher relative expression in woolly buds than the veraison berry reference tissue. The high relative expression of VvTPPE in bud tissue suggests a possible role for this gene in inflorescence initiation and development in grapevine. In a recent grapevine GeneChip® (Affymetrix, Santa Clara, USA) microarray study, supplementary material provided by the researchers showed VvTPPE decreased at least two-fold in grapevine buds as they developed over the course of two growing seasons (Diaz-Riquelme et al., 2012), which is in agreement with the decrease in relative expression observed in this research (Figure 5.17).

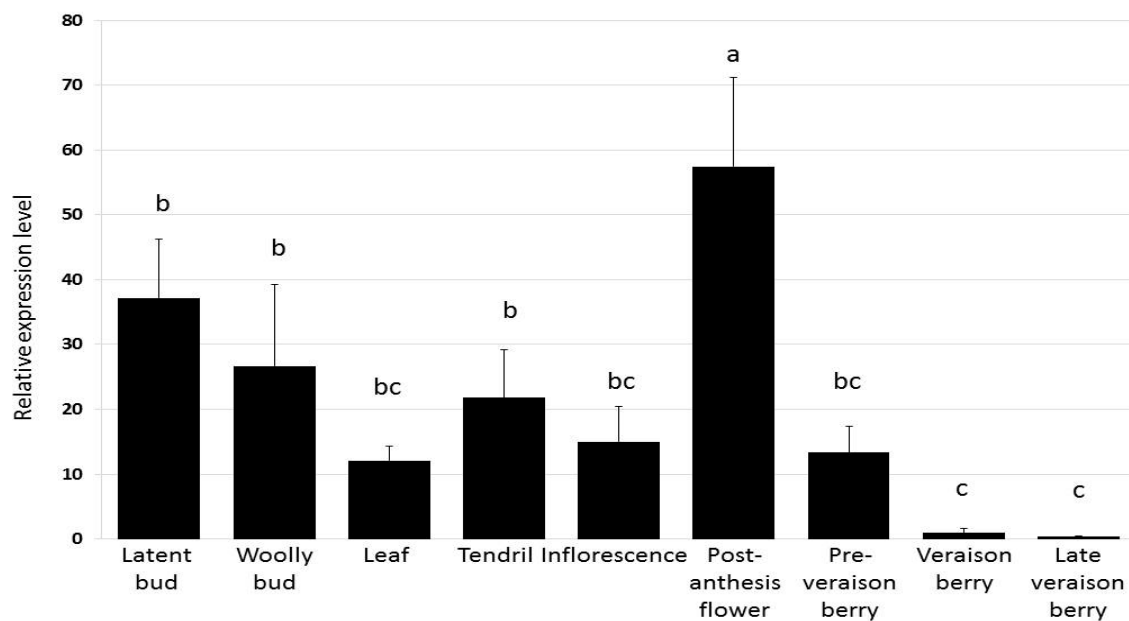


Figure 5.17 Relative expression of VvTPPE assayed in nine ‘Pinot noir’ tissue types.

The tissues listed below the charts were collected from the Lincoln University vineyard as described in Section 5.2.3. Bars represent the mean of the three biological replicates of each tissue type relative to the veraison berry tissue. Standard deviations of the means are represented by lines above the bars. Tissues with the same letter above the bars indicates the means are not significantly different ($p < 0.5$) as determined by the Tukey-Kramer test after ANOVA.

As shown in Figure 4.5 of Chapter 4 (page 48), VvTPPE is highly similar in sequence to the Arabidopsis TPP genes AtTPPE, AtTPPH, AtTPPI, and AtTPPJ. Microarray data of these TPP genes in Arabidopsis shows high relative expression during most stages of the plant’s life cycle (Days 6-50), with specific expression in the inner cell layers, roots, cotyledons, and petioles (Li et al., 2008). VvTPPE expression was not tested on similar tissue types in grapevine, so similarities between VvTPPE and its nearest Arabidopsis homologues cannot be inferred. GUS expression assays of these genes in Arabidopsis found specific expression of the genes in leaves, roots, and stamens (Vandesteene et al., 2012). As shown in Figure 5.17, VvTPPE also had high relative expression in leaves and post-anthesis flowers (containing stamens), indicating that VvTPPE has similar expression patterns to its nearest homologues in Arabidopsis.

Besides the Arabidopsis TPP genes, the VvTPPE sequence (along with VvTPPB) also groups with the maize RAMOSA3 (RA3) gene (Figure 4.5, page 48), which has been shown to influence inflorescence architecture (Satoh-Nagasawa et al., 2006). As discussed with VvTPPB, this suggests that VvTPPE may have a similar role in regulating inflorescence architecture in grapevine. The ability of all grapevine TPP genes to complement a yeast mutant strain lacking TPP activity suggests that VvTPPE is capable of trehalose biosynthesis in grapevine, as discussed in Section 5.3.1 of this chapter. Investigations into the possible role of VvTPPE in trehalose biosynthesis and grapevine inflorescence architecture regulation are discussed in Chapter 7.

In grapevine, VvTPPE was previously found to be expressed in all tissue types examined (root, stem leaf), with the highest expression in stems (Fernandez et al., 2012). Stem tissue was not examined as part of this research, so confirmation of the high relative expression of VvTPPE in grapevine stems cannot be made. However, the wider range of tissues examined in this experimental dataset shows the high relative expression of this gene in all tissues examined, except berries from the veraison stage and later (Figure 5.17).

The VvTPPF gene was not studied in this assay. As discussed in Appendix E, VvTPPF only showed a faint band after RT-PCR on an agarose gel that could not be dismissed as an artefact of the gel. As the tissue types used for RT-PCR were also used to assay gene transcript activity in this experiment, it was decided to exclude VvTPPF in this gene expression assay.

The results of the transcriptome assay discussed here show that many of the grapevine TPP family genes have high relative expression in the same tissues. Such overlapping expression of genes from the same gene family is surprising, especially given that all of these genes are capable of dephosphorylating T6P into trehalose. As discussed in Section 5.3.1, only one grapevine TPP gene is hypothesized to be involved in trehalose biosynthesis, given that there is only one Arabidopsis TPP gene that is involved in the trehalose biosynthesis pathway. Instead, the other Arabidopsis genes are believed to be involved in regulation of the signal molecule T6P in a highly specific manner (Vandesteene et al., 2012). Therefore, the high relative expression of so many grapevine TPP gene family genes in post-anthesis flowers in particular is quite perplexing as several genes seem to overlap in specificity. The high relative expression of so many VvTPP genes may indicate a highly localized and specialized role for these TPP genes in pollen fertility, ovule development, and seed development in grapevine. Further work into the reproductive fitness of grapevine needs to be done to elucidate the role of the grapevine TPP gene family in fertility.

Of particular interest to this research is the high relative expression of many of the grapevine TPP genes in bud stages, particularly the maize RA3 homologues VvTPPB and VvTPPE. Further analysis into the potential roles of these genes, as well as VvTPPA, in relation to flowering pathway genes during inflorescence initiation and development is described in Chapter 7.

5.4 Conclusions and future prospects

The trehalose biosynthesis pathway is of much interest to plant researchers, initially due to its role in abiotic defence (Muller et al., 1995; Elbein et al., 2003) and more recently because of its role in inflorescence architecture (Satoh-Nagasawa et al., 2006) and carbohydrate status signalling (Zhang et al., 2009; O'Hara et al., 2013). Recently, trehalose biosynthesis was investigated in grapevine, with partial characterization of the TREHALOSE-6-PHOSPHATE SYNTHASE (TPS) and TREHALOSE-6-

PHOSPHATE PHOSPHATASE (TPP) gene families published (Fernandez et al., 2012). As part of this current research, the grapevine genome has had seven TPS and seven TPP genes identified. In our investigations into grapevine inflorescence architecture and outer arm development, the characterization of these VvTPS and VvTPP genes was carried out by a series of experiments to identify a) whether the genes were present in grapevine, b) identify biosynthetically active VvTPS and VvTPP genes, and c) quantify VvTPS and VvTPP expression in grapevine tissue. This current work confirms many of the findings of the previous research into trehalose biosynthesis in grapevine, and supplements their work with screening of additional grapevine TPS and TPP family genes and tissue types, with a focus on the role of the pathway in inflorescence architecture and carbohydrate signalling.

5.4.1 Grapevine TPS and TPP genes can complement yeast mutant strains

To test for trehalose biosynthesis capability in the grapevine TPS and TPP genes identified in Chapter 4, a series of complementation experiments using the model organism *Saccharomyces cerevisiae* (Baker's yeast) was performed. Yeast genotypes that had mutant TPS or TPP genes were transformed with plasmids developed as described in Chapter 2 containing the grapevine TPS or TPP genes. For the VvTPS genes, the yeast *tps1Δ:TRP1* mutant was transformed with plasmids that utilized either the endogenous yeast TPS1 promoter or the yeast constitutive TEF1 promoter. As shown in Figure 5.8, the only grapevine gene capable of complementing the yeast *tps1Δ:TRP1* mutant was the Class I grapevine TPS gene VvTPS1. This is similar to results observed in Arabidopsis, where only the Arabidopsis Class I TPS gene (AtTPS1) was able to complement the yeast *tps1Δ* mutant (Vandesteene et al., 2010). As no grapevine Class II TPS genes were able to complement the yeast *tps1Δ* mutant, regardless of which promoter was used, it was determined that using the native yeast TPS1 promoter was just as effective in complementation experiments as the constitutive promoter. To the best of our knowledge, no other researchers have investigated using the native TPS1 promoter in yeast complementation experiments. To further test the efficiency of grapevine TPS1 in replacing the mutant *tps1Δ* enzyme in the yeast trehalose enzyme complex, kinetic experiments designed to measure growth of the transformed yeast *tps1Δ:TRP1* containing VvTPS1 or ScTPS1 (control) over a period of time can be done. This will help to quantify the ability of the complemented yeast containing the grapevine TPS gene to grow in relation to the native yeast TPS1 gene.

In the complementation experiments for the grapevine TPP gene family, the yeast *tps2Δ:LEU2* genotype was transformed with plasmids that had the VvTPP genes driven by the endogenous yeast TPS2 promoter. As shown in Figure 5.9, all of the grapevine TPP genes were able to complement the yeast *tps2Δ* mutant using the native TPS2 promoter. This indicates that the native yeast TPS2

promoter is sufficient to activate transcription of the grapevine TPP family genes. In addition, the successful complementation of the yeast *tps2Δ* mutant shows that all of the grapevine TPP genes seem capable of functioning in the yeast trehalose synthase enzyme complex. This confirms the results for VvTPPA as published by Fernandez et al. (2012) and is similar to results observed in the Arabidopsis TPP gene family (Vandesteene et al., 2012). As in the grapevine TPS gene family complementation study, a series of kinetic experiments to measure the efficiency of grapevine TPP gene complementation in the yeast *tps2Δ* mutant using ScTPS2 as a control would assist in measuring the enzyme activity of the grapevine TPP genes in relation to the endogenous yeast TPP enzyme.

5.4.2 Transcript variation of grapevine TPS and TPP genes among different tissues

To accurately measure TPS and TPP gene expression in grapevine, a series of transcription assay experiments were undertaken to quantify transcript abundance of the genes within grapevine tissues. As described in Section 5.3.2, VvTPS and VvTPP genes were screened on 'Pinot noir' tissue collected from the Lincoln University vineyard during the course of a growing cycle and the relative expression of the VvTPS and VvTPP genes were compared to the veraison berry tissue in the remaining tissues.

The lone Class I grapevine TPS gene (VvTPS1) had the highest relative expression in woolly buds and the lowest relative expression in late veraison berries (Figure 5.7). The remaining Class II grapevine TPS genes tested (VvTPS2-6) all had higher relative expression levels in the bud developmental stages when compared to the veraison berry tissue (Figures 5.8-5.12), with the exception of VvTPS6 expression in latent buds, which was slightly lower in expression when compared to the veraison berry tissue (Figure 5.12). The overlapping expression of so many grapevine TPS genes in bud tissue suggests that regulation of trehalose biosynthesis is tightly regulated in this tissue. Further work investigating the role of some of these genes in relation to flowering during bud development is discussed in Chapter 7.

With the exception of VvTPPA (Figure 5.13), all of the VvTPP genes had high relative expression in post-anthesis flowers when compared to the veraison berry reference sample (Figures 5.14-5.17). VvTPPD had the highest relative expression of all the grapevine TPP genes in post-anthesis flowers, with more than a 100-fold difference in expression (Figure 5.16). This may be due to the need for trehalose in grapevine fertility, as was observed in Arabidopsis pollen (Munoz-Bertomeu et al., 2010). The overlapping expression of so many grapevine TPP genes in post-anthesis flowers suggests that trehalose biosynthesis is highly localized and tightly regulated in this tissue. The potential role of grapevine TPP genes in fertility is quite interesting and would be of great value to investigate.

Many of the grapevine TPP genes also had higher relative expression in the bud tissues tested when compared to the veraison berry reference sample (Figures 5.13-5.17). This suggests that trehalose biosynthesis is tightly regulated in buds and may indicate a role for these genes in inflorescence development within the tissue. As some of the grapevine TPP genes (VvTPPB and VvTPPE) are similar in sequence to the maize RAMOSA3 gene, it is of particular interest to this research to determine whether TPP expression in grapevine can affect inflorescence architecture as observed with the maize RAMOSA3 gene. Investigations into the possible role of some of these TPP genes during bud development in relation to the flowering pathway are described in Chapter 7.

5.4.3 Future work in grapevine TPS and TPP characterization

Although a strong foundation for characterization of the trehalose biosynthesis pathway in grapevine has begun with the results of this work, there is still a lot of work that needs to be done to fully understand the role of this pathway in grapevine. Of particular interest to this work is the localization of trehalose pathway genes in grapevine buds, either during inflorescence primordia initiation or outer arm differentiation. In an attempt to localize gene expression activity *in situ*, probes have been developed to identify transcript activity for some of the grapevine trehalose pathway genes (VvTPS1 and VvTPPE). Grapevine buds have been collected and processed for microscope sectioning several times, but complications with natural disasters (the 2010 and 2011 Christchurch earthquakes) and subsequent access to suitable equipment have led to poor tissue preservation, leading to unusable samples. A final round of tissue collection was processed recently, and it is hoped that the tissue will be viable and sufficient for use in *in situ* hybridization experiments.

As described in Section 5.4.1, a series of yeast kinetic experiments should help to characterize the biosynthetic capability of the grapevine TPS and TPP genes in a model species. Other biochemical experiments can also be performed to help elucidate the role of VvTPS and VvTPP in grapevine. In yeast, trehalose is synthesized in a multi-enzyme complex (Bell et al., 1998) and inclusion in complexes have been suggested for Class II TPS family enzymes in Arabidopsis (Geelen et al., 2007) and rice (Zang et al., 2011). To test if similar complexes are involved in grapevine Class II TPS enzyme activity, yeast-two hybrid assays using grapevine cDNA in the bait plasmid can be carried out to identify possible enzyme complex partners.

In addition to the role of grapevine Class II TPS genes in complexes, further research into TPS gene involvement in signalling pathways such as the SnRK1 and 14-3-3 signalling cascades would be very informative. Experiments such as kinase activity assays would help to identify which grapevine TPS genes are involved in signalling within the plant. As research into signalling cascades in other plant species expands, it is becoming clear that plant development is quite complex and signalling plays a very important role.

Besides the complex formation and signalling roles of the TPS and TPP enzymes, measurements of the metabolites formed during trehalose biosynthesis would aid in elucidating the role of this pathway in grapevine. Both trehalose and its precursor T6P are rapidly synthesized and degraded in most plant species (Muller et al., 1995; Goddijn et al., 1997), making measurements of these metabolites difficult. Currently, the method used for measuring T6P levels in plants employs liquid chromatography coupled to tandem mass spectrometry (LC-MS/MS), which is not sensitive enough for trehalose measurements (Carillo et al., 2013). Instead, trehalose levels in plants are measured using gas chromatography coupled to mass spectrometry (GC-MS) (Parrou and Francois, 1997), which involves very expensive equipment. During the course of this research, we attempted to measure the levels of T6P and trehalose in latent bud tissue with LC-MS using an MS ion trap. Unfortunately, this method was not sensitive enough to measure either T6P or trehalose in the tissues sampled. Accurate measurements of T6P and trehalose require equipment not currently available at Lincoln University. Recently, a protocol was published that allowed for accurate measurement of both T6P and trehalose after enzymatic digestion in plant tissue using LC-MS/MS (Carillo et al., 2013). As LC-MS/MS is somewhat less expensive and more available than GC-MS equipment, it may be possible to measure the metabolites from the trehalose pathway in grapevine using this protocol. This will require some time to prepare the samples and cost involved in shipping and processing the material, but will provide valuable information regarding trehalose biosynthesis in grapevine.

The role of the grapevine TPS and TPP gene families in the grapevine species needs to be fully elucidated. This is typically done by transforming the species with constructs to either overexpress or silence the genes of interest. As grapevine is a woody perennial, stable transformation experiments in the species takes a very long time to complete (about three years). During the course of this research, a set of overexpression and silencing constructs for two of the genes (VvTPS1 and VvTPPE) were developed in an attempt to transform grapevine somatic embryos for characterization of these two genes in the species. These experiments were abandoned due to time constraints and the limited space available for transgenic plants on the Lincoln University campus. Hopefully, transformation of grapevine to either reduce or overexpress the TPS and TPP gene families will be done at some point. Transformation experiments are the best way to conclusively prove which genes are involved in trehalose biosynthesis (as hypothesized for VvTPS1), enzyme complex formation or signalling cascades (as hypothesized for Class II TPS genes), grapevine fertility (as hypothesized for most TPP genes), and inflorescence architecture (as hypothesized for many TPS and TPP genes).

Chapter 6

Characterization of the BA1/LAX1 gene in grapevine

6.1 Introduction

The BARREN STALK1/LAX PANICLE1 (BA1/LAX1) gene family is a clade of the large basic helix-loop-helix (bHLH) transcription factor gene family. Mutants of the BA1/LAX1 clade have been shown to alter inflorescence morphology in plants (Komatsu et al., 2003; Gallavotti et al., 2004; Yang et al., 2012). In maize, the *barren stalk1* (*ba1*) phenotype is characterized by a complete lack of tillers, axillary buds, and female inflorescences (ears) while the male inflorescences (tassels) are of reduced length with no secondary branching (Gallavotti et al., 2004). In rice, the *lax panicle 1* (*lax1*) phenotype is characterized by reduced inflorescence (panicle) branches and a reduction or complete loss of flowers (spikelets) (Komatsu et al., 2001). In Arabidopsis, the BA1 orthologue REGULATOR OF AXILLARY MERISTEM FORMATION (ROX) was shown to have a similar, but less intense phenotype. Arabidopsis *rox* mutants had reduced lateral branching from the basal axils of the plant when grown in short day conditions, then transferred to long-day photoperiods (Yang et al., 2012). This phenotype was overcome as the plant matured, with normal lateral branching and floral development occurring (Yang et al., 2012). The milder mutant phenotype in Arabidopsis was in part explained as being due to the reduced number of branching events that occur in the species when compared to the multiple branching events that occur in grasses, as well as possible redundant regulation with the axillary meristem regulator genes LATERAL SUPPRESSOR (LAS) and REGULATOR OF AXILLARY MERISTEM (RAX) controlling lateral bud development in the species (Yang et al., 2012).

Besides the possible redundant regulation of lateral bud development in Arabidopsis, the slight phenotype observed in *rox* mutants may be due to the linkage of the AtROX gene to an APRATAXIN (APTX) gene. In sequence databases, such as TAIR and NCBI, the Arabidopsis ROX gene is annotated as the first exon of the APTX gene. Previous work by other researchers shows that AtROX can be successfully isolated by itself by RT-PCR (Woods et al., 2011; Yang et al., 2012). However, the putative STOP codon for AtROX is located within the predicted first intron and the next potential START codon for APTX is in the middle of the second predicted exon of AtAPTX. In addition, sequence and phylogenetic tree analysis results described in Section 4.3.2 of Chapter 4 indicates that AtROX is not in the BA1/LAX1 clade of bHLH genes. Therefore, the tightly linked AtROX gene to AtAPTX suggests that AtROX may not in fact be involved in lateral bud development, but have a completely different function altogether.

Transcription factors bind directly to DNA to promote or inhibit transcription. Transcription factors are classified based on their DNA-binding regions (Latchman, 1993). The bHLH transcription factor group is characterized by having two α -helices separated by a loop, with the DNA binding motif helix containing a large number of basic amino acids (Carretero-Paulet et al., 2010). In plants, bHLH transcription factors have been shown to be involved many processes- from pathogen resistance to hormone signalling to flowering (Gallavotti et al., 2008; Carretero-Paulet et al., 2010; Ito et al., 2012; Kumar et al., 2012). bHLH transcription factors are known to bind to DNA at E-box sites (5'CANNTG3') in the promoter region of genes (Carretero-Paulet et al., 2010). The bHLH clade that includes BA1/LAX1 is not believed to bind to the typical E-box site of other bHLHs, but where or how it binds to DNA is currently unknown (Gallavotti et al., 2004). This clade comprises both monocots and dicots, although the two groups form separate branches within the clade (Woods et al., 2011). Within the dicot branch of the BA1/LAX1 bHLH clade, Woods et al. (2011) mapped one putative grapevine BA1/LAX1 homologue, indicating the presence of at least one BA1/LAX1 gene in the species.

In maize, the BA1 gene was shown to control sites of tissue divergence by limiting auxin transport into dividing cells (Gallavotti et al., 2008; Woods et al., 2011). Auxin is a group of plant hormones that maintains apical dominance by repressing cytokinin synthesis (another group of plant hormones), which are responsible for promoting cell division (Müller and Leyser, 2011). Auxin is produced in higher quantities in the shoot apex of a growing plant (Ljung et al., 2001) and is transported down the plant through the phloem to the roots in a process called polar auxin transport (Müller and Leyser, 2011). The maintenance of the auxin polar gradient is believed to control apical dominance. Changes in auxin levels within the plant are believed to cause lateral branching to occur by a negative feedback loop with cytokinin synthesis (Müller and Leyser, 2011). As cytokinins are produced throughout the plant, activation of cytokinin synthesis in turn activates mitosis and undifferentiated cells (such as inflorescence primordia) begin to differentiate (Müller and Leyser, 2011). Lateral branching begins when the auxin gradient within the stem is altered by a pooling of auxin in the L1 layer of the stem adjacent to the primordia (Heisler et al., 2005). The auxin pooling is caused by differential expression of the auxin efflux transporter PINFORMED (PIN; Heisler et al., 2005).

In maize, the PIN auxin transporter is highly expressed at all branching points during the plant's development (Gallavotti et al., 2008). The increase in PIN expression in turn leads to increased auxin accumulation within the L1 cell layers (Gallavotti et al., 2008), which then leads to the development of new organs or meristems. These new organs or meristems then develop independently of the primary organ or meristem, as per the conversion model of meristem development as proposed by Irish (1997). The maize BA1 gene was found to regulate axillary meristem formation by limiting polar

auxin transport upstream of PIN from subtending bracts on the inflorescence meristem to the potential site of the new axillary meristem (Gallavotti et al., 2008). In the conversion model of meristem development, this suggests that BA1 can regulate not only the development of lateral branching in vegetative and reproductive structures upstream of the polar auxin transport pathway, but also the branching events that occur on these lateral branches once they have begun development independently of the primary meristem.

In agreement with its role as a “gatekeeper” of auxin transport, BA1/LAX1 expression is highly localized. *In situ* experiments from several plant species show BA1/LAX1 expression in an arc pattern in anlagen at the border between the stem and the primordia as well as at the border between secondary branching events in inflorescence meristems and floral meristems (Gallavotti et al., 2004; Woods et al., 2011). BA1/LAX1 is believed to control the overall size of the developing anlagen by regulating the number of cells that accumulate in the anlagen before differentiation (Gallavotti et al., 2004). As BA1/LAX1 is expressed both before and after anlagen initiation as described above, it is believed to have dual roles as an auxin regulator (in anlagen differentiation) and as an auxin signal (in anlagen initiation) (Gallavotti et al., 2008). Intriguingly, the auxin efflux transporter PIN is also highly localized to a narrow region in the meristem between the primary shoot and the branch point (Reinhardt et al., 2003). If BA1/LAX1 does in fact regulate branching upstream of the polar auxin transport, it may be regulating the expression of PIN at the branching boundary.

In grapevine, the inflorescences for the following growing season are formed during the current growing season within the latent bud located on the base of each petiole along the shoot (Morrison, 1991). The inflorescence primordia develops from undifferentiated primordia (anlagen) that appears after three to eight leaf primordia develop within the latent bud (Srinivasan and Mullins, 1981). Anlagen can develop into inflorescence primordia, tendril primordia, or a combination of the two tissue types (May, 2004). Typically the first few anlagen formed become inflorescences, while the anlagen that form later develop into tendrils (Boss et al., 2003). Differentiation of the anlagen into the final tissue type begins during anthesis of the current year’s inflorescences (Morrison, 1991). For anlagen that become inflorescences, the tissue undergoes an initial division which will later become the main inflorescence and the outer arm (Srinivasan and Mullins, 1981). The main inflorescence primordia undergoes several rounds of branching to form secondary and tertiary branch primordia before entering dormancy (Srinivasan and Mullins, 1981; May, 2004; Vasconcelos et al., 2009). The outer arm primordia also undergoes some branching (Srinivasan and Mullins, 1981), but significantly less than the main branch primordia. BA1/LAX1 expression in the inflorescence primordia at different stages of the growth cycle may explain how a single inflorescence primordia can have such a wide range of phenotypes after differentiation.

To elucidate the role of BA1/LAX1 in grapevine, expression of the gene across several grapevine tissues was investigated by a transcript assay experiment. Complementation experiments using the Arabidopsis BA1/LAX1 homologue mutant *rox* were initiated, but given the recent publication of its minor mutant phenotype (Yang et al., 2012) and poor sequence homology to the other members of the BA1/LAX1 clade of the bHLH gene family as discussed in Section 4.3.2 of Chapter 4, it was decided that the Arabidopsis *rox* mutant was not suitable for complementation with VvBA1/LAX1. The results described below show that the single VvBA1/LAX1 gene identified in Chapter 4 is expressed during times of rapid cell division, suggesting a role for VvBA1/LAX1 in auxin-mediated regulation of development- similar to the observations seen in other species.

6.2 Materials & Methods

6.2.1 Cloning of VvBA1/LAX1

VvBA1/LAX1 expression was verified in grapevine by RT-PCR as described in Appendix E, and then the whole gene was amplified from the cDNA sample showing the strongest expression using TaKaRa PrimeStar™ reagents (Norrie Biotech, NZ). The reaction was set up as a “proofreading PCR” as described in Appendix A using VvBA1/LAX1 primers (Appendix B) containing the CACC leader sequence on the forward primer for topoisomerase cloning in the Invitrogen pENTR™/D-TOPO® cloning kit (Invitrogen, NZ). The PCR product was run on a 1% agarose gel and excised for purification. The PCR products were gel purified using the Axygen® Axyprep™ DNA Gel Extraction Kit (Raylab, NZ). The purified PCR product was cloned into the Invitrogen pENTR™/D-TOPO® cloning kit (Invitrogen, NZ) as per the manufacturer’s instructions. The cloned plasmid was transformed into *E. coli* DH5α competent cells by heat shock as per the kit’s protocol and plated onto LB plates (Appendix C) containing 50mg/L kanamycin. Transformed colonies were checked for the presence of the plasmid containing the VvBA1/LAX1 gene by PCR (Appendix A-Colony PCR) using the reagents and cycle described in Appendix A with M13 primers that flank the insertion site (Appendix B). The PCR product was run on a 1% agarose gel and 3 positive colonies were sequenced to ensure correct amplification.

6.2.2 Quantitative expression assay of VvBA1/LAX1 in grapevine tissue by qRT-PCR

Sample collection

To accurately measure the amount of VvBA1/LAX1 expression within grapevine, additional ‘Pinot noir’ tissue was collected from the Lincoln University vineyard during the 2012-13 growing season for qRT-PCR assays. ‘Pinot noir’ clone 113 tissue was collected throughout the growing season from nine plants pooled into three biological replicates (n=3). The tissue collected was as follows: latent bud, woolly bud, leaf (~225 mm²), tendril (~50mm), E-L stage 17 inflorescence(Coombe, 1995), post-anthesis flowers, pre-veraison berry (3.7 °Brix at 25.0°C), veraison berry (11.5 °Brix at 21.6 °C) and

late veraison berry (16.1 °Brix at 22.1 °C). Representative images of the tissue types collected are in Figure 6.1. The tissue was collected in 2mL microcentrifuge tubes and snap-frozen in liquid nitrogen on site. The frozen tissue was then transferred to -80°C for storage until ready for RNA extraction.

RNA extraction and cDNA synthesis

The 'Pinot noir' tissue types described above were ground in liquid nitrogen and aliquots of ~100 mg were put in 2mL microcentrifuge tubes. RNA was extracted from each of the samples using the Sigma Spectrum™ Plant Total RNA kit (Sigma-Aldrich, NZ) with the On-Column DNase treatment protocol. The extracted RNA was quantified using an Invitrogen Qubit® fluorometer with the Qubit® RNA buffer and dye (Life Technologies, NZ) and calibrated with the supplied standards. RNA quality was checked on a 1.5% denaturing agarose gel (Sambrook and Russell, 2001) and visualized by UV excitation of ethidium bromide on a BioRad GelDoc apparatus (Bio Rad Laboratories Pty Ltd, NZ). Contamination of RNA with proteins or extraction reagents was measured on a Nanodrop™ spectrophotometer (ThermoFischer Scientific, NZ).

Good quality, pure RNA was used to synthesize complimentary DNA (cDNA) using the TaKaRa BluePrint™ RT-PCR kit (Norrie Biotech, NZ). 300ng of RNA was used in a 10µL reaction with oligo dTs provided by the manufacturer. The cDNA was synthesized according to protocol and subsequently diluted 20-fold with sterile water. The synthesized cDNA was checked for amplification and lack of genomic DNA (gDNA) contamination by PCR (cDNA check PCR; Appendix A).

qRT-PCR assays

A qRT-PCR assay was performed on the cDNA synthesized from the tissues described above using TaKaRa SYBR® Premix ExTaq™ II PCR reagents (Norrie Biotech, NZ). The assay was done using the Illumina Eco™ Real Time PCR System (dnature, NZ) with the nine tissue types in three biological replicates (27 samples total) repeated in triplicate spread across two 48-well plates. For the assay, a master mix containing the reagents and the qRT-PCR primers (Appendix B) was made and the cDNA template and master mix were aliquoted into the qRT-PCR plates by an Eppendorf epMotion 5070 liquid handling robot (Eppendorf, NZ) to reduce any pipetting error. In addition to the test samples, each plate contained a plate control sample of woolly bud from replicate two cDNA amplifying a fragment of the Actin gene with qRT ACT primers (Table 3.1, page 26) repeated in triplicate to normalize any plate variation. For each assay, digested plasmid containing the cloned VvBA1/LAX1 gene was used to create a 5-point standard curve of 10-fold dilutions, which the concentrations 1×10^{-2} , 1×10^{-4} , 1×10^{-6} , 1×10^{-7} and 1×10^{-8} (ng/µL) were used as both an internal positive control for the assay and to determine the PCR efficiency of the reactions. Sterile water was used in place of cDNA in the same reaction mix for a negative control to check for contamination of the reagents. Both the

standard curve and water samples were repeated in triplicate. The qRT-PCR reaction is described in Appendix A.

Raw data from the qRT-PCR assays was entered into the Illumina EcoStudy 4.0 software (Illumina, NZ) for plate normalization. The plate-normalized data was then exported to Excel and the average quantification cycle (C_q) and standard deviation for each tissue type was calculated from the three biological replicates. The averaged C_q and standard deviation values for the pooled replicates was normalized to the geometric mean of three reference genes (N2227, SAND, TRU5) that were found to be the most stable reference genes for this experimental set as described in Chapter 3. The average relative expression of the tissues was compared to the pooled veraison berry sample in Excel by the Pfaffl method as described in Vandesompele et al. (2002) and Appendix A. A bar graph of the normalized relative average expression of the tissue types was generated in Excel.

Statistical analysis

Post-hoc analysis of the normalized relative expression of VvBA1/LAX1 in the tissue types tested was performed by the Tukey-Kramer test after ANOVA using the GenStat 15 software package (VSN International, Ltd.). Means significantly different at $\alpha=0.05$ are indicated by different letters above each bar in the graph.

6.3 Results & discussion

6.3.1 Transcript variation of grapevine VvBA1/LAX1 genes among different tissues

To accurately measure VvBA1/LAX1 gene expression in grapevine, qRT-PCR assays were done on the tissue types shown in Figure 6.1. Three biological replicates of the nine tissue types were collected and run as described in Section 6.2.2. The raw data was normalized to the geometric mean of the three reference genes found to be most stably expressed in these tissues as described in Chapter 3 (N2227, SAND, TRU5) and expression of the VvBA1/LAX1 in each tissue type was compared to the expression level in veraison berry tissue. After normalization, the relative expression levels of the three biological replicates was tested for differences between the tissue types by analysis of variance (ANOVA) and significant differences between the tissues were tested by the Tukey-Kramer test ($p<0.05$).

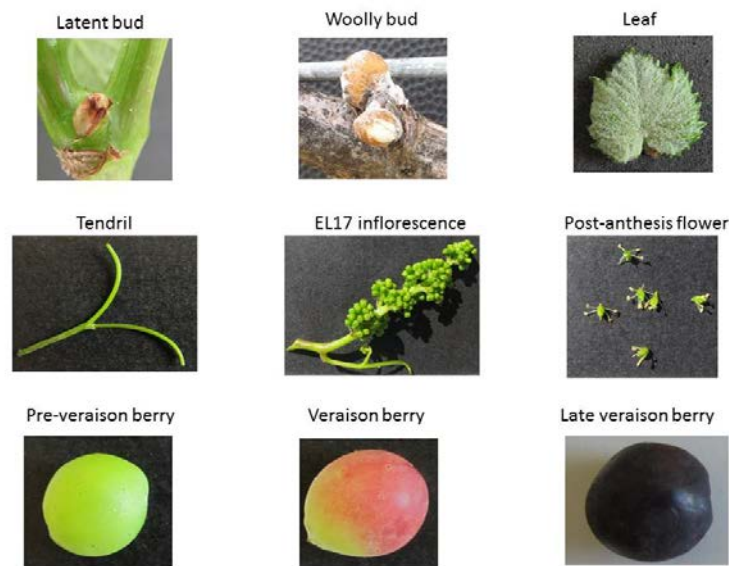


Figure 6.1 Grapevine 'Pinot noir' tissue types used to quantify VvBA1/LAX1 transcript activity by qRT-PCR.

The woolly bud tissue had the highest average relative VvBA1/LAX1 expression of all tissue types tested (Figure 6.2). Based on observations of BA1/LAX1 in other plant species, the high relative expression of VvBA1/LAX1 in woolly buds is expected, as this tissue is not only the site of the shoot apical meristem after budburst, but is also the site of inflorescence primordia that is undergoing differentiation before budburst (May, 2000). In other plant species, BA1/LAX1 genes have been shown to be necessary for the proper maintenance of the apical meristem and cell division, especially in regards to new organ formation and divergence points (Gallavotti et al., 2008; Woods et al., 2011). Surprisingly, the next highest relative expression of VvBA1/LAX1 was in post-anthesis flower tissue (Figure 6.2). No previous BA1/LAX1 research has looked at expression in mature flowers, so the function of VvBA1/LAX1 within this tissue type can only be hypothesized. VvBA1/LAX1 expression in post-anthesis flowers may be due to the role of auxin in pollen formation and anther drop after maturity, as was observed in *Arabidopsis* (Cecchetti et al., 2013; Yang et al., 2013). Further work needs to be done to clarify what role VvBA1/LAX1 has in grapevine reproductive fitness. VvBA1/LAX1 expression was nearly ten times higher in latent buds than the veraison berry reference tissue (Figure 6.2). The high relative expression of VvBA1/LAX1 in latent bud was expected, as this tissue is undergoing several rounds of division and organ initiation (leaf primordia, inflorescence primordia) before dormancy (May, 2000). The high relative expression of VvBA1/LAX1 in the leaf tissue (about seven times higher than the reference tissue) was also expected, as studies into BA1/LAX1 gene expression have shown that this gene family is often expressed in serrated leaves (Woods et al., 2011), such as those of grapevine. Again, this is believed to be due to the BA1/LAX1 gene family's role in regulating auxin movement between cells (Woods et al., 2011).

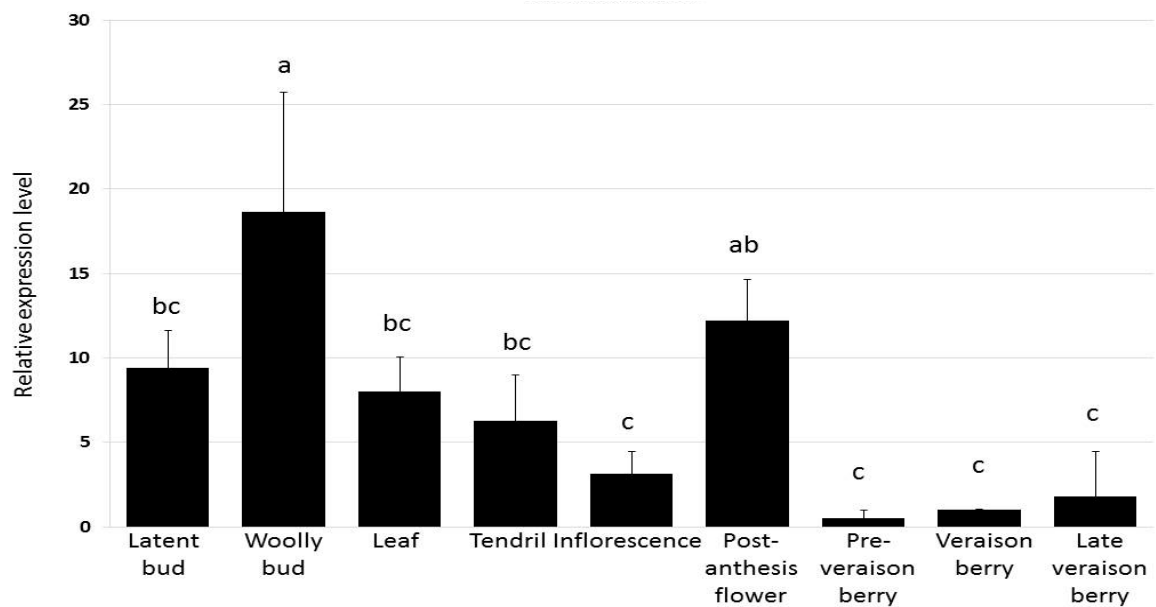


Figure 6.2 Quantitative relative expression of grapevine VvBA1/LAX1 gene activity in three biological replicates of nine ‘Pinot noir’ tissue types.

The tissues listed below the chart were collected from the Lincoln University vineyard as described in Section 6.2.2. Bars represent the mean of the three biological replicates of each tissue type relative to the veraison berry tissue. Standard deviations of the means are represented by lines above the bars. Tissues with the same letter above the bars indicates the means are not significantly different ($p < 0.5$) as determined by the Tukey-Kramer test after ANOVA.

Although the difference in relative expression between the tendril and EL-17 stage inflorescence (Coombe, 1995) tissues was not significant, the inflorescence tissue had about half the VvBA1/LAX1 expression of tendrils (Figure 6.2). The higher VvBA1/LAX1 expression in tendrils rather than inflorescences is surprising, as the expression of VvBA1/LAX1 was predicted to be reduced in this tissue type. However, given the highly specific expression pattern of VvBA1/LAX1 the transcript may be a smaller proportion of the total transcript pool in post-anthesis flowers, which would lead to a lower relative expression of VvBA1/LAX1 in this compound tissue type when compared to the more simplified structure of the tendril.

The berry developmental stages all had the same relative expression level to each other (Figure 6.2), indicating that VvBA1/LAX1 does not affect the ripening process in grapevine. Given the role auxin has in the ripening process in grapevine berries (Lijavetzky et al., 2012; Ziliotto et al., 2012; Boettcher et al., 2013), this result is a little surprising. However, BA1/LAX1 is believed to have a highly specific role in auxin signalling- namely branching events and organ initiation (Gallavotti et al., 2008; Woods et al., 2011), so other transcription factors may be involved in auxin-mediated ripening of grapevine berries.

6.4 Conclusions and future prospects

The BARREN1/LAX PANICLE1 (BA1/LAX1) clade of the large bHLH family of transcription factors is of much interest to this research due to its role in inflorescence architecture and auxin-based cell division regulation (Gallavotti et al., 2004; Gallavotti et al., 2008). Originally identified in rice and maize by its mutant phenotype (Komatsu et al., 2001; Ritter et al., 2002), BA1/LAX1 is believed to limit lateral organ formation by regulating the amount of cells that can form in the developing primordia before differentiation (Gallavotti et al., 2008). In mutants lacking functional BA1/LAX1 genes, no lateral meristems form on inflorescences, giving the plants an almost tendril-like appearance (Komatsu et al., 2001; Gallavotti et al., 2004). Given the role of BA1/LAX1 in inflorescence architecture in other species, and the fact that grapevine inflorescences and tendrils are derived from the same primordia, we hypothesized that BA1/LAX1 may have a similar role in grapevine inflorescence architecture.

As discussed in Chapter 4, there is a single grapevine BA1/LAX1 gene that is closer in sequence similarity to the maize BA1 and rice LAX1 genes than to the Arabidopsis ROX gene. Complementation experiments using the Arabidopsis *rox* mutant to determine if VvBA1/LAX1 is involved in auxin-mediated regulation of lateral branching were initiated but had to be abandoned once data from a recent publication showed only a slight mutant phenotype (Yang et al., 2012) and concerns over the exact nature of the AtROX locus arose. Instead, the focus turned to a transcriptomic approach to determine where in grapevine VvBA1/LAX1 was expressed. Measurement of VvBA1/LAX1 by qRT-PCR assays on grapevine tissues showed high relative expression in woolly and latent buds, leaves, and post-anthesis flowers. The high relative expression of VvBA1/LAX1 in bud tissue is of much interest to this work, as it may indicate that this gene is involved not only in inflorescence primordia initiation within latent buds, but also the final differentiation of the inflorescence primordia within woolly buds. This hypothesis is investigated further in Chapter 7.

The very preliminary results described here for VvBA1/LAX1 expression in grapevine is the first examination of this gene in this species. Furthermore, this research is the first to show high expression of any BA1/LAX1 genes in mature flowers. Given its potential role in not only inflorescence architecture but also in the determination of anlagen differentiation, there is still a large body of research needed. To support the transcriptional evidence provided here, localization of VvBA1/LAX1 activity within grapevine buds is needed. Probes to identify VvBA1/LAX1 transcript activity have been developed for *in situ* hybridization experiments. Grapevine buds have been collected and processed for microscope sectioning several times, but complications with natural disasters (the 2010 and 2011 Christchurch earthquakes) and subsequent issues with access to suitable equipment have led to poor tissue preservation, leading to unusable samples. A final round

of tissue collection was processed recently, and it is hoped that the tissue will be viable and sufficient for use in *in situ* hybridization experiments.

As described above, complementation experiments in *Arabidopsis* were abandoned as the AtROX gene was determined to be too divergent from the other BA1/LAX1 genes. Overexpression studies of VvBA1/LAX1 in wild-type *Arabidopsis* are being considered as a possible way to help to characterize this gene. Ideally, characterization of VvBA1/LAX1 gene function should be done using grapevine plants transformed with constructs to either silence or overexpress the gene, but given the time constraints of grapevine transformation and the limited space available for transgenic plant research in New Zealand, these experiments are not likely to take place as part of this research project.

In addition to the research needed to assist in the characterization of VvBA1/LAX1 in grapevine, there is a surprising lack of research being done in the grapevine community on auxin regulation of the inflorescence development. In contrast, numerous reports have been published on auxin regulation of the ripening process in grapevine berries (Coombe, 1972; Lijavetzky et al., 2012; Ziliotto et al., 2012; Boettcher et al., 2013; Cakir et al., 2013), which indicates that the role of hormones such as auxin in grapevine development is well known. Characterization of auxin signalling during reproductive development in grapevine is sorely needed and would provide much valuable data for researchers into grapevine fruitfulness.

Chapter 7

Investigating the impact of carbohydrate supply on the flowering process in grapevine

7.1 Introduction

Plants require carbohydrates to fuel the metabolic processes necessary for survival and development- obtained either through conversion of the sun's energy via photosynthesis or by breakdown of stored carbohydrates such as starch. Recently, the role of carbohydrate supply in the flowering process has become the focus of much research in plants, as numerous experiments have shown the importance of carbohydrates at this important point in the life cycle of the plant (Coneva et al., 2012; Matsoukas et al., 2012; Stitt and Zeeman, 2012; Matsoukas et al., 2013). In grapevine, much research has gone into the role of carbohydrates on fruitfulness, with recent research within the Winefield group studying the physiological impact of carbohydrate limitation in inflorescence development (Eltom, 2013). This research aims to supplement the physiological research into carbohydrate limitation and inflorescence development with molecular research into the genetic causes of inflorescence architecture alterations due to carbohydrate limitations.

7.1.1 Carbohydrate in flowering

The transition from the vegetative stage to a reproductive state in plants requires the concerted timing of several factors, such as age, season, and health. To gauge the overall health of the plant, carbohydrate supply is often used as to indicate the plant's ability to undergo the transition to a reproductive state. Proper phloem transport of sucrose and other carbohydrates is integral for maintenance of apical dominance and inflorescence development (Barratt et al., 2011). Arabidopsis mutants that cannot recognize the presence of sugars or their related signals show earlier transition to flowering under reduced photoperiods, similar to phenotypes obtained in mutants of the floral repressor genes *TERMINAL FLOWER1* (TFL1), TFL2, and *HASTY1* (HST1) (Matsoukas et al., 2012). Similarly, excess sugar in plants leads to a repression of floral meristem identity gene *LEAFY* (LFY) (Ohto et al., 2001).

Starch supply and breakdown is integral for Arabidopsis flowering when grown in sub-optimal conditions. Under periods of limited daylight, Arabidopsis, a facultative long-day plant, require the breakdown of starch reserves for the transition to flowering (Corbesier et al., 1998). Arabidopsis starch mutants have delayed flowering when compared to the wild-type due to a lack of starch reserve mobilization and photosynthetic activity under reduced photoperiods (Corbesier et al.,

1998). The reason why starch breakdown is believed to play a role in the transition to flowering under short photoperiods is believed to be due to the production of sucrose, which has been shown to have a significant role in signalling the plant's ability to flower. Sucrose is a product of not only the breakdown of starch reserves, but also photosynthesis (Bernier et al., 1993). In *Arabidopsis*, the transition to flowering is preceded by a temporary increase in sucrose content (Corbesier et al., 1998). The increase in sucrose content before the flowering transition occurs is believed to be due to the sugar acting as a floral induction signal because the increase is observed before the cells in the apical meristem undergo mitosis, and so is not due to increased energy demands within the cells (Bernier et al., 1993).

As with many plant signals, other carbohydrates can also act as energy signals for the transition to flowering. Many of the *Arabidopsis* mutants that are insensitive to glucose have early flowering phenotypes under short photoperiods (Matsoukas et al., 2013). These GLUCOSE INSENSITIVE (GIN) mutants are actually mutants of enzymes involved in abscisic acid (ABA) synthesis, which leads to the loss of glucose recognition (Matsoukas et al., 2013). As shown in Figure 1.2 of Chapter 1, ABA is a hormone that represses FT expression, which is one of the major floral pathway integrators. The overexpression of the HEXOKINASE1 (HXK1) gene in *Arabidopsis*, which acts as a glucose sensor, led to the loss of apical dominance caused by a reduction in auxin signalling (Kelly et al., 2012). As discussed in Chapter 6, a reduction in auxin leads to increased cytokinin signalling and lateral branch formation. Another glucose molecule, UDP-glucose, was found to be necessary for proper transition to flowering and pollen fertility in *Arabidopsis* (Park et al., 2010). Of particular interest to this research is the role of the trehalose precursor, trehalose-6-phosphate (T6P), in the signalling of carbohydrate status during the transition to flowering.

T6P has been implicated in signalling carbohydrate status for many developmental processes in plants (Schluepmann et al., 2003; Lunn et al., 2006; Martins et al., 2013). As discussed in Section 5.1.2 of Chapter 5, the trehalose intermediate T6P is used in the SnRK1 signalling pathway as an indicator of carbohydrate status to regulate gene transcription. In addition to its role in SnRK1 signalling, T6P has also been shown to affect floral meristem development (Schluepmann et al., 2003; Wahl et al., 2013). This molecule is the focus of much of this research due to the observed role of T6P in inflorescence architecture in maize (Satoh-Nagasawa et al., 2006), in which increased levels of T6P lead to increased basal branching of the inflorescence. Increased T6P levels during inflorescence development may explain the presence of fruitful outer arms on grapevine bunches.

7.1.2 Carbohydrate in grapevine

Carbohydrate status in grapevine has been the focus of much research within the viticulture industry, and is an excellent resource to demonstrate the relationship between carbohydrates and

inflorescence development. The amount of starch reserves in grapevine are directly correlated with the number and size of inflorescences that develop (Bennett et al., 2005; Lebon et al., 2008), and numerous defoliation studies have shown how limiting carbohydrates during the period from budburst to anthesis affect flower development (Caspari et al., 1998; Sabbatini and Howell, 2010; Nicolosi et al., 2012; Tardaguila et al., 2012; Pastore et al., 2013). Carbohydrate limitation affects not only flower development during the current year, but can also affect both the number and size of inflorescences that develop the following year (Candolfi-Vasconcelos and Koblet, 1990; Bennett et al., 2005). In 'Pinot noir' vines, half of the starch reserves were depleted during the period of inflorescence differentiation (budburst to anthesis), but was later recuperated post-anthesis (Zapata et al., 2004). The effect of carbohydrate limitation on inflorescence development is quite clear, but little work has been done to study the effect of carbohydrate limitation in outer arm development.

Grapevine outer arms are highly correlated with large inflorescences (Tarter and Poni, 2010). As carbohydrate supply, namely starch, has been shown to affect inflorescence size, it can be assumed that vines with surplus carbohydrate will have larger inflorescences and in turn a higher chance of forming fruitful outer arms. Recent work within the Winefield group has shown that limiting carbohydrate by girdling during dormancy can reduce fruitful outer arm development by up to 50% on shoots affected by the girdling treatment (Eltom, 2013). Conversely, girdling during inflorescence primordia development (thereby limiting carbohydrate export to the rest of the vine) leads to an increase in fruitful outer arm development on the girdled shoot the following season (Eltom, 2013). This indicates that carbohydrate status affects not only the development of inflorescence primordia during the first growing season, but also the differentiation of the inflorescence the following year.

7.1.3 Molecular biology of flowering in grapevine

The genes involved in general floral development are described in Section 1.1 of Chapter 1, and those characterized in grapevine are reviewed here. In grapevine, inflorescence primordia initiation begins in the latent buds during the first year of growth (Srinivasan and Mullins, 1981; Carmona et al., 2008; Vasconcelos et al., 2009). Early in inflorescence primordia development, VvTFL1A had high expression within the developing latent buds (Carmona et al., 2007). As the inflorescence primordia develops, the floral genes VvFL (LFY) and VvMADS8 (SOC1) as well as the photoperiod regulator gene VvCO1 were highly expressed (Almada et al., 2009), and the 'florigen' gene VvFT had high expression levels in other parts of the plant (Sreekantan and Thomas, 2006; Carmona et al., 2007). In addition, VvSPL genes from the age-dependent floral pathway also had high transcript expression (Diaz-Riquelme et al., 2012). The inflorescence primordia undergoes several rounds of division, forming not only an outer and inner arm but also secondary and tertiary branching before entering dormancy (Srinivasan and Mullins, 1981). During dormancy, little activity occurs in the inflorescence primordia,

although mitosis has been observed in ‘Pinot noir’ buds (Jones et al., 2009). The following season, the inflorescence primordia undergoes the final sets of division and differentiates into floral structures before budburst (Srinivasan and Mullins, 1981; Vasconcelos et al., 2009). At this time VvTFL1A and VvFL transcript activity resumes (Carmona et al., 2002; Carmona et al., 2007) and expression of other floral meristem identity genes such as VvAP1 were initiated (Calonje et al., 2004; Diaz-Riquelme et al., 2009). After budburst, the inflorescence develops floral structures and the overall architecture is set. The floral repressor VvTFL1A decreases in transcript activity and the ‘florigen’ gene VvFT increases in activity in the plant throughout the second growing season (Carmona et al., 2007).

As discussed above, the breakdown of starch into sucrose and other disaccharides is believed to signal the energy status of the plant and its ability to transition to a floral state. In grapevine, carbohydrate limitation has been shown to affect flowering both in the current year as well as the following growing season due to the initiation of inflorescence primordia during the current season. To test if carbohydrate limitation also affects floral pathway genes, a series of experiments were carried out investigating both the physiological impacts of carbohydrate limitation as well as transcriptional activity of several floral pathway genes and carbohydrate metabolism genes.

7.2 Materials & methods

7.2.1 Single node cuttings

Shoot collection

‘Pinot noir’ clone 777 on 101-14 rootstock shoots were collected from row 469 of the Brancott Estate in the Marlborough region of New Zealand from 15-17 May, 2010. The shoots were collected from an experimental field trial set up by Amber Parker as part of her PhD thesis (Parker, 2012). The shoots collected were from 2-cane VSP-trained vines that had been pruned to either 6-node or 12-node shoots during the growing season of 2009-2010. From each of the 6- or 12-node pruned vines, one large and one small diameter sized shoot was collected and stored at Lincoln University at 4°C until the shoots were divided for use as single node cuttings.

Experimental setup and data collection

The shoots collected for single node cuttings described above were grown in blocks of three with the experiment repeated three times (December 2010, April 2011, December 2011). The shoots were grown in the greenhouse at the Lincoln University campus in polystyrene trays floating in tap water with no additional supplements. The small and large diameter shoots from each 6- or 12-node pruned vine were grown side-by-side, with the distribution of 6- or 12-node pruned shoots distributed randomly within the blocks. The shoots were pruned into single node cuttings by cutting each shoot

between the internode. When possible, the single node cuttings were restricted in length to ~45-50 mm to further limit the amount of possible available carbohydrate.

Measurements of shoot diameter and length were collected during the setup of each experiment using digital callipers. Flowering and outer arm data were collected every other day during the course of the experiment.

Statistical analysis

Data from the experiment was collated in Excel. Bar graphs of the data were done in Excel. ANOVA and tests for significance were done using the GenStat 15 software package (VSN International, Ltd.).

7.2.2 Quantitative gene expression assays in grapevine bud developmental stages by qRT-PCR

Tissue collection

Buds or shoots from 'Pinot noir' clone 777 on 101-14 rootstock were collected from row 460 of the Brancott Estate in the Marlborough region of New Zealand during the 2010-11 growing season. The vines in row 460 were trained as 2-cane VSP and were cultivated under standard commercial viticulture practices. Buds from either small or large diameter shoots were collected from three general positions along the shoot: basal (nodes 1-4), middle (nodes 5-8), and apical (nodes 9-12). The buds were collected as three biological replicates (n=3) from vines randomly selected along the row. Latent buds were collected in the vineyard on Feb 11, 2011. The tissue was collected in 2mL microcentrifuge tubes and snap-frozen in liquid nitrogen on site and transported back to Lincoln University the same day on dry ice. The frozen tissue was then transferred to -80°C for storage until ready for RNA extraction. Dormant buds were collected in the vineyard on June 15, 2011. Tissue collection and storage was as described above. Dormant shoots from the vines were also collected at the same time and stored at Lincoln University at 4°C until the shoots were divided for single node cuttings.

In March 2012, the shoots collected for single node cuttings were grown for harvesting budswell and woolly buds. The shoots were grown in the greenhouse at the Lincoln University campus in polystyrene trays floating in tap water with no additional supplements. The vines were grown in groups of the three biological replicates with small and large diameter shoots from the same vine growing side by side. Budswell and woolly buds from the vines were harvested as the buds reached the desired developmental stage. The buds were collected from three general positions along the shoot: basal (nodes 1-4), middle (nodes 5-8), and apical (nodes 9-12). The tissue was collected in 2mL microcentrifuge tubes and snap-frozen in liquid nitrogen on site. The frozen tissue was then transferred to -80°C for storage until ready for RNA extraction.

RNA extraction and cDNA synthesis

RNA from the tissue described above was extracted and quality checked as described in 5.2.1. For cDNA synthesis, 300ng of RNA was used in a 10 μ L reaction with oligo dTs provided by the manufacturer. The cDNA was synthesized according to protocol and subsequently diluted 20-fold with sterile water. The cDNA quality was checked by PCR (cDNA check PCR; Appendix A).

qRT-PCR assays

A qRT-PCR assay was performed on the cDNA synthesized from the tissues above using TaKaRa SYBR® Premix ExTaq™ II PCR reagents (Norrie Biotech, NZ). The assay was done using the Illumina Eco™ Real Time PCR System (dnature, NZ) with the two groups of four bud developmental stages in three biological replicates (24 samples total) repeated in triplicate spread across two 48-well plates. For the assay, a master mix containing the reagents and the qRT-PCR primers (Appendix B) was made and the cDNA template and master mix were aliquoted into the qRT-PCR plates by an Eppendorf epMotion 5070 liquid handling robot (Eppendorf, NZ) to reduce any pipetting error. In addition to the test samples, each plate contained a plate control sample of woolly bud from the middle node positions of large diameter shoots from replicate three cDNA amplifying a fragment of the Actin gene with qRT ACT primers (Table 3.1, page 26) repeated in triplicate to normalize any plate variation. For each assay, digested plasmid containing the cloned gene being studied was used to create a 5-point standard curve of 10-fold dilutions, of which the concentrations 1x10⁻², 1x10⁻⁴, 1x10⁻⁶, 1x10⁻⁷ and 1x10⁻⁸ (ng/ μ L) were used as both an internal positive control for the assay and to determine the PCR efficiency of the reactions. Sterile water was used in place of cDNA in the same reaction mix for a negative control to check for contamination of the reagents. Both the standard curve and water samples were repeated in triplicate. The qRT-PCR reaction is described in Appendix A.

Raw data from the qRT-PCR assays was entered into the Illumina EcoStudy 4.0 software (Illumina, NZ) for plate normalization. The plate-normalized data was then exported to Excel and the average quantification cycle (C_q) and standard deviation for each tissue type was calculated from the three biological replicates. The averaged C_q and standard deviation values for the pooled replicates was normalized to the geometric mean of three reference genes (AP2mu, TIP41, TRU5) that were found by geNorm analysis (Vandesompele et al., 2002) to be the most stable reference genes for this set of tissues as described in Chapter 3. The average relative expression of the tissues was compared to the pooled basal dormant bud sample in Excel by the Pfaffl method as described in Vandesompele et al. (2002) and Appendix A. A bar graph of the normalized relative average expression of the buds was generated in Excel.

Statistical analysis

Post-hoc analysis of the normalized relative expression of the genes assayed in the tissues described above was performed by the Tukey-Kramer test after ANOVA using the GenStat 15 software package (VSN International, Ltd.). Means significantly different at $\alpha=0.05$ are indicated by different letters or an asterisk above each bar in the graph.

7.3 Results & discussion

7.3.1 Determination of fruitful outer arm development with limited carbohydrate by single node cuttings

Data from the single node cuttings were pooled into three bins per shoot position (basal, middle, and apical). For the shoots that were pruned to 6 nodes, the basal shoot position consisted of nodes 1-2, the middle shoot position consisted of nodes 3-4, and the apical shoot position consisted of nodes 5-6. For the shoots that were pruned to 12 nodes, the basal shoot position consisted of nodes 1-4, the middle shoot position consisted of shoots 5-8, and the apical shoot position consisted of nodes 9-12. As shown in Figure 7.1, both pruning treatments (6-node or 12-node) had diameter sizes that were significantly different for each of the three shoot positions when large diameter shoots were compared to the small diameter shoots. This indicates that the two class systems adopted for comparing floral data in the single node cuttings are sufficiently different to identify any size effects in outer arm formation. In addition, the comparison between 6-node and 12-node pruned shoots indicates similar diameter sizes for the two pruning treatments (Figure 7.1). For the 6-node pruned shoots the mean diameter difference between large and small class shoots was 3.19 mm (basal), 3.37 mm (mid), and 3.63mm (apical). For the 12-node pruned shoots, the mean diameter difference between large and small class shoots was 2.89 mm (basal), 3.00 mm (middle), and 2.83 mm (apical). Overall, the basal shoot positions had the largest mean diameter and the apical shoot positions had the lowest mean diameter for both pruning treatments.

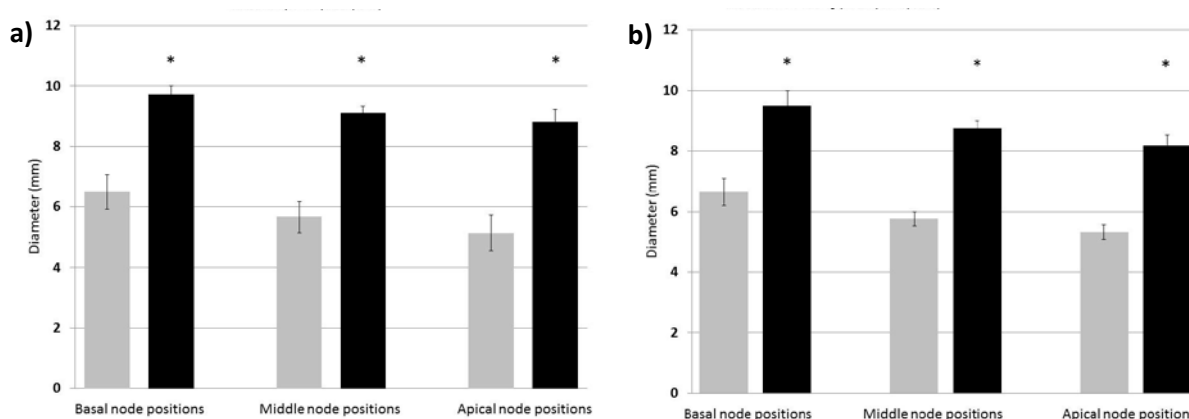


Figure 7.1 Mean diameter (mm) of small or large diameter class single node cuttings per shoot position from 6-node (a) or 12-node (b) pruned shoots.

Diameter sizes are the means of three replicates with a minimum of 6 vines per replicate. Cuttings taken from the small diameter class shoots are represented by the grey bars. Cuttings taken from the large diameter class shoots are represented by the black bars. Standard deviations for each of the mean values are indicated by vertical bars. Mean large diameter class shoots with an asterisk (*) indicate significantly different ($p < 0.5$) diameter size per shoot position when compared to the small diameter class shoots at same position as determined by the Tukey-Kramer test after ANOVA.

To account for both the diameter and the length of each single node cutting, the volume of each cutting was calculated based on a cylindrical shape. The calculated volumes of small and large diameter class canes for both 6-node and 12-node pruned shoots showed that large diameter class shoots had significantly larger volumes when compared to the small diameter class shoots at the same position (Figure 7.2). For the 6-node pruned shoots the mean volume difference between large and small class shoots was 1319.07 mm^3 (basal), 1875.79 mm^3 (middle) and 1784.44 mm^3 (apical). For the 12-node pruned shoots, the mean volume difference between large and small class shoots was 1458.29 mm^3 (basal), 1691.63 mm^3 (middle) and 1512.54 mm^3 (apical). The volume measurements are a more accurate description of the total possible carbohydrate supply for each cutting as length measurements are also included in the calculations. This is best demonstrated with cuttings from the basal shoot position, in which the larger diameter measurements observed in Figure 7.1 are offset by the reduced length of the cuttings due to the reduced internode distance between the basal nodes. This leads to a smaller overall volume measurement for cuttings from the basal node positions, while the middle node positions have the largest mean volume for both pruning treatments due to the longer internode distances and larger diameter measurements (Figure 7.2). The mean volumes for basal shoot position cuttings was slightly lower in the shoots pruned to 6 nodes when compared to shoots in the 12-node treatment, but the middle and apical volumes for the two pruning treatments were similar (Figure 7.2). The difference in mean volume measurements for the 6-node treatment when compared to the 12-node treatment is due to only two node positions being evaluated in the 6-node treatment versus four nodes being evaluated in the 12 node treatment.

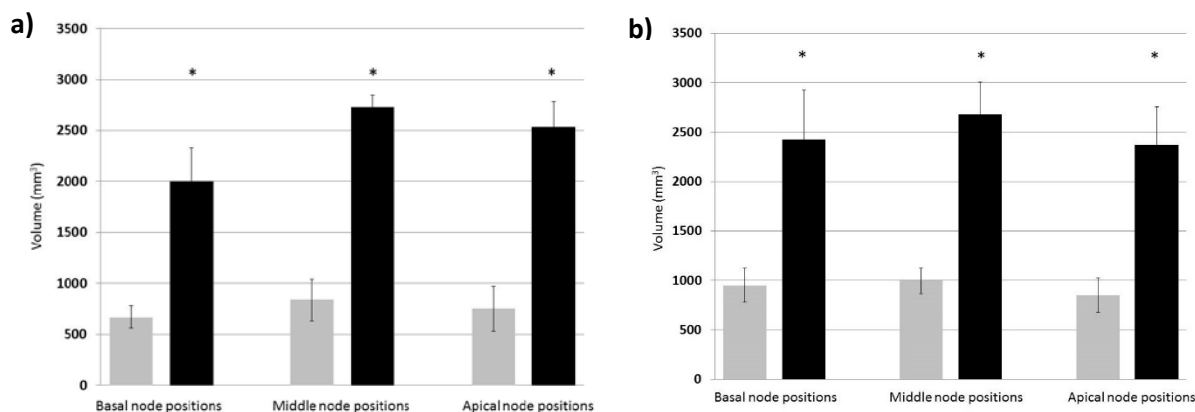


Figure 7.2 Mean volume (mm³) of small or large diameter class single node cuttings per shoot position from 6-node (a) or 12-node (b) pruned shoots.

Volumes are the means of three replicates with a minimum of 6 vines per replicate. Cuttings taken from the small diameter class shoots are represented by the grey bars. Cuttings taken from the large diameter class shoots are represented by the black bars. Standard deviations for each of the mean values are indicated by vertical bars. Mean large diameter class shoots with an asterisk (*) indicate significantly different ($p < 0.5$) volumes per shoot position when compared to the small diameter class shoots at same position as determined by the Tukey-Kramer test after ANOVA.

Flowering data collected from the single node cuttings showed that the pruning treatments initiated during the previous growing season had a significant effect on the size of the outer arm that formed from each treatment (Appendix F). There was a much higher frequency of fruitful outer arms for both the 6-node and 12-node pruned shoots on the basal inflorescence of each shoot (Appendix F), so the results of only the basal inflorescences will be discussed here. The shoots pruned to 6 nodes during the growing season had a much lower frequency of forming fruitful outer arms when compared to the 12-node treatment, regardless of the diameter class (Figure 7.3). For the 6-node pruned shoots, only large diameter class shoots from the middle position had a significantly higher frequency of fruitful outer arms, while the small diameter class shoots often did not form any fruitful outer arms (Figure 7.3 (a)). This may indicate that there is a minimum volume requirement for fruitful outer arms to form from single node cuttings, as the large diameter class shoots from the middle node positions had a mean volume of 2751.12 mm³, while the large diameter shoots from basal node positions had a mean volume of only 2009.48 mm³. Similar results were observed in previous work within our research group, in which the cane cross sectional area (mm²) was compared to the frequency of fruitful outer arms on basal bunches of ‘Sauvignon blanc’ shoots (Eltom, 2013). This work showed that there was a minimum cane area required before fruitful outer arms formed, and a window of about 100 mm² in which the majority of fruitful outer arms developed (Eltom, 2013).

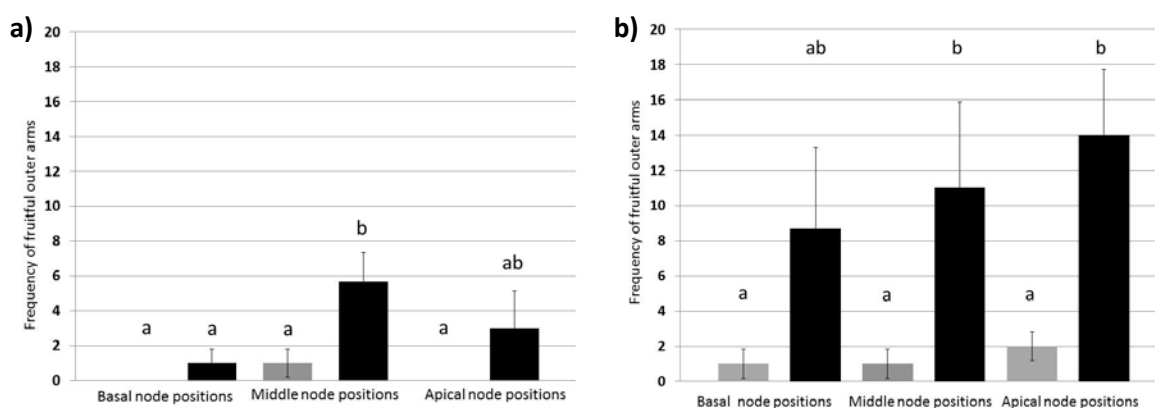


Figure 7.3 Mean frequency of fruitful outer arms from single node cuttings grown from small or large diameter class shoots from 6-node (a) or 12-node (b) pruned shoots.

Fruitful outer arm frequencies are the means of three replicates with a minimum of 6 vines per replicate. Cuttings taken from the small diameter class shoots are represented by the grey bars. Cuttings taken from the large diameter class shoots are represented by the black bars. Standard deviations for each of the mean values are indicated by vertical bars. Frequencies with the same letter above the bars indicates the means are not significantly different ($p < 0.5$) as determined by the Tukey-Kramer test after ANOVA.

For the 12-node pruned shoots, there was a difference in the mean frequency of fruitful outer arms between small and large diameter class shoots at the basal position but the difference was not significant at this shoot position. There was a ten-fold difference in the frequency of fruitful outer arms that formed on large diameter shoots at both the middle and apical shoot positions (Figure 7.3 (b)). The frequency of fruitful outer arms that formed appeared to increase in the large diameter shoots as the location of the shoots increased from basal to apical (Figure 7.3 (b)), although the differences at each shoot position were not significant. The volume measurements of the 12-node pruned shoots were not that much different than the measurements from the 6-node pruned shoots, yet the frequency of fruitful outer arms that formed was much higher in the 12-node treatment (Figure 7.3). This indicates that the volume of the cuttings alone does not dictate the frequency of fruitful outer arms that develop on basal inflorescences from single node cuttings. Other factors, such as hormone signalling or gene expression must also be a factor in determining the size of the outer arm that forms on inflorescences.

Overall, the frequency of fruitful outer arm development on basal inflorescences from single node cuttings was higher in the shoots that were pruned to 12 nodes during the growing season. The increased frequency of fruitful outer arms on the basal inflorescences was much higher in cuttings grown from large diameter class shoots when compared to cuttings grown from small diameter class shoots at the same position (Figure 7.3). The frequency of fruitful outer arm formation cannot be attributed to cutting size alone, as cuttings grown from shoots pruned to 6 nodes had similar volume measurements to those pruned to 12 nodes. This indicates that other signals at a molecular level are regulating the size of fruitful outer arms on grapevine inflorescences.

To investigate whether genetic cues were regulating outer arm development in grapevine, a series of assays were performed on grapevine bud developmental stages harvested from shoots collected from the same vineyard as the shoots used in the single node cuttings experiment described above. The assays were designed to measure gene expression of some of the trehalose pathway genes described in Chapter 5 as well as the transcription factor gene VvBA1/LAX1 in conjunction with several flowering pathway genes.

7.3.2 Transcript variation of grapevine trehalose pathway families, VvBA1/LAX1, and flowering pathway genes in grapevine developmental bud stages

Transcription activity across four bud developmental stages (latent bud, dormant bud, budswell bud, woolly bud) was measured from buds collected from either small or large diameter class shoots that were pruned to 12 nodes during the growing season. The buds were pooled into three bins per shoot position (basal, middle, and apical) during collection and screened based on the shoot position. Three biological replicates of the four bud developmental stages were collected and run as described in Section 7.2.2. The raw data was normalized to the geometric mean of the three reference genes found to be most stably expressed in the bud developmental stages by geNorm in Chapter 3 (AP2mu, TIP41, TRU5) and expression of the genes in each tissue type was compared to the expression level of the same gene in the small diameter class basal shoot position of the dormant bud. After normalization, the relative expression levels of the three biological replicates was tested for differences between the bud developmental stages and by bud stage*diameter class*shoot position by analysis of variance (ANOVA) and significant differences between the tissues were tested by the Tukey-Kramer test ($p < 0.5$).

Flowering pathway gene expression in grapevine bud developmental stages

In this study, three floral pathway genes were screened across the bud developmental series: VvCO1, VvFL, and VvTFL1A. VvFT was investigated for use in this research, but was not found to have measurable levels of transcript activity in the bud tissues tested (data not shown). VvCO1 was selected for screening in this experiment as it had been shown to be expressed in a similar pattern to the trehalose biosynthesis gene AtTPS1 in Arabidopsis (Wahl et al., 2013). CO1 is a photoperiod signalling gene whose expression is closely linked to FT gene expression by direct activation of FT (Wigge et al., 2005). Given its role as an activator of FT, VvCO1 transcript activity suggests a correlated activation of VvFT during long-day photoperiods, although this assumption cannot be taken as fact since interaction of VvCO1 with VvFT has not been investigated in grapevine. VvFL was selected for screening as it has been shown in other grapevine research to maintain floral meristem indeterminacy during inflorescence differentiation before budburst (Carmona et al., 2002). This gene is also of interest in this work due to its hypothesized role in maintaining a pluripotent cell state in all meristems (Carmona et al., 2002), which may indicate an interaction with the auxin-signalling

transcription factor VvBA1/LAX1. Finally, VvTFL1A was selected for this experiment due to the role of TFL in regulating inflorescence architecture and determinacy in all plant species studied, particularly when interacting with FL (Prusinkiewicz et al., 2007). VvTFL1A is of particular interest to this research as it is known to affect inflorescence architecture in grapevine (Fernandez et al., 2010).

As seen in Figure 7.4(a), VvCO1 had the highest expression in latent buds. As the latent buds were the only developmental stage collected during long days, the high relative activity of VvCO1 in this tissue is in agreement with its role as a long-day photoperiod signal. The high level of VvCO1 expression in latent buds was also observed by Almada et al. (2009), confirming their observations. The mean expression level of VvCO1 in latent buds was 3.4 times higher than the reference sample (dormant buds). Almada et al. (2009) found the highest relative expression of VvCO1 in November in Chile, so earlier sampling of latent buds in this experiment may have also found higher expression levels of the gene. VvCO1 expression decreased during the dormant period and the following spring before budburst, again also in agreement with previous findings (Almada et al., 2009).

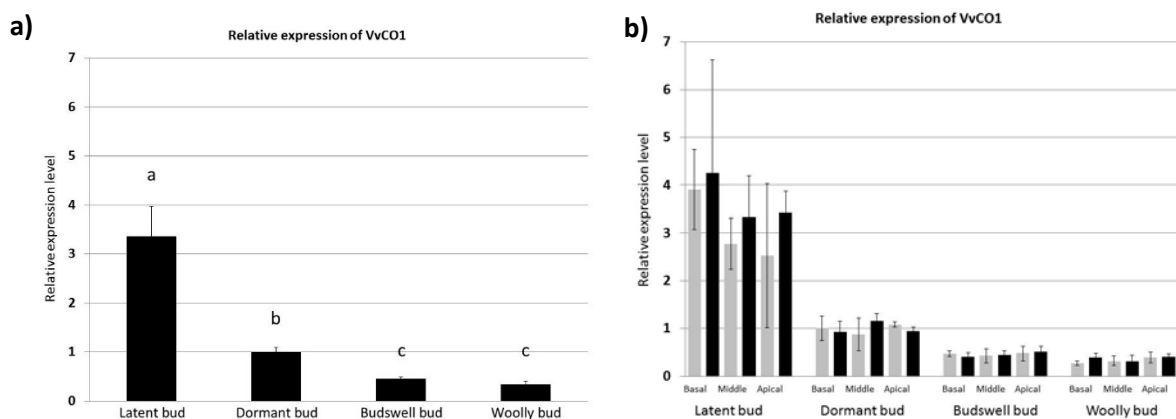


Figure 7.4 Relative expression of VvCO1 in grapevine bud developmental stages. VvCO1 expression levels are shown as grouped developmental stages (a) or separated into small or large diameter class shoots (b).

Relative expression values are the means of three biological replicates with three individuals per replicate. Standard deviations of the means are indicated by vertical lines above the bars. In (a), frequencies with the same letter above the bars indicates the means are not significantly different ($p < 0.5$) as determined by the Tukey-Kramer test after ANOVA. In (b), small diameter class shoots are represented by the grey bars, while large diameter class shoots are represented by the black bars.

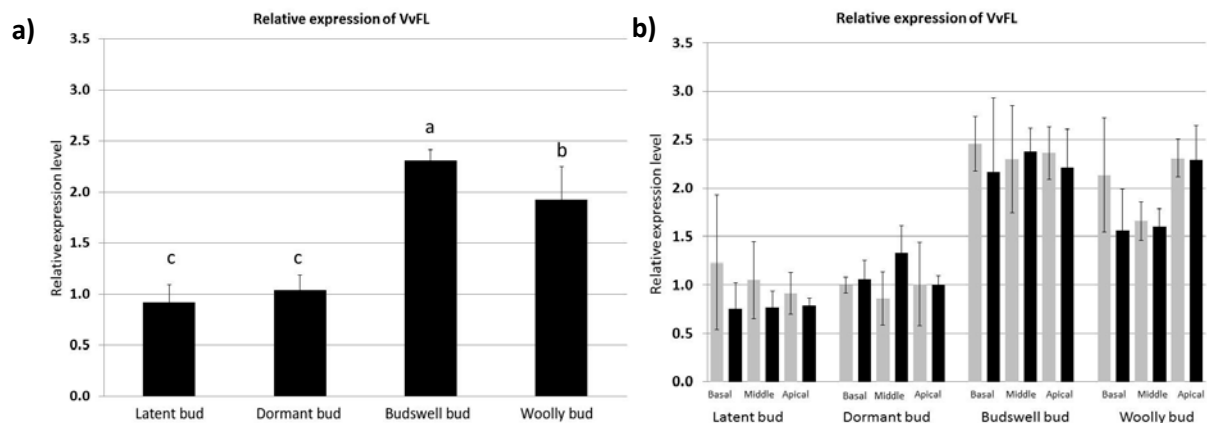


Figure 7.5 Relative expression of VvFL in grapevine bud developmental stages. VvFL expression levels are shown as grouped developmental stages (a) or separated into small or large diameter class shoots (b).

Relative expression values are the means of three biological replicates with three individuals per replicate. Standard deviations of the means are indicated by vertical lines above the bars. In (a), frequencies with the same letter above the bars indicates the means are not significantly different ($p < 0.5$) as determined by the Tukey-Kramer test after ANOVA. In (b), small diameter class shoots are represented by the grey bars, while large diameter class shoots are represented by the black bars.

As shown in Figure 7.5(a), VvFL had the highest expression level in budswell buds, in agreement with work by other researchers (Carmona et al., 2002; Diaz-Riquelme et al., 2012). For this study, the mean expression level of VvFL in budswell buds was 2.2 times higher than the dormant buds reference samples and 2.5 times higher than the bud developmental stage with the lowest VvFL relative expression (latent buds). High relative expression of VvFL in budswell buds is in agreement with its proposed role in maintaining floral meristem indeterminacy during inflorescence differentiation before budburst (Carmona et al., 2002). There was no difference in expression observed in any of the bud developmental stages collected from small or large diameter class shoots (Figure 7.4(b)), indicating that carbohydrate status within the shoot does not affect VvFL gene expression.

Similar to VvFL, VvTFL1A relative gene expression was highest in budswell buds (Figure 7.6(a)). The results observed here for VvTFL1A are in agreement with work by other researchers, in which VvTFL1A has high expression in budswell buds (Carmona et al., 2007; Diaz-Riquelme et al., 2012),

although RT-PCR experiments by Carmona et al. (2007) found the highest relative expression in latent buds. High relative expression of VvTFL1A in budswell buds is in agreement with its proposed role of maintaining floral meristem indeterminacy during inflorescence differentiation before budburst (Carmona et al., 2007) and may indicate that the final inflorescence architecture in

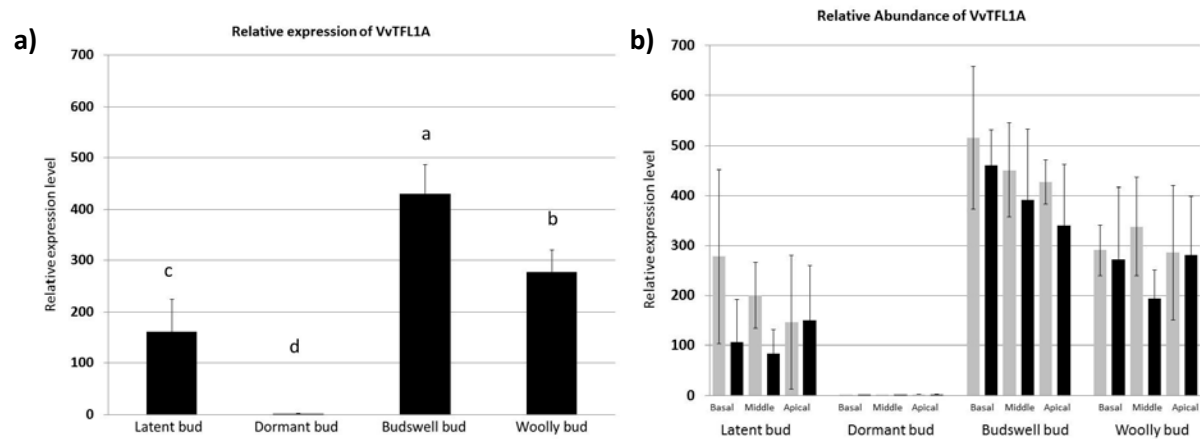


Figure 7.6 Relative expression of VvTFL1A in grapevine bud developmental stages. VvTFL1A expression levels are shown as grouped developmental stages (a) or separated into small or large diameter class shoots (b).

Relative expression values are the means of three biological replicates with three individuals per replicate. Standard deviations of the means are indicated by vertical lines above the bars. In (a), frequencies with the same letter above the bars indicates the means are not significantly different ($p < 0.5$) as determined by the Tukey-Kramer test after ANOVA. In (b), small diameter class shoots are represented by the grey bars, while large diameter class shoots are represented by the black bars.

grapevine is not determined until the second season of growth. As shown in Figure 7.6(b), there is a general trend for large diameter class shoots to have lower relative expression of VvTFL1A in both latent buds and budswell buds, although the difference is not statistically significant due to the high standard deviation observed for this gene within the different biological replicates. This may indicate some carbohydrate effect on VvTFL1A gene expression, although more experiments will need to be done to confirm this.

The floral pathway gene expression patterns observed in this study are similar to those seen by other researchers for each of the genes investigated. VvCO1, a long-day photoperiod signal gene has the highest relative expression in latent buds (the only buds collected during a long-day photoperiod). The expression of VvCO1 in latent buds suggests that the 'florigen' gene VvFT may also be transcriptionally active in grapevine at this period, although no expression in buds was observed (data not shown). This may indicate that VvFT, after activation by VvCO1, is stimulating inflorescence primordia initiation in latent buds during long-day photoperiods. It is well known that inflorescence primordia initiation occurs in latent buds during the first growing season (Srinivasan and Mullins, 1981; May, 2000), so VvFT may likely be the molecular cue for inflorescence initiation in grapevine. The other flowering pathway genes assayed for this experiment, VvFL and VvTFL1A both had their

highest relative expression in budswell buds, indicating that this developmental stage is integral for determining the final architecture of the inflorescence and likely the outer arm in grapevine. The interaction of VvFL and VvTFL1A has not yet been studied in grapevine, but if the interaction of these genes are similar to observations in other plant species (Prusinkiewicz et al., 2007), then the final determination of inflorescence architecture and outer arm formation is not completed until just before budburst. More work needs to be done to elucidate the molecular biology of the grapevine flowering process, particularly in regards to inflorescence initiation and differentiation before budburst.

VvBA1/LAX1 gene expression in grapevine bud developmental stages

As discussed in Section 6.1 of Chapter 6, VvBA1/LAX1 is believed to regulate inflorescence architecture by limiting auxin to pluripotent cells before differentiation. VvBA1/LAX1 is of particular interest to this research due to the *barren stalk1* phenotype of maize BA1 mutants, in which there is no inflorescence branching-leading to a single, sterile stalk (Gallavotti et al., 2004). To supplement the partial characterization of VvBA1/LAX1 as described in Chapter 6, the gene was screened on grapevine bud developmental stages to determine if VvBA1/LAX1 may also be involved in inflorescence branching and architecture in the same manner as maize BA1.

As shown in Figure 7.7(a), VvBA1/LAX1 had the highest relative expression in budswell buds, which indicates a potential role for this gene in the final floral determination in grapevine inflorescences before budburst. The floral pathway genes VvFL and VvTFL1A also had the highest relative expression in budswell buds (Figures 7.5(a) and 7.6(a)). This suggests that VvBA1/LAX1 may act in concert with these floral pathway genes to regulate the final architecture of the grapevine inflorescence before budburst. The interaction of VvBA1/LAX1 with these floral meristem maintenance genes would incorporate hormonal signalling into the flowering process in grapevine.

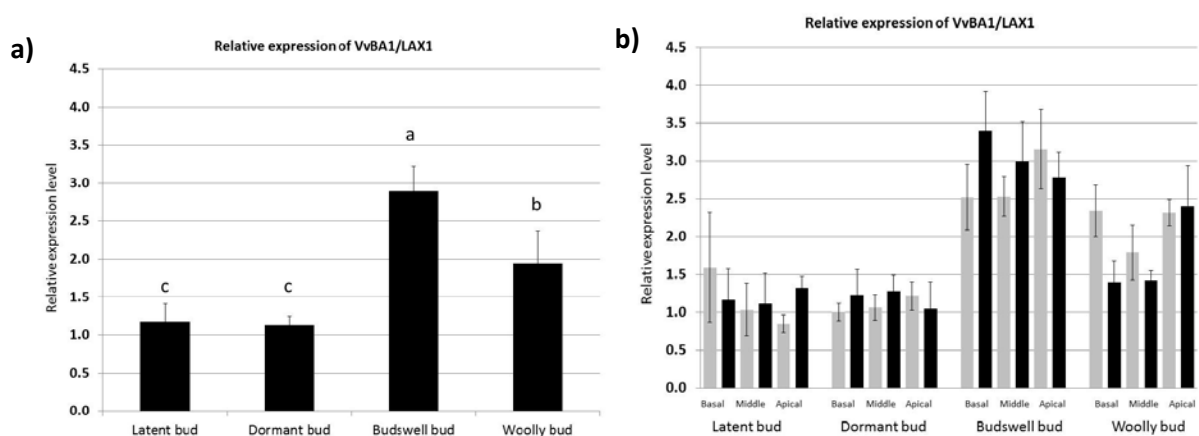


Figure 7.7 Relative expression of VvBA1/LAX1 in grapevine bud developmental stages. VvBA1/LAX1 expression levels are shown as grouped developmental stages (a) or separated into small or large diameter class shoots (b).

Relative expression values are the means of three biological replicates with three individuals per replicate. Standard deviations of the means are indicated by vertical lines above the bars. In (a), frequencies with the same letter above the bars indicates the means are not significantly different ($p < 0.5$) as determined by the Tukey-Kramer test after ANOVA. In (b), small diameter class shoots are represented by the grey bars, while large diameter class shoots are represented by the black bars.

There is no effect of shoot diameter size on VvBA1/LAX1 expression in any of the bud stages tested (Figure 7.7(b)), although some of the bud stages appear to have differences in gene expression between the two diameter classes, particularly at the basal and middle shoot positions. Recently, a link between carbohydrates and auxin biosynthesis has been found in Arabidopsis (Sairanen et al., 2012). To the best of our knowledge no studies have been done to investigate the role of carbohydrates in auxin or any other hormone signalling in grapevine flowering. Such a study would be very useful in the species, as both carbohydrates and hormones are known to affect the development and fruitset of grape bunches.

The high relative expression of VvBA1/LAX1 in budburst tissue suggests that auxin signalling is involved in inflorescence differentiation in grapevine. This is similar to results observed in maize, in which BA1 regulates branching and subsequent differentiation of inflorescences by limiting auxin into undifferentiated cells (Gallavotti et al., 2004). Further work needs to be done to confirm the role of VvBA1/LAX1 in inflorescence differentiation. Localization of VvBA1/LAX1 in inflorescence primordia from budburst buds by *in situ* hybridization was initiated but was abandoned due to difficulties with tissue fixation and time constraints. Other experiments such as transgenic approaches to identify VvBA1/LAX1 function in grapevine would also be very informative. Perhaps the most vital research into the regulation of flowering in grapevine would be to investigate the potential interaction of carbohydrates with hormonal signalling during inflorescence development.

Trehalose pathway family gene expression in grapevine bud developmental stages

The trehalose biosynthesis pathway gene families are of particular interest in regards to their possible role in the flowering process in grapevine. In Arabidopsis, AtTPS1 has been shown to affect gene expression of both the 'florigen' gene FT, as well as several genes from the age-dependent flowering pathway gene family SPL (Wahl et al., 2013). In addition, the signal molecule T6P has been shown to significantly alter inflorescence architecture in maize (Sato-Nagasawa et al., 2006). To the best of our knowledge, this is the first study of trehalose biosynthesis gene family expression across bud developmental stages in grapevine.

Two grapevine TPS family genes were selected to test for gene expression across the grapevine bud developmental stages from small and large diameter shoots to test for possible roles in carbohydrate signalling and the flowering process. VvTPS1 was selected for assay due to its hypothesised role as the only grapevine TPS gene involved in trehalose biosynthesis. VvTPS5 was selected for assay due to its seemingly specific expression in grapevine buds, as discussed in Section 5.3.2 of Chapter 5.

Three grapevine TPP family genes were assayed on the bud developmental stages from small and large diameter class shoots to examine their potential role in carbohydrate signalling during the flowering process. VvTPPA was assayed due to previously published work that purported this gene to be the grapevine TPP gene involved in trehalose biosynthesis (Fernandez et al., 2012). The other two grapevine TPP genes assayed, VvTPPB and VvTPPE, were selected due to their sequence similarity to the Arabidopsis TPP gene identified as being involved in trehalose biosynthesis (AtTPPB) and their similarity to the maize TPP gene (RA3) that was identified as being involved in the classic *ramosa3* mutant phenotype that is characterized by increased basal branching in inflorescences.

As shown in Figure 7.8(a), VvTPS1 had the highest relative expression in latent buds. The high relative expression of VvTPS1 in latent buds coincides with the period of inflorescence primordia initiation within grapevine buds and may suggest a role for signalling the carbohydrate status of the plant during this period. Floral pathway genes that have high expression patterns in latent buds include VvCO1 (this work and Almada et al., 2009), VvTFL1A (Carmona et al., 2007), and VvSPLs (Diaz-Riquelme et al., 2012). The concurrent high relative expression of VvTPS1 with members of the VvSPL gene family is quite exciting, as similar expression patterns have been observed in Arabidopsis with AtTPS1 and AtSPLs and are hypothesized to show carbohydrate signalling directly within the shoot apical meristem to initiate the age dependant flowering pathway (Wahl et al., 2013).

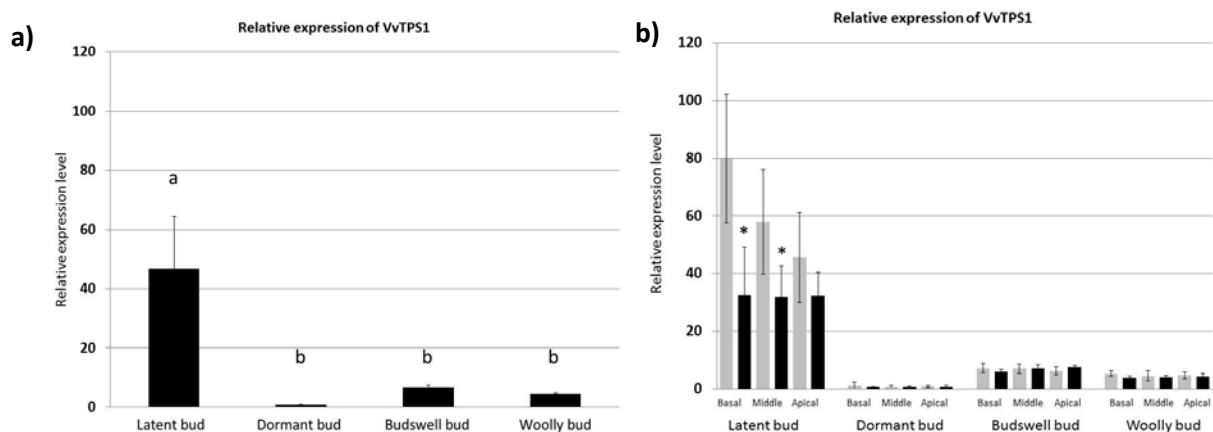


Figure 7.8 Relative expression of VvTPS1 in grapevine bud developmental stages. VvTPS1 expression levels are shown as grouped developmental stages (a) or separated into small or large diameter class shoots (b).

Relative expression values are the means of three biological replicates with three individuals per replicate. Standard deviations of the means are indicated by vertical lines above the bars. In (a), frequencies with the same letter above the bars indicates the means are not significantly different ($p < 0.5$) as determined by the Tukey-Kramer test after ANOVA. In (b), small diameter class shoots are represented by the grey bars, while large diameter class shoots are represented by the black bars. Large diameter class shoots with an asterisk (*)

indicate significantly different ($p < 0.5$) volumes per shoot position when compared to the small diameter class shoots at same position as determined by the Tukey-Kramer test after ANOVA.

As shown in Figure 7.8(b), there is a size effect in VvTPS1 gene expression in small diameter shoots when compared to large diameter shoots in latent buds at the basal and middle shoot positions. There also appears to be a slight size effect in latent buds at the apical position, although the difference in expression between small and large diameter shoots at this position is not statistically significant. Intriguingly, the small diameter shoots have a higher relative expression of VvTPS1 than the large diameter shoots. This is contrary to expected results, in which shoots with large diameters were anticipated to have higher VvTPS1 expression. The reduced expression of VvTPS1 in large diameter class shoots may indicate a feedback effect of the gene or even gene repression from an unknown transcription factor in large diameter shoots.

VvTPS5 had the highest relative expression in latent buds, followed closely by budswell buds (Figure 7.9(a)). Other than the work described in previous chapters, no other research has been done on this gene in grapevine, so functions of this gene can only be hypothesized. As described in Section 5.3.3 of Chapter 5, VvTPS5 is not believed to function as part of the trehalose biosynthesis pathway as this gene cannot complement a yeast strain that lacks a functional TPS gene. As shown in Figure 5.6(e), VvTPS5 has the highest mean relative expression in bud tissue (latent bud and woolly bud), which may indicate a signalling role for this gene in buds. The relative expression of VvTPS5 in both latent and budswell buds is much lower than the expression levels of VvTPS1, which may mean a more specialized role for VvTPS5 in bud tissue. As shown in Figure 7.9(b), VvTPS5 expression was reduced in large diameter shoots from the basal and middle node positions of latent buds, but the

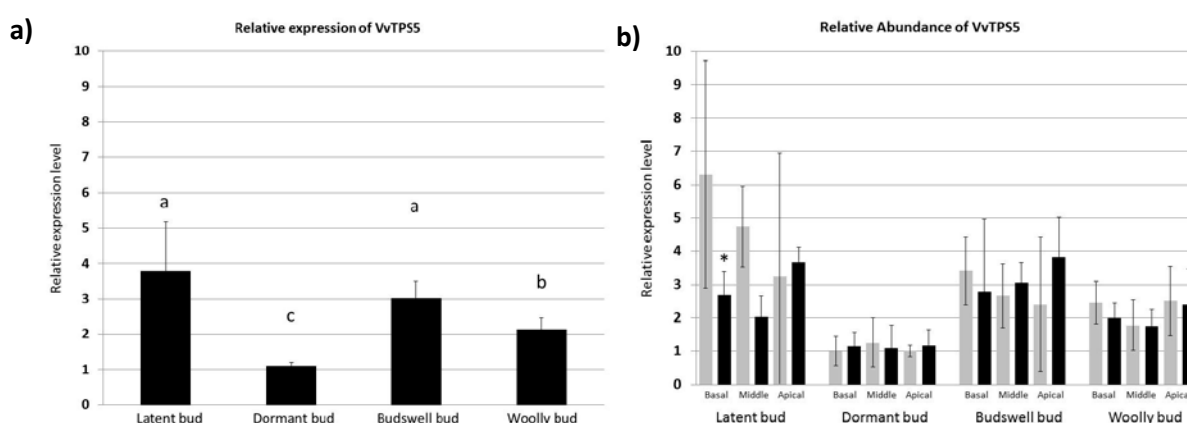


Figure 7.9 Relative expression of VvTPS5 in grapevine bud developmental stages. VvTPS5 expression levels are shown as grouped developmental stages (a) or separated into small or large diameter class shoots (b).

Relative expression values are the means of three biological replicates with three individuals per replicate. Standard deviations of the means are indicated by vertical lines above the bars. In (a), frequencies with the

same letter above the bars indicates the means are not significantly different ($p < 0.5$) as determined by the Tukey-Kramer test after ANOVA. In (b), small diameter class shoots are represented by the grey bars, while large diameter class shoots are represented by the black bars. Large diameter class shoots with an asterisk (*) indicate significantly different ($p < 0.5$) volumes per shoot position when compared to the small diameter class shoots at same position as determined by the Tukey-Kramer test after ANOVA.

difference in latent buds in the middle position was not significant. The reason for reduced gene expression of grapevine TPS genes in large diameter shoots is unknown, and can only be hypothesized to be caused by either a feedback effect or transcriptional repression.

The relative expression of VvTPPA (Figure 7.10(a)) has a similar expression pattern to that of VvTPS1, although at a much lower expression level. VvTPPA may be involved in regulating inflorescence primordia initiation in latent buds, as the expression pattern of the gene is similar to that of VvCO1 (Figure 7.4(a)). VvTPPA has previously been implicated in cold stress response (Fernandez et al., 2012), so determining if this gene is involved in temperature signalling in grapevine would be very interesting. The high expression of VvTPPA in latent buds may indicate both a temperature and carbohydrate signalling role for this gene during inflorescence initiation in grapevine.

Similar to the grapevine TPS genes described above, there is a much lower expression level of VvTPPA in latent buds collected from large diameter shoots when compared to small diameter class shoots at all node positions, although only the middle position was statistically significant (Figure 7.10(b)). Contrary to the results from the grapevine TPS genes tested, a reduced relative expression of grapevine TPP genes in the large diameter class shoots was expected, as reduced TPP activity would lead to an increase in the presence of the signal molecule T6P, which has been shown to increase inflorescence size and architecture in other plant species (Schluepmann et al., 2003; Satoh-Nagasawa et al., 2006).

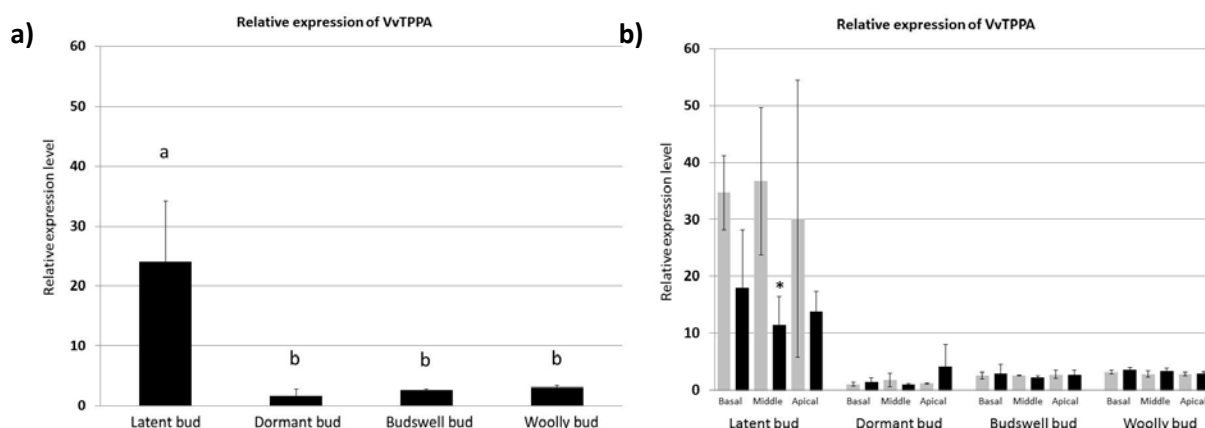


Figure 7.10 Relative expression of VvTPPA in grapevine bud developmental stages. VvTPPA expression levels are shown as grouped developmental stages (a) or separated into small or large diameter class shoots (b).

Relative expression values are the means of three biological replicates with three individuals per replicate. Standard deviations of the means are indicated by vertical lines above the bars. In (a), frequencies with the

same letter above the bars indicates the means are not significantly different ($p < 0.5$) as determined by the Tukey-Kramer test after ANOVA. In (b), small diameter class shoots are represented by the grey bars, while large diameter class shoots are represented by the black bars. Large diameter class shoots with an asterisk (*) indicate significantly different ($p < 0.5$) volumes per shoot position when compared to the small diameter class shoots at same position as determined by the Tukey-Kramer test after ANOVA.

VvTPPB had the highest relative expression in budswell buds (Figure 7.11(a)). Intriguingly, the expression pattern of VvTPPB is similar to that of VvTFL1A (Figure 7.6(a)), although at a much lower level of expression. Given that VvTPPB was the only trehalose pathway gene with increased activity in budswell buds, this gene may incorporate a carbohydrate status signal in the flowering process during the final determination of the inflorescence architecture and outer arm. As described above, VvTPPB and VvTPPE are the two grapevine genes closest in sequence similarity to the maize RAMOSA3 gene, which has been shown to alter inflorescence architecture by regulating levels of T6P in the inflorescence meristem (Satoh-Nagasawa et al., 2006). It is tempting to hypothesize that grapevine TPP genes have evolved specialized roles to regulate T6P levels in grapevine inflorescence primordia to reflect the perennial nature of the species. More research into the functions of grapevine TPP genes during inflorescence development needs to be done to confirm if such a hypothesis is possible.

Unlike the relative expression patterns of the other grapevine TPS and TPP genes tested, VvTPPB does not appear to have any change in expression between the large and small diameter class shoots in the bud stage showing the highest relative expression (Figure 7.11(b)). This suggests that VvTPPB may not have a role in carbohydrate signalling, or that VvTPPB expression in budswell buds is required regardless of carbohydrate status.

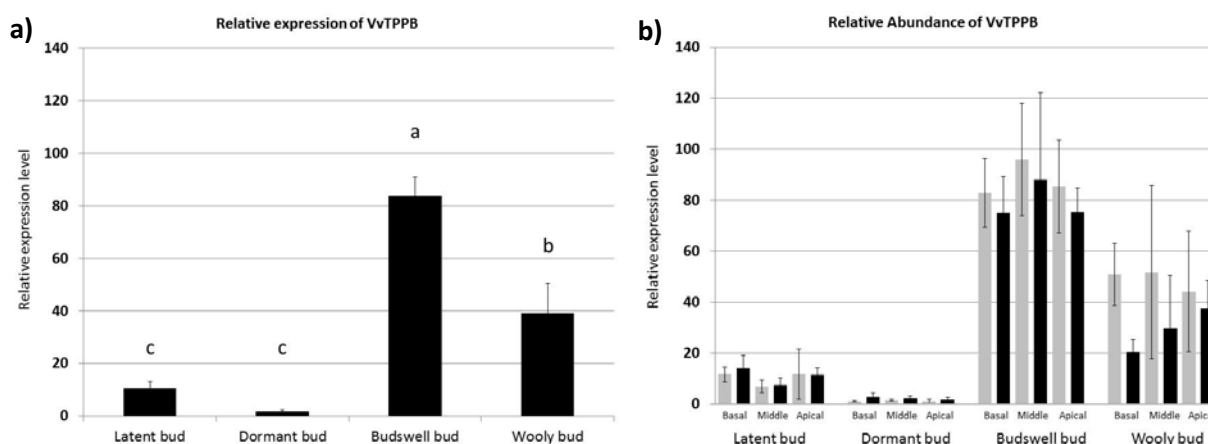


Figure 7.11 Relative expression of VvTPPB in grapevine bud developmental stages. VvTPPB expression levels are shown as grouped developmental stages (a) or separated into small or large diameter class shoots (b).

Relative expression values are the means of three biological replicates with three individuals per replicate. Standard deviations of the means are indicated by vertical lines above the bars. In (a), frequencies with the same letter above the bars indicates the means are not significantly different ($p < 0.5$) as determined by the

Tukey-Kramer test after ANOVA. In (b), small diameter class shoots are represented by the grey bars, while large diameter class shoots are represented by the black bars.

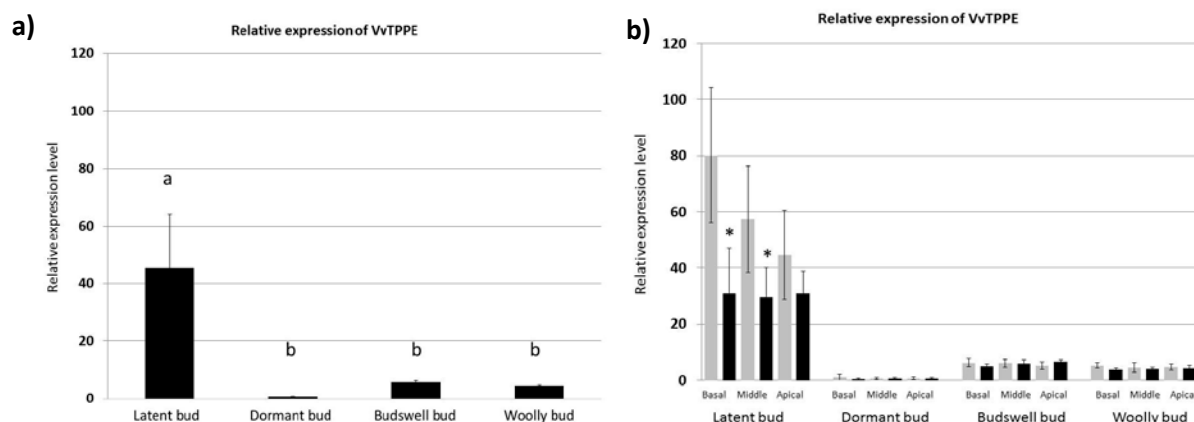


Figure 7.12 Relative expression of VvTPPE in grapevine bud developmental stages. VvTPPE expression levels are shown as grouped developmental stages (a) or separated into small or large diameter class shoots (b).

Relative expression values are the means of three biological replicates with three individuals per replicate. Standard deviations of the means are indicated by vertical lines above the bars. In (a), frequencies with the same letter above the bars indicates the means are not significantly different ($p < 0.5$) as determined by the Tukey-Kramer test after ANOVA. In (b), small diameter class shoots are represented by the grey bars, while large diameter class shoots are represented by the black bars. Large diameter class shoots with an asterisk (*) indicate significantly different ($p < 0.5$) volumes per shoot position when compared to the small diameter class shoots at same position as determined by the Tukey-Kramer test after ANOVA.

VvTPPE had the highest relative expression level in latent buds (Figure 7.12(a)). As discussed in Section 4.3.1 of Chapter 4, VvTPPE may be the grapevine TPP gene involved in trehalose biosynthesis, although other grapevine TPP genes cannot be ruled out due to the ability of all grapevine TPP genes to complement the yeast mutant strain deficient in TPP activity (see Figure 5.5, page 66). As shown in Figure 7.12(b), VvTPPE relative expression had similar levels to that of VvTPS1 (Figure 7.8(b)) for all shoot and diameter positions for every bud developmental stage. This leads us to conclude that VvTPPE expression is tightly linked to VvTPS1 expression and is the most likely candidate for trehalose biosynthesis in grapevine, rather than the previously published VvTPPA (Fernandez et al., 2012). In addition, the high expression of this gene during latent buds indicates a possible role for VvTPPE in signalling the carbohydrate status of the plant during inflorescence primordia formation.

There is a significantly reduced level of VvTPPE expression in large diameter shoots at the basal and middle node positions of latent buds (Figure 7.12(b)). This is again similar to the expression pattern observed in VvTPS1 (Figure 7.8(b)). As discussed with VvTPPA, the reduced expression pattern of VvTPPE is the expected pattern for reduced TPP activity in large diameter shoots, which would lead to an increase in the signal molecule T6P.

The presence of TPS and TPP family genes in grapevine bud developmental stages, as well as the differential expression of many of these genes in large diameter shoots when compared to small diameter shoots from the same plant indicate that some, if not all of the grapevine TPS and TPP genes assayed here are involved in carbohydrate signalling during the flowering process in grapevine. The high expression of VvTPS1 and VvTPPE in latent buds indicates that the trehalose biosynthesis pathway is likely involved in regulating inflorescence primordia initiation. The differential expression of these genes in the two diameter classes examined indicates that carbohydrate supply affects gene transcription of these genes- although the reduced expression of VvTPS1 in large diameter class shoots was an unanticipated result.

A likely explanation for the reduced expression of the VvTPS genes in large diameter shoots is some sort of negative-feedback loop, in which higher carbohydrate supply within the buds leads to transcriptional repression of VvTPS genes. This regulation may be due to the SnRK1 signalling pathway, in which T6P inhibits SnRK1 inhibition. As SnRK1 inhibits anabolic growth processes, a certain level of inhibition must be reached that is no longer beneficial for the plant (i.e. too much growth), so there must be a regulatory mechanism that would inhibit the regulation of SnRK1. A similar model is proposed by Schlueppman et al. (2012), although their model is based on sucrose-mediated regulation of T6P synthesis.

The reduced expression of the grapevine TPP genes (except VvTPPB) in large diameter shoots implies that there is an increase in the signal molecule T6P that is believed to be responsible for the inflorescence phenotype in the maize *ramosa3* mutant. A similar role for T6P may be involved in grapevine, in which shoots with surplus carbohydrate (as inferred from the large diameter) have reduced TPP enzymes, which would lead to higher levels of T6P within latent buds during inflorescence primordia initiation, causing not only larger inflorescences but also a higher frequency of large, fruitful outer arms. VvTPPA has previously been implicated in temperature stress response (Fernandez et al., 2012). The high relative expression of VvTPPA in latent buds suggests that this gene could be involved in signalling both temperature and carbohydrate status during inflorescence primordia initiation. In budswell buds, VvTPPB has the highest relative expression of all the trehalose pathway genes assayed. This suggests that VvTPPB may be involved in signalling during inflorescence differentiation in the period before budburst. However, the lack of differential expression between the shoot diameter classes suggests that gene expression of VvTPPB is not dependant on carbohydrate supply. VvTPPE has the highest relative expression in latent buds and shows a significantly different expression pattern between the two shoot classes at the basal and middle node positions, which suggests that trehalose biosynthesis may be involved in carbohydrate status signalling during inflorescence primordia initiation during this bud developmental stage.

Further work into the regulation of inflorescence initiation and differentiation needs to be done to help elucidate the possible role for TPS and TPP genes in carbohydrate signalling during reproductive development in grapevine. Localization studies showing expression of the trehalose pathway genes in the same tissues as the flowering pathway genes described above would help confirm the role of TPS and/or TPP genes in signalling carbohydrate status within the flowering pathway. As discussed in Section 5.4 of Chapter 5, the localization of VvTPS1 and VvTPPE in grapevine buds by *in situ* hybridization was initiated but was abandoned due to difficulties with tissue fixation and time constraints. The surprising result showing reduced VvTPS gene expression in large diameter class shoots indicates a possible feedback loop regulating these genes. Experiments such as yeast two-hybrid assays would help to identify interactions with any genes that might be regulating transcription of the VvTPS genes. Experiments to measure T6P and trehalose levels in grapevine during bud development would be very helpful, but quite difficult to do given the rapid degradation of T6P and trehalose in plants and the limited availability of the equipment required to measure these metabolites.

Other carbohydrate pathways gene expression in bud developmental stages

To test if other sugar molecules or biosynthesis genes besides the trehalose pathway gene family are involved in carbohydrate signalling in grapevine, members of the sucrose biosynthesis pathway were also assayed on the bud developmental stages studied here. The sucrose synthesis pathway was chosen for screening due to the observed effect of sucrose signalling in floral initiation in other plant species (Bernier et al., 1993). In addition, there is a high similarity in the sucrose and trehalose biosynthesis pathways (Goddijn and van Dun, 1999; Avonce et al., 2006). Similar to trehalose, the initial precursors to sucrose are the product of the Calvin-Benson cycle (Rolland et al., 2002). Sucrose is synthesized from UDP-glucose and fructose-6-phosphate into the intermediate sucrose-6-phosphate (S6P) by the enzyme SUCROSE PHOSPHATE SYNTHASE (SPS), which is then dephosphorylated by the enzyme SUCROSE PHOSPHATE PHOSPHATASE (SPP) to get the sucrose molecule (Goddijn and van Dun, 1999). To date, no studies have been done on the sucrose biosynthesis pathway in grapevine, so a single grapevine SPS gene was selected based on sequence homology to the Arabidopsis homologue AtSPS1 (Lutfiyya et al., 2007) and two grapevine SPP genes were selected based on their high sequence similarity to each other as well as to the Arabidopsis homologue AtSPP1 (Lunn, 2003).

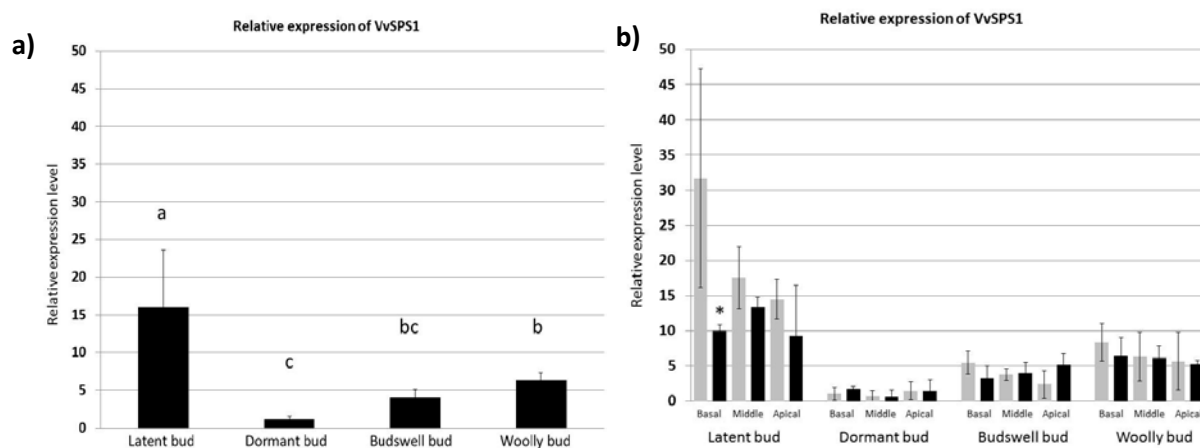


Figure 7.13 Relative expression of VvSPS1 in grapevine bud developmental stages. VvSPS1 expression levels are shown as grouped developmental stages (a) or separated into small or large diameter class shoots (b).

Relative expression values are the means of three biological replicates with three individuals per replicate. Standard deviations of the means are indicated by vertical lines above the bars. In (a), frequencies with the same letter above the bars indicates the means are not significantly different ($p < 0.5$) as determined by the Tukey-Kramer test after ANOVA. In (b), small diameter class shoots are represented by the grey bars, while large diameter class shoots are represented by the black bars. Large diameter class shoots with an asterisk (*) indicate significantly different ($p < 0.5$) volumes per shoot position when compared to the small diameter class shoots at same position as determined by the Tukey-Kramer test after ANOVA.

As shown in Figure 7.13(a), VvSPS1 had the highest relative expression in latent buds. The expression patterns of VvSPS1 is somewhat similar to that of VvTPS1 (Figure 7.8(a)), in that latent buds had the highest gene expression. VvSPS1 differs from VvTPS1 expression, however, in that VvSPS1 expression in woolly buds was higher than the expression of VvSPS1 in dormant buds. This may be due to more products of starch degradation during the stages before budburst being shunted into sucrose synthesis rather than trehalose synthesis. VvSPS1 expression was similar to the expression of the photoperiod signalling gene VvCO1. This may suggest a possible role for this gene is sucrose signalling during inflorescence initiation as suggested for the floral transition in *Arabidopsis* (Corbesier et al., 1998). This hypothesis requires much more research into the role of sucrose during floral development as well as characterization of the sucrose synthesis pathway in grapevine.

Similar to the TPS gene family genes tested, VvSPS1 appears to have reduced expression in latent buds from large diameter class shoots (Figure 7.13(b)), although the buds collected from the basal node position were the only ones that showed a statistically significant difference. It is unclear why large diameter shoots would have a lower relative expression of VvSPS1, but a similar pattern was observed in the VvTPS genes assayed. As discussed with the VvTPS genes above, there may be a feedback loop effect on gene transcription in large diameter class shoots. SPS genes in particular may be down-regulated in grapevine in large diameter shoots due to the sucrose precursors being diverted for starch synthesis instead.

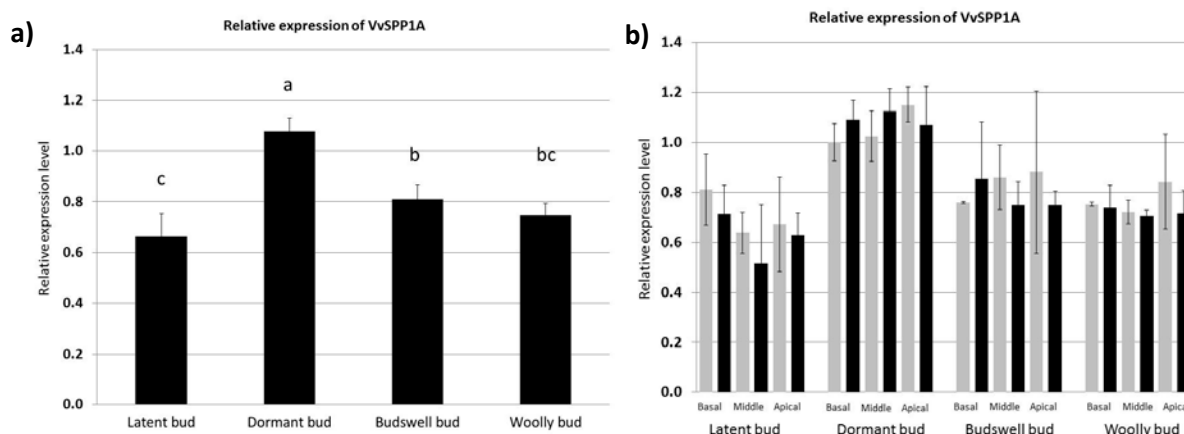


Figure 7.14 Relative expression of VvSPP1A in grapevine bud developmental stages. VvSPP1A expression levels are shown as grouped developmental stages (a) or separated into small or large diameter class shoots (b).

Relative expression values are the means of three biological replicates with three individuals per replicate. Standard deviations of the means are indicated by vertical lines above the bars. In (a), frequencies with the same letter above the bars indicates the means are not significantly different ($p < 0.5$) as determined by the Tukey-Kramer test after ANOVA. In (b), small diameter class shoots are represented by the grey bars, while large diameter class shoots are represented by the black bars.

As shown in Figure 7.14(a), the grapevine SPP homologue VvSPP1A had the highest mean relative expression in dormant buds. This expression pattern is opposite to the pattern observed for all VvTPP genes assayed (VvTPPA, VvTPPB, and VvTPPE), and does not match the expression pattern of any of the floral pathway genes assayed in this study (VvCO1, VvFL, and VvTFL1A). In addition, VvSPP1A expression is quite different to the expression pattern of VvSPS1 (Figure 7.13(a)), indicating that VvSPP1A is not working in conjunction with VvSPS1 for sucrose synthesis. As with the grapevine TPP gene family, the grapevine SPP gene family consists of multiple genes of which only two (VvSPP1A and VvSPP1B) were investigated in this study. Regardless, the higher relative expression of VvSPP1A during the dormant bud stage indicates that this gene may play a role in carbohydrate metabolism during the dormant period in grapevine.

VvSPP1A does not have significantly different levels of expression in large diameter shoots when compared to small diameter shoots from the same bud developmental stage and shoot position (Figure 7.14(b)). This indicates that VvSPP1A is not involved in carbohydrate signalling in grapevine, although more work needs to be done to elucidate the role of this gene. Instead, VvSPP1A may be involved in other signalling pathways during the dormant period, or have a completely different function in grapevine.

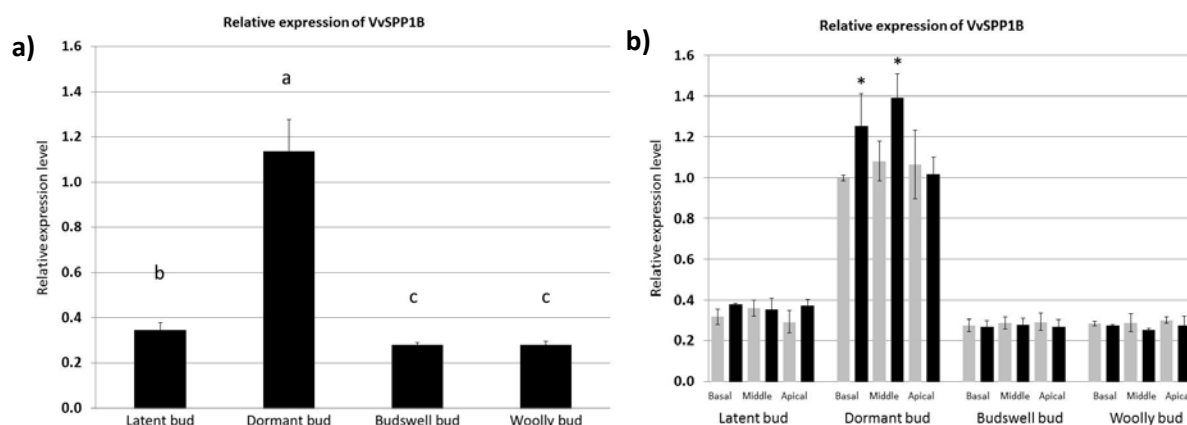


Figure 7.15 Relative expression of VvSPP1B in grapevine bud developmental stages. VvSPP1B expression levels are shown as grouped developmental stages (a) or separated into small or large diameter class shoots (b).

Relative expression values are the means of three biological replicates with three individuals per replicate. Standard deviations of the means are indicated by vertical lines above the bars. In (a), frequencies with the same letter above the bars indicates the means are not significantly different ($p < 0.5$) as determined by the Tukey-Kramer test after ANOVA. In (b), small diameter class shoots are represented by the grey bars, while large diameter class shoots are represented by the black bars. Large diameter class shoots with an asterisk (*) indicate significantly different ($p < 0.5$) volumes per shoot position when compared to the small diameter class shoots at same position as determined by the Tukey-Kramer test after ANOVA.

Similar to VvSPP1A, VvSPP1B had the highest mean relative expression in dormant buds (Figure 7.15(a)). This indicates that VvSPP1B is also not involved in sucrose biosynthesis with VvSPS1, as the expression patterns of these two genes are quite different (Figure 7.13(a)). In addition, the expression pattern of VvSPP1B is dissimilar to the expression pattern of the floral pathway genes examined (VvCO1, VvFL, and VvTFL1A). However, the high relative expression of the gene in dormant buds suggests an alternate role for VvSPP1B in grapevine. The mean relative expression of VvSPP1B is four times higher in dormant buds than the bud developmental stage with the lowest relative expression of the gene (budswell). This indicates that VvSPP1B expression is quite active in dormant buds and may indicate a role for the gene in carbohydrate metabolism and signalling during dormancy in grapevine.

As seen in Figure 7.15(b), there is a diameter effect on VvSPP1B expression in dormant buds at the basal and middle node positions. This suggests that VvSPP1B may be involved in carbohydrate signalling during the dormant period, although the signalling pathway in which the VvSPP1B interacts is unknown. Intriguingly, VvSPP1B is the only carbohydrate gene assayed in which the relative expression of the gene was higher in the large diameter class shoots than the small diameter class shoots.

Given the purported role of sucrose signalling in floral development in plants, some of the genes involved in sucrose biosynthesis were investigated alongside trehalose biosynthesis genes to see what influence, if any, these genes may have in inflorescence development in grapevine. One

grapevine SPS gene (VvSPS1) and two highly similar grapevine SPP genes (VvSPP1A and VvSPP1B) were assayed across four grapevine bud developmental stages collected from small or large diameter class shoots to determine whether they had expression patterns that may indicate a role for the genes in signalling during inflorescence development.

The expression pattern of VvSPS1 (Figure 7.13(a)) was similar to the floral pathway gene VvCO1 and had an expression pattern somewhat like that of the trehalose biosynthesis gene VvTPS1. This suggests that VvSPS1 may be involved in sucrose signalling during inflorescence initiation within latent buds in grapevine. The similarity in expression pattern with VvTPS1 indicates that VvSPS1 is likely involved in sucrose biosynthesis, as both sucrose and trehalose are formed from products of the Calvin-Benson cycle so are likely expressed in similar patterns. The VvSPP genes assayed in this research (VvSPP1A and VvSPP1B) both had their highest expression in dormant buds (Figures 7.14(a) and 7.15(a)). These genes did not match the expression patterns of any other genes investigated, including VvSPS1. This indicates that neither grapevine SPP gene assayed is involved in sucrose biosynthesis with VvSPS1 and are not likely to be involved in floral signalling. The high relative expression of both VvSPP genes studied, particularly VvSPP1B, in dormant buds may indicate a role for these genes in maintaining adequate energy levels within the buds during the dormant period. A complete characterization of the sucrose synthesis pathway in grapevine needs to be done to determine what role, if any, these genes have in sucrose signalling during reproductive development.

7.4 Conclusions and future prospects

To investigate a link between carbohydrate supply and inflorescence size, particularly in regards to outer arm development, a series of experiments were performed using shoots from either small or large diameter class shoots from the same vine. In the first set of experiments, the shoots were harvested and partitioned into single node cuttings to investigate the effects of carbohydrate supply on outer arm formation the following season. The shoots collected for this experiment were harvested from the field trials of another researcher, in which a pruning treatment of 6 or 12 nodes was also included in the experiment (Parker, 2012). For both pruning treatments, both diameter and volume measurements were significantly greater in the large diameter class shoots, indicating that dividing the shoots into these two classes was acceptable for identifying diameter effects on the flowering data. The flowering data from the single node cuttings was subsequently analysed based on the diameter class of the shoot from which the cutting was taken. The outer arm that developed from these cuttings was analysed from the basal inflorescence only, as the other inflorescences that formed fruitful outer arms were too few to be relevant. On the basal inflorescences, the frequency of fruitful outer arms was much higher on the shoots collected from the 12-node pruning treatment. In addition, the frequency of fruitful outer arms from the 12-node pruning treatment was much

higher from shoots in the large diameter class than the small diameter class. While the higher frequency of fruitful outer arms on large diameter class shoots can be attributed to increased carbohydrate supply, the difference in fruitful outer arm frequency between the two pruning treatments cannot be attributed to carbohydrate status alone, as both pruning treatments had similar volume measurements for all shoot positions. This indicates that other factors, likely at the molecular level, are regulating outer arm development in grapevine

To investigate what could be regulating outer arm formation at a molecular level, a series of assays was performed on grapevine bud developmental stages using flowering pathway genes in conjunction with trehalose pathway genes, the transcription factor VvBA1/LAX1, and sucrose pathway genes. The current hypothesis on trehalose pathway genes is that many of these genes are involved in signalling carbohydrate status to the plant during different periods of growth and development. As inflorescence size and outer arm development in grapevine is highly variable, the aim of this work is to study whether trehalose pathway genes are indeed involved in carbohydrate signalling during inflorescence development and/or differentiation in grapevine. In addition to the trehalose pathway gene families, the bHLH transcription factor VvBA1/LAX1 also became a gene of interest to us in inflorescence architecture and outer arm differentiation due to its role in auxin-mediated regulation of cell differentiation in other plant species. To test if the trehalose pathway genes or VvBA1/LAX1 are involved in signalling during the flowering process in grapevine, a series of qRT-PCR assays were done on bud developmental stages collected from small or large diameter class shoots harvested from a commercial vineyard in Marlborough, New Zealand or single node cuttings grown in the greenhouse from shoots collected from the same vineyard. The expression patterns of the trehalose pathway genes and VvBA1/LAX1 were correlated to the expression patterns of three floral pathway genes (VvCO1, VvFL, and VvTFL1A). A fourth floral pathway gene, VvFT, was also investigated but did not amplify in any of the bud developmental stages tested (data not shown).

VvBA1/LAX1 had the highest relative expression in budswell buds, a period in which inflorescence primordia are undergoing final differentiation before budburst. The flowering pathway genes VvFL and VvTFL1A also had high relative expression in this bud developmental stage, indicating a possible role for the VvBA1/LAX1 in regulating inflorescence differentiation in concert with other flowering pathway genes. The high relative expression of VvBA1/LAX1 in budswell buds may indicate how auxin signalling may regulate the final architecture of both the main inflorescence and the outer arm. As the inflorescences begin to differentiate, VvBA1/LAX1 may limit the amount of division occurring at each branch point, leading to an inflorescence with reduced branching (a more open bunch) and even a tendril rather than a fruitful outer arm. There was a slight difference in VvBA1/LAX1 relative expression between small and large diameter class shoots at the basal node positions observed in this study, but the difference was not significant. More work needs to be done to localize

VvBA1/LAX1 expression in grapevine, as well as fully characterize the function of this gene in the species. Previous research has shown a link between auxin signalling and carbohydrate supply in other plant species, and it would be quite informative to determine if there is a similar interaction in grapevine.

VvTPS1 and VvTPPE are the two genes most likely to be involved in trehalose biosynthesis in grapevine. Both genes appear to have differential expression in latent buds between small and large diameter class shoots, indicating a possible role for carbohydrate signalling during latent bud development. As inflorescence primordia initiate in latent buds, the differential expression of these genes may signal to the plant the carbohydrate status of the vine, and aid in the development of larger inflorescences (and in turn larger outer arms) during the initiation and early division of inflorescence primordia. In addition, the selective expression of VvTPS5 in both latent and budswell buds may indicate a specialized role for this gene in floral development in grapevine. The high relative expression of VvTPPA in latent buds and VvTPPB in budswell buds also may indicate specialized roles for these grapevine TPP genes in the initiation and differentiation of inflorescences in the species, as well. Further work needs to be done to localize and characterize these genes within the buds to incorporate the trehalose pathway into the flowering process in grapevine.

VvSPS1 showed a similar expression profile to the flowering pathway gene VvCO1 and VvTPS1. This suggests that VvSPS1 may be involved in sucrose signalling during inflorescence initiation in grapevine. The VvSPP genes investigated in this research did not show similarities to any of the flowering pathway genes investigated, indicating that either these genes are not involved in carbohydrate signalling in grapevine or the interaction of these genes in the flowering process was not discovered during the course of this work. As no work has been done to characterize the sucrose biosynthesis pathway in grapevine, much more research needs to be done before any conclusions can be drawn about whether sucrose biosynthesis genes are involved in signalling during the flowering process.

Chapter 8

Conclusions and future prospects

This research project was initiated to identify the molecular causes for fruitful outer arm development in grapevine. In red wine varieties such as 'Pinot noir', fruitful outer arms can reduce the value of the finished product when used in winemaking due to the ripening delay of up to two weeks in berries from the outer arm when compared to the rest of the bunch. To maintain the value of their crop, red wine viticulturists often remove fruitful outer arms by hand during the growing season or just before harvest to prevent the fruitful outer arm berries from being used in the winemaking process. This adds a substantial cost to the viticulturists, so methods to either prevent fruitful outer arms or predict seasons in which fruitful outer arms will be present in high proportions within the vineyard are currently being examined.

As part of the industry-driven research goal, this research project was tasked with identifying genes that may be involved in fruitful outer arm development in grapevine. Much research into flowering pathway genes has already been done in grapevine by other researchers (for review see Vasconcelos et al., 2009), so the focus of this research turned to genes outside of the general flowering model that have been shown to alter inflorescence morphology and architecture in other plant species. The first gene to attract our attention was a TREHALOSE PHOSPHATE PHOSPHATASE (TPP) gene in maize that is part of the classic *ramosa3* mutant phenotype, which is characterized by an increase in the number of branching events that occur at the base of the meristem for both male and female inflorescences (Satoh-Nagasawa et al., 2006). It was found that loss of the maize RA3 gene, which is in fact a TPP gene, leads to the *ramosa3* phenotype. As fruitful outer arms in grapevine appear to be caused by increased basal branching comparable to that of the *ramosa3* mutation, TPP genes in grapevine also seemed likely to cause a similar surplus of basal inflorescence branching. Further research into genes involved in trehalose biosynthesis revealed that the genes and the products of the pathway are involved in many other biological processes, including carbohydrate signalling via the SnRK1 signalling pathway (Baena-Gonzalez and Sheen, 2008; Zhang et al., 2009). As fruitful outer arms are often found on larger than average inflorescences (Tarter and Poni, 2010), trehalose biosynthesis pathway genes seemed highly likely to be involved in fruitful outer arm development by signalling carbohydrate status within grapevine. It was decided that the bulk of this research project would entail the identification and characterization of the trehalose biosynthesis pathway gene family in grapevine.

The trehalose biosynthesis pathway consists of the production of trehalose from products of the Calvin-Benson cycle. Glucose-6-phosphate and UDP-glucose are synthesized into the trehalose

intermediate molecule trehalose-6-phosphate (T6P) by the enzyme TREHALOSE-6-PHOSPHATE SYNTHASE (TPS). T6P is then dephosphorylated into trehalose by the enzyme TREHALOSE PHOSPHATE PHOSPHATASE (TPP) (Figure 5.1; Müller et al., 1999). As described in Section 4.3.1 of Chapter 4, seven TPS family genes and seven TPP family genes were identified in grapevine. The seven TPS family genes identified agrees with findings from other researchers (Fernandez et al., 2012). In addition to the six TPP family genes identified by both ourselves and Fernandez et al. (2012), this research identified an additional, previously unidentified TPP gene (VvTPPG).

To identify which grapevine TPS and TPP genes are capable of trehalose biosynthesis, the two gene families were partially characterized by complementation of yeast strains that lacked functional TPS or TPP gene activity. Before these complementation experiments could be initiated, plasmids had to be constructed containing stable promoters that could be used in all of the mutant yeast strains to be tested. A total of three plasmid constructs were developed, one containing a constitutive yeast promoter, one containing the endogenous yeast TPS promoter, and one containing the endogenous yeast TPP promoter. As described in Section 2.3 of Chapter 2, the two plasmid constructs containing the endogenous yeast TPS and TPP promoters were sufficient to drive expression of the yeast TPS or TPP genes. These two plasmids were then used to transform the yeast mutant strains with the grapevine TPS and TPP gene family genes to see which genes, if any, are capable of trehalose biosynthesis.

As demonstrated in Section 5.3.1, there is only one grapevine TPS gene (VvTPS1) capable of complementing the yeast *tps* mutant strain. This is the first work to identify a functional TPS gene in grapevine, and is similar to results observed in other plant species in which a single TPS gene family gene is biosynthetically active while the other gene members have other, unknown functions (Vandesteene et al., 2010). Conversely, all grapevine TPP genes tested were capable of complementing the yeast *tpg* mutant strain. This research is the first to test nearly the entire grapevine TPP gene family for functionality by yeast complementation. In addition, the finding that all grapevine TPP genes tested are capable of phosphatase activity as described in this work are similar to findings for TPP gene families in other plant species (Vandesteene et al., 2012).

While the identification of trehalose biosynthesis gene families was underway, another maize mutant phenotype attracted our attention. The *barren stalk* mutation is caused by the loss of maize BA1 function and is characterized by a complete lack of inflorescence branching, leading to a single, sterile stalk for a tassel and no female inflorescences forming (Gallavotti et al., 2004). As grapevine inflorescences and tendrils are formed from the same uncommitted primordia (May, 2000), the maize BA1 gene also became a gene of interest not only for fruitful outer arm development, but also as a possible cause for the regulation of fruitfulness versus tendrilness in grapevine. As there is only

a single BA1 homologue in grapevine (this work; Woods et al., 2011), it was decided that identification and characterization of the BA1/LAX1 gene family would also be carried out for this research project. As discussed in Section 4.3.2 of Chapter 4, the grapevine BA1/LAX1 gene, VvBA1/LAX1, has not yet been studied by any other grapevine researchers and is more similar to the maize and rice homologues than the Arabidopsis homologue AtROX.

To fully characterize gene function in plants, genetic modification is often carried out to either knockout gene expression or overexpress the gene. These experiments are routinely done in annual species such as Arabidopsis and maize, but are much rarer in perennial species such as grapevine due to the low frequency of obtaining transformed plants and the long juvenile period required. In addition, the genetic modification of plants is tightly regulated in New Zealand, leading to limited availability for space to undertake genetic modification experiments at many research institutions, including Lincoln University. Transgenic experiments in which grapevine genes are used to complement mutant strains in annual species such as Arabidopsis are often done to circumvent the time and space limitations involved in transformation experiments in perennial species. As this research successfully showed gene function by yeast complementation for VvTPS1 and all of the VvTTP genes, transformation experiments using grapevine genes in Arabidopsis mutants would not provide any further useful information. Instead, a transcriptomic approach was undertaken to help characterize the gene families of interest in grapevine.

Before any transcriptomic experiments could be done, it was determined that a library of potential reference genes for transcript normalization needed to be identified and validated in grapevine due to the limited number and the outdated standards used to develop the reference genes currently in use within the grapevine community. Ten potential reference genes that were identified as being the most stable genes in the heterologous model species Arabidopsis (Czechowski et al., 2005) were selected for screening, in addition to the four reference genes currently in use within the Winefield research group. As discussed in Section 3.3 of Chapter 3, this led to a total of 11 potential reference genes that were screened across two experimental tissue sets. The 11 potential reference genes were validated as acceptable for use in transcript normalization using two different methods across one of the experimental sets- the highly popular Excel applet GeNorm (Vandesompele et al., 2002) or a basic analysis of variance (ANOVA) test (Khanlou and Van Bockstaele, 2012). As discussed in Section 3.3 of Chapter 3, the results of the two tests were highly similar, indicating that the 11 reference genes were suitable for use in transcript normalization in grapevine across the experimental data sets studied.

Once suitable reference genes were identified and validated, the characterization of the three gene families of interest was initiated. As described in Section 5.3.1 of Chapter 5, the grapevine TPS and

TPP gene families were screened across nine different tissue types for transcript activity. As expected from gene families with multiple members, the members of the TPS and TPP gene families showed variable expression across the different tissue types, indicating specialized and/or localized functions for these genes in grapevine. Of particular interest to this research was the increased expression of some of the TPS and TPP genes in the bud stages examined.

As described in Section 6.3 of Chapter 6, the results from the transcriptomic experiment with the grapevine BA1/LAX1 gene, VvBA1/LAX1, showed high relative expression in several tissue types. The high relative expression of VvBA1/LAX1 in some of the tissue types was similar to observations made in other plant species with BA1/LAX1 genes (Woods et al., 2011). Of particular interest to this research was the high relative expression of VvBA1/LAX1 in the bud stages examined.

To further characterize the role of the TPS, TPP and BA1/LAX1 gene families in grapevine inflorescence development, another set of transcriptomic experiments was undertaken studying members of the three gene families across four bud developmental stages harvested from both small and large diameter shoots. In addition to the gene families of interest, several genes from the general flowering pathway were also assayed to determine if the genes from the TPS, TPP and BA1/LAX1 gene families had similar expression patterns- which would indicate a possible interaction of the genes of interest with the flowering pathway in grapevine. Members of the sucrose biosynthesis pathway were also assayed to determine if this pathway also involved in carbohydrate signalling during the flowering process in grapevine, as has been found in other plant species (Corbesier et al., 1998).

As described in Section 7.3.2 of Chapter 7, all of the TPS and TPP genes examined have high relative expression in at least one of the bud developmental stages tested. In addition, most of the TPS and TPP genes examined have differential expression between the two diameter shoot classes, indicating a possible role for signalling carbohydrate status for these genes. Intriguingly, gene expression was reduced in large diameter class shoots, indicating a possible regulation of these genes, possibly through a feedback loop. The TPS and TPP genes had similar expression patterns to some of the flowering pathway genes assayed, indicating that some if not all of these genes are involved in regulating either inflorescence primordia initiation within latent buds or inflorescence differentiation in budswell buds the following growing season. There were only two TPS and TPP genes with nearly identical expression patterns in all of the bud stages and shoot classes examined-VvTPS1 and VvTPPE. This leads us to hypothesize that these two genes are the only TPS and TPP genes involved in trehalose biosynthesis, while the other members of each gene family have other specialized roles.

As shown in Section 7.3.2 of Chapter 7, the VvBA1/LAX1 gene had its highest relative expression in budswell buds, indicating a possible role for this gene in inflorescence differentiation before

budburst. The floral meristem maintenance genes VvFL and VvTFL1A also had the highest relative expression in budswell buds, which suggests that VvBA1/LAX1 may incorporate a hormone signal into the flowering process while VvFL and VvTFL1A manipulate the final architecture of the inflorescence and possibly outer arm the following growing season.

The sucrose biosynthesis pathway genes assayed across the bud developmental stages and diameter shoot classes did not show as strong of an expression pattern as the trehalose biosynthesis pathway genes. As discussed in Section 7.3.2 of Chapter 7, the SPS homologue VvSPS1 had a similar expression pattern to that of VvTPS1, but at a much lower level of expression. VvSPS1 may be involved in carbohydrate signalling during the flowering process as its highest relative expression was in latent buds- a period in which inflorescence primordia initiation occurs. VvSPS1 had differential expression between the two diameter classes at the basal position of latent buds, further indicating a possible role for carbohydrate signalling in grapevine. The two SPP genes assayed in this experimental set both had their highest expression in dormant buds. These results suggest that neither of these genes are involved in the flowering process, as little inflorescence development occurs during the dormant period. In addition, neither SPP gene examined is likely to be involved in sucrose biosynthesis with VvSPS1 as the expression patterns are too dissimilar. However, the high relative expression of both VvSPP1A and VvSPP1B in dormant buds suggests that these two genes may be involved in energy regulation within the buds during the dormant period. VvSPP1B in particular is quite interesting due to the very high expression of this gene in dormant buds and the differential expression in the basal and middle node positions between the two shoot diameter classes.

To supplement the transcriptomic assays on the bud developmental stages, a series of experiments investigating fruitful outer arm development was done using single node cuttings from small and large diameter class shoots harvested from a field trial set up to investigate pruning treatments in grapevine. Small and large diameter class shoots were collected from vines pruned to either 6 or 12 nodes during the growing season to see what effect the pruning treatment and the shoot diameter size would have on fruitful outer arm formation the following season. As described in Section 7.3.1 of Chapter 7, there was sufficient difference in the diameter measurements between the two groups to categorize them as different classes, although the calculated volume measurement of the cuttings portrayed a more accurate picture of the total potential available carbohydrates for each single node cutting. For both pruning treatments, there were too few fruitful outer arms on the upper inflorescences, so only basal inflorescences were used for further analysis. The shoots pruned to 6 nodes had a much lower frequency of fruitful outer arms on the basal inflorescences, indicating that limiting carbohydrate assimilation during the first year of growth will affect fruitful outer arm development the following year. There was little difference in the frequency of fruitful outer arms

from the small and large diameter class shoots for the 6 node treatment, with the exception of the middle node positions, in which the large diameter class had significantly more fruitful outer arms than the small diameter class. The shoots pruned to 12 nodes had significantly more fruitful outer arms form on the basal inflorescences than the 6 node treatment, and there were significantly more fruitful outer arms on large diameter class shoots, particularly at the middle and apical node positions. The results from the 12 node pruning treatment suggest that small diameter class shoots may reduce the frequency of fruitful outer arm formation the following year if the vines were not severely pruned to limit carbohydrate assimilation during the first growing season.

Given the results of the experiments performed in this research project, it cannot be said definitively that genes from the trehalose biosynthesis pathway or its products are involved in fruitful outer arm formation in grapevine. Before such statements can be made, localization of the grapevine TPS and TPP genes within inflorescence primordia needs to be identified. During the course of this research, localization of the two genes believed to be involved in trehalose biosynthesis, VvTPS1 and VvTPPE, by *in situ* hybridization was initiated but not completed due to difficulties in tissue fixation and time constraints. In addition to gene localization, more research into how the grapevine TPS and TPP genes function in grapevine needs to be done. Ideally, a transgenic approach to either knockdown or overexpress these genes in grapevine would take place to characterize the function of these genes *in planta*. As described above, transgenic experiments in grapevine are quite difficult to do, given the length of time required to achieve transformants and the limited space for the plants. To overcome this hurdle, a transposon-tagged population of 'Sauvignon blanc' grapevine is currently being developed within the Winefield research group. As transposons are naturally occurring in grapevine, the plants are not engineered and so can be grown under standard conditions. The benefit of this transposon-tagged population is the high activity of the transposons selected, which allows for an increased possibility of mutation of many genes each generation. It is hoped that this grapevine population can be used to study the effects of grapevine TPS and TPP mutation in the near future. Biochemical experiments to measure T6P and trehalose levels in grapevine, particularly during the periods of inflorescence primordia initiation in latent buds and inflorescence differentiation in budswell buds would help to elucidate whether trehalose biosynthesis metabolites are being used to signal carbohydrate status during the flowering process in grapevine. Finally, assays to identify gene interactions, such as yeast two-hybrid assays or kinase activity assays would provide invaluable information into the function of the grapevine TPS and TPP gene family members that are not involved in trehalose biosynthesis.

Similarly, the results from the experiments discussed here do not conclusively show that VvBA1/LAX1 is involved in regulating outer arm development or tendril formation in grapevine. Localization of VvBA1/LAX1 in grapevine inflorescence primordia first needs to be done to show that the gene is in

fact active within the inflorescence. During the course of this research, localization of the VvBA1/LAX1 gene by *in situ* hybridization was initiated but not completed due to difficulties in tissue fixation and time constraints. In addition, transgenic approaches as described above or utilization of the transposon-tagged mutant population being developed by our group would help to show whether VvBA1/LAX1 can regulate inflorescence development for both outer arms and the inflorescence itself. An overexpression experiment using VvBA1/LAX1 in Arabidopsis was investigated, but due to the slight phenotype of the mutant and the poor sequence similarity of AtROX1 to other BA1/LAX1 genes, was not performed. An intriguing lead to follow up on is the potential interaction of carbohydrates and hormones such as auxin in grapevine fruitfulness. Finally, the interaction of VvBA1/LAX1 with other genes by yeast two hybrid assays or other gene-gene interaction experiments would be quite informative for this auxin-signalling transcription factor.

In conclusion, three gene families were identified and characterized in grapevine to investigate their potential role in fruitful outer arm formation. The trehalose biosynthesis pathway gene families, TPS and TPP were identified as having seven genes per family. The grapevine TPS gene family has only one biosynthetically active gene (VvTPS1) while all members of the grapevine TPP gene family investigated are capable of phosphorylating the trehalose intermediary molecule T6P into trehalose in yeast. The single grapevine BA1/LAX1 gene, VvBA1/LAX1, was identified and tested for transcript activity across a range of grapevine tissue types along with the VvTPS and VvTPP genes. As several of the genes showed high expression in bud stages, a further transcript assay experiment was performed to examine gene expression of these genes across a range of bud developmental stages collected from shoots with small and large diameters in conjunction with several major flowering pathway genes. The genes from the grapevine TPS, TPP and BA1/LAX1 gene families showed similar expression patterns with the flowering pathway genes and most also showed differential expression between the two diameter class shoots, suggesting a possible carbohydrate signalling function. The bud developmental stage transcriptomic experiment was supplemented with a physiological experiment examining the role of pruning treatments and shoot diameter size on fruitful outer arm development using single node cuttings. The results of the physiological experiment showed that shoot diameter had an effect on fruitful outer arm development for one of the pruning treatments, but diameter size (and by inference carbohydrate supply) alone was not sufficient to explain the difference in fruitful outer arm formation in grapevine.

This research is the first step in identifying potential genes involved in fruitful outer arm development in grapevine. The results of this work show that there are grapevine genes involved in trehalose biosynthesis, which are members of two gene families (TPS and TPP). This work also shows that there is a grapevine VvBA1/LAX1 gene that is more similar to the monocot BA1/LAX1 genes than the Arabidopsis homologue AtROX. The work presented here shows that the genes from the three

gene families investigated have differential expression patterns throughout grapevine tissues, suggesting specialized roles for the genes. The differential expression of several of the genes in grapevine bud developmental stages indicates a possible role for some of these genes in regulating inflorescence architecture and fruitful outer arm development in conjunction with flowering pathway genes via carbohydrate signalling during the flowering process. The findings of this work allow for a more focused look at specific genes (in particular VvTPS1, VvTPPE and VvBA1/LAX1) during inflorescence initiation and differentiation in grapevine to identify the causes of fruitful outer arm development.

Once the characterization of the grapevine trehalose pathway genes and VvBA1/LAX1 has been further elucidated, it is hoped that manipulation of these genes will allow for selection of grapevine varieties or clonal variants that have reduced fruitful outer arms, particularly in red wine varieties such as 'Pinot noir'. Utilization of the transposon-tagged mutant grapevine population being developed by our group should help to facilitate the identification of mutants that show altered inflorescence architecture, particularly in outer arm development. By using these mutants, identification of ways to trigger transposon-induced mutation of genes in red wine varieties will speed up the development of superior lines for release to commercial vineyards. The implementation of these superior lines should lower the cost of red wine production, as hand removal of fruitful outer arms before harvest will be significantly reduced. This will increase both the profitability and the quality of red wine production in New Zealand, which is of great benefit to all members of the industry.

Appendix A

General protocols

Many of the experiments performed for this research used the same general lab protocols. To avoid repetition throughout the thesis, the protocols are described below and referenced in the necessary chapters.

A.1 Polymerase chain reaction (PCR)

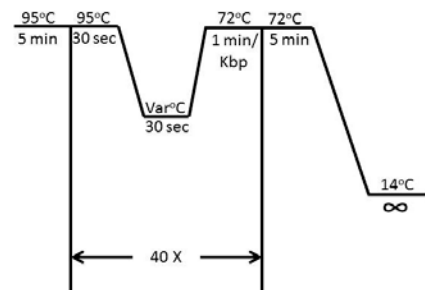
Since its development in the 1980's, the polymerase chain reaction (PCR) has revolutionized molecular biology by allowing researchers to not only detect very low levels of gene expression, but also to synthesize DNA to study gene function in model species. PCR is currently a standard experiment run in all molecular labs for various purposes. As PCR has become so popular, numerous variants of the protocol have been developed. The PCR experiments run for this research are described in this section.

A.1.1 General PCR

The general PCR protocol is used for minor experiments such as checking primer specificity. For this protocol, the DNA template comes from various sources, such as genomic DNA (gDNA), DNA derived from reverse transcription from mRNA, or plasmids. The reagents used for this protocol were from the TaKaRa ExTaq® line (Norrie Biotech, NZ). The protocol is as shown in Table A1.1

Table A.1.1 General PCR protocol

Reagents	Stock Concentration	Final Concentration
10X ExTaq Buffer	10X	1X
dNTPs	10mM	2.5mM
ExTaq Polymerase	5U/μL	1.25U
Sterile water	N/A	As needed
Forward Primer	10mM	2.5mM
Reverse Primer	10mM	2.5mM
Template	Varies	0.5-1ng/μL

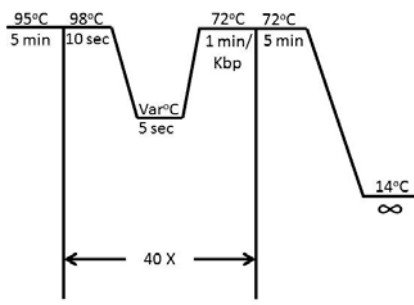


A.1.2 Proofreading PCR

The proofreading PCR utilizes 3'-5' exonuclease activity of some polymerases to ensure specific strand amplification. This protocol was used in this research for gene amplification for cloning so was done in 3x 50µL reactions to ensure plenty of PCR product after gel cleanup. The reagents for this protocol were from the TaKaRa PrimeSTAR® line (Norrie Biotech, NZ). The protocol is as described in Table A.1.2

Table A.1.2 Proofreading PCR protocol

Reagents	Stock Concentration	Final Concentration
5X PrimeSTAR Buffer	5X	1X
dNTPs	10mM	2.5mM
PrimeSTAR Polymerase	2.5U/µL	1.25U/50µL
Sterile water	N/A	As needed
Forward Primer	10mM	2.5mM
Reverse Primer	10mM	2.5mM
Template	Varies	1ng/µL

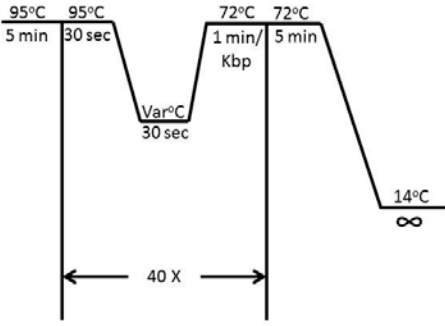


A.1.3 Colony PCR

Colony PCRs were done on transformed *Escherichia coli* DH5α colonies to check for the presence of plasmid containing the correct insert. The template for this protocol was picks of each colony straight from the selection plate. The reagents used for this reaction were from Qiagen (BioStrategy, Ltd.,NZ), with the dNTPs sold separately. The protocol is as described in Table A.1.3 with the primers used as listed in the main text.

Table A.1.3 Colony PCR protocol

Reagents	Stock Concentration	Final Concentration
10X Qiagen PCR Buffer	10X	1X
dNTPs	10mM	2.5mM
Qiagen Taq Polymerase	5U/µL	1.25U
Sterile water	N/A	As needed
Forward Primer	10mM	2.5mM
Reverse Primer	10mM	2.5mM
Template	Unknown	Varies



A.1.4 FTA card PCR

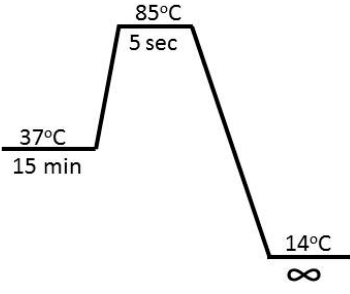
To test transformed *Saccharomyces cerevisiae* genotypes for the presence of plasmid and insert, a modified Colony PCR was done in which transformed *S. cerevisiae* colonies were loaded onto Whatman FTA® cards (Thermo Fisher, NZ) and punches of the cards were used as template for the PCR reaction. The protocol for FTA card development is as described by Borman et al. (2010) and summarized here. Colony picks of the transformed yeast genotypes were suspended in 100 µL sterile water and ~40 µL of the mixture was aliquoted onto a circle of the Whatman FTA® Elute Micro cards and allowed to dry overnight. In preparation for PCR, 1.2mm punches of the card were loaded into PCR tubes and washed twice with 100 µL FTA reagent for two minutes each, followed by a rinse with 100 µL sterile water for two minutes. The liquid was removed and the card punches were allowed to air dry for a minimum of five minutes before the addition of the PCR master mix. The card punches were used as templates for 50 µL colony PCR reactions as described in section A.1.3 using primers listed in the main text.

A.1.5 Reverse-transcriptase PCR (RT-PCR)

Reverse-transcriptase PCR (RT-PCR) was done to screen different grapevine tissue types for transcription activity of each of the genes studied for this research. This was done using RNA extracted from the tissues using the Sigma Spectrum™ Plant Total RNA kit (Sigma-Aldrich, NZ) with the On-Column DNase treatment protocol. Quality control checks were done as described in the main text. The reverse transcriptase reaction was done using TaKaRa BluePrint™ reagents (Norrie Biotech, NZ) and a 1:1 ratio of oligo dTs and random 6-mers as described in Table A.1.4.

Table A.1.4 RT reaction protocol for gene screening

Reagents	Stock Concentration	Final Concentration
5X BluePrint Buffer	5X	1X
BluePrint Enzyme Mix	Unknown	0.5 µL/10 µL
Sterile water	N/A	As needed
Oligo dT Primer	50 µM	25 pmol
Random 6-mers	100 µM	50 pmol
Template	Varies	50 ng/µL

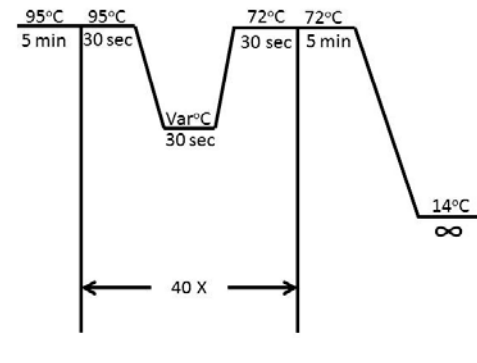


The diagram illustrates the thermal profile for the RT-PCR reaction. It begins with a 15-minute hold at 37°C. This is followed by a 5-second ramp to 85°C. Finally, the reaction enters an infinite hold (indicated by the infinity symbol ∞) at 14°C.

The cDNA synthesized from the reaction was diluted 5-fold with sterile water before being used in the RT-PCR reaction. To confirm product from the RT reaction, the diluted cDNA was checked for template amplification by PCR using RT-Actin primers (Appendix B). The protocol is as described in Table A.1.5.

Table A.1.5 cDNA check PCR protocol

Reagents	Stock Concentration	Final Concentration
10X ExTaq Buffer	10X	1X
dNTPs	10mM	2.5mM
ExTaq Polymerase	5U/ μ L	1.25U
Sterile water	N/A	As needed
RT-Actin F	10mM	2.5mM
RT-Actin R	10mM	2.5mM
Template	Varies	5 μ L/20 μ L rxn



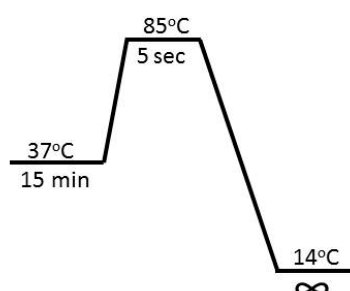
Once the cDNA was confirmed to be present and amplifying in PCR reactions, the RT-PCR reaction was performed using the general PCR protocol as described in section A.1.1 using the primers listed in the main text and Appendix B with 5 μ L of the diluted cDNA as template in a 20 μ L reaction.

A.1.6 Quantitative reverse-transcriptase PCR (qRT-PCR)

To accurately measure the amount of gene transcription occurring in each tissue type tested, quantitative reverse-transcription PCR (qRT-PCR) was performed. For these experiments, RNA was extracted and checked for purity from the tissues as described in the main text. The reverse transcriptase reaction was done using TaKaRa BluePrint™ reagents (Norrie Biotech, NZ) using only oligo dTs as described in Table A.1.6.

Table A.1.6 qRT-PCR protocol

Reagents	Stock Concentration	Final Concentration
5X BluePrint Buffer	5X	1X
BluePrint Enzyme Mix	Unknown	0.5 μ L/10 μ L
Sterile water	N/A	As needed
Oligo dT Primer	50 μ M	25 pmol
Template	Varies	30 ng/ μ L



The cDNA synthesized from the reaction was diluted 20-fold with sterile water before being used in the qRT-PCR reaction and checked for amplification by cDNA check PCR as described in section A.1.4. The reagents used for this reaction were from the TaKaRa SYBR® Premix ExTaq™ II (Tli RNaseH plus) line (Norrie Biotech, NZ). The qRT-PCR protocol is as described in Table A.1.7 with the primers used as listed in Appendix B. The reaction was done in an Illumina Eco™ Real Time PCR System (dnature,

NZ). The cDNA template and master mix was aliquoted into the qRT-PCR plates by an Eppendorf epMotion 5070 liquid handling robot (Eppendorf, NZ) to reduce any pipetting error.

Table A.1.7 qRT-PCR protocol

Reagents	Stock Concentration	Final Concentration
2X SYBR ExTaq II Buffer	2X	1X
Sterile water	N/A	As needed
Forward Primer	10 mM	2.5 mM
Reverse Primer	10 mM	2.5 mM
Template	~10 ng/μL	~40 ng

A.2 Quantitative reverse-transcriptase PCR (qRT-PCR) data analysis

After the qRT-PCR cycle was complete, the raw data was entered into the Illumina EcoStudy 4.0 software (Illumina, NZ) for plate normalization. The plate-normalized data was then exported to Excel and the average Cq and standard deviation for each tissue type was calculated from the biological replicates. The averaged Cq and standard deviation values for the pooled replicates was used in the geNorm application for Excel and normalized to the geometric mean of 3 reference genes listed in the main text relative to the reference sample as listed in the main text by the Pflaffl method as described in Vandesompele et al. (2002) and reviewed here.

For normalization of the data to the reference genes, the mean threshold cycle number (Ct) of each sample (from the pooled biological replicates) was subtracted from the lowest Ct valued sample (ΔCt). The PCR efficiency of the reaction (as determined by the 5-point standard curve) was raised to the power of ΔCt to give the *Q* value ($Q = E^{\Delta Ct}$). The *Q* value of the gene of interest is then divided by the geometric mean of *Q* values of the three reference genes to give the normalization factor, NF ($NF = \frac{Q_{GOI}}{GEOMEAN(Q_{RG1}, Q_{RG2}, Q_{RG3})}$). Relative expression of each sample was then determined by NF value of each sample divided by the NF value of the reference sample (listed in main text) to give the RE value ($RE = \frac{NF_s}{AVG(LB_1, LB_2, LB_3)}$). Meanwhile, standard deviation for the pooled biological replicates was determined using the population standard deviation function in Excel (STDEV.P). The standard deviation was then multiplied by the *Q* value of the sample which was in turn multiplied by the natural logarithm of the PCR efficiency to get the standard deviation of the *Q* value (SD *Q*) (Vandesompele et al., 2002). The standard deviation of the normalization factor for each sample (SD NF_s) was determined by the equation:

$$SD NF_S = NF_S \sqrt{\left(\frac{SD Q_{RG1}}{3 * Q_{RG1}}\right)^2 + \left(\frac{SD Q_{RG2}}{3 * Q_{RG2}}\right)^2 + \left(\frac{SD Q_{RG3}}{3 * Q_{RG3}}\right)^2} \text{ (Vandesompele et al., 2002).}$$

Finally, the standard deviation of the RE value (SD RE) was determined by the equation:

$$SD RE_S = RE_S \sqrt{\left(\frac{SD Q_S}{Q_S}\right)^2 + \left(\frac{SD NF_S}{NF_S}\right)^2} \text{ (Vandesompele et al., 2002).}$$

The relative expression value (RE) and its corresponding standard deviation (SD RE_s) were used to generate charts in Excel. Statistical tests for significance were done as described in the main text.

Appendix B

Primers used for this research

B.1 Plasmid backbone primers

Name	Forward primer	Reverse primer	Notes
M13	GTAAACGACGGCCAG	CAGGAAACAGCTATGAC	For use on pENTR plasmids
pYEX-BX	CATATAGAAGTCATCGA	TTTGACGCTACCACATT	For use on pYex plasmids
T7	TAATACGACTCACTATAGGG		For use on pTOPO-TA plasmids with M13 R

B.2 Reference gene fragment cloning primers

Name	Forward primer	Reverse primer	Amplicon
ACT	CTTGCATCCCTCAGCACCTT	TCCTGTGGACAATGGATGGA	199 bp
AP2mu	TTCTAATGAAATGCTTCCTCTCTGG	GTTCTTAATTGTTGGCAATACTCG	282 bp
EF1 α	AAAATAAAGCGGACGATCTAT	GGAAGCCTCCTATCATCAAAA	85 bp
GAPDH	TTCTCGTTGAGGGCTATTCCA	CCACAGACTTCATCGGTGACA	70 bp
HLK	GGTGATGACTCTGTGCTTTCTGAAG	TGCTATAGATGAATGCAATGGAAGA	297 bp
HYP	CCAAGCCAGGTGAAAAGAAATG	TCATGCACTAGCAACTCCAGAGAC	221 bp
N2227	ATGTCAATGAGCGAAGATGAGGA	TTGAAGGGTAGTGAGACAATAAAGCC	211 bp
PP2A	ATTTATTCCTATGTCGGAGGTGTT	TCATCCTGTGTCAGATCCTCAAATA	423 bp
SAND	CAACATCCTTTACCCATTGACAGA	GCATTTGATCCACTTGCAGATAAG	76 bp
TIIP41	GGAAATGTTGACGGATGGAC	AACTTCAACTGGTGGCAAGG	253 bp
TRU5	GAAGTTCTGGCTTCAGTTGCTG	TCGGTACTTGGTGGAGTAGTCTTT	297 bp

B.3 Whole gene amplification primers

Name	Forward primer	Reverse primer	Amplicon
VvTPS1	CACCATGCCCCGGGAACAAGTACAACGGTAT	TTAAAAAGAAGACTTGGCTCCAGC	2784 bp
VvTPS2	CACCATGGTGTCTGAGATCGTATT	CTATAGAGGAACCGGTTGCTCTGAGAC	2565 bp
VvTPS3	CACCATGGTCTCAAGGTCCTATTCTAATCTC	TTACTCTCTGTCGATAATCGCC	2604 bp
VvTPS4	CACCATGATGTCAAGATCGTATACCAATCTTTTA	TCAAGGAGAGCTTGCTTCAAGTTCGGGAGA	2566 bp
VvTPS5	CACCATGGCCTCAAGATCATGTGCAA	TCATATCCGCAACAAGCTTCC	2583 bp
VvTPS6	CACCATGGTGTCAAGATCATCATATACAA	TCAAGCAACACTTTCAAAGGAGAA	2589 bp
VvTPS7	CACCATGATGTCAAGATCGTATACC	TTATTCTGTTGATGCTTGCGGGGGCTG	2122 bp
VvTPPA	CACCATGGATCTGAAGTCCAATCA	TTATAGTGCACTTGACTTCTTCCACATCAC	1158 bp
VvTPPB	CACCATGACCAACCAGAATGTGGCGG	TCAGTCTCTACTCAATATATC	1128 bp
VvTPPC/G	CACCATGGATTTGAAGTCGAACCATGCT	CTATGCTCCTCTTCCTTCTGAAT	1182 bp
VvTPPD	CACCATGGACAGGGAACCCATCC	TCATGAATTTCCAGCGAAG	948 bp
VvTPPE	CACCATGACGAGGCAGAATGTAGTTG	TTACACCCTGTATTGCCTCATTGACAGT	1098 bp
VvTPPF	CACCATGTCTTGCTATGCTAACATTGCG	CTAATCAACAGAATGACCAGAAAATGAG	1242 bp
VvBA1/LAX1	CACCATGGATTATCCCAGCAG	CTAATAGTAGTTCACGGACGC	486 bp
AtTPS1	CACCATGCCTGGAAATAAGTACAACCTG	TTAAGGTGAGGAAGTGGTGTCTCAGC	2829 bp
AtTPPB	CACCATGACTAACCAGAATGTCATCGTTTCC	TCACTCTTCTCCCACTGTCTTCCTTCCA	1125 bp
AtROX	CACCATGGATGATTTCATCTTC	CTAGGACGAGTCACGTTCTTGCT	517 bp

B.4 RT-PCR primers

Name	Forward primers	Reverse primer	Amplicon
VvTPS1	AGAGATAAGTGCCGGGGGTCTA	TACCTTTCGCCCTGTAAATGTT	745 bp
VvTPS2	TGTTGGTTATTGGGCTCGTAGTT	CAAGCCCTGCATCAGTCTAA	922 bp
VvTPS3	AGGTGCTGGGGTATTGGTTTTGGTTTAG	AGGAAGCCCCTTTGCCCTTATTATCACT	744 bp
VvTPS4	GATTATGATGGGACTGTAATGCCTC	ACACAAAATCAGCCTGCCTTC	550 bp
VvTPS5	AAAAAGTTGTGGAGCCTGTGATGAGAT	GGTAAGATAATTCGCCCCAAAGATGC	691 bp
VvTPS6	GTGGCAGGGGGAAAACTCT	TGCTACACTTGGGCTTCATACTA	648 bp
VvTPS7	ATTGAGGGTTGATGTTGACTTGAC	ATAGCCCCTCTTTGACTGATACTCCA	535 bp
VvTPPA	CTGTGATTGACTGGGATAAGGGAAAAAG	GGGGAGATAATAGGGACCAAAACTGA	636 bp
VvTPPB	CGGTAGAGTCGGTGCCTGGGTGGATTC	GGTGGATTTGGTTTTCTCTAGCAGGG	499 bp
VvTPPC/G	ATGCCATGAAATCGTCCTCTCCTCCTC	CCTTCGCCCATGGGTTAGTCGTA	645 bp
VvTPPD	GGATGTGATTTGGGATTCATACAA	GAGCCTTTTATGTTCTTGGTTCGT	474 bp
VvTPPE	GCACGCTTTCGCCCATAGTTGAT	AGAGCCTTCCCTTTGTCCCATTTA	502 bp
VvTPPF	AATAACTGGGTCTCAGCCTTTCAG	TTCATCAGTTCGATCATCTCCAAT	816 bp
VvBA1/LAX1	ATGGATTATCCCAGCAGCAGCAA	CTAATAGTAGTTCACGGACGC	486 bp

B.5 qRT-PCR primers

Name	Forward primer	Reverse primer	Notes
VvTPS1	CAAGAACAGACGTTCCCGAGTA	CAAGAGAACGATCCAGGTGATG	123 bp
VvTPS2	GCTAGAAGCCGGAAGAACTTG	CCCCTTGGGCCTTAGAAAATAA	93 bp
VvTPS3	GTGTTCTTGCCAATGAGCCAGTT	TGCCGCATTGTTACAAGGAGAC	115 bp
VvTPS4	TAGCCAGGCCAAGGAGATGTTAGA	TTCCGCAACCACACCTTTACTGA	127 bp
VvTPS5	TGATGGGGATTCTGATGTTTGT	GCACCATTTGGCAGTCACTTTA	97 bp
VvTPS6	AGCCACAGGGAGTCAGTAAAGG	GTCCCCAATGCACATCACA	98 bp
VvTPPA	AAAGCAATGCATTTTACTCACTCA	ATAGTGCACTTGACTTCTTCCACATC	90 bp
VvTPPB	GCATTGGCCGAGCAGGTTAG	CGTTTCCCTGTCCCATTGAT	112 bp
VvTPPC/G	GGAAGAAGCCGTCAGAAGGTTTAT	ATGGTCATTGCAGGCTGTGTATCT	114 bp
VvTPPD	GAAGTGGTAGAATCTGTGCTGGAA	TTCTATAAGAGGGCGAACCTCAAG	87 bp
VvTPPE	CCCCACCCGTGTCAAATC	GTGCCGTCGTAGTCCAAAAA	144 bp
VvBA1/LAX1	CGATGACCCGTCTCTGCTCT	CCGGCGCTGTAGTGGTTATGT	119 bp
VvCO1	TGCCTACAGCTACAACCCTTCA	GGATGCGAGATTGAGATTGAGA	114 bp
VvFL	CTACTAAGGTGACGAACCAGGTGTTAG	TAGTGTGCGATCTTGGGTTTGTGAT	82 bp
VvFT	CCCTTTCTCAGGTCCATCACTC	CTCAAGTCATCCCCTCCAATGT	125 bp
VvTFL1A	AGCAGAAACGCCGACAAACA	TTCCCTTTGGGCATTGAAGA	126 bp
VvSPS1	AAGGAGGAGGTGTTTAATCCCA	CACGTGAGTTCCTTGTTGCTATC	115 bp
VvSPP1A	TGCAAAATCTGAAAGTGGATTATCAT	CCACACCTGAAATTTCTTCCTTG	137 bp
VvSPP1B	CTATTGAAAAACGTGGGTTGG	GCCTTAACTTCTTAGCAAATATG	122 bp

Appendix C

Media used for this research

C.1 Bacterial media

C.1.1 LB media (1L)

Tryptone (Ft. Richards Lab, NZ)	10 g
NaCl (Total Lab Systems, NZ)	10 g
Yeast extract (Ft. Richards Lab, NZ)	5 g
Microbiological agar (if needed) (Sigma Aldrich, NZ)	15 g

C.2 Yeast media

C.2.1 YPD media (complete rich media) (1L)

Yeast extract (Ft. Richards Lab, NZ)	10 g
Peptone (Ft. Richards Lab, NZ)	20 g
Galactose or glucose (ThermoFischer Scientific NZ, Ltd.)	20 g
Microbiological agar (if needed) (Sigma Aldrich, NZ)	15 g

C.2.2 Selection media for plasmids containing the URA selection marker (1L)

Yeast nitrogen base without amino acids and ammonium sulphate (Sigma Aldrich, NZ)	1.7 g
Ammonium sulphate (ThermoFischer Scientific NZ, Ltd.)	5 g
Synthetic complete dropout mix minus Uracil (Sigma Aldrich, NZ)	15 g
Galactose or glucose (ThermoFischer Scientific NZ, Ltd.)	20 g
Microbiological agar (if needed) (Sigma Aldrich, NZ)	15 g

Adjust to pH of 5.6 with 1N NaOH before the addition of agar (if used)

C.2.3 Minimal media (1L)

Yeast nitrogen base without amino acids and ammonium sulphate (Sigma Aldrich, NZ)	1.7 g
Ammonium sulphate (ThermoFischer Scientific NZ, Ltd.)	5 g
Uracil (Sigma Aldrich, NZ)	0.037 g
Synthetic complete dropout mix minus Uracil (Sigma Aldrich, NZ)	15 g
Galactose or glucose (ThermoFischer Scientific NZ, Ltd.)	20 g
Microbiological agar (if needed) (Sigma Aldrich, NZ)	15 g

Adjust to pH of 5.6 with 1N NaOH before the addition of agar (if used)

Appendix D

Sequence data for this work

D.1 Sequence results after cloning yeast promoters into pYexBx

Reference Coordinates	370	380	390	400	410	420	430	440
► Translate ► Consensus	CTTTCCTTACATCACACCCAATCCCCACAAGTGATCCCCACACACCATAGCTTCAAAATGTTTCTACTCCT							
► pYEXBx S...372>5323) →	cttTCCTTACATCACACCCAATCCCCACAAGTGATCCCCACACACCATAGCTTCAAAATGTTTCTACTCCT							
► pYex_TEF...12(4>884) ←	CTTTCCTTACATCACACCCAATCCCCACAAGTGATCCCCACACACCATAGCTTCAAAATGTTTCTACTCCT							
► pYex_TEF...1(17>807) →	CTTTCCTTACATCACACCCAATCCCCACAAGTGATCCCCACACACCATAGCTTCAAAATGTTTCTACTCCT							
Reference Coordinates	450	460	470	480	490	500	510	520
► Translate ► Consensus	TTTTTACTCTTCCAGATTTTCTCGGACTCCGCGCATCGCCGTACCACTTCAAAACACCCAAGCACAGCATACTAAATTTCCCC							
► pYEXBx S...372>5323) →	TTTTTACTCTTCCAGATTTTCTCGGACTCCGCGCATCGCCGTACCACTTCAAAACACCCAAGCACAGCATACTAAATTTCCCC							
► pYex_TEF...12(4>884) ←	TTTTTACTCTTCCAGATTTTCTCGGACTCCGCGCATCGCCGTACCACTTCAAAACACCCAAGCACAGCATACTAAATTTCCCC							
► pYex_TEF...1(17>807) →	TTTTTACTCTTCCAGATTTTCTCGGACTCCGCGCATCGCCGTACCACTTCAAAACACCCAAGCACAGCATACTAAATTTCCCC							
Reference Coordinates	530	540	550	560	570	580	590	600
► Translate ► Consensus	TCTTTCCTCCTCTAGGGTGTCGTTAATTACCCGTAATAAGGTTTGAAAAAGAAAAAGAGACCGCCTCGTTTCTTTTT							
► pYEXBx S...372>5323) →	TCTTTCCTCCTCTAGGGTGTCGTTAATTACCCGTAATAAGGTTTGAAAAAGAAAAAGAGACCGCCTCGTTTCTTTTT							
► pYex_TEF...12(4>884) ←	TCTTTCCTCCTCTAGGGTGTCGTTAATTACCCGTAATAAGGTTTGAAAAAGAAAAAGAGACCGCCTCGTTTCTTTTT							
► pYex_TEF...1(17>807) →	TCTTTCCTCCTCTAGGGTGTCGTTAATTACCCGTAATAAGGTTTGAAAAAGAAAAAGAGACCGCCTCGTTTCTTTTT							
Reference Coordinates	610	620	630	640	650	660	670	680
► Translate ► Consensus	CTTCGTCGAAAAAGGCAATAAAAATTTTATCACGTTTCTTTTCTTGAAAATTTT-T-GATTTTTTCTCTTTCGA							
► pYEXBx S...372>5323) →	CTTCGTCGAAAAAGGCAATAAAAATTTTATCACGTTTCTTTTCTTGAAAATTTT-T-GATTTTTTCTCTTTCGA							
► pYex_TEF...12(4>884) ←	CTTCGTCGAAAAAGGCAATAAAAATTTTATCACGTTTCTTTTCTTGAAAATTTT-T-GATTTTTTCTCTTTCGA							
► pYex_TEF...1(17>807) →	CTTCGTCGAAAAAGGCAATAAAAATTTTATCACGTTTCTTTTCTTGAAAATTTT-T-GATTTTTTCTCTTTCGA							

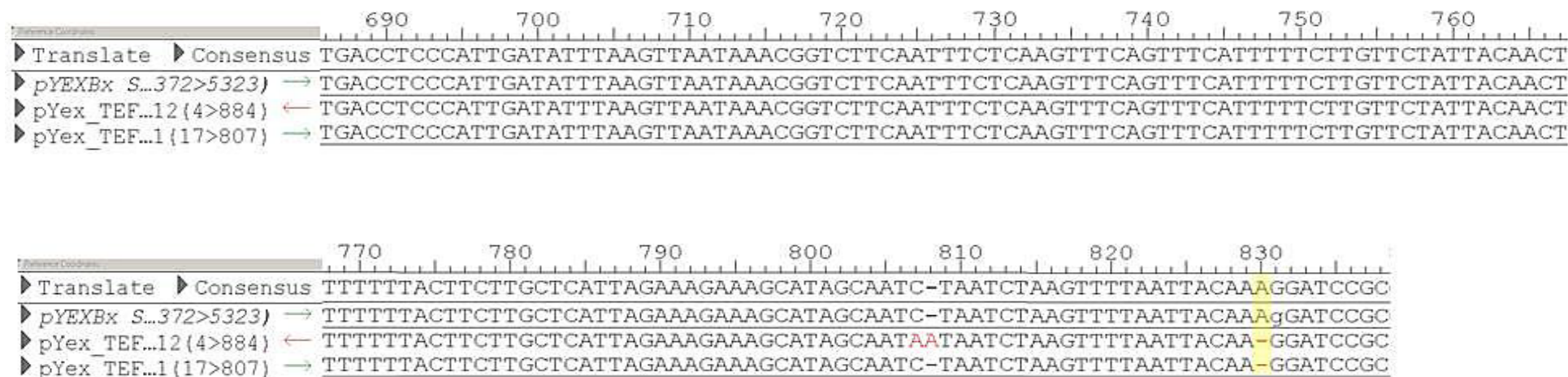


Figure D.1 Yeast TEF1 constitutive promoter sequence alignment.

Sequence results as shown by the SeqManager program in the Lasergene 9 software suite (Burland, 2000). The top row displays the consensus of the reference sequence (2nd row) when compared to the forward (4th row) and reverse (3rd row) sequence results. The reference sequence was generated by inserting the ScTEF1 promoter sequence generated from the S288c genotype obtained from the NCBI database into the CUP1 promoter site of pYexBx. The first nucleotide of the promoter sequence is highlighted in grey. The sequenced nucleotides that diverge from the reference sequence are highlighted in yellow.

		370	380	390	400	410	420	430	440
► Translate	► Consensus	AGCTTGTGGTTGTGTCAGGGGTGATAGCCATATCTTCGTGCTCTTGTGTCATTGTTCTGTTCCATCTGCACCAGAACAAAG							
► pYEXBx S...368>5382	→	agcttGTGGTTGTGTCAGGGGTGATAGCCATATCTTCGTGCTCTTGTGTCATTGTTCTGTTCCATCTGCACCAGAACAAAG							
► pYex_TPS..._2(9>887)	←	AGCTTGTGGTTGTGTCAGGGGTGATAGCCATATCTTCGTGCTCTTGTGTCATTGTTCTGTTCCATCTGCACCAGAACAAAG							
► pYex_TPS..._(10>873)	→	AGCTTGTGGTTGTGTCAGGGGTGATAGCCATATCTTCGTGCTCTTGTGTCATTGTTCTGTTCCATCTGCACCAGAACAAAG							

		450	460	470	480	490	500	510	520
► Translate	► Consensus	AACAAAAGAACAAG3AACAAAGTCCAAGCACGTGAGCGCTGTTTATAAGGGGATTGACGAGGGATCGGGCCTAGAGTGC							
► pYEXBx S...368>5382	→	AACAAAAGAACAAG3AACAAAGTCCAAGCACGTGAGCGCTGTTTATAAGGGGATTGACGAGGGATCGGGCCTAGAGTGC							
► pYex_TPS..._2(9>887)	←	AACAAAAGAACAAG3AACAAAGTCCAAGCACGTGAGCGCTGTTTATAAGGGGATTGACGAGGGATCGGGCCTAGAGTGC							
► pYex_TPS..._(10>873)	→	AACAAAAGAACAAG3AACAAAGTCCAAGCACGTGAGCGCTGTTTATAAGGGGATTGACGAGGGATCGGGCCTAGAGTGC							

		530	540	550	560	570	580	590	600
► Translate	► Consensus	CAGCGCGCCAGGGAGAGGGAGCCCCCTGGGCCCTCATCCGCAGGCTGATAGGGGTACCCCCGCTGGGCAGGTCAGGGCAGGG							
► pYEXBx S...368>5382	→	CAGCGCGCCAGGGAGAGGGAGCCCCCTGGGCCCTCATCCGCAGGCTGATAGGGGTACCCCCGCTGGGCAGGTCAGGGCAGGG							
► pYex_TPS..._2(9>887)	←	CAGCGCGCCAGGGAGAGGGAGCCCCCTGGGCCCTCATCCGCAGGCTGATAGGGGTACCCCCGCTGGGCAGGTCAGGGCAGGG							
► pYex_TPS..._(10>873)	→	CAGCGCGCCAGGGAGAGGGAGCCCCCTGGGCCCTCATCCGCAGGCTGATAGGGGTACCCCCGCTGGGCAGGTCAGGGCAGGG							

		610	620	630	640	650	660	670	680
► Translate	► Consensus	GCTCTCAGGGGGGCGCCATGGACAAACTGCACTGAGGTTCTAAGACACATGTATTATTGTGAGTATGTATATATAGAGA							
► pYEXBx S...368>5382	→	GCTCTCAGGGGGGCGCCATGGACAAACTGCACTGAGGTTCTAAGACACATGTATTATTGTGAGTATGTATATATAGAGA							
► pYex_TPS..._2(9>887)	←	GCTCTCAGGGGGGCGCCATGGACAAACTGCACTGAGGTTCTAAGACACATGTATTATTGTGAGTATGTATATATAGAGA							
► pYex_TPS..._(10>873)	→	GCTCTCAGGGGGGCGCCATGGACAAACTGCACTGAGGTTCTAAGACACATGTATTATTGTGAGTATGTATATATAGAGA							

		690	700	710	720	730	740	750	760
► Translate	► Consensus	GAGATTAAGGCGTACAGCCGGGTGGTAGAGATTGATTAACCTGGTAGTCTTATCTTGTCAATTGAGTTTCTGTCAGTTTCTT							
► pYEXBx S...368>5382	→	GAGATTAAGGCGTACAGCCGGGTGGTAGAGATTGATTAACCTGGTAGTCTTATCTTGTCAATTGAGTTTCTGTCAGTTTCTT							
► pYex_TPS..._2(9>887)	←	GAGATTAAGGCGTACAGCCGGGTGGTAGAGATTGATTAACCTGGTAGTCTTATCTTGTCAATTGAGTTTCTGTCAGTTTCTT							
► pYex_TPS..._(10>873)	→	GAGATTAAGGCGTACAGCCGGGTGGTAGAGATTGATTAACCTGGTAGTCTTATCTTGTCAATTGAGTTTCTGTCAGTTTCTT							

	770	780	790	800	810	820	830	840
► Translate ► Consensus	CTTGAACAAGCACGCAGCTAAGTAAGCAACAAAGCAGGCTAACAACTAGGTACTCACATACAGACTTAGGATCCGC							
► pYEXBx S...368>5382) →	CTTGAACAAGCACGCAGCTAAGTAAGCAACAAAGCAGGCTAACAACTAGGTACTCACATACAGACTTAGGATCCGC							
► pYex_TPS..._2(9>887) ←	CTTGAACAAGCACGCAGCTAAGTAAGCAACAAAGCAGGCTAACAACTAGGTACTCACATACAGACTTAGGATCCGC							
► pYex_TPS..._(10>873) →	CTTGAACAAGCACGCAGCTAAGTAAGCAACAAAGCAGGCTAACAACTAGGTACTCACATACAGACTTAGGATCCGC							

Figure D.2 Yeast TPS1 constitutive promoter sequence alignment.

Sequence results as shown by the SeqManager program in the Lasergene 9 software suite (Burland, 2000). The top row displays the consensus of the reference sequence (2nd row) when compared to the forward (4th row) and reverse (3rd row) sequence results. The reference sequence was generated by inserting the ScTPS1 promoter sequence generated from the S288c genotype obtained from the NCBI database into the CUP1 promoter site of pYexBx. The first and last nucleotides of the promoter sequence are highlighted in grey.

370 380 390 400 410 420 430 440

► Translate ► Consensus TTCTCCTTCCAACGGTCAACCCCTTCTTTCTATTCTCTTCTCGTTCTCTACGTAAGGAACTTGTAAGGAAAAAA

► pYEX-BX(4371>5353) → TTCTCCTTCCAACGGTCAACCCCTTCTTTCTATTCTCTTCTCGTTCTCTACGTAAGGAACTTGTAAGGAAAAAA

► pYex_TPS... (10>863) ← TTCTCCTTCCAACGGTCAACCCCTTCTTTCTATTCTCTTCTCGTTCTCTACGTAAGGAACTTGTAAGGAAAAAA

► pYex_TPS... (23>844) → TTCTCCTTCCAACGGTCAACCCCTTCTTTCTATTCTCTTCTCGTTCTCTACGTAAGGAACTTGTAAGGAAAAAA

450 460 470 480 490 500 510 520

► Translate ► Consensus TTTGGTGCCATACAGGGAAATCGGCAGTGAGACGGAGCGGCCGAGGGTCTGATTATAGGGGTAGTTACGCTCCTACTATGA

► pYEX-BX(4371>5353) → TTTGGTGCCATACAGGGAAATCGGCAGTGAGACGGAGCGGCCGAGGGTCTGATTATAGGGGTAGTTACGCTCCTACTATGA

► pYex_TPS... (10>863) ← TTTGGTGCCATACAGGGAAATCGGCAGTGAGACGGAGCGGCCGAGGGTCTGATTATAGGGGTAGTTACGCTCCTACTATGA

► pYex_TPS... (23>844) → TTTGGTGCCATACAGGGAAATCGGCAGTGAGACGGAGCGGCCGAGGGTCTGATTATAGGGGTAGTTACGCTCCTACTATGA

530 540 550 560 570 580 590 600

► Translate ► Consensus CGATCAAGGAGAGACAATCTCGATTCTCATTCTTTCTTTGGGACAATACGCCTTTAACCCCCCATTTTCGGACATCC

► pYEX-BX(4371>5353) → CGATCAAGGAGAGACAATCTCGATTCTCATTCTTTCTTTGGGACAATACGCCTTTAACCCCCCATTTTCGGACATCC

► pYex_TPS... (10>863) ← CGATCAAGGAGAGACAATCTCGATTCTCATTCTTTCTTTGGGACAATACGCCTTTAACCCCCCATTTTCGGACATCC

► pYex_TPS... (23>844) → CGATCAAGGAGAGACAATCTCGATTCTCATTCTTTCTTTGGGACAATACGCCTTTAACCCCCCATTTTCGGACATCC

610 620 630 640 650 660 670

► Translate ► Consensus CTGGAAGTCTCAGCTGATTCATTTAAATACTATCAATTTCGGTGTACTTTCGGAGATCTTTCAGTCAGCTTTTCC

► pYEX-BX(4371>5353) → CTGGAAGTCTCAGCTGATTCATTTAAATACTATCAATTTCGGTGTACTTTCGGAGATCTTTCAGTCAGCTTTTCC

► pYex_TPS... (10>863) ← CTGGAAGTCTCAGCTGATTCATTTAAATACTATCAATTTCGGTGTACTTTCGGAGATCTTTCAGTCAGCTTTTCC

► pYex_TPS... (23>844) → CTGGAAGTCTCAGCTGATTCATTTAAATACTATCAATTTCGGTGTACTTTCGGAGATCTTTCAGTCAGCTTTTCC

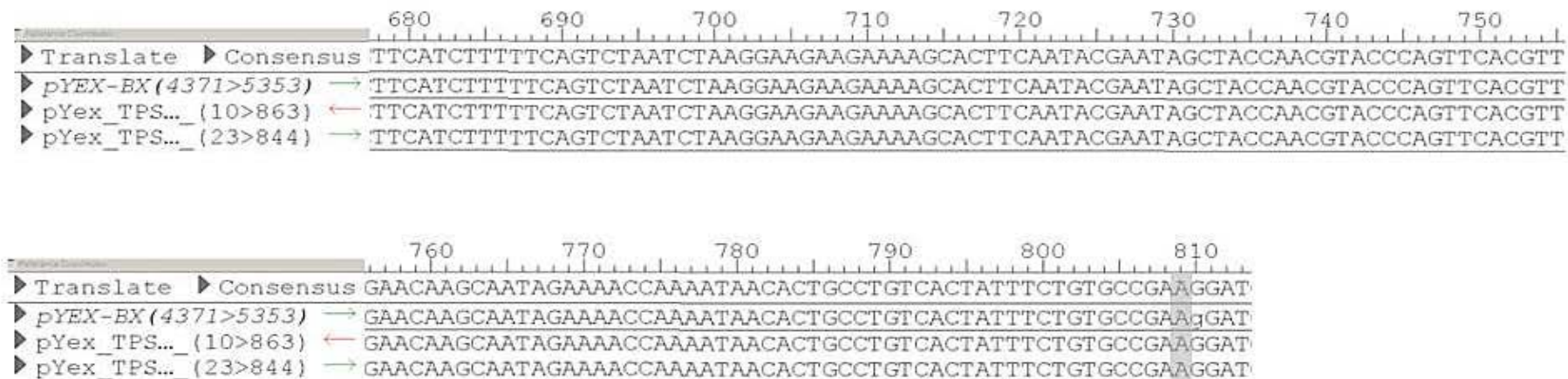


Figure D.3 Yeast TPS2 constitutive promoter sequence alignment.

Sequence results as shown by the SeqManager program in the Lasergene 9 software suite (Burland, 2000). The top row displays the consensus of the reference sequence(2nd row) when compared to the forward (4th row) and reverse (3rd row) sequence results. The reference sequence was generated by inserting the ScTPS2 promoter sequence generated from the S288c genotype obtained from the NCBI database into the CUP1 promoter site of pYexBx. The first and last nucleotides of the promoter sequence are highlighted in grey.

D.2 Class II TPS genes sequence alignment of the glycosyltransferase and phosphatase regions

EcOtsA	R	I	A	P	P	D	E	H	A	-	-	-	-	-	-	-	-	A	S	A	G	G	L	A	V	G	I	L	G	A	L	K	A	-	-	A	G	G	L	W	F	G	W	S	G	-	-	-		
ScTPS1	R	L	P	V	T	I	T	K	N	S	-	S	-	T	G	Q	Y	E	A	M	S	S	G	G	L	V	T	A	L	L	-	G	V	K	E	-	-	F	E	A	R	W	F	G	W	S	G	-	-	-
AtTPS1	R	L	P	V	S	A	V	R	R	G	E	D	S	-	-	W	S	L	E	I	S	A	G	G	L	V	S	A	L	L	-	G	V	K	E	-	-	F	E	A	R	W	I	G	W	A	G	V	N	V
VvTPS1	R	L	P	V	S	A	I	R	R	G	E	E	S	-	-	W	S	L	E	I	S	A	G	G	L	V	S	A	L	L	-	G	V	K	E	-	-	F	E	A	R	W	I	G	W	A	G	V	N	V
VvTPS2	Q	L	P	I	R	A	Q	R	K	S	E	N	N	N	G	W	I	F	S	W	D	E	N	S	L	L	L	Q	L	K	D	G	L	G	D	D	E	I	E	V	I	Y	V	G	C	L	K	E	E	I
VvTPS3	Q	L	P	L	R	A	H	R	S	S	D	G	S	G	E	W	C	F	S	W	D	E	D	S	L	L	L	Q	L	K	D	G	L	P	D	D	-	M	E	V	L	Y	V	G	S	L	R	V	D	V
VvTPS4	Q	L	P	V	K	A	K	R	R	P	D	N	K	G	-	W	S	F	S	W	D	E	D	S	L	L	L	Q	L	K	D	G	L	P	D	D	-	M	E	V	L	Y	V	G	S	L	R	V	D	V
VvTPS5	M	L	P	L	H	A	Q	R	D	K	-	V	T	A	K	W	C	F	S	L	D	E	D	A	L	L	L	H	L	K	D	G	F	S	P	E	-	T	E	V	I	Y	V	G	S	L	K	V	E	I
VvTPS6	F	L	P	L	L	A	Q	K	D	L	-	N	T	G	R	W	C	F	S	F	D	E	D	A	L	L	L	Q	M	K	D	G	F	S	S	E	-	T	D	V	V	Y	V	G	S	L	K	V	D	V
VvTPS7	Q	L	P	V	K	A	N	R	R	A	D	D	R	G	-	W	V	F	S	W	N	E	D	S	L	L	L	Q	L	K	E	G	L	P	E	D	-	M	E	V	L	Y	V	G	S	L	R	V	D	V

EcOtsA	E	T	G	N	E	D	Q	P	L	K	K	V	K	K	G	N	I	T	W	A	S	F	N	L	S	E	Q	D	L	D	E	Y	Y	N	Q	F	S	N	A	V	L	W	P	A	F	H	Y	R	-	L	
ScTPS1	P	D	D	E	K	D	Q	V	R	K	D	L	L	E	K	F	N	A	V	P	I	F	-	L	S	D	E	I	A	D	L	H	Y	Y	N	G	F	S	N	N	I	L	W	P	L	F	H	Y	H	-	L
AtTPS1	P	D	E	V	G	Q	K	A	L	T	K	A	L	A	E	K	R	C	I	P	V	F	-	L	D	E	I	V	H	Q	Y	Y	Y	N	G	Y	C	N	N	I	L	W	P	L	F	H	Y	L	G	L	
VvTPS1	P	D	E	A	G	Q	R	A	L	T	K	A	L	A	E	K	M	C	I	P	V	F	-	L	D	E	I	V	H	Q	Y	Y	Y	N	G	Y	C	N	N	I	L	W	P	L	F	H	Y	L	G	L	
VvTPS2	H	P	C	E	Q	D	E	V	S	Q	I	L	L	E	T	F	K	C	V	P	T	F	-	L	P	P	D	L	F	T	R	Y	Y	H	G	F	C	K	Q	Q	L	W	P	L	F	H	Y	M	-	L	
VvTPS3	D	P	S	E	Q	D	D	V	A	Q	T	L	L	E	T	F	K	C	V	P	A	F	-	I	P	P	E	L	F	S	K	F	Y	H	G	F	C	K	Q	Q	L	W	P	L	F	H	Y	M	-	L	
VvTPS4	D	S	N	E	Q	D	D	V	S	Q	V	L	L	D	R	F	K	C	V	P	A	F	-	L	P	Q	D	I	L	S	K	F	Y	H	G	F	C	K	Q	Q	L	W	P	L	F	H	Y	M	-	L	
VvTPS5	D	A	S	E	Q	E	E	V	A	Q	K	L	L	E	D	F	N	C	V	P	T	F	-	L	P	H	D	L	H	K	K	F	Y	H	G	F	C	K	Q	Q	L	W	P	L	F	H	Y	M	-	L	
VvTPS6	D	T	S	E	Q	E	E	V	A	E	R	L	L	A	E	F	N	C	V	P	T	F	-	L	P	P	D	L	Q	K	K	F	Y	H	G	F	C	K	Q	Y	L	W	P	L	F	H	Y	M	-	L	
VvTPS7	D	L	T	E	Q	E	E	V	S	Q	I	L	L	E	T	F	K	C	V	P	T	F	-	L	P	H	D	V	L	E	K	F	Y	H	G	F	C	K	K	L	L	W	P	L	F	H	Y	M	-	L	

EcOtsA	D	L	V	-	-	-	-	-	Q	F	Q	R	P	A	W	D	G	Y	L	R	V	N	A	L	L	A	D	K	L	L	P	L	L	Q	-	D	D	D	I	I	W	I	H	D	Y	H	L	L	P		
ScTPS1	-	-	-	-	-	P	G	E	I	N	F	D	E	N	A	W	L	A	Y	N	E	A	N	Q	T	F	T	N	E	I	A	K	T	M	N	-	H	N	D	L	I	W	V	H	D	Y	H	L	M	F	
AtTPS1	P	Q	E	D	R	L	A	T	T	R	S	F	Q	S	Q	F	A	A	Y	K	K	A	N	Q	M	F	A	D	V	V	N	K	H	Y	E	-	E	G	D	V	V	W	C	H	D	Y	H	L	M	F	
VvTPS1	P	Q	E	D	R	L	A	T	T	R	S	F	Q	S	Q	F	A	A	Y	K	K	A	N	Q	M	F	A	D	V	V	N	K	H	Y	E	-	E	G	D	V	V	W	C	H	D	Y	H	L	M	F	
VvTPS2	P	L	S	P	D	L	G	-	G	R	F	N	R	S	L	W	Q	A	Y	V	S	V	N	K	I	F	A	D	R	I	M	E	V	I	N	P	E	D	D	F	V	W	I	H	D	Y	H	L	M	V	
VvTPS3	P	L	S	P	D	L	G	-	G	R	F	D	R	S	L	W	Q	A	Y	V	S	V	N	K	I	F	A	D	R	K	V	M	E	V	I	T	P	D	E	D	F	V	W	V	H	D	Y	H	L	M	V
VvTPS4	P	F	S	A	N	H	G	-	G	R	F	D	R	S	L	W	E	A	Y	V	S	A	N	K	I	F	S	Q	R	V	I	E	V	L	N	P	E	D	D	Y	V	W	V	I	H	D	Y	H	L	M	V
VvTPS5	P	M	C	P	D	H	G	-	D	R	F	D	R	V	L	W	Q	A	Y	V	S	A	N	K	I	F	A	D	K	V	R	E	V	I	N	P	E	D	D	Y	V	W	I	H	D	Y	H	L	M	V	
VvTPS6	P	M	S	P	E	H	C	-	N	R	F	D	R	F	L	W	Q	A	Y	V	S	A	N	K	I	F	A	D	K	V	M	E	V	I	N	P	E	E	D	Y	V	W	I	H	D	Y	H	L	M	V	
VvTPS7	P	F	S	A	D	H	G	-	G	R	F	D	R	S	M	W	E	A	Y	V	W	A	N	K	L	F	S	Q	K	V	I	E	A	I	N	P	D	D	Y	V	W	I	H	D	Y	H	L	M	V		

EcOtsA	F	A	H	E	L	R	-	-	-	-	-	K	R	G	V	N	N	R	I	G	F	F	L	H	I	P	F	P	T	P	E	I	F	N	A	L	P	T	Y	D	T	L	L	E	Q	L	C	D	Y	D	
ScTPS1	V	P	E	M	L	R	V	K	I	H	E	K	Q	L	Q	N	V	K	V	G	W	F	L	H	T	P	F	P	S	S	E	I	Y	R	I	L	P	V	R	Q	E	I	L	K	G	V	L	S	C	D	
AtTPS1	L	P	K	C	L	K	-	-	-	-	-	E	Y	N	S	K	M	K	V	G	W	F	L	H	T	P	F	P	S	S	E	I	H	R	T	L	P	S	R	S	E	L	L	L	H	S	V	L	A	A	D
VvTPS1	L	P	K	C	L	K	-	-	-	-	-	K	Y	N	S	E	M	K	V	G	W	F	L	H	T	P	F	P	S	S	E	I	H	R	T	L	P	S	R	S	E	L	L	L	H	S	V	L	A	A	D
VvTPS2	L	P	T	F	L	R	-	-	-	-	-	K	R	F	N	R	V	K	L	G	F	F	L	H	S	P	F	P	S	S	E	I	Y	R	T	L	P	I	R	E	E	L	L	R	A	L	L	N	S	D	
VvTPS3	L	P	T	F	L	R	-	-	-	-	-	K	R	F	N	R	V	K	L	G	F	F	L	H	S	P	F	P	S	S	E	I	Y	R	T	L	P	V	R	D	E	L	L	R	A	L	L	N	S	D	
VvTPS4	L	P	T	F	L	R	-	-	-	-	-	K	R	F	N	R	L	R	M	G	F	F	L	H	S	P	F	P	S	S	E	I	Y	R	T	L	P	V	R	D	E	I	L	K	A	L	L	N	S	D	
VvTPS5	L	P	T	F	L	R	-	-	-	-	-	K	R	F	H	R	V	K	L	G	F	F	L	H	S	P	F	P	S	S	E	I	Y	R	T	L	P	V	R	D	E	I	L	R	G	L	L	N	C	D	
VvTPS6	L	P	T	F	L	R	-	-	-	-	-	K	R	F	Y	R	V	K	L	G	F	F	L	H	S	P	F	P	S	S	E	I	Y	R	T	L	P	V	R	D	D	I	L	K	A	L	L	N	A	D	
VvTPS7	L	P	T	F	L	R	-	-	-	-	-	R	H	F	N	Q	L	R	M	G	F	F	L	H	S	P	F	P	S	S	E	I	Y	R	T	L	P	V	R	E	E	I	L	K	A	L	L	N	S	D	

EcOtsA	L	L	G	F	Q	T	E	N	D	R	L	A	F	L	D	C	L	S	N	L	T	R	V	T	T	R	S	A	K	S	H	T	A	W	-	-	-	G	K	A	F	R	T	E	V	Y	P	I	G	I
ScTPS1	L	V	G	F	H	T	Y	D	Y	A	R	H	F	L	S	S	V	Q	R	V	L	N	V	N	T	L	P	N	-	-	-	-	G	V	E	Y	Q	G	R	F	V	N	V	G	A	F	P	I	G	I
AtTPS1	L	V	G	F	H	T	Y	D	Y	A	R	H	F	V	S	A	C	T	R	I	L	G	L	E	G	T	P	E	-	-	-	-	G	V	E	D	Q	G	R	L	T	R	V	A	A	F	P	I	G	I
VvTPS1	L	V	G	F	H	T	Y	D	Y	A	R	H	F	V	S	A	C	T	R	I	L	G	L	E	G	T	P	E	-	-	-	-	G	V	E	D	Q	G	R	L	T	R	V	A	A	F	P	I	G	I
VvTPS2	L	I	G	F	H	T	F	D	Y	A	R	H	F	L	S	C	C	S	R	M	L	G	L	S	Y	E	S	K	R	G	Y	I	G	L	E	Y	Y	G	R	T	V	S	I	K	I	L	P	V	G	I
VvTPS3	L	I	G	F	H	T	F	D	Y	A	R	H	F	L	S	C	C	S	R	M	L	G	L	A	Y	Q	S	K	R	G	Y	I	G	L	E	Y	Y	G	R	T	V	S	I	K	I	L	P	V	G	I
VvTPS4	L	I	G	F	H	T	F	D	Y	A	R	H	F	L	S	C	C	S	R	M	L	G	L	E	Y	Q	S	K	R	G	Y	I	G	L	E	Y	Y	G	R	T	V	G	I	K	I	M	P	V	G	V
VvTPS5	L	I	G	F	Q	T	F	D	Y	A	R	H	F	L	S	C	C	S	R	M	L	G	L	D	Y	E	S	K	R	G	H	I	G	L	E	Y	S	G	R	T	V	Y	I	K	I	L	P	V	G	V
VvTPS6	L	V	G	F	H	T	F	D	Y	A	R	H	F	L	S	C	C	S	R	M	L	G	L	N	Y	E	S	K	R	G	H	I	G	L	E	Y	F	G	R	T	V	Y	V	K	I	L	P	V	G	I
VvTPS7	L	I	G	F	H	T	F	D	Y	A	R	H	F	L	S	C	C	S	R	M	L	G	L	E	Y	Q	S	K	R	G	Y	I	G	L	E	Y	Y	G	R	T	V	G	I	K	I	M	P	V	G	I

EcOtsA	E	P	K	E	I	A	K	Q	A	A	G	P	-	L	P	P	K	L	A	Q	L	K	A	E	L	-	-	K	N	V	Q	N	I	F	S	V	E	R	L	D	Y	S	K	G	L	P	E	R	F	L
ScTPS1	D	V	D	K	F	T	D	G	L	K	K	E	S	V	Q	K	R	I	Q	Q	L	K	E	T	F	-	-	K	G	C	K	I	I	V	G	V	D	R	L	D	Y	I	K	G	V	P	Q	K	L	H
AtTPS1	D	S	D	R	F	I	R	A	L	E	V	P	E	V	I	Q	H	M	K	E	L	K	E	R	F	-	-	A	G	R	K	V	M	L	G	V	D	R	L	D	M	I	K	G	I	P	Q	K	I	L
VvTPS1	D	S	H	R	F	I	R	A	L	D	A	P	Q	V	Q	D	R	I	N	E	L	K	R	T	F	-	-	T	G	R	K	V	M	L	G	V	D	R	L	D	M	I	K	G	I	P	Q	K	I	L
VvTPS2	H	M	G	Q	L	Q	S	V	L	S	L	P	E	T	E	E	K	V	A	E	L	I	K	Q	F	C	D	Q	D	R	I	M	L	L	G	V	D	D	M	D	I	F	K	G	I	S	L	K	L	L
VvTPS3	H	M	G	Q	L	R	S	V	L	N	L	P	E	T	D	S	R	V	A	E	L	R	D	Q	F	-	-	R	G	Q	T	V	L	L	G	V	D	D	M	D	I	F	K	G	I	S	L	K	L	L
VvTPS4	H	M	G	Q	I	E	S	V	L	R	F	A	D	K	E	W	R	V	G	E	L	K	Q	Q	F	-	-	E	G	K	T	V	L	L	G	V	D	D	M	D	I	F	K	G	V	N	L	K	L	L
VvTPS5	H	M	G	R	L	E	S	V	L	N	L	H	S	T	S	A	K	I	K	E	I	Q	K	Q	F	-	-	E	G	K	K	L	I	L	G	V	D	D	M	D	I	F	K	G	I	S	L	K	F	L
VvTPS6	H	M	G	Q	L	E	S	A	L	N	L	P	S	T	S	I	K	V	K	E	I	Q	E	Q	F	-	-	K	G	K	K	I	I	L	G	V	D	D	M	D	I	F	K	G	I	S	L	K	L	L
VvTPS7	H	M	G	R	I	A	S	V	M	K	L	A	D	K	E	K	K	V	G	E	L	K	Q	Q	F	-	-	E	G	K	T	V	L	L	G	V	N	D	M	D	I	F	K	G	I	N	L	K	L	L

EcOtsA	A	Y	E	A	L	L	E	K	Y	P	Q	H	H	G	K	I	R	Y	T	Q	I	A	P	T	S	R	G	D	V	Q	A	Y	Q	D	I	R	H	Q	L	E	N	E	A	G	R	I	N	G	K	Y
ScTPS1	A	M	E	V	F	L	N	E	H	P	E	W	R	G	K	V	V	L	V	Q	V	A	V	P	S	R	G	D	V	E	E	Y	Q	Y	L	R	S	V	V	N	E	L	V	G	R	I	N	G	Q	F
AtTPS1	A	F	E	K	F	L	E	E	N	A	N	W	R	D	K	V	V	L	L	Q	I	A	V	P	T	R	T	D	V	P	E	Y	Q	K	L	T	S	Q	V	H	E	I	V	G	R	I	N	G	R	F
VvTPS1	A	F	E	K	F	L	E	E	N	S	E	W	Q	Q	K	V	V	L	L	Q	I	A	V	P	T	R	T	D	V	P	E	Y	Q	K	L	T	S	Q	V	H	E	I	V	G	R	I	N	G	R	F
VvTPS2	A	M	E	Q	L	L	V	Q	H	P	E	W	Q	G	K	V	V	L	V	Q	I	A	N	P	A	R	G	R	G	K	D	V	K	E	V	Q	T	E	T	F	S	T	V	K	R	I	N	E	T	F
VvTPS3	A	M	E	Q	L	L	T	Q	H	P	D	K	R	G	K	V	V	L	V	Q	I	A	N	P	A	R	G	R	G	K	D	V	Q	E	V	Q	S	E	T	H	A	T	V	R	R	I	N	E	T	F
VvTPS4	A	M	E	Q	M	L	T	Q	H	P	K	W	Q	G	R	A	V	L	V	Q	I	A	N	P	A	R	G	S	G	R	D	L	E	V	I	Q	A	E	I	Q	A	S	C	K	R	I	N	E	N	F
VvTPS5	A	V	E	Q	L	L	Q	Q	H	P	E	L	Q	G	K	L	V	L	V	Q	I	V	N	P	A	R	S	T	G	K	D	V	Q	E	A	K	R	E	T	Y	L	T	A	E	R	I	N	E	T	Y
VvTPS6	A	M	E	H	L	L	Q	H	Y	E	E	L	R	G	E	L	V	L	V	Q	I	V	N	P	A	R	S	T	G	K	D	V	Q	E	A	K	R	E	T	Y	A	I	T	E	R	I	N	A	N	F
VvTPS7	A	M	E	Q	L	L	Q	Q	H	S	K	W	Q	G	K	T	V	L	V	Q	I	A	N	P	A	R	G	K	G	A	D	L	E	E	I	Q	A	E	I	R	E	S	C	R	R	I	N	E	E	F

EcOtsA	G	Q	L	G	W	T	P	L	Y	Y	L	N	Q	H	F	D	R	K	L	L	M	K	I	F	R	Y	S	D	V	G	L	V	T	P	L	R	D	G	M	N	L	V	A	K	E	Y	V	A	A	Q	
ScTPS1	G	T	V	E	F	V	P	I	H	F	M	H	K	S	I	P	F	E	E	L	I	S	L	Y	A	V	S	D	V	C	L	V	S	S	T	R	D	G	M	N	L	V	S	Y	E	Y	I	A	C	Q	
AtTPS1	G	T	L	T	A	V	P	I	H	H	L	D	R	S	L	D	F	H	A	L	C	A	L	Y	A	V	T	D	V	A	L	V	T	S	S	L	R	D	G	M	N	L	V	S	Y	E	F	V	A	C	Q
VvTPS1	G	T	L	T	A	V	P	I	H	H	L	D	R	S	L	D	F	H	A	L	C	A	L	Y	A	V	T	D	V	A	L	V	T	S	S	L	R	D	G	M	N	L	V	S	Y	E	F	V	A	C	Q
VvTPS2	G	K	P	G	Y	D	P	V	V	L	I	D	E	P	L	K	F	Y	E	R	I	A	Y	Y	V	V	A	E	C	C	L	V	T	A	V	R	D	G	M	N	L	I	P	Y	E	Y	I	I	S	R	
VvTPS3	G	R	P	G	Y	H	P	V	V	L	I	D	T	P	L	Q	F	Y	E	R	I	A	Y	Y	V	T	A	E	C	C	L	V	T	A	V	R	D	G	M	N	L	I	P	Y	E	Y	I	I	C	R	
VvTPS4	G	Q	P	G	Y	E	P	I	V	F	I	D	R	P	V	S	L	S	E	K	A	A	F	Y	T	I	A	E	C	V	V	V	T	A	V	R	D	G	M	N	L	I	P	Y	E	Y	I	V	S	R	
VvTPS5	G	S	P	N	Y	E	P	V	I	L	I	D	R	P	V	A	R	Y	E	K	S	A	Y	Y	A	V	A	E	C	C	I	V	N	A	V	R	D	G	M	N	L	V	P	Y	K	Y	I	V	C	R	
VvTPS6	G	F	P	G	Y	E	P	V	V	L	I	D	H	P	V	P	F	Y	E	K	T	A	Y	Y	A	L	A	E	C	C	I	V	N	A	V	R	D	G	M	N	L	M	P	Y	N	Y	I	V	C	R	
VvTPS7	G	E	P	G	Y	E	P	I	V	F	V	D	R	P	V	S	I	S	E	R	I	A	Y	Y	S	I	A	E	C	V	V	V	T	A	V	R	D	G	M	N	L	T	P	Y	E	Y	I	V	C	R	

Appendix E

RT-PCR assay on grapevine tissues

E.1 Trehalose biosynthesis pathway gene families

As described in Section 5.2.1, a series of RT-PCR experiments were performed on grapevine tissues collected from the Lincoln University campus to determine which tissues had expression of the trehalose pathway genes. Once expression of the genes was identified in a given tissue type, the whole gene was amplified from the same cDNA used in the RT-PCR assay to clone the gene. The cloned genes were then used for complementation experiments in yeast or transcript experiments. The results of the experiments are described in Section 5.3

E.1.1 Materials & methods

Sample collection

To identify where in the grapevine the trehalose biosynthesis genes are expressed, 'Pinot noir' tissue was collected during the 2009-10 growing season from the Lincoln University (LU) campus vineyard (LU-V) or Mullins vines grown in the greenhouse (LU-G). The tissue was collected in 2 mL microcentrifuge tubes and snap-frozen in liquid nitrogen on site. The frozen tissue was then transferred to -80°C for storage until ready for RNA extraction. The tissue types collected were as follows: Root tip (~15mm; LU-G), Woolly bud (LU-V), Latent bud (LU-V), EL-15 Inflorescence (LU-G; Coombe, 1995), Tendril (~30mm, LU-G), Leaf (~225mm²; LU-G), Vegetative shoot tip (~7mm; LU-G), Pre-veraison berry (LU-G), Véraison berry (LU-G) and Ripe berry (LU-G). Representative images of the tissue types collected are in Figure E.1.



Figure E.1 Grapevine 'Pinot noir' tissue types used to screen for VvTPS and VvTPP transcript activity by RT-PCR.

RNA extraction and cDNA synthesis

The 'Pinot noir' tissue types described above were ground in liquid nitrogen and aliquots of ~100 mg were put in 2mL microcentrifuge tubes. Extra aliquots were returned to -80°C for long-term storage. RNA was extracted from each of the samples using the Sigma Spectrum™ Plant Total RNA kit (Sigma-Aldrich, NZ) with the On-Column DNase treatment protocol. The extracted RNA was quantified using an Invitrogen Qubit® fluorometer with the Qubit® RNA buffer and dye (Life Technologies, NZ) and calibrated with the supplied standards. RNA quality was checked on a 1.5% denaturing agarose gel (Sambrook and Russell, 2001) and visualized by UV excitation of ethidium bromide on a BioRad GelDoc apparatus (BioRad Laboratories Pty Ltd, NZ). Contamination of RNA with proteins or extraction reagents was measured on a Nanodrop™ spectrophotometer (ThermoFischer Scientific, NZ). Good quality, pure total RNA was used to synthesize complimentary DNA (cDNA) using the TaKaRa BluePrint™ RT-PCR kit (Norrie Biotech, NZ). For RT-PCR assays, 500ng of total RNA was used in a 10µL reaction with a 1:1 ratio of oligo dTs and random hexamers provided by the manufacturer. The cDNA was synthesized according to the kit's protocol and subsequently diluted 5-fold with sterile water. The synthesized cDNA was checked for amplification and lack of genomic DNA (gDNA) contamination by PCR (cDNA check PCR; Appendix A).

Genomic DNA (gDNA) extraction

To indicate what gDNA contamination would look like in contaminated cDNA after synthesis, a sample of genomic DNA was included in the RT-PCRs. Genomic DNA was extracted from 'Pinot noir' leaves (~225 mm², LU-G) using a Machery Nagel NucleoSpin® II genomic DNA extraction kit (Total Lab Systems, NZ). The DNA was checked for quality on a 1% agarose gel containing 2% ethidium bromide and visualized by UV light in a BioRad GelDoc apparatus (Bio Rad Laboratories Pty Ltd, NZ).

The gDNA was quantified on an Invitrogen Qubit® fluorometer with the Qubit® dsDNA, BR (Broad Range) buffer and dye kit (Life Technologies, NZ). The gDNA was then diluted to 10 ng/μL in sterile water for further use.

RT-PCR to identify VvTPS and VvTPP gene expression in grapevine tissues

RT-PCR was performed on the cDNA synthesized from the tissues described above using TaKaRa ExTaq™ PCR reagents (Norrie Biotech, NZ). The RT-PCR reaction was set up as per the manufacturer's instructions with 5μL of diluted cDNA used as template using VvTPS or VvTPP primers (Appendix B; Custom Science, NZ) that amplify a ~500bp~1000bp fragment of the gene of interest. The RT-PCR protocol is described in Appendix A and was run in an Eppendorf Mastercycler© gradient thermocycler (Eppendorf, NZ). A control RT-PCR reaction was run at the same time using the same cDNA template and Actin RT-PCR primers (Appendix B) that flank an intron to show that all of the tissue cDNA amplified a PCR product and was free of genomic DNA (gDNA) contamination.

E.1.2 Results & discussion

As shown in Chapter 4, there are seven predicted TREHALOSE-6-PHOSPHATE SYNTHASE (TPS) and seven predicted TREHALOSE-6-PHOSPHATE PHOSPHATASE (TPP) genes in grapevine. Initial identification of VvTPS and VvTPP transcript activity was done on cDNA synthesized from RNA collected from the tissue types shown in Figure E.1 by RT-PCR using primers that amplified up to ~1000 bp of product. As shown in Figure E.2, there is differential expression of VvTPS and VvTPP genes in the tissue types tested. VvTPS7 has faint bands that appear in the same tissue types that show strong VvTPS4 expression. As VvTPS7 could not be amplified in its entirety from any of the tissues showing expression of the gene by RT-PCR (see Section 5.3.1), this suggests that the bands observed for VvTPS7 in Figure E.2 are due to non-specific amplification of VvTPS4 from VvTPS7 primers. VvTPPF did not amplify a product in any of the tissues assayed, with the possible exception of latent bud. The faint band observed on the agarose gel in latent bud tissue from the VvTPPF RT-PCR assay is likely an artefact of the gel.

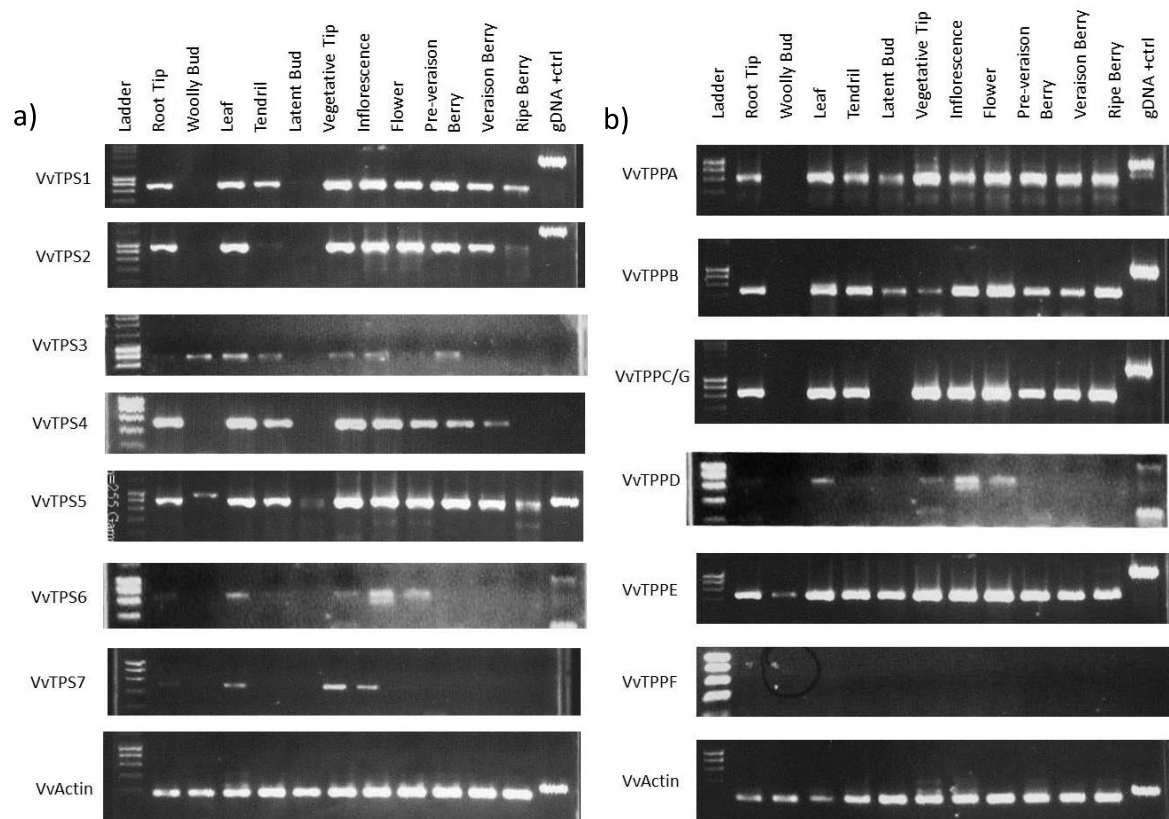


Figure E.1 Gel images of VvTPS and VvTPP transcript activity on 'Pinot noir' grapevine tissues as determined by RT-PCR.

The tissues listed above the gels were collected from the Lincoln university campus as described in Section E.1.1. a) VvTPS gene expression across the tissue types tested. b) VvTPP gene expression across the tissue types tested.

E.2 VvBA1/LAX1

As described in Section 6.2.1, an RT-PCR assay was done to determine where in grapevine VvBA1/LAX1 was transcribed. Once expression of the gene was identified in a given tissue type, the whole gene was amplified from the same cDNA used in the RT-PCR assay to clone the gene. The cloned gene was going to be used in a complementation study using the *Arabidopsis rox* mutant, but the experiment was abandoned due to the minor phenotype of the mutant and concerns over the AtROX locus as described in Section 6.1.

E.2.1 Materials & methods

Sample collection

To identify where in the grapevine *VvBA1/LAX1* is expressed, 'Pinot noir' tissue was collected during the 2009-10 growing season from the Lincoln University (LU) campus vineyard (LU-V) or Mullins vines grown in the greenhouse (LU-G). The tissue was collected in 2 mL microcentrifuge tubes and snap-frozen in liquid nitrogen on site. The frozen tissue was then transferred to -80°C for storage until ready for RNA extraction. The tissue types collected were as follows: Root tip (~15mm; LU-G), Woolly bud (LU-V), Latent bud (LU-V), E-L stage 15 Inflorescence (Coombe, 1995), Tendril (~60mm, LU-G), Leaf (~225mm²; LU-G) and Vegetative shoot tip (~7mm; LU-G). Representative images of the tissue types collected are in Figure E.3.

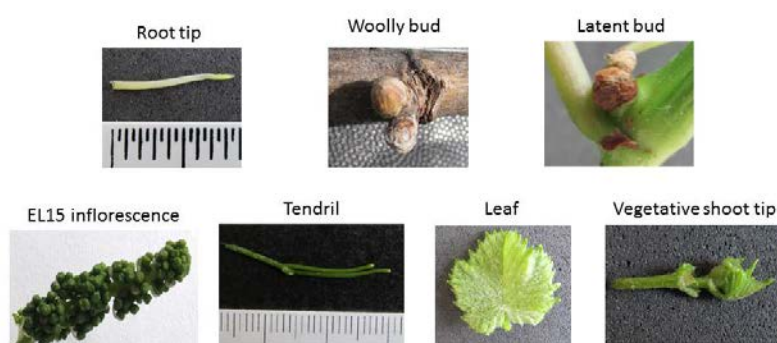


Figure E.3 Grapevine 'Pinot noir' tissue types used to screen for *VvBA1/LAX1* transcript activity by RT-PCR.

RNA extraction and cDNA synthesis

The 'Pinot noir' tissue types described above were ground in liquid nitrogen and aliquots of ~100 mg were put in 2mL microcentrifuge tubes. Extra aliquots were returned to -80°C for long-term storage. RNA was extracted and cDNA was synthesized as described in Section E.1.1.

Genomic DNA (gDNA) extraction

Genomic DNA was extracted from 'Pinot noir' leaves as described in Section E.1.1.

RT-PCR to identify *VvBA1/LAX1* expression in grapevine tissues

RT-PCR was performed on the cDNA synthesized from the tissues described above using TaKaRa ExTaq™ PCR reagents. The RT-PCR reaction was set up as per the manufacturer's instructions with 5uL of diluted cDNA used as template and the *VvBA1/LAX1* primers (Appendix B) used to amplify the gene of interest. The RT-PCR protocol is described in Appendix A and was run in an Eppendorf Mastercycler© gradient thermocycler (Eppendorf, NZ). A control RT-PCR reaction was run at the same time using the same cDNA template and Actin primers Actin RT-PCR F/R (Appendix B) that flank

an intron to show that all of the tissue cDNA amplified a PCR product and was free of genomic DNA (gDNA) contamination.

E.2.2 Results & discussion

Based on *in silico* analysis of the BA1/LAX1 clade of the bHLH gene family of transcription factors described in Chapter 4, there is a single predicted BA1/LAX1 gene in grapevine. To identify where in grapevine the BA1/LAX1 gene is being transcribed, the 'Pinot noir' tissue shown in Figure E.3 were collected from the Lincoln University campus and used to screen for VvBA1/LAX1 activity by RT-PCR. As shown in Figure E.4, there is VvBA1/LAX1 transcript activity in all tissues tested except woolly bud tissue.

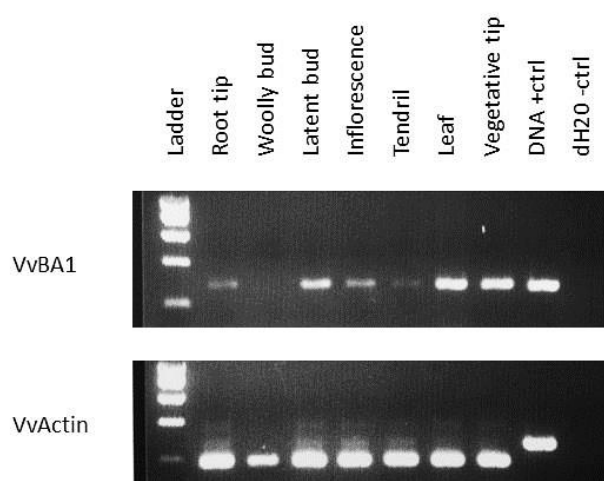


Figure E. 4 Gel image of VvBA1/LAX1 transcript activity on 'Pinot noir' grapevine tissues as determined by RT-PCR.

Appendix F

Additional tables and charts for this work

F.1 ANOVA table of reference genes tested on the 'Pinot noir' confirmation population tissue types

Gene Symbol	Tissue Type	Sum Squares of Variance		F value	Significance	Mean Variance ¹ (-1/ \bar{X})	V_W (SS_W/MV)	V_B (SS_B/MV)	Stability value ² ($V_W * V_B$)
		Within Group (SS_W)	Between Group (SS_B)						
ACT	Latent bud	0.0151	0.1530						
	Woolly bud	0.0003	0.0864						
	Leaf	0.0164	0.0055						
	Tendrill	0.0381	0.2098						
	Inflorescence	0.0298	0.0405						
	Post anthesis flower	0.0124	0.0108						
	Pre veraison berry	0.0934	0.0116						
	Veraison berry	0.0025	0.2221						
	Late veraison berry	0.0253	0.2000						
	Total	0.2334	0.9397	7.6064	0.0002	3.4733	0.0672	0.2706	0.0182

Gene Symbol	Tissue Type	Sum Squares of Variance		F value	Significance	Mean Variance ¹ (-1/X)	V _W (SS _W /MV)	V _B (SS _B /MV)	Stability value ² (V _W *V _B)
		Within Group (SS _W)	Between Group (SS _B)						
AP2mu	Latent bud	0.0100	0.1558						
	Woolly bud	0.0066	0.0438						
	Leaf	0.0146	0.1612						
	Tendrill	0.0256	0.0009						
	Inflorescence	0.0556	0.1402						
	Post anthesis flower	0.0131	0.0680						
	Pre veraison berry	0.0531	0.0191						
	Veraison berry	0.0017	0.1111						
	Late veraison berry	0.1168	0.0714						
	Total	0.2971	0.7714	5.8419	0.0009	2.3362	0.1272	0.3302	0.0420
EF1a	Latent bud	0.0118	0.0017						
	Woolly bud	0.0047	0.3583						
	Leaf	0.0494	0.0674						
	Tendrill	0.0726	0.0725						
	Inflorescence	0.0160	0.0548						
	Post anthesis flower	0.0063	0.0294						
	Pre veraison berry	0.0861	0.2535						
	Veraison berry	0.0002	0.0637						
	Late veraison berry	0.0368	0.1224						
	Total	0.2838	1.0237	8.1160	0.0001	2.5801	0.1100	0.3967	0.0436

Gene Symbol	Tissue Type	Sum Squares of Variance		F value	Significance	Mean Variance ¹ (-1/ \bar{X})	V _W (SS _W /MV)	V _B (SS _B /MV)	Stability value ² (V _W *V _B)
		Within Group (SS _W)	Between Group (SS _B)						
GAPDH	Latent bud	0.0050	0.0477						
	Woolly bud	0.0021	0.1476						
	Leaf	0.0159	0.0710						
	Tendrill	0.0215	0.1084						
	Inflorescence	0.0317	0.0492						
	Post anthesis flower	0.0003	0.0648						
	Pre veraison berry	0.0932	0.1678						
	Veraison berry	0.0073	0.0155						
	Late veraison berry	0.0554	0.0354						
	Total	0.2325	0.7074	6.8460	0.0004	3.8957	0.0597	0.1816	0.0108
HLK	Latent bud	0.0126	0.1458						
	Woolly bud	0.0047	0.1662						
	Leaf	0.0261	0.0094						
	Tendrill	0.0189	0.0053						
	Inflorescence	0.0932	0.0863						
	Post anthesis flower	0.0065	0.0037						
	Pre veraison berry	0.1604	0.3785						
	Veraison berry	0.0022	0.0014						
	Late veraison berry	0.0770	0.0055						
	Total	0.4017	0.8021	4.4930	0.0039	3.4336	0.1170	0.2336	0.0273

Gene Symbol	Tissue Type	Sum Squares of Variance		F value	Significance	Mean Variance ¹ (-1/ \bar{X})	V_W (SS_W/MV)	V_B (SS_B/MV)	Stability value ² ($V_W * V_B$)
		Within Group (SS_W)	Between Group (SS_B)						
HYP	Latent bud	0.0036	0.3128						
	Woolly bud	0.0039	0.2516						
	Leaf	0.0242	0.1643						
	Tendrill	0.0218	0.3597						
	Inflorescence	0.0211	0.0012						
	Post anthesis flower	0.0153	0.0378						
	Pre veraison berry	0.2292	0.8623						
	Veraison berry	0.0310	0.2683						
	Late veraison berry	0.0704	0.1522						
	Total	0.4206	2.4101	12.8930	0.0000	2.3788	0.1768	1.0132	0.1791
N2227	Latent bud	0.0011	0.2093						
	Woolly bud	0.0009	0.0553						
	Leaf	0.0045	0.0027						
	Tendrill	0.0308	0.0497						
	Inflorescence	0.0607	0.0478						
	Post anthesis flower	0.0099	0.0060						
	Pre veraison berry	0.0356	0.1019						
	Veraison berry	0.0080	0.0069						
	Late veraison berry	0.0497	0.0785						
	Total	0.2011	0.5580	6.2440	0.0006	3.0148	0.0667	0.1851	0.0123

Gene Symbol	Tissue Type	Sum Squares of Variance		F value	Significance	Mean Variance ¹ (-1/ \bar{X})	V_W (SS_W/MV)	V_B (SS_B/MV)	Stability value ² ($V_W * V_B$)
		Within Group (SS_W)	Between Group (SS_B)						
PP2A	Latent bud	0.0027	0.3626						
	Woolly bud	0.0050	0.1520						
	Leaf	0.0069	0.1855						
	Tendrils	0.0315	0.0305						
	Inflorescence	0.0553	0.0322						
	Post anthesis flower	0.0179	0.2072						
	Pre veraison berry	0.0858	0.0003						
	Veraison berry	0.0053	0.0271						
	Late veraison berry	0.1067	0.0042						
	Total	0.3171	1.0017	7.1080	0.0003	2.5739	0.1232	0.3892	0.0479
SAND	Latent bud	0.0143	0.0126						
	Woolly bud	0.0025	0.0391						
	Leaf	0.0028	0.0849						
	Tendrils	0.0032	0.0694						
	Inflorescence	0.0459	0.1886						
	Post anthesis flower	0.0256	0.0174						
	Pre veraison berry	0.0542	0.5178						
	Veraison berry	0.0078	0.0001						
	Late veraison berry	0.0295	0.0211						
	Total	0.1858	0.9512	11.5180	0.0000	4.8766	0.0381	0.1951	0.0074

Gene Symbol	Tissue Type	Sum Squares of Variance		F value	Significance	Mean Variance ¹ (-1/ \bar{X})	V_W (SS_W/MV)	V_B (SS_B/MV)	Stability value ² ($V_W * V_B$)
		Within Group (SS_W)	Between Group (SS_B)						
TIP41	Latent bud	0.0002	0.0000						
	Woolly bud	0.0085	0.0416						
	Leaf	0.0208	0.0577						
	Tendrill	0.0315	0.0792						
	Inflorescence	0.0718	0.0632						
	Post anthesis flower	0.0201	0.0247						
	Pre veraison berry	0.0058	0.0905						
	Veraison berry	0.0995	0.1417						
	Late veraison berry	0.0622	0.2322						
	Total	0.3202	0.7307	5.1340	0.0019	2.1244	0.1507	0.3440	0.0519
TRU5	Latent bud	0.0110	0.0030						
	Woolly bud	0.0010	0.0054						
	Leaf	0.0271	0.0011						
	Tendrill	0.0395	0.0022						
	Inflorescence	0.0658	0.1982						
	Post anthesis flower	0.0104	0.0330						
	Pre veraison berry	0.0830	0.1546						
	Veraison berry	0.0050	0.0222						
	Late veraison berry	0.0204	0.1347						
	Total	0.2632	0.5544	4.7380	0.0029	3.3696	0.0781	0.1645	0.0129

F.2 Single node cuttings supplementary charts

Frequency of fruitful outer arms from basal or apical inflorescence

For the two pruning treatments, the frequency of fruitful outer arms was compared across all node positions at both the basal and apical inflorescences. The data shown in Figures F.1 and F.2 are the total number of fruitful inflorescences observed at either the basal or apical inflorescence position per shoot diameter class. As shown in Figure F.1, there is a significantly higher frequency of fruitful outer arms for both the small and large diameter class shoots on the basal inflorescences, as the apical inflorescences did not have any fruitful outer arms, regardless of shoot class.

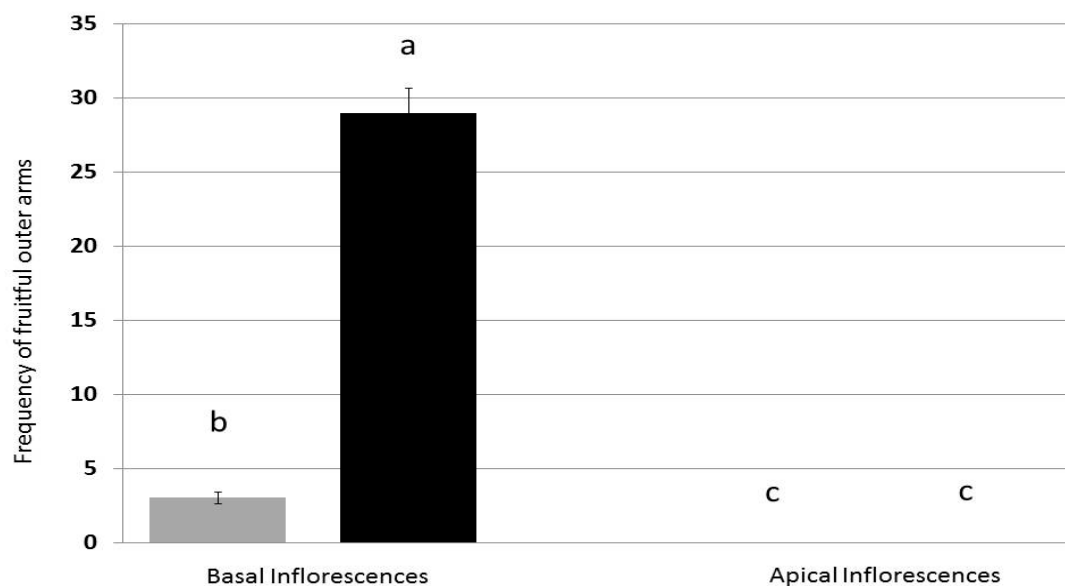


Figure F.1 Frequency of fruitful outer arms from single node cuttings grown from small or large diameter class shoots from the 6-node pruned shoots.

Fruitful outer arm frequencies are the sum of three replicates. Cuttings taken from the small diameter class shoots are represented by the grey bars. Cuttings taken from the large diameter class shoots are represented by the black bars. Standard deviations for each of the mean values are indicated by vertical bars. Frequencies with the same letter above the bars indicates the means are not significantly different ($p < 0.5$) as determined by the Tukey-Kramer test after ANOVA.

As shown in Figure F.2, there are significantly more fruitful outer arms on the basal inflorescences from the large diameter shoots when compared to the small diameter class shoots. There is a higher frequency of fruitful outer arms on the apical inflorescences from the large diameter shoots when compared to the small diameter shoots, but the difference is not significant (Figure F.2). In the 12 node pruning treatment, there are more fruitful outer arms observed for both shoot classes on the apical inflorescences when compared to the 6 node pruning treatment.

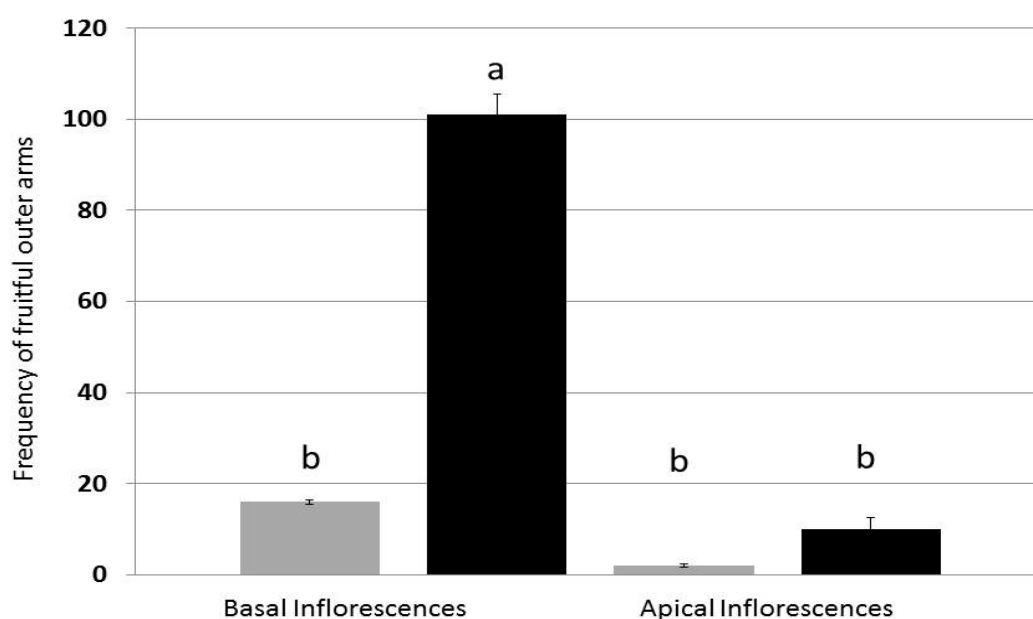


Figure F.2 Frequency of fruitful outer arms from single node cuttings grown from small or large diameter class shoots from 12-node pruned shoots.

Fruitful outer arm frequencies are the means of three replicates with a minimum of 6 vines per replicate. Cuttings taken from the small diameter class shoots are represented by the grey bars. Cuttings taken from the large diameter class shoots are represented by the black bars. Standard deviations for each of the mean values are indicated by vertical bars. Frequencies with the same letter above the bars indicates the means are not significantly different ($p < 0.5$) as determined by the Tukey-Kramer test after ANOVA.

Weighted frequency of outer arms from basal or apical inflorescences per shoot position from small or large diameter class shoots

To determine the overall size of the outer arms that formed on the inflorescences from the single node cuttings done from the 6- or 12-node pruning treatments, the outer arms were scored as categorical data. Outer arms that formed tendrils were given a value of 1. Outer arms that had only a few flowers develop were given a value of 2. Outer arms that had between three to nine flowers develop were given a value of 3. Outer arms that had ten to fifteen flowers were given a value of 4. Outer arms with more than fifteen flowers were given a value of 5. To calculate the weighted frequency of the outer arms, the frequency of outer arms observed for each category value per shoot position was multiplied by the category value. The weighted frequency was then averaged across each shoot position and shoot class to generate the mean weighted frequency value. An example of the calculations done to determine the mean weighted frequency of the outer arm is shown in Table F.1

Table F.1 Example calculation to determine the mean weighted frequency of the outer arm from basal inflorescences for the apical shoot position from large diameter class shoots

A	B	C	D	E	F	G	H	I	J	K	L
Observed frequency						Weighted values					
	Class 1	Class 2	Class 3	Class 4	Class 5	Weight CI1 Col B *1	Weight CI2 Col B *2	Weight CI3 Col B *3	Weight CI4 Col B *4	Weight CI5 Col B *5	Avg weight Avg ColG:Col K/5
Rep1											
Node 9	3	0	0	2	3	3	0	0	8	15	5.2
Node 10	3	0	1	2	3	3	0	3	8	15	5.8
Node 11	4	1	0	0	1	4	2	0	0	5	2.2
Node 12	1	0	1	1	1	1	0	3	4	5	2.6
Rep2											
Node 9	1	0	1	3	1	1	0	3	12	5	4.2
Node 10	2	0	2	0	0	2	0	6	0	0	1.6
Node 11	3	0	0	0	1	3	0	0	0	5	1.6
Node 12	2	0	0	2	0	2	0	0	8	0	2
Rep3											
Node 9	5	0	0	2	2	5	0	0	8	10	4.6
Node 10	3	0	0	2	1	3	0	0	8	5	3.2
Node 11	2	2	0	2	0	2	4	0	8	0	2.8
Node 12	2	0	0	1	0	2	0	0	4	0	1.2
Mean weight										3.083333333	

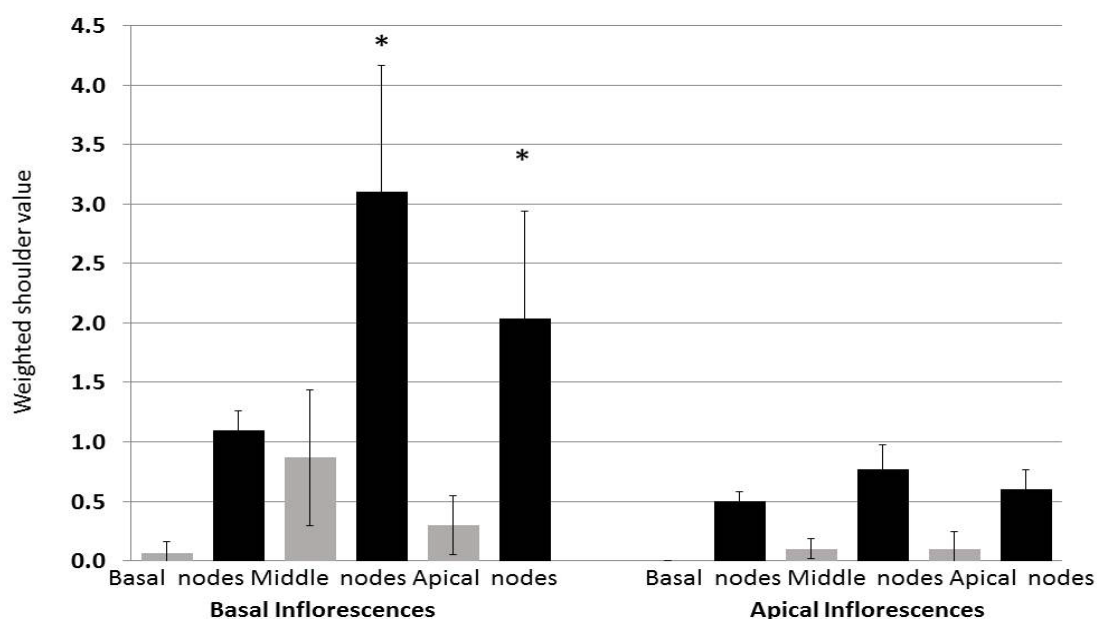


Figure F.3 Mean weighted frequency of outer arms from single node cuttings grown from small or large diameter class shoots from 6-node pruned shoots.

The weighted fruitful outer arm frequencies are the means of three replicates with a minimum of 6 vines per replicate. Cuttings taken from the small diameter class shoots are represented by the grey bars. Cuttings taken from the large diameter class shoots are represented by the black bars. Standard deviations for each of the mean values are indicated by vertical bars. Mean large diameter class shoots with an asterisk (*) indicate significantly different ($p < 0.5$) weighted frequencies per shoot position when compared to the small diameter class shoots at same position as determined by the Tukey-Kramer test after ANOVA.

As shown in Figure F.3, the large diameter class shoots had weighted outer arm values higher than the values calculated for the small diameter class shoots at the same node positions. This indicates that there is a higher frequency of fruitful outer arms that developed on the large diameter shoots at all node positions. There was a higher weighted outer arm value for both shoot classes at all positions for the outer arms from the basal inflorescences when compared to the apical inflorescences (Figure F.3). The weighted values for the outer arms from the apical inflorescences at all node positions is less than 1, indicating that most if not all of the outer arms that formed on the apical inflorescences were tendrils (Category value 1). The findings here are in agreement with the observations shown in Figure F.1.

The weighted outer arm values calculated of the basal inflorescences from the 12-node pruning treatment are similar to those observed in the 6-node pruning treatment (Figure F.4). The large diameter class shoots at all node and inflorescence positions had higher weighted outer arm values than the small diameter class shoots at the same positions. There was also a much higher weighted outer arm value for both shoot classes at all basal inflorescences when compared to the same class and shoot positions in the apical inflorescences. These results are in agreement with observations shown in Figure F.2. The large diameter class shoots had a higher mean outer arm value on the basal

inflorescences from the 12-node pruning treatment (Figure F.4) when compared to the 6-node pruning treatment (Figure F.3), particularly at the basal and apical shoot positions. This indicates that the 12-node treatment lead to a higher frequency of fruitful outer arms in large diameter shoots on the basal inflorescences when compared to the 6-node treatment. This is in agreement with the findings discussed in Chapter 7.

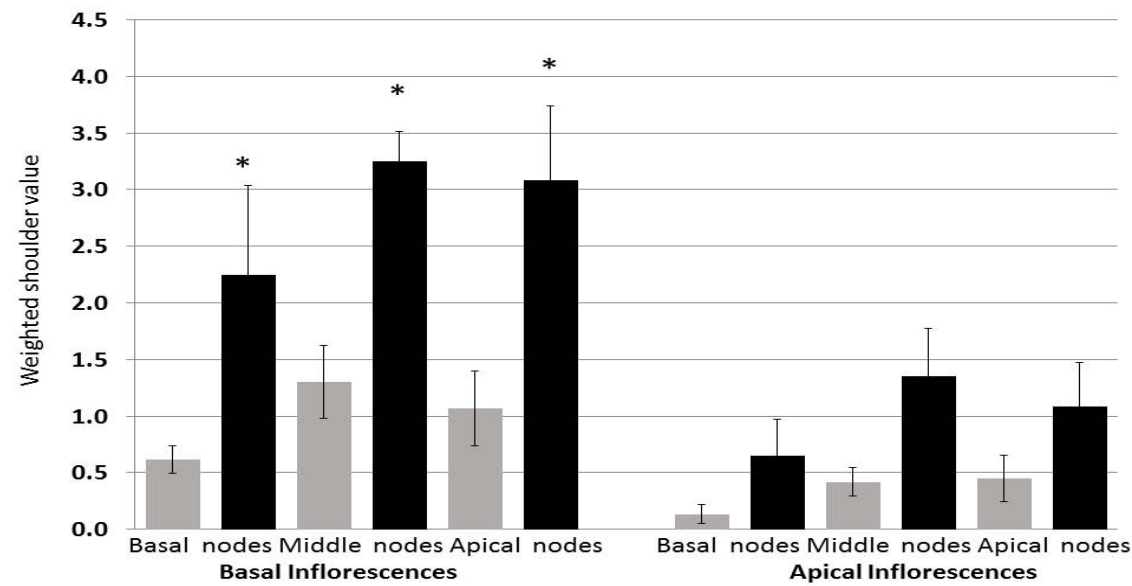


Figure F.4 Mean weighted frequency of fruitful outer arms from single node cuttings grown from small or large diameter class shoots from 12-node pruned shoots.

The weighted fruitful outer arm frequencies are the means of three replicates with a minimum of 6 vines per replicate. Cuttings taken from the small diameter class shoots are represented by the grey bars. Cuttings taken from the large diameter class shoots are represented by the black bars. Standard deviations for each of the mean values are indicated by vertical bars. Mean large diameter class shoots with an asterisk (*) indicate significantly different ($p < 0.5$) weighted frequencies per shoot position when compared to the small diameter class shoots at same position as determined by the Tukey-Kramer test after ANOVA.

References

- Almada R, Cabrera N, Casaretto JA, Ruiz-Lara S, Villanueva EG** (2009) VvCO and VvCOL1, two CONSTANS homologous genes, are regulated during flower induction and dormancy in grapevine buds. *Plant Cell Reports* **28**: 1193-1203
- Altschul SF, Gish W, Miller W, Myers EW, Lipman DJ** (1990) Basic local alignment search tool. *Journal of Molecular Biology* **215**: 403-410
- Avonce N, Leyman B, Mascorro-Gallardo JO, Van Dijck P, Thevelein JM, Iturriaga G** (2004) The Arabidopsis trehalose-6-P synthase AtTPS1 gene is a regulator of glucose, abscisic acid, and stress signaling. *Plant Physiology* **136**: 3649-3659
- Avonce N, Leyman B, Thevelein J, Iturriaga G** (2005) Trehalose metabolism and glucose sensing in plants. *Biochemical Society Transactions* **33**: 276-279
- Avonce N, Mendoza-Vargas A, Morett E, Iturriaga G** (2006) Insights on the evolution of trehalose biosynthesis. *Bmc Evolutionary Biology* **6**
- Baena-Gonzalez E, Rolland F, Thevelein JM, Sheen J** (2007) A central integrator of transcription networks in plant stress and energy signalling. *Nature* **448**: 938-U910
- Baena-Gonzalez E, Sheen J** (2008) Convergent energy and stress signaling. *Trends in Plant Science* **13**: 474-482
- Barratt DHP, Koelling K, Graf A, Pike M, Calder G, Findlay K, Zeeman SC, Smith AM** (2011) Callose synthase GSL7 is necessary for normal phloem transport and inflorescence growth in Arabidopsis. *Plant Physiology* **155**: 328-341
- Bell W, Sun WN, Hohmann S, Wera S, Reinders A, De Virgilio C, Wiemken A, Thevelein JM** (1998) Composition and functional analysis of the *Saccharomyces cerevisiae* trehalose synthase complex. *Journal of Biological Chemistry* **273**: 33311-33319
- Benlloch R, Berbel A, Serrano-Mislata A, Madueno F** (2007) Floral initiation and inflorescence architecture: a comparative view. *Annals of Botany* **100**: 659
- Bennett J, Jarvis P, Creasy GL, Trought MCT** (2005) Influence of defoliation on overwintering carbohydrate reserves, return bloom, and yield of mature 'Chardonnay' grapevines. *American Journal of Enology and Viticulture* **56**: 386
- Bernier G, Havelange A, Houssa C, Petitjean A, Lejeune P** (1993) Physiological signals that induce flowering. *Plant Cell* **5**: 1147-1155
- Blazquez MA, Ferrandiz C, Madueno F, Parcy F** (2006) How floral meristems are built. *Plant Molecular Biology* **60**: 855-870
- Blazquez MA, Lagunas R, Gancedo C, Gancedo JM** (1993) Trehalose-6-phosphate, a new regulator of yeast glycolysis that inhibits hexokinases. *Febs Letters* **329**: 51-54
- Blazquez MA, Santos E, Flores CL, Martinez-Zapater JM, Salinas J, Gancedo C** (1998) Isolation and molecular characterization of the Arabidopsis TPS1 gene, encoding trehalose-6-phosphate synthase. *Plant Journal* **13**: 685-689
- Blazquez MA, Soowal LN, Lee I, Weigel D** (1997) LEAFY expression and flower initiation in Arabidopsis. *Development* **124**: 3835-3844
- Boettcher C, Burbidge CA, Boss PK, Davies C** (2013) Interactions between ethylene and auxin are crucial to the control of grape (*Vitis vinifera* L.) berry ripening. *Bmc Plant Biology* **13**: 222-222
- Bomblies K, Wang RL, Ambrose BA, Schmidt RJ, Meeley RB, Doebley J** (2003) Duplicate FLORICAULA/LEAFY homologs *zfl1* and *zfl2* control inflorescence architecture and flower patterning in maize. *Development* **130**: 2385
- Borman AM, Fraser M, Linton CJ, Palmer MD, Johnson EM** (2010) An improved protocol for the preparation of total genomic DNA from isolates of yeast and mould using Whatman FTA filter papers. *Mycopathologia* **169**: 445-449
- Boss PK, Bastow RM, Mylne JS, Dean C** (2004) Multiple pathways in the decision to flower: Enabling, promoting, and resetting. *Plant Cell* **16**: S18-S31
- Boss PK, Buckeridge EJ, Poole A, Thomas MR** (2003) New insights into grapevine flowering. *Functional Plant Biology* **30**: 593-606

- Bradley D, Ratcliffe O, Vincent C, Carpenter R, Coen E** (1997) Inflorescence commitment and architecture in Arabidopsis. *Science* **275**: 80
- Burland TG** (2000) DNASTAR's Lasergene sequence analysis software. *Methods in molecular biology* (Clifton, N.J.) **132**: 71-91
- Bustin SA, Benes V, Garson JA, Hellemans J, Huggett J, Kubista M, Mueller R, Nolan T, Pfaffl MW, Shipley GL, Vandesompele J, Wittwer CT** (2009) The MIQE Guidelines: Minimum Information for Publication of Quantitative Real-Time PCR Experiments. *Clinical Chemistry* **55**: 611-622
- Butt TR, Sternberg EJ, Gorman JA, Clark P, Hamer D, Rosenberg M, Crooke ST** (1984) Copper metallothionein of yeast, structure of the gene, and regulation of expression. *Proceedings of the National Academy of Sciences of the United States of America-Biological Sciences* **81**: 3332-3336
- Cakir B, Kilickaya O, Olcay AC** (2013) Genome-wide analysis of Aux/IAA genes in *Vitis vinifera*: cloning and expression profiling of a grape Aux/IAA gene in response to phytohormone and abiotic stresses. *Acta Physiologiae Plantarum* **35**: 365-377
- Calonje M, Cubas P, Martinez-Zapater JM, Carmona MJ** (2004) Floral meristem identity genes are expressed during tendril development in grapevine. *Plant Physiology* **135**: 1491-1501
- Candolfi-Vasconcelos MC, Koblet W** (1990) Yield, fruit-quality, bud fertility and starch reserves of the wood as a function of leaf removal in *Vitis vinifera*- evidence of compensation and stress recovering. *Vitis* **29**: 199-221
- Carillo P, Feil R, Gibon Y, Satoh-Nagasawa N, Jackson D, Blaesing OE, Stitt M, Lunn JE** (2013) A fluorometric assay for trehalose in the picomole range. *Plant Methods* **9**
- Carmona MJ, Calonje M, Martínez-Zapater JM** (2007) The FT/TFL1 gene family in grapevine. *Plant Molecular Biology* **63**: 637-650
- Carmona MJ, Chaib J, Martinez-Zapater JM, Thomas MR** (2008) A molecular genetic perspective of reproductive development in grapevine. *Journal of Experimental Botany* **59**: 2579-2596
- Carmona MJ, Cubas P, Martinez-Zapater JM** (2002) VFL, the grapevine FLORICAULA/LEAFY ortholog, is expressed in meristematic regions independently of their fate. *Plant Physiology* **130**: 68-77
- Carretero-Paulet L, Galstyan A, Roig-Villanova I, Martinez-Garcia JF, Bilbao-Castro JR, Robertson DL** (2010) Genome-wide classification and evolutionary analysis of the bHLH family of transcription factors in Arabidopsis, Poplar, Rice, Moss, and Algae. *Plant Physiology* **153**: 1398-1412
- Caspari HW, Lang A, Alspach P** (1998) Effects of girdling and leaf removal on fruit set and vegetative growth in grape. *American Journal of Enology and Viticulture* **49**: 359-366
- Cecchetti V, Altamura MM, Brunetti P, Petrocelli V, Falasca G, Ljung K, Costantino P, Cardarelli M** (2013) Auxin controls Arabidopsis anther dehiscence by regulating endothecium lignification and jasmonic acid biosynthesis. *Plant Journal* **74**: 411-422
- Chary SN, Hicks GR, Choi YG, Carter D, Raikhel NV** (2008) Trehalose-6-phosphate synthase/phosphatase regulates cell shape and plant architecture in Arabidopsis. *Plant Physiology* **146**: 97-107
- Chen X, Zhang Z, Liu D, Zhang K, Li A, Mao L** (2010) SQUAMOSA promoter-binding protein-like transcription factors: Star players for plant growth and development. *Journal of Integrative Plant Biology* **52**: 946-951
- Cho YH, Hong JW, Kim EC, Yoo SD** (2012) Regulatory functions of SnRK1 in stress-responsive gene expression and in plant growth and development. *Plant Physiology* **158**: 1955-1964
- Coneva V, Guevara D, Rothstein SJ, Colasanti J** (2012) Transcript and metabolite signature of maize source leaves suggests a link between transitory starch to sucrose balance and the autonomous floral transition. *Journal of Experimental Botany* **63**: 5079-5092
- Coombe BG** (1972) The regulation of set and development of the grape berry. *In*. ISHS, pp 261-274
- Coombe BG** (1995) Growth stages of the grapevine: adoption of a system for identifying grapevine growth stages. *Australian Journal of Grape and Wine Research* **1**: 104-110
- Corbesier L, Lejeune P, Bernier G** (1998) The role of carbohydrates in the induction of flowering in *Arabidopsis thaliana*: comparison between the wild type and a starchless mutant. *Planta* **206**: 131-137

- Czechowski T, Stitt M, Altmann T, Udvardi MK, Scheible W-R** (2005) Genome-wide identification and testing of superior reference genes for transcript normalization in Arabidopsis. *Plant Physiology* **139**: 5-17
- Danilveskaya ON, Meng X, Ananiev EV** (2010) Concerted modification of flowering time and inflorescence architecture by ectopic expression of TFL1-like genes in Zea mays. *Plant Physiology*
- Devirgilio C, Burckert N, Bell W, Jenö P, Boller T, Wiemken A** (1993) Disruption of Tps2, the gene encoding the 100-Kda subunit of the trehalose-6-phosphate synthase phosphatase complex in *Saccharomyces cerevisiae*, causes accumulation of trehalose-6-phosphate and loss of trehalose-6-phosphate phosphatase activity. *European Journal of Biochemistry* **212**: 315-323
- Diaz-Riquelme J, Grimplet J, Martinez-Zapater JM, Carmona MJ** (2012) Transcriptome variation along bud development in grapevine (*Vitis vinifera* L.). *Bmc Plant Biology* **12**
- Diaz-Riquelme J, Lijavetzky D, Martinez-Zapater JM, Jose Carmona M** (2009) Genome-Wide Analysis of MIKCC-Type MADS Box Genes in Grapevine. *Plant Physiology* **149**: 354-369
- Dunn GM, Martin SR** (2007) A functional association in *Vitis vinifera* L. cv. 'Cabernet Sauvignon' between the extent of primary branching and the number of flowers formed per inflorescence. *Australian Journal of Grape and Wine Research* **13**: 95-100
- Edgar RC** (2004) MUSCLE: multiple sequence alignment with high accuracy and high throughput. *Nucleic Acids Research* **32**: 1792-1797
- Elbein AD, Pan YT, Pastuszak I, Carroll D** (2003) New insights on trehalose: a multifunctional molecule. *Glycobiology* **13**: 17-27
- Eltom MAM** (2013) The influence of temperature and carbohydrate availability on the bunch architecture of *Vitis vinifera* L. 'Sauvignon blanc'. Lincoln University
- Felsenstein J** (1985) Confidence-limits on phylogenies - an approach using the bootstrap. *Evolution* **39**: 783-791
- Fernandez L, Torregrosa L, Segura V, Bouquet A, Martinez-Zapater JM** (2010) Transposon-induced gene activation as a mechanism generating cluster shape somatic variation in grapevine. *Plant Journal* **61**: 545-557
- Fernandez O, Vandesteene L, Feil R, Baillieul F, Lunn JE, Clement C** (2012) Trehalose metabolism is activated upon chilling in grapevine and might participate in *Burkholderia phytofirmans* induced chilling tolerance. *Planta* **236**: 355-369
- Galet P** (2000) General Viticulture. Oenoplurimedia, Chateau de Chaintre, France
- Gallavotti A, Malcomber S, Gaines C, Stanfield S, Whipple C, Kellogg E, Schmidt RJ** (2011) BARREN STALK FASTIGIATE1 is an AT-hook protein required for the formation of maize ears. *Plant Cell* **23**: 1756-1771
- Gallavotti A, Yang Y, Schmidt RJ, Jackson D** (2008) The relationship between auxin transport and maize branching. *Plant Physiology* **147**: 1913-1923
- Gallavotti A, Zhao Q, Kyojuka J, Meeley RB, Ritter M, Doebley JF, Pe ME, Schmidt RJ** (2004) The role of barren stalk1 in the architecture of maize. *Nature* **432**: 630-635
- Gamm M, Heloir M-C, Kelloniemi J, Poinssot B, Wendehenne D, Adrian M** (2011) Identification of reference genes suitable for qRT-PCR in grapevine and application for the study of the expression of genes involved in pterostilbene synthesis. *Molecular Genetics and Genomics* **285**: 273-285
- Geelen D, Royackers K, Vanstraelen M, De Bus M, Inze D, Van Dijck P, Thevelein JM, Leyman B** (2007) Trehalose-6-P synthase AtTPS1 high molecular weight complexes in yeast and Arabidopsis. *Plant Science* **173**: 426-437
- Gietz RD, Woods RA** (2002) Transformation of yeast by lithium acetate/single-stranded carrier DNA/polyethylene glycol method. *In* Guide to Yeast Genetics and Molecular and Cell Biology, Pt B, Vol 350, pp 87-96
- Goddijn OJM, van Dun K** (1999) Trehalose metabolism in plants. *Trends in plant science* **4**: 315-319
- Goddijn OJM, Verwoerd TC, Voogd E, Krutwagen P, deGraaf P, Poels J, vanDun K, Ponstein AS, Damm B, Pen J** (1997) Inhibition of trehalase activity enhances trehalose accumulation in transgenic plants. *Plant Physiology* **113**: 181-190

- Greer DH, Sicard SM** (2009) The net carbon balance in relation to growth and biomass accumulation of grapevines (*Vitis vinifera* cv. 'Semillon') grown in a controlled environment. *Functional Plant Biology* **36**: 645-653
- Guerinier T, Millan L, Crozet P, Oury C, Rey F, Valot B, Mathieu C, Vidal J, Hodges M, Thomas M, Glab N** (2013) Phosphorylation of p27(KIP1) homologs KRP6 and 7 by SNF1-related protein kinase-1 links plant energy homeostasis and cell proliferation. *Plant Journal* **75**: 515-525
- Gunstream S, Hellemans J, Menezes A, Owens B, Rose S, Sander R, Vandesompele J** (2011) qPCR application guide: Experimental overview, protocol, troubleshooting. *In*, Ed 3. IDT, Online
- Gutierrez L, Mauriat M, Guenin S, Pelloux J, Lefebvre J-F, Louvet R, Rusterucci C, Moritz T, Guerineau F, Bellini C, Van Wuytswinkel O** (2008) The lack of a systematic validation of reference genes: a serious pitfall undervalued in reverse transcription-polymerase chain reaction (RT-PCR) analysis in plants. *Plant Biotechnology Journal* **6**: 609-618
- Harthill JE, Meek SEM, Morrice N, Pegg MW, Borch J, Wong BHC, MacKintosh C** (2006) Phosphorylation and 14-3-3 binding of Arabidopsis trehalose-phosphate synthase 5 in response to 2-deoxyglucose. *Plant Journal* **47**: 211-223
- Hayworth D** (2009) Tech tip #45: Anneal complementary pairs of oligonucleotides. *In*, Ed 1. Thermo Fisher Scientific, Online, pp 1-2
- He YH** (2012) Chromatin regulation of flowering. *Trends in Plant Science* **17**: 556-562
- Heazlewood JE, Wilson S, Clark RJ, Gracie AJ** (2006) Pruning effects on Pinot Noir vines in Tasmania (Australia). *Vitis* **45**: 165-171
- Heisler MG, Ohno C, Das P, Sieber P, Reddy GV, Long JA, Meyerowitz EM** (2005) Patterns of auxin transport and gene expression during primordium development revealed by live imaging of the Arabidopsis inflorescence meristem. *Current Biology* **15**: 1899-1911
- Hepworth SR, Valverde F, Ravenscroft D, Mouradov A, Coupland G** (2002) Antagonistic regulation of flowering-time gene SOC1 by CONSTANS and FLC via separate promoter motifs. *Embo Journal* **21**: 4327-4337
- Hiraoka K, Yamaguchi A, Abe M, Araki T** (2013) The florigen genes FT and TSF modulate lateral shoot outgrowth in *Arabidopsis thaliana*. *Plant and Cell Physiology* **54**: 352-368
- Hunter JJ, Ruffner HP, Volschenk CG** (1995) Starch concentrations in grapevine leaves, berries and roots and the effect of canopy management. *South African Journal for Enology and Viticulture* **16**: 35-40
- Irish EE** (1997) Class II tassel seed mutations provide evidence for multiple types of inflorescence meristems in maize (Poaceae). *American Journal of Botany* **84**: 1502-1515
- Ito S, Song YH, Josephson-Day AR, Miller RJ, Breton G, Olmstead RG, Imaizumi T** (2012) FLOWERING BHLH transcriptional activators control expression of the photoperiodic flowering regulator CONSTANS in Arabidopsis. *Proceedings of the National Academy of Sciences of the United States of America* **109**: 3582-3587
- Iturriaga G, Suarez R, Nova-Franco B** (2009) Trehalose metabolism: from osmoprotection to signaling. *International Journal of Molecular Sciences* **10**: 3793-3810
- Jackson DI** (1991) Environmental and hormonal effects on development of early bunch stem necrosis. *American Journal of Enology and Viticulture* **42**: 290-294
- Jackson RS** (2000) Introduction. *In* Wine Science: Principles, Practice, Perception, Ed Second. Elsevier Inc., pp 1-12
- Jaillon O, Aury JM, Noel B, Policriti A, Clepet C, Casagrande A, Choisne N, Aubourg S, Vitulo N, Jubin C** (2007) The grapevine genome sequence suggests ancestral hexaploidization in major angiosperm phyla. *Nature* **449**: 463-467
- Jiang W, Fu FL, Zhang SZ, Wu L, Li WC** (2010) Cloning and characterization of functional trehalose-6-phosphate synthase gene in Maize. *Journal of Plant Biology* **53**: 134-141
- Jones DT, Taylor WR, Thornton JM** (1992) The rapid generation of mutation data matrices from protein sequences. *Computer Applications in the Biosciences* **8**: 275-282
- Jones JE, Menary RC, Wilson SJ** (2009) Continued development of *V. vinifera* inflorescence primordia in winter dormant buds. *Vitis* **48**: 103-105

- Jossier M, Bouly J-P, Meimoun P, Arjmand A, Lessard P, Hawley S, Grahame Hardie D, Thomas M** (2009) SnRK1 (SNF1-related kinase 1) has a central role in sugar and ABA signalling in *Arabidopsis thaliana*. *Plant Journal* **59**: 316-328
- Kaufmann K, Wellmer F, Muino JM, Ferrier T, Wuest SE, Kumar V, Serrano-Mislata A, Madueno F, Krajewski P, Meyerowitz EM, Angenent GC, Riechmann JL** (2010) Orchestration of floral initiation by APETALA1. *Science* **328**: 85-89
- Kelly G, David-Schwartz R, Sade N, Moshelion M, Levi A, Alchanatis V, Granot D** (2012) The pitfalls of transgenic selection and new roles of AtHXK1: A high level of AtHXK1 expression uncouples hexokinase1-dependent sugar signaling from exogenous sugar. *Plant Physiology* **159**: 47-51
- Khanlou KM, Van Bockstaele E** (2012) A critique of widely used normalization software tools and an alternative method to identify reliable reference genes in red clover (*Trifolium pratense* L.). *Planta* **236**: 1381-1393
- Kobayashi Y, Kaya H, Goto K, Iwabuchi M, Araki T** (1999) A pair of related genes with antagonistic roles in mediating flowering signals. *Science* **286**: 1960-1962
- Kolbe A, Tiessen A, Schluepmann H, Paul M, Ulrich S, Geigenberger P** (2005) Trehalose 6-phosphate regulates starch synthesis via posttranslational redox activation of ADP-glucose pyrophosphorylase. *Proceedings of the National Academy of Sciences of the United States of America* **102**: 11118-11123
- Komatsu K, Maekawa M, Ujiie S, Satake Y, Furutani I, Okamoto H, Shimamoto K, Kyojuka J** (2003) LAX and SPA: Major regulators of shoot branching in rice. *Proceedings of the National Academy of Sciences of the United States of America* **100**: 11765-11770
- Komatsu M, Maekawa M, Shimamoto K, Kyojuka J** (2001) The LAX1 and FRIZZY PANICLE 2 genes determine the inflorescence architecture of rice by controlling rachis-branch and spikelet development. *Developmental Biology* **231**: 364-373
- Kosmas SA, Argyrokastritis A, Loukas MG, Eliopoulos E, Tsakas S, Kaltsikes PJ** (2006) Isolation and characterization of drought-related trehalose 6-phosphate-synthase gene from cultivated cotton (*Gossypium hirsutum* L.). *Planta* **223**: 329-339
- Krstic M, G. Moulds, W. Panagiotopoulos, S. West** (2003) Growing Quality Grapes to Winery Specification. Winetitles, Adelaide, Australia
- Kumar SV, Lucyshyn D, Jaeger KE, Alos E, Alvey E, Harberd NP, Wigge PA** (2012) Transcription factor PIF4 controls the thermosensory activation of flowering. *Nature* **484**: 242-U127
- Kunikowska A, Byczkowska A, Doniak M, Kazmierczak A** (2013) Cytokinins resume: their signaling and role in programmed cell death in plants. *Plant Cell Reports* **32**: 771-780
- Latchman DS** (1993) Transcription factors- and overview. *International Journal of Experimental Pathology* **74**: 417-422
- Lebon G, Duchene E, Brun O, Magne C, Clement C** (2004) Flower abscission and inflorescence carbohydrates in sensitive and non-sensitive cultivars of grapevine. *Sexual Plant Reproduction* **17**: 71-79
- Lebon G, Wojnarowicz G, Holzapfel B, Fontaine F, Vaillant-Gaveau N, Clement C** (2008) Sugars and flowering in the grapevine (*Vitis vinifera* L.). *Journal of Experimental Botany* **59**: 2565-2578
- Lee H, Suh SS, Park E, Cho E, Ahn JH, Kim SG, Lee JS, Kwon YM, Lee I** (2000) The AGAMOUS-LIKE 20 MADS domain protein integrates floral inductive pathways in Arabidopsis. *Genes & Development* **14**: 2366-2376
- Leyman B, Van Dijck P, Thevelein JM** (2001) An unexpected plethora of trehalose biosynthesis genes in *Arabidopsis thaliana*. *Trends in plant science* **6**: 510-513
- Li P, Ma S, Bohnert HJ** (2008) Coexpression characteristics of trehalose-6-phosphate phosphatase subfamily genes reveal different functions in a network context. *Physiologia Plantarum* **133**: 544-556
- Lijavetzky D, Carbonell-Bejerano P, Grimplet J, Bravo G, Flores P, Fenoll J, Hellin P, Carlos Oliveros J, Martinez-Zapater JM** (2012) Berry flesh and skin ripening features in *Vitis vinifera* as assessed by transcriptional profiling. *Plos One* **7**
- Liu C, Zhou J, Bracha-Drori K, Yalovsky S, Ito T, Yu H** (2007) Specification of Arabidopsis floral meristem identity by repression of flowering time genes. *Development* **134**: 1901-1910

- Ljung K, Bhalerao RP, Sandberg G** (2001) Sites and homeostatic control of auxin biosynthesis in *Arabidopsis* during vegetative growth. *Plant Journal* **28**: 465-474
- Lunn JE** (2003) Sucrose-phosphatase gene families in plants. *Gene* **303**: 187-196
- Lunn JE** (2007) Gene families and evolution of trehalose metabolism in plants. *Functional Plant Biology* **34**: 550-563
- Lunn JE, Feil R, Hendriks JHM, Gibon Y, Morcuende R, Osuna D, Scheible WR, Carillo P, Hajirezaei MR, Stitt M** (2006) Sugar-induced increases in trehalose 6-phosphate are correlated with redox activation of ADP glucose pyrophosphorylase and higher rates of starch synthesis in *Arabidopsis thaliana*. *Biochemical Journal* **397**: 139-148
- Lutfiyya LL, Xu N, D'Ordine RL, Morrell JA, Miller PW, Duff SMG** (2007) Phylogenetic and expression analysis of sucrose phosphate synthase isozymes in plants. *Journal of Plant Physiology* **164**: 923-933
- Martins MCM, Hejazi M, Fettke J, Steup M, Feil R, Krause U, Arrivault S, Vosloh D, Figueroa CM, Ivakov A, Yadav UP, Piques M, Metzner D, Stitt M, Lunn JE** (2013) Feedback inhibition of starch degradation in *Arabidopsis* leaves mediated by trehalose 6-phosphate. *Plant Physiology* **163**: 1142-1163
- Matsoukas IG, Massiah AJ, Thomas B** (2012) Florigenic and antiflorigenic signaling in plants. *Plant and Cell Physiology* **53**: 1827-1842
- Matsoukas IG, Massiah AJ, Thomas B** (2013) Starch metabolism and antiflorigenic signals modulate the juvenile-to-adult phase transition in *Arabidopsis*. *Plant Cell and Environment* **36**: 1802-1811
- May P** (2000) From bud to berry, with special reference to inflorescence and bunch morphology in *Vitis vinifera* L. *Australian Journal of Grape and Wine Research* **6**: 82-98
- May P** (2004) Flowering and Fruitset in Grapevines. Lythrum Press, Adelaide
- McDonald JH** (2009) Handbook of Biological Statistics. *In*, Ed 2. Sparky House Publishing, Baltimore, MD
- Morrison JC** (1991) Bud development in *Vitis vinifera* L. *Botanical Gazette* **152**: 304-315
- Muller J, Boller T, Wiemken A** (1995) Trehalose and trehalase in plants: Recent developments. *Plant Science* **112**: 1-9
- Mullins MG, A. Bouquet, L.E. Williams** (1992) Biology of the grapevine. Cambridge University Press, Cambridge, UK
- Munoz-Bertomeu J, Cascales-Minana B, Irls-Segura A, Mateu I, Nunes-Nesi A, Fernie AR, Segura J, Ros R** (2010) The plastidial glyceraldehyde-3-phosphate dehydrogenase is critical for viable pollen development in *Arabidopsis*. *Plant Physiology* **152**: 1830-1841
- Müller D, Leyser O** (2011) Auxin, cytokinin and the control of shoot branching. *Annals of Botany* **107**: 1203-1212
- Müller J, Wiemken A, Aeschbacher R** (1999) Trehalose metabolism in sugar sensing and plant development. *Plant Science* **147**: 37-47
- Nakagawa M, Shimamoto K, Kyojuka J** (2002) Overexpression of RCN1 and RCN2, rice TERMINAL FLOWER 1/CENTRORADIALIS homologs, confers delay of phase transition and altered panicle morphology in rice. *The Plant Journal* **29**: 743-750
- New Zealand Winegrowers** (2013) New Zealand Winegrowers Annual Report 2013. *In*. New Zealand Winegrowers
- Nicolosi E, Continella A, Gentile A, Cicala A, Ferlito F** (2012) Influence of early leaf removal on autochthonous and international grapevines in Sicily. *Scientia Horticulturae* **146**: 1-6
- Nunes C, O'Hara LE, Primavesi LF, Delatte TL, Schluepmann H, Somsen GW, Silva AB, Fevereiro PS, Wingler A, Paul MJ** (2013) The trehalose 6-phosphate/SnRK1 signaling pathway primes growth recovery following relief of sink limitation. *Plant Physiology* **162**: 1720-1732
- Nunes C, Primavesi LF, Patel MK, Martinez-Barajas E, Powers SJ, Sagar R, Fevereiro PS, Davis BG, Paul MJ** (2013) Inhibition of SnRK1 by metabolites: Tissue-dependent effects and cooperative inhibition by glucose 1-phosphate in combination with trehalose 6-phosphate. *Plant Physiology and Biochemistry* **63**: 89-98
- O'Hara LE, Paul MJ, Wingler A** (2013) How do sugars regulate plant growth and development? New insight into the role of trehalose-6-phosphate. *Molecular Plant* **6**: 261-274

- Ohto M, Onai K, Furukawa Y, Aoki E, Araki T, Nakamura K** (2001) Effects of sugar on vegetative development and floral transition in arabidopsis. *Plant Physiology* **127**: 252-261
- OIV** (2010) International Organisation of Vine and Wine-Statistics. *In*, Vol 2010
- OIV** (2012) Statistical report on world vitiviniculture 2012. *In*. OIV
- Okita TW, Nakata PA, Anderson JM, Sowokinos J, Morell M, Preiss J** (1990) The subunit structure of potato tuber ADP-glucose pyrophosphorylase. *Plant Physiology* **93**: 785-790
- Park J-I, Ishimizu T, Suwabe K, Sudo K, Masuko H, Hakozaki H, Nou I-S, Suzuki G, Watanabe M** (2010) UDP-glucose pyrophosphorylase is rate limiting in vegetative and reproductive phases in *Arabidopsis thaliana*. *Plant and Cell Physiology* **51**: 981-996
- Parker A** (2012) Modelling phenology and maturation of the grapevine *Vitis vinifera* L.: varietal differences and the role of leaf area to fruit weight ratio manipulations. Lincoln University, New Zealand
- Parrou JL, Francois J** (1997) A simplified procedure for a rapid and reliable assay of both glycogen and trehalose in whole yeast cells. *Analytical Biochemistry* **248**: 186-188
- Partow S, Siewers V, Bjørn S, Nielsen J, Maury J** (2010) Characterization of different promoters for designing a new expression vector in *Saccharomyces cerevisiae*. *Yeast* **27**: 955-964
- Pastore C, Zenoni S, Fasoli M, Pezzotti M, Tornielli GB, Filippetti I** (2013) Selective defoliation affects plant growth, fruit transcriptional ripening program and flavonoid metabolism in grapevine. *Bmc Plant Biology* **13**
- Paul M** (2007) Trehalose 6-phosphate. *Current Opinion in Plant Biology* **10**: 303-309
- Podolyan A, White J, Jordan B, Winefield C** (2010) Identification of the lipoxygenase gene family from *Vitis vinifera* and biochemical characterisation of two 13-lipoxygenases expressed in grape berries of 'Sauvignon Blanc'. *Functional Plant Biology* **37**: 767-784
- Prusinkiewicz P, Erasmus Y, Lane B, Harder LD, Coen E** (2007) Evolution and development of inflorescence architectures. *Science* **316**: 1452-1456
- Ramon M, De Smet I, Vandesteene L, Naudts M, Leyman B, Van Dijck P, Rolland F, Beeckman T, Thevelein JM** (2009) Extensive expression regulation and lack of heterologous enzymatic activity of the Class II trehalose metabolism proteins from *Arabidopsis thaliana*. *Plant, Cell & Environment* **32**: 1015-1032
- Ratcliffe OJ, Amaya I, Vincent CA, Rothstein S, Carpenter R, Coen ES, Bradley DJ** (1998) A common mechanism controls the life cycle and architecture of plants. *Development* **125**: 1609-1615
- Ratcliffe OJ, Bradley DJ, Coen ES** (1999) Separation of shoot and floral identity in *Arabidopsis*. *Development* **126**: 1109-1120
- Reid KE, Olsson N, Schlosser J, Peng F, Lund ST** (2006) An optimized grapevine RNA isolation procedure and statistical determination of reference genes for real-time RT-PCR during berry development. *Bmc Plant Biology* **6**
- Reinhardt D, Pesce ER, Stieger P, Mandel T, Baltensperger K, Bennett M, Traas J, Friml J, Kuhlmeier C** (2003) Regulation of phyllotaxis by polar auxin transport. *Nature* **426**: 255-260
- Ritter MK, Padilla CM, Schmidt RJ** (2002) The maize mutant *barren stalk1* is defective in axillary meristem development. *American Journal of Botany* **89**: 203-210
- Robaglia C, Thomas M, Meyer C** (2012) Sensing nutrient and energy status by SnRK1 and TOR kinases. *Current Opinion in Plant Biology* **15**: 301-307
- Rolland F, Baena-Gonzalez E, Sheen J** (2006) Sugar sensing and signaling in plants: Conserved and novel mechanisms. *Annual Review of Plant Biology* **57**: 675-709
- Rolland F, Moore B, Sheen J** (2002) Sugar sensing and signaling in plants. *Plant Cell* **14**: S185-S205
- Romanos MA, Scorer CA, Clare JJ** (1992) Foreign gene expression in yeast- a review. *Yeast* **8**: 423-488
- Sabbatini P, Howell GS** (2010) Effects of early defoliation on yield, fruit composition, and harvest season cluster rot complex of grapevines. *Hortscience* **45**: 1804-1808
- Sairanen I, Novak O, Pencik A, Ikeda Y, Jones B, Sandberg G, Ljung K** (2012) Soluble carbohydrates regulate auxin biosynthesis via PIF proteins in *Arabidopsis*. *Plant Cell* **24**: 4907-4916
- Samach A, Smith HM** (2013) Constraints to obtaining consistent annual yields in perennials. II: Environment and fruit load affect induction of flowering. *Plant Science* **207**: 168-176
- Sambrook J, Russell DW** (2001) Molecular cloning: a laboratory manual. CSHL press

- Satoh-Nagasawa N, Nagasawa N, Malcomber S, Sakai H, Jackson D** (2006) A trehalose metabolic enzyme controls inflorescence architecture in maize. *Nature* **441**: 227-230
- Schluepmann H, Berke L, Sanchez-Perez GF** (2012) Metabolism control over growth: a case for trehalose-6-phosphate in plants. *Journal of Experimental Botany* **63**: 3379-3390
- Schluepmann H, Pellny T, van Dijken A, Smeekens S, Paul M** (2003) Trehalose 6-phosphate is indispensable for carbohydrate utilization and growth in *Arabidopsis thaliana*. *Proceedings of the National Academy of Sciences of the United States of America* **100**: 6849-6854
- Schluepmann H, van Dijken A, Aghdasi M, Wobbes B, Paul M, Smeekens S** (2004) Trehalose mediated growth inhibition of *Arabidopsis* seedlings is due to trehalose-6-phosphate accumulation. *Plant Physiology* **135**: 879-890
- Selim M, Legay S, Berkelmann-Loehnertz B, Langen G, Kogel KH, Evers D** (2012) Identification of suitable reference genes for real-time RT-PCR normalization in the grapevine-downy mildew pathosystem. *Plant Cell Reports* **31**: 205-216
- Shannon S, Meeks-Wagner DR** (1991) A mutation in the *Arabidopsis* TFL1 gene affects inflorescence meristem development. *The Plant Cell Online* **3**: 877
- Sheen J, Zhou L, Jang JC** (1999) Sugars as signaling molecules. *Current opinion in plant biology* **2**: 410-418
- Shima S, Matsui H, Tahara S, Imai R** (2007) Biochemical characterization of rice trehalose-6-phosphate phosphatases supports distinctive functions of these plant enzymes. *FEBS journal* **274**: 1192-1201
- Smeekens S, Ma JK, Hanson J, Rolland F** (2010) Sugar signals and molecular networks controlling plant growth. *Current Opinion in Plant Biology* **13**: 274-279
- Smith AM, Stitt M** (2007) Coordination of carbon supply and plant growth. *Plant Cell and Environment* **30**: 1126-1149
- Sohn EJ, Rojas-Pierce M, Pan S, Carter C, Serrano-Mislata A, Madueño F, Rojo E, Surpin M, Raikhel NV** (2007) The shoot meristem identity gene TFL1 is involved in flower development and trafficking to the protein storage vacuole. *Proceedings of the National Academy of Sciences* **104**: 18801
- Sreekantan L, Mathiason K, Grimplet J, Schlauch K, Dickerson JA, Fennell AY** (2010) Differential floral development and gene expression in grapevines during long and short photoperiods suggests a role for floral genes in dormancy transitioning. *Plant Molecular Biology* **73**: 1-15
- Sreekantan L, Thomas MR** (2006) VvFT and VvMADS8, the grapevine homologues of the floral integrators FT and SOC1, have unique expression patterns in grapevine and hasten flowering in *Arabidopsis*. *Functional Plant Biology* **33**: 1129-1139
- Srinivasan C, Mullins MG** (1981) Physiology of flowering in the grapevine-A review. *American Journal of Enology and Viticulture* **32**: 47-63
- Stitt M, Zeeman SC** (2012) Starch turnover: pathways, regulation and role in growth. *Current Opinion in Plant Biology* **15**: 282-292
- Strasser B, Alvarez MJ, Califano A, Cerdán PD** (2009) A complementary role for ELF3 and TFL1 in the regulation of flowering time by ambient temperature. *The Plant Journal* **58**: 629-640
- Tamura K, Peterson D, Peterson N, Stecher G, Nei M, Kumar S** (2011) MEGA5: Molecular evolutionary genetics analysis using maximum likelihood, evolutionary distance, and maximum parsimony methods. *Molecular Biology and Evolution* **28**: 2731-2739
- Tardaguila J, Blanco JA, Poni S, Diago P** (2012) Mechanical yield regulation in winegrapes: comparison of early defoliation and crop thinning. *Australian Journal of Grape and Wine Research* **18**: 344-352
- Tarter ME, Poni S** (2010) A *Vitis vinifera* cluster's wing-related structural characteristics and their associations with yield and berry composition. *HortScience* **45**: 1270-1277
- Tesic D, Woolley DJ, Hewett EW, Martin DJ** (2002) Environmental effects on cv 'Cabernet Sauvignon' (*Vitis vinifera* L.) grown in Hawke's Bay, New Zealand. 1. Phenology and characterisation of viticultural environments. *Australian Journal of Grape and Wine Research* **8**: 15-26
- Teusink B, Walsh MC, van Dam K, Westerhoff HV** (1998) The danger of metabolic pathways with turbo design. *Trends in Biochemical Sciences* **23**: 162-169

- Thevelein JM, Hohmann S** (1995) Trehalose synthase- guard to the gate of glycolysis in yeast. Trends in Biochemical Sciences **20**: 3-10
- Tsai AYL, Gazzarrini S** (2012) AKIN10 and FUSCA3 interact to control lateral organ development and phase transitions in Arabidopsis. Plant Journal **69**: 809-821
- van Dijken AJH, Schluepmann H, Smeeckens SCM** (2004) Arabidopsis trehalose-6-phosphate synthase 1 is essential for normal vegetative growth and transition to flowering. Plant Physiology **135**: 969-977
- Vandesompele J, De Preter K, Pattyn F, Poppe B, Van Roy N, De Paepe A, Speleman F** (2002) Accurate normalization of real-time quantitative RT-PCR data by geometric averaging of multiple internal control genes. Genome Biology **3**
- Vandesteene L, Lopez-Galvis L, Vanneste K, Feil R, Maere S, Lammens W, Rolland F, Lunn JE, Avonce N, Beeckman T, Van Dijck P** (2012) Expansive evolution of the TREHALOSE-6-PHOSPHATE PHOSPHATASE gene family in Arabidopsis. Plant Physiology **160**: 884-896
- Vandesteene L, Ramon M, Le Roy K, Van Dijck P, Rolland F** (2010) A single active trehalose-6-P synthase (TPS) and a family of putative regulatory TPS-like proteins in Arabidopsis. Molecular Plant **3**: 406-419
- Vasconcelos MC, Greven M, Winefield CS, Trought MCT, Raw V** (2009) The flowering process of *Vitis vinifera*: a review. Am. J. Enol. Vitic. **60**: 411-434
- Vogel G, Aeschbacher RA, Muller J, Boller T, Wiemken A** (1998) Trehalose-6-phosphate phosphatases from *Arabidopsis thaliana*: identification by functional complementation of the yeast tps2 mutant. Plant Journal **13**: 673
- Vogel G, Fiehn O, Jean-Richard-dit-Bressel L, Boller T, Wiemken A, Aeschbacher RA, Wingler A** (2001) Trehalose metabolism in Arabidopsis: occurrence of trehalose and molecular cloning and characterization of trehalose-6-phosphate synthase homologues. Journal of Experimental Botany **52**: 1817
- Wahl V, Ponnu J, Schlereth A, Arrivault S, Langenecker T, Franke A, Feil R, Lunn JE, Stitt M, Schmid M** (2013) Regulation of flowering by trehalose-6-phosphate signaling in *Arabidopsis thaliana*. Science **339**: 704-707
- Wang AM, Doyle MV, Mark DF** (1989) Quantitation of messenger-RNA By the polymerase chain-reaction. Proceedings of the National Academy of Sciences of the United States of America **86**: 9717-9721
- Wang YJ, Hao YJ, Zhang ZG, Chen T, Zhang JS, Chen SY** (2005) Isolation of trehalose-6-phosphate phosphatase gene from tobacco and its functional analysis in yeast cells. Journal of plant physiology **162**: 215-223
- Wendland J** (2003) PCR-based methods facilitate targeted gene manipulations and cloning procedures. Current Genetics **44**: 115-123
- Wigge PA, Kim MC, Jaeger KE, Busch W, Schmid M, Lohmann JU, Weigel D** (2005) Integration of spatial and temporal information during floral induction in Arabidopsis. Science **309**: 1056-1059
- Winegrowers NZ** (2009) Annual Report 2008. In. New Zealand Winegrowers
- Woods DP, Hope CL, Malcomber ST** (2011) Phylogenomic analyses of the BARREN STALK1/LAX PANICLE1 (BA1/LAX1) genes and evidence for their roles during axillary meristem development. Molecular Biology and Evolution **28**: 2147-2159
- Wu W, Pang Y, Shen GA, Lu J, Lin J, Wang J, Sun X, Tang K** (2006) Molecular cloning, characterization and expression of a novel trehalose-6-phosphate synthase homologue from Ginkgo biloba. Journal of Biochemistry and Molecular Biology **39**: 158
- Yang F, Wang Q, Schmitz G, Muller D, Theres K** (2012) The bHLH protein ROX acts in concert with RAX1 and LAS to modulate axillary meristem formation in Arabidopsis. Plant Journal **71**: 61-70
- Yang J, Tian L, Sun M-X, Huang X-Y, Zhu J, Guan Y-F, Jia Q-S, Yang Z-N** (2013) AUXIN RESPONSE FACTOR17 Is Essential for Pollen Wall Pattern Formation in Arabidopsis. Plant Physiology **162**: 720-731

- Yant L, Mathieu J, Dinh TT, Ott F, Lanz C, Wollmann H, Chen X, Schmid M** (2010) Orchestration of the floral transition and floral development in Arabidopsis by the bifunctional transcription factor APETALA2. *Plant Cell* **22**: 2156-2170
- Yoo S-C, Chen C, Rojas M, Daimon Y, Ham B-K, Araki T, Lucas WJ** (2013) Phloem long-distance delivery of FLOWERING LOCUS T (FT) to the apex. *Plant Journal* **75**: 456-468
- Zang B, Li H, Li W, Deng XW, Wang X** (2011) Analysis of trehalose-6-phosphate synthase (TPS) gene family suggests the formation of TPS complexes in rice. *Plant Molecular Biology* **76**: 507-522
- Zapata C, Deléens E, Chaillou S, Magné C** (2004) Partitioning and mobilization of starch and N reserves in grapevine (*Vitis vinifera* L.). *Journal of plant physiology* **161**: 1031-1040
- Zhang SL, Yao AY, Bai HL, Ren J, Jia WS, Zhang LS, Hu JF** (2008) The VAP1 gene expression in relation to GAs effect on tendrils, buds and flowers development in "Xiangfei" grapevine. *Scientia Horticulturae* **117**: 225-230
- Zhang YH, Primavesi LF, Jhurreea D, Andralojc PJ, Mitchell RAC, Powers SJ, Schluepmann H, Delatte T, Wingler A, Paul MJ** (2009) Inhibition of SNF1-related protein kinase1 activity and regulation of metabolic pathways by trehalose-6-phosphate. *Plant Physiology* **149**: 1860-1871
- Ziliotto F, Corso M, Rizzini FM, Rasori A, Botton A, Bonghi C** (2012) Grape berry ripening delay induced by a pre-veraison NAA treatment is paralleled by a shift in the expression pattern of auxin- and ethylene-related genes. *BMC Plant Biology* **12**